Advancing the Field of Soft Scorpionates Ligated to Carbyne, Aminocarbyne and Tricarbido Complexes

by

Steven Scott Welsh

MChem (Hons) (Heriot-Watt University, Edinburgh)

October 2022

A thesis submitted for the degree of Doctor of Philosophy of

The Australian National University

Australian National University

Author's Declaration

This thesis is an account of the work conducted at the Research School of Chemistry, Australian National University between October 2018 and October 2022. The information documented therein, unless otherwise referenced, is my own original work.

Steven S. Welsh

October 2022

Acknowledgements

Upon review of my time as a PhD candidate, it's hard to believe some of the events which have taken place over the past four years. These have included the incipient threat of bushfires and choking smoke, the SARS-CoV-2 (COVID-19) pandemic, and the strict lockdowns which followed. Combined with the universally acknowledged personal stresses and strains which accompany all PhD programs (the abundancy of which cannot be overemphasised), my academic journey has been unpredictable to say the least. However, due to the people who have helped me continuously navigate the uncertain landscape which presented itself, I've successfully (miraculously) managed to progress through the PhD program. To all of these people, I owe a massive debt of gratitude.

(Prof.) Tony Hill, thank-you for giving me the opportunity to return to the ANU and for proving yourself to not only be a font of infinite chemical knowledge, but also a great supervisor. Both you and Mark have repeatedly displayed incredible generosity, especially when volunteering to host group dinners and trips outside of Canberra. Furthermore, I would never have re-joined the ANU RSC without the advice, guidance and reassurance of Mark Ellison and Alannah MacLeod. The impact which you've all had on my time here has been profound, and one which I will continue to hold dear.

As for all the members of Hill Group: Ben, Cheesheng, Harrison, Lachlan, Liam, Richie, Ryan, Yong Shen, and all of the project students who have worked in Hill Group over my time at the ANU. Not only have you all proven to be brilliant scientists, colleagues and friends, but you have (and still) find endless ways of enriching our lives both in-and-out of the lab. I only hope that I have been able to reciprocate this in kind, if not at least in part. I wish to extend this sentiment to all members of the HDR cohort, project students and undergraduates alike, and I wish you all the best of luck, wherever your chemistry careers take you.

Aside from the chemistry, one of the most significant things which drew me back to Canberra were the people I met during my year spent as an exchange student, back in 2015-2016. Although there are far too many people to list here, I would like to acknowledge two people who I believe went above and beyond, and helped me to maintain my sanity (and at times erode it) as we all simultaneously negotiated our postgraduate studies: Patrick Yates and Harrison Barnett. Thanks for your friendship and endless support!

(THIS PAGE INTENTIONALLY LEFT BLANK)

Abstract

The application of soft Scorpionate ligand systems, such as the bidentate ligand dihydrobis(methimazolyl)borate, (**Bm**) and dihydrobis(*N*-*tert*-butyl-5-mercaptotetrazolyl)-borate, (**Hbt**); and the analogous tridentate ligand systems hydrotris(methimazolyl)borate, (**Tm**) and hydrotris(*N*-*tert*-butyl-5-mercaptottrazolyl)borate, (**Htt**), remain to be relatively rare in the field of organometallic chemistry. In part, this is due to their relative infancy in the field of Scorpionate coordination chemistry, which has previously been dominated by the use of pyrazolyl-based systems. Throughout the work detailed in this thesis, these four ligand systems have been utilised in the preparation of various tungsten and molybdenum carbyne, aminocarbyne and tricarbido complexes, including propargylidynes.

The propargylidyne complexes reported herein were prepared *via* the semi-generalisable oxide abstraction synthetic route. This method has notable advantages over alternative synthetic procedures, including allowing for the convenient incorporation of an appropriate ligand system in a 'one-pot' process and affording relatively high reaction yields. Through this method, a short list of propargylidyne complexes were prepared, featuring a range of silyl-, alkyl-, and aryl- termini: [**Tm**W(CO)$_2$(≡CC≡CR)] (R = SiMe$_3$ (**2.1**), Si^{i}Pr$_3$ (**2.3**), ^{t}Bu (**2.4**), Ph (**2.5**)). It is possible to form the molybdenum analogue of complex **2.1** *via* a similar synthetic approach through the addition of [Mo(CO)$_6$] instead of the tungsten variant, thereby affording [**Tm**Mo(CO)$_2$(≡CC≡CSiMe$_3$)] (**2.2**). However, it was noted that complex **2.2** was isolated in diminished yields compared to complex **2.1**, and also afforded broadly similar spectroscopic results. Hence, of the remaining propargylidyne complexes, their molybdenum analogues were not synthetically targeted.

Propargylidyne complexes are known to contain several reactive sites. In an effort to probe these various sites, complex **2.1** was reacted with an excess of elemental iodine in order to effect complete oxidative decarbonylation at the tungsten centre. However, results showed that the intended reaction had not been carried out, and instead a mono-cationic complex of the form [**Tm**W(CO)$_2$I(≡CC≡CSiMe$_3$)][I$_3$] (**2.6**) was isolated. This complex is notably unusual, as instead of the loss of one or both carbonyl ligands from the metal centre these have both been retained. Instead, a single iodine atom was found to have coordinated to the tungsten centre, which subsequently caused the slippage of one **Tm** methimazolyl arm into a semi-bridging position between the tungsten atom and the carbyne carbon. This was conclusively shown *via* single crystal x-ray diffraction.

In previously published reports, the silylpropargylidyne complex [**Tp***W(CO)$_2$(≡CC≡CSiMe$_3$)] (**Tp*** = hydrotris(3,5-dimethylpyrazolyl)borate) was successfully used to prepare a range of bimetallic tricarbido complexes, [**Tp***W(CO)$_2${μ-CC≡C}(ML$_n$)] (M = Ru, Rh, Ir, Hg, Au). Aided by the fact that complex **2.1** could be prepared in multi-gram quantities, attempts were made to similarly prepare bimetallic tricarbido structural analogues featuring the **Tm** ligand by sequential *in-situ* desilylation and metalation *via* halide metathesis. Despite concerted and repeated attempts to incorporate several metal species, only two complexes were deemed to have been formed: [**Tm**W(CO)$_2${μ-CC≡C}(ML$_n$)] (ML$_n$ = Au(PPh$_3$) (**2.7**), Rh(CO)(PPh$_3$)$_2$ (**2.8**). In both cases, full spectroscopic analysis proved to be difficult, due in part to low reaction yields and further exacerbated by difficulties during purification of the crude reaction mixtures. Despite this, a single crystal of complex **2.8** was grown and analysed *via* single crystal x-ray diffraction. This returned an agreeable structural model, and confirmed that complex **2.8** had successfully been prepared *via* this synthetic route. Regrettably, structural data was not obtained for complex **2.7**.

Often, metallocarbyne complexes may serve as late common intermediates and may be further functionalised without the need for extensive synthetic procedures. A prime example of such a complex is [Br(pic)$_2$(CO)$_2$W≡C(Mesityl)] (pic = γ-picoline), which has the ability to undergo three-fold ligand substitution upon the addition of a suitable Scorpionate pro-ligand. Four complexes of the form [L$_n$W(CO)$_2${≡C-(Mesityl)}] (L$_n$ = **Bm** (**3.1**), **Tm** (**3.2**), **Hbt** (**3.3**), **Htt** (**3.4**)) were successfully prepared through this effective synthetic route.

Further success was obtained using the oxide abstraction synthetic route, albeit in the preparation of more conventional metallocarbyne complexes. A range of **Tm**-ligated tungsten and molybdenum metallocarbyne complexes bearing a range of conjugated and poly-aromatic species of the form [**Tm**M(CO)$_2${≡C-R}] (M = W, R = thienyl (**3.5**), 2-naphthyl (**3.6**), 9-phenanthryl (**3.8**), 9-anthracenyl (**3.10**), 1-pyrenyl (**3.12**), 3-perylenyl (**3.14**), 9-(10-phenyl-anthracenyl) (**3.21**); M = Mo, 2-naphthyl (**3.7**), 9-phenanthryl (**3.9**), 9-anthracenyl (**3.11**), 1-pyrenyl (**3.13**), 3-perylenyl (**3.15**)) were prepared. However, more structurally intricate examples of complexes bearing PAH's were soon prepared and included the tungsten propargylidynes [**Tm**W(CO)$_2${≡CC≡C-R] (R = 3-phenanthryl (**3.16**), 9-anthracenyl (**3.17**), 1-pyrenyl (**3.18**)).

As an aside, two **Tp***-ligated tungsten metallocarbyne complexes bearing the uncommon 1,2,4,5-dehydro[2.2]paracyclophane moiety were successfully isolated. The

tungsten stannyl carbyne [**Tp***$(CO)_2W{\equiv}C(SnBu_3)$] was reacted separately with 1-bromo-1,2,4,5-dehydro[2.2]paracyclophane and 1,9/10-dibromo-1,2,4,5-dehydro[2.2]paracyclophane in a modified Stille coupling reaction to afford the complexes [**Tp***$(CO)_2W${≡C(1-(1,2,4,5-dehydro[2.2]paracyclophane)}] (**3.19**) and [**Tp***$(CO)_2W{\equiv}C]_2$-{1,9/10-(1,2,4,5-dehydro[2.2]paracyclophane)} (**3.20**). Hence, this novel approach has afforded some of the first **Tp***-ligated tungsten metallocarbyne complexes which bear cyclophane frameworks.

While working with the dibrominated compound 9,10-dibromoanthracene, it was noted that through the careful stoichiometric addition of *n*BuLi it is possible to selectively effect mono-lithiation at either the 9- or 10-position. This approach was quickly utilised, and allowed for the preparation of the bromo-anthracenyl functionalised complex [**Tm**$W(CO)_2${≡C(9-[10-bromo-anthracenyl])}] (**3.22**). This complex proved to be seminal in the preparation of even more structurally intricate materials. For example, the post-synthetic modification of complex **3.22** *via* reaction with excess elemental sulfur was carried out to try and form the complex [**Tm**$W(CO)_2${SC(9-[10-bromo-anthracenyl])}] (**3.23**), which bears a bridging sulfur atom. Although some spectroscopic results (namely those afforded by ESI-MS and elemental analysis) indicate that this complex was successfully formed, the material produced proved to be unstable in halogenated NMR solvents and quickly decomposed. Hence, further work still remains to be carried out on the isolation and characterisation of this complex.

However, more successful attempts to further derivatise complex **3.22** were carried out. A triptycenyl-complex was formed through the reaction of complex **3.22** with benzyne (generated through the Kobayashi method). The benzyne generated *in situ* was found to bind and ring-fuse to the central anthracenyl-ring, thereby forming the complex [**Tm**$W(CO)_2${≡C(9-[10-bromo-triptycenyl])}] (**3.24**).

Further success was achieved in the preparation of butterfly complexes [**Tm**$W(CO)_2${≡C(9-[10-bromo-anthracenyl])}]$_2$Pt (**3.25**) and [**Tm**$W(CO)_2${≡C(9-[10-bromo-anthracenyl])}]$_2$Pd (**3.26**) through the addition of $[Pt(nbe)_3]$ (nbe = norbornene) and $[Pd_2(dba)_3{\cdot}CHCl_3]$ (dba = dibenzylideneacetone), respectively, to complex **3.22**. Plus, complexes of the form [**Tm**$W(CO)_2${μ-≡C-(9,10-anthracenyl)-C≡}$W(CO)_2$**Tp***] (**3.27**) and [**Tm**$W(CO)_2${μ-≡C-(9,10-anthracenyl)-C≡}$Mo(CO)_2$**Tp***] (**3.28**) were prepared and isolated in good yields.

Lastly, a range of aminocarbyne complexes featuring both tungsten and molybdenum centres, as well as **Tm** and **Htt** ligand systems were prepared. Of those ligated with **Tm**, they included [**Tm**M(CO)$_2${≡C–NR$_2$}] (M = Mo, R = Et (**4.1**); M = W, R = Ph (**4.6**); M = Mo, R = Ph (**4.7**). Likewise, those ligated with the rarely encountered **Htt** ligand system included [(**Htt**)M(CO)$_2${≡C–NR$_2$}] (M = W, R = Et (**4.2**); M = Mo, R = Et (**4.3**); M = W, R = ^{i}Pr (**4.4**); M = Mo, R = ^{i}Pr (**4.5**); M = W, R = Ph (**4.8**). More complex secondary amines were also utilised to form [**Tm**W(CO)$_2${≡C((*R*)-dimethylbenzylamine)}] (**4.9**), [(**Htt**)W(CO)$_2${≡C((*R*,*R*)-bis[1-phenylethyl]amine)}] (**4.10**), [**Tm**W(CO)$_2${≡C(*N*,*N*′-diphenylbenzidine)}] (**4.11**), [(**Htt**)W(CO)$_2${≡C(*N*,*N*′-diphenylbenzidine)}] (**4.12**) and the di-substituted complex [(**Htt**)W-(CO)$_2${μ-CN(Ph)-Ph-Ph-N(Ph)C≡}W(CO)$_2$(**Htt**)] (**4.13**).

Contents

Author's Declaration i

Acknowledgements ii

Abstract iv

Contents viii

List of Abbreviations xii

CHAPTER 1. - INTRODUCTION. **1**

1.1 General Introduction **2**

1.2 Methimazole-based Ligand Systems ..... Error! Bookmark not defined.

1.3 *N-'butyl*-5-mercaptotetrazole-based Ligand Systems **18**

1.4 Chapter 1 - References ..... Error! Bookmark not defined.

CHAPTER 2. – PROPARGYLIDYNE & TRICARBIDO COMPLEXES **27**

2.1 Introduction to Propargylidyne Complexes **28**

2.2 Background and Scope **28**

2.3 Propargylidyne Complexes **30**

2.3.1 Synthesis of Propargylidyne Complexes **31**

2.3.2 Bonding in Propargylidyne Complexes **34**

2.4 Tricarbido Complexes **35**

2.5 Recent Advances in Propargylidyne and Tricarbido Chemistry **38**

2.5.1 Preparation of the First Selenolatopropargylidyne **38**

2.5.2 A New *Pseudo*-Sonogashira ($\{C_2\}+\{C_1\}$) Route to Forming Propargylidynes **40**

2.5.3 Installation of Si, Sn, Pb, P, and As at Propargylidyne Termini **42**

2.5.4 Polycyclic Aromatic Hydrocarbon Propargylidynes **45**

2.6 Results & Discussion: Routes to Propargylidyne and Tricarbido Complexes **47**

2.6.1 Summary of Spectral Features – Chapter 2 Complexes **47**

2.6.2 Synthesis of [TmM(CO)$_2$(≡CC≡CSiMe$_3$)] (M = Mo, W) **48**

2.6.3 Synthesis of [TmW(CO)$_2$(≡CC≡CSi^{i}Pr$_3$)] **53**

2.6.4 Synthesis of [TmW(CO)$_2$(≡CC≡CR)] (R = ^{t}Bu, Ph) **55**

2.6.5 Synthesis of [TmW(CO)$_2$I(≡CC≡CSiMe$_3$)][I$_3$] **58**

2.6.6 Synthesis of [TmW(CO)$_2${μ-≡CC≡C}(Au(PPh$_3$))] **60**

2.6.7 Synthesis of [TmW(CO)$_2${μ-≡CC≡C}(Rh(CO)(PPh$_3$)$_2$)] **64**

2.6.8 Attempted Synthesis of other Tricarbido Complexes **68**

2.7 Summary **70**

2.8 Chapter 2 - References **71**

CHAPTER 3. PAH FUNCTIONALISED METALLOCARBYNE COMPLEXES 72

3.1 Introduction to Polycyclic Aromatic Hydrocarbon-containing Complexes **73**

3.2 Background and Scope **73**

3.3 Results & Discussion: Routes to PAH Functionalised Metallocarbyne Complexes **74**

3.3.1 Summary of Spectral Features – Chapter 3 Complexes **74**

3.3.2 Synthesis of [(L$_{fac}$)W(CO)$_2${≡C-(Mesityl)}] (L$_{fac}$ = Bm, Tm, Hbt, Htt) **76**

3.3.3 Synthesis of [TmW(CO)$_2${≡C-(Thienyl)}] **79**

3.3.4 Synthesis of [TmM(CO)$_2${≡C-(1-Naphthyl)}] (M = Mo, W) **81**

3.3.5 Synthesis of [TmM(CO)$_2${≡C-(9-Phenanthryl)}] (M = Mo, W) **84**

3.3.6 Synthesis of [TmM(CO)$_2${≡C-(9-Anthracenyl)}] (M = Mo, W) **86**

3.3.7 Synthesis of [TmM(CO)$_2${≡C-(1-Pyrenyl)}] (M = Mo, W) **88**

3.3.8 Synthesis of [TmM(CO)$_2${≡C-(3-Perylenyl)}] (M = Mo, W) **90**

3.3.9 Synthesis of [TmW(CO)$_2${≡CC≡C-R)}] (R = 3-Phenanthryl, 9-Anthracenyl, 1-Pyrenyl) **93**

3.3.10 Synthesis of Tp*(CO)$_2$W{≡C(1-(1,2,4,5-dehydro[2.2]paracyclophane)} and [Tp*(CO)$_2$W≡C]$_2$-{1,9/10-(1,2,4,5-dehydro[2.2]paracyclophane)} **97**

3.3.11 Synthesis of [Tm(CO)$_2$W{≡C(9-[10-phenyl-anthracenyl])}] **103**

3.3.12 Synthesis of [TmW(CO)$_2${≡C(9-[10-bromo-anthracenyl])}] **106**

3.3.13 Synthesis of [TmW(CO)$_2${SC(9-[10-bromo-anthracenyl])}] **108**

3.3.14 Synthesis of [TmW(CO)$_2${≡C(9-[10-bromo-triptycenyl])}] **110**

3.3.15 Synthesis of [TmW(CO)$_2${≡C(9-[10-bromo-anthracenyl])}]$_2$Pt and [Tm-W(CO)$_2${≡C(9-[10-bromo-anthracenyl])}]$_2$Pd **112**

3.3.16 Synthesis of [TmW(CO)$_2${μ-≡C-(9,10-anthracenyl)-C≡}M(CO)$_2$Tp*] (M = Mo, W)… **117**

3.4 Summary **120**

3.5 Chapter 3 - References **122**

CHAPTER 4. – AMINOCARBYNE COMPLEXES 123

4.1 Introduction **124**

4.2 Background and Scope **124**

4.3 Synthesis of Group 6 Aminocarbyne Complexes **127**

4.3.1 Preparation from Isocyanide Ligands **127**

4.3.2 Preparation from Carbonyl Ligands **130**

4.4 Results & Discussion: Routes to Tm & Htt Ligated Aminocarbyne Complexes **134**

4.4.1 General Reaction Procedure **134**

4.4.2 Summary of Spectral Features – Chapter 4 Complexes **136**

4.4.3 Synthesis of [TmMo(CO)$_2${≡CN(Et$_2$)}] (4.1) **136**

4.4.4 Synthesis of [(Htt)M(CO)$_2${≡CN(Et$_2$)}] (M = Mo, W) **140**

4.4.5 Synthesis of [(Htt)M(CO)$_2${≡CN(*i*Pr$_2$)}] (M = Mo, W) **145**

4.4.6 Synthesis of [TmM(CO)$_2${≡CN(Ph$_2$)}] (M = Mo, W) **149**

4.4.7 Synthesis of [(Htt)W(CO)$_2${≡CN(Ph$_2$)}] **152**

4.4.8 Synthesis of [TmW(CO)$_2${≡C((*R*)-dimethylbenzylamine)}] **154**

4.4.9 Synthesis of [(Htt)W(CO)$_2${≡C((*R*,*R*)-bis(1-phenylethyl)amine)}] **158**

4.4.10 Synthesis of [TmW(CO)$_2${≡C(*N*,*N*′-diphenylbenzidine)}] **160**

4.4.11 Synthesis of [(Htt)W(CO)$_2${≡C(*N*,*N*′-diphenylbenzidine)}] and [(Htt)W-(CO)$_2${μ-CN(Ph)-Ph-Ph-N(Ph)C≡}W(CO)$_2$(Htt)] **162**

4.5 Analysis of Cyclic Voltammetry Data **164**

4.6 Summary **167**

4.7 Chapter 4 - References **169**

CHAPTER 5. - EXPERIMENTAL **170**

5.1 General Procedures **171**

5.2 Compounds **173**

5.2.1 Ligand Systems **173**

5.2.2 Chapter 2 – Propargylidyne & Tricarbido Complexes **174**

5.2.3 Chapter 3 – Polycyclic Aromatic Hydrocarbon-containing Carbynes **185**

5.2.4 Chapter 4 – Aminocarbyne Complexes **215**

5.3 Chapter 5 - References and Notes **228**

CHAPTER 6. – CONCLUDING REMARKS **229**

6.1 Concluding Remarks **230**

List of Abbreviations

Bm	dihydrobis(methimazolyl)borate
Bp	dihydrobis(pyrazolyl)borate
Cp	cyclopentadienyl
Cp*	1,2,3,4,5-pentamethylcyclopentadienyl
DMSO	dimethylsulfoxide
ESI	Electrospray Ionisation
Hbt	dihydrobis(*N-tert*-butyl-5-mercaptotetrazolyl)borate
HOMO	Highest Occupied Molecular Orbital
Htt	hydrotris(*N-tert*-butyl-5-mercaptottrazolyl)borate
IMCT	Inter-Molecular Charge Transfer
IR	infrared
J	coupling constant
L_{fac}	facially capping ligand
LUMO	Lowest Unoccupied Molecular Orbital
m/z	Mass/charge ratio
Me, Et, Pr …	methyl, ethyl, propyl …
MeCN	acetonitrile
MHz	Megahertz
MLCT	Metal to Ligand Charge Transfer
MS	Mass Spectrometry
mt	methimazolyl
NLO	Non-Linear Optics
NMR	Nuclear Magnetic Resonance

PAH	Polycyclic Aromatic Hydrocarbon
Ph	phenyl
ppm	parts per million
pz	pyrazolyl
s, d, t, m …	singlet, doublet, triplet, multiplet …
TBAF	tetra-*n*-butylammonium fluoride
TBAT	tetrabutylammonium difluorotriphenylsilicate
^{t}Bu	*tert*-butyl
TFAA	trifluoroacetic anhydride
THF	tetrahydrofuran
Tm	hydrotris(methimazolyl)borate
Tp	hydrotris(pyrazolyl)borate
Tp*	hydrotris(3,5-dimethylpyrazolyl)borate
v/v	volume per volume
δ	chemical shift
Δ	reflux temperature
ν	IR band (cm^{-1})

CHAPTER 1.

INTRODUCTION

1.1 General Introduction

This body of work is primarily focused with synthetically incorporating two distinct classes of soft poly(azolyl)borate ligands which, up until now, have only received marginal attention compared to those found in existing literature. The bidentate ligand systems dihydrobis(methimazolyl)borate, (**Bm**) and dihydrobis(*N*-*tert*-butyl-5-mercaptotetrazolyl)-borate, (**Hbt**); and the analogous tridentate ligand systems hydrotris(methimazolyl)borate, (**Tm**) and hydrotris(*N*-*tert*-butyl-5-mercaptottrazolyl)borate, (**Htt**) have been utilised widely throughout the synthetic procedures herein. Where deemed to be appropriate, the more commonly encountered pyrazole-based Scorpionate ligand hydrotris(3,5-dimethylpyrazol-1-yl)borate (**Tp***) has also been used (**Figure 1.1**).

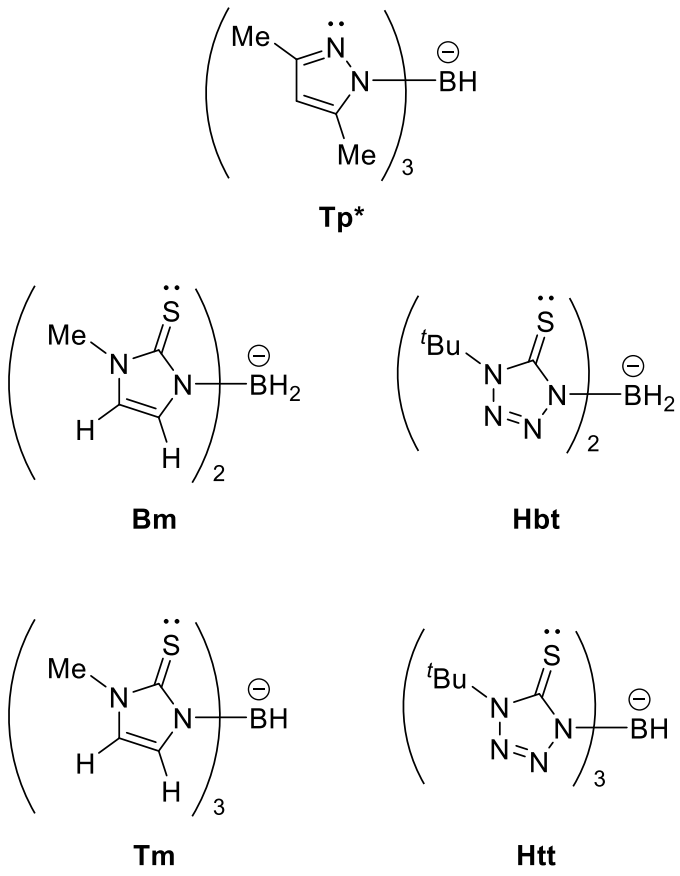

Figure 1.1. Molecular structures of **Tp***, **Bm**, **Hbt**, **Tm** and **Htt**.

Before delving into the topic of Scorpionate ligands and their chemistries, it is worthwhile noting that throughout pre-existing literature* a uniform naming and

* Numbers of which greatly surpass 2000 individual publications at the time of writing.

abbreviation system for the unambiguous description all Scorpionate ligands has never been adopted. Instead, one will often find several nomenclatures being used, even between papers published in the same journal volume! Current authors in the field are rapidly adopting the use of concise and easily understandable notations in an attempt to rectify this issue. To further promote this venture and to avoid confusion to the reader, particularly when using two- and three-letter abbreviations, the nomenclatures which have been used in this body of work have been based on abbreviations which are most commonly found in literature. Certainly, if the scope of this work was solely focused on pyrazole-based Scorpionate ligands, a detailed naming system has already been outlined by Trofimenko in his 1993 review of the topic,[1] which in itself was inspired by the work of D. Curtis and his "*very useful abbreviation*" of the hydrotris(pyrazolyl)borate ligand (see below).[2,3] With regards to methimazole-based Scorpionates, these too have been already denoted in their initial report by Reglinski and co-workers.[4] However, given that several Scorpionate ligands have been used throughout this work, some of which lack an agreed upon abbreviation, a conscious effort has been made to only refer to each ligand using the naming scheme detailed in the following paragraphs.

Scorpionates, so-called due to their preferred facially-capping coordination mode (**Figure 1.2**),[1†] were first prepared by Trofimenko in 1966 with the report of a new tridentate ligand: hydrotris(pyrazolyl)borate (**Tp**).[5]

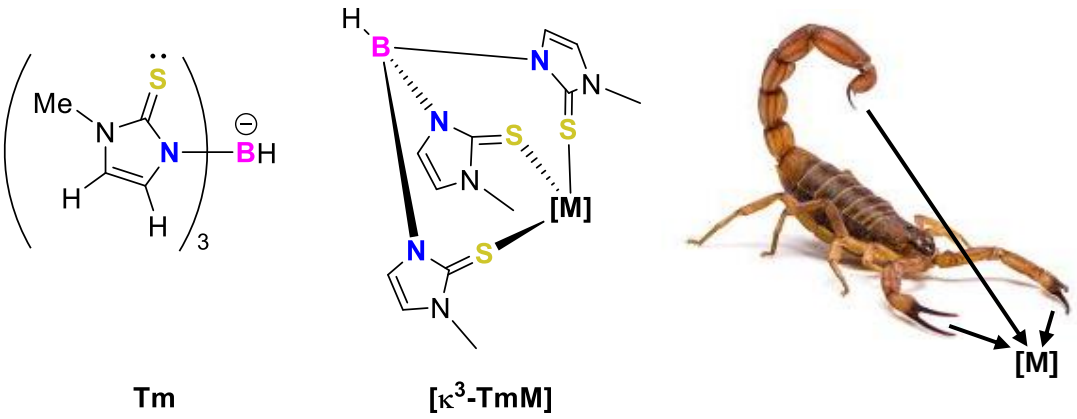

Figure 1.2. *Left*: Molecular structure of **Tm** with highlighted atoms. *Centre*: **Tm** bound to a metal center (**M**) in a facial binding mode. *Right*: Cartoon depicting a scorpion gripping a metal center and striking it with its barbed tail – giving rise to the name of this homologue, 'Scorpionate' ligands.

† Initially, Trofimenko was inspired by the South American three-toed sloth *Bradypus tridactylus* and considered referring to the series as 'Bradypate' ligands. However, upon the realization that the claws on the feet of this species curve in the same direction, the analogy of a scorpion's pincers and barbed tail were found to more appropriately depict the facial-binding mode these compounds adopt with metal centers.[6]

The report of **Tp**, along with the dimethyl-substituted hydrotris(3,5-dimethylpyrazol-1-yl)borate (**Tp***) ligand are widely regarded as the seminal examples of the first generation of Scorpionate ligands and irrespective of their age continue to be utilised in studies being carried out to this day.[6] Cyclopentadienyl ligands and tris(pyrazolyl)borates are often directly compared to one another since both are anionic, six-electron donors, which cap a face of a coordination polyhedron. However, there are incredibly significant differences between the two. For instance, cyclopentadienyl ligands can act as pi-electron acceptors while **Tp** does not possess this characteristic. With regards to the donor abilities of cyclopentadienyl ligands and **Tp**, cyclopentadienyl ligands are softer donors compared to **Tp**, which bears three σ-donating nitrogen atoms.[7] Furthermore, the drastically different topology of the two ligands allows for enhanced steric protection of the metal centre in the case of **Tp**. This has led to the utilisation of the bulky second generation of Scorpionate ligands to stabilise coordinatively unsaturated transition metal complexes.[8]

Prior to the development of Scorpionates bearing heterocyclic-bound soft donor atoms (see below), Riordan and co-workers were quick to realise the potential which the inclusion of soft donor atoms may have, particularly when attempting to gain coordinative access to low valent transition metal centres. Hence, they drew significant inspiration from Trofimenko's second generation of Scorpionates which also displayed similar characteristics. This led to the development of the first examples of monoanionic tripodal ligands bearing soft donor groups in the form of poly(thioether)borates.[9] Quickly following the initial report of the tetrakis((methylthio)methyl)borate (**RTt**) ligand,[10] attention was refocussed to the successful formation of the first tris(thioether)borates, in the form of the phenyltris(thioether)borates.[11] It is notable that since the early reports of poly(thioether)borate ligands, they have been widely modified to incorporate various coordination sites, including several examples of hybrid ligands which bear both thioether and pyrazolyl donor groups.[12,13]

Continuous expansion of the field, predominantly wrought by increasingly easy access to varied heterocyclic starting materials and simple synthetic routes, has led to the preparation of 'soft' Scorpionate ligands like **Bm**, **Tm**, **Hbt** and **Htt**, which will be the focus of the chemistry discussed throughout this body of work.

All the aforementioned ligands have the ability to coordinate to a metal centre *via* up to three donor groups. In general circumstances this can result in: the facial capping of a metal ion; the bridging of the ligand's donor groups around the meridian of the relevant

coordination polyhedron; or, as is found with some ligands, the flexibility to adopt either arrangement. In the case of Scorpionates, their coordination is limited by their rigidity and steric encumbrance which cannot be overcome to allow them to branch across the meridian of a coordination polyhedron, thereby making them exclusively facially capping ligands.

Macrocyclic, tridentate ligands bearing a set of soft [S_3] donor atoms, such as 1,4,7-trithiacyclononane,‡ have already been widely used throughout the field of organometallic chemistry.[14] Given that thioether macrocycles bear no charge, molecules of this type may not offer a commensurate graded difference from ligands such as the monoanionic [N_3]-donor, **Tp**. Hence, it is hoped that through the use of **Tm**, which also bears a negative charge, this may be a more suitable scaffold to interrogate the differences between these [N_3] and [S_3] systems.

Although it is far beyond the scope of this work, it should be noted that an even more intrinsically detailed study may be possible with the help of hybrid tripodal ligands, which bear both pyrazolyl- and methimazolyl-groups.[15,16] Furthermore, it may be appropriate to consider using Janus Scorpionates, which bear the name of the Roman god *Janus*, the god of gates and doors, who was (crucially) described as having a two-faced figure.[17–19] Hence, it is no surprise that these ligands have been referred to as hybrids of **Tp** and **Tm**,[20] and are closely related to Bailey's and Marchiò's thioxotriazolyl-borates.[15,21] Although uncommon, the series may be expanded further through the use of the [Se_3] Scorpionate donors if results prove to be promising, or if additional data is required.[22]

1.2 Methimazole-based Ligand Systems

Efforts to prepare a soft analogue of Trofimenko's pyrazolylborates were initially spurred by the search for chemical systems which could better model metalloenzymes operating in sulfur-rich environments,[23] such as proteins containing copper[24,25] and zinc,[26–30] as well as molybdenum and tungsten pterin-based proteins.[31] The framework of this new soft Scorpionate ligand was intended to broadly resemble that of the existing pyrazolylborates. Hence, a literature search commenced for an appropriate heterocycle which met the following selection prerequisites: the heterocycle must contain five atoms; a sulfur donor atom must be contained within the ring; and an acidic N–H group must be present directly

‡ Also referred to as [9]aneS_3 and 1,4,7-trithionane. CAS Registry No.: 6573-11-1.

adjacent to the sulfur atom. Surprisingly, few examples of suitable heterocycles could be sourced, nor synthesised. It was eventually realised that the heterocycle methimazole, which is duplicitously labelled as 1-methyl-2-mercaptoimidazole by chemical manufacturers, may not react as if it contains an S–H group. Instead, under normal conditions, the alternative thione-containing tautomer is the predominant structure (**Figure 1.3**).[32]

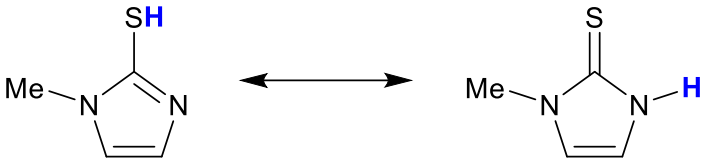

Figure 1.3. Tautomerisation of methimazole.

Armed with this new information, a new soft Scorpionate designated as '**Tm**' was successfully prepared by Reglinski and co-workers in an analogous manner to that of **Tp**, where methimazole was used in place of pyrazole to yield a tripodal [S_3] Scorpionate.[4] The original route to preparing **Tp** involved nothing more than the mixing and heating of pyrazole and an appropriate alkali-metal borohydride in the absence of solvent. When done stoichiometrically, and with careful temperature control of the reaction mixture, the di-, tri- and tetrakis(pyrazolyl)borate compounds could be selectively prepared in significant yields. Although this route was simplistic, problems associated with improper mixing and heating of the reaction often led to inhomogeneous product mixtures. Although **Tm** can also be prepared in the melt, attempts to selectively prepare less substituted variants suffered from similar issues. Given these problems could be attributed to the lack of solvent to regulate mixing and reaction temperature, a more refined route involving refluxing methimazole with an alkali-metal borohydride in xylene was established to form **Tm** (**Scheme 1.1**) so that these problems may be negated, and also allow for solvent-based methodologies to selectively prepare **Bm**.[33–37]

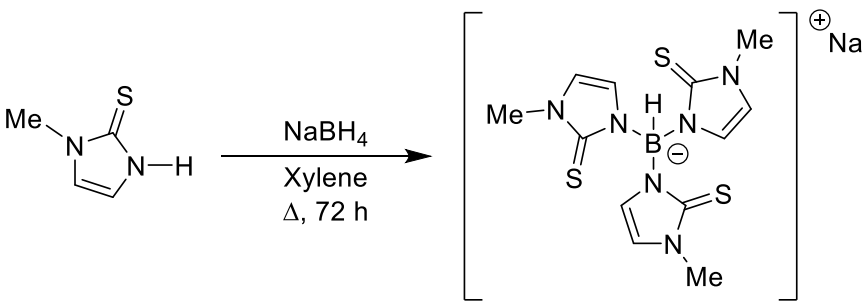

Scheme 1.1. Preparation of Na[**Tm**] using a high-boiling solvent.

Furthermore, by carrying out the above reaction at 50°C in a THF solution, it is possible to form the trihydro(methimazolyl)borate pro-ligand, which has been utilised in the study of rhenium and technetium complexes.[38] It is also noteworthy that the tetrakis(methimazolyl)borate (i.e. **mtTm**) compound is currently unknown, unlike the tetrakis(pyrazolyl)borate (**pzTp**) analogue; more than likely as a result of the rapid decomposition of methimazole[§] at the elevated temperatures required to achieve four-fold substitution around a central boron atom.[23]

By carrying out the reaction in xylene at 50°C, it is possible to access **Bm**; the bipodal [S_2] variant of **Tm**.[39,40] Coordination of **Bm** primarily occurs through both sulfur atoms (κ^2-*S*,*S*′), but additionally the borohydride hydrogens possess the ability to coordinate to a metal centre (κ^3-*S*,*S*′,*H* or κ^2-*S*,*H*) and thereby serve as a hemilabile donor. When coordinating to a metal centre, **Bm** may be described as either a four-electron donor with a negative charge located on the boron atom, or as a three-electron donor with a negative charge located on the metal centre (**Figure 1.4**).

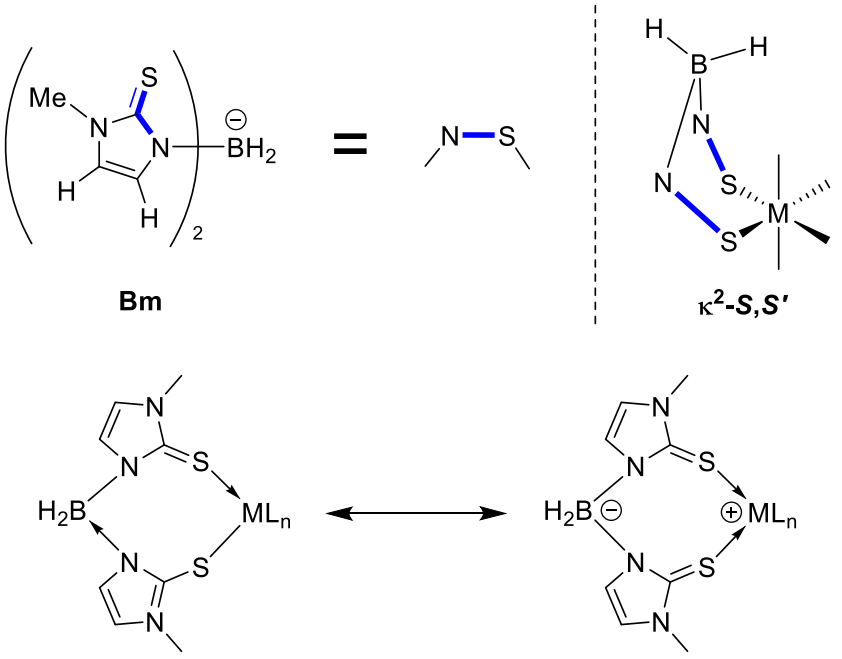

Figure 1.4. Coordination of **Bm** and its canonical forms.

Bonding descriptions become more complex once the possibility of B–H σ-bonding is considered, as this contributes a further two-electrons into the system *via* a three-centre two-electron (3c-2e) bond. Although the term *agostic* was originally used to describe C–H–M

[§] Methimazole will decompose when exposed to temperatures approaching, and in excess of, 180°C.

bonds, the B–H–M bonding observed in **Bm** chemistry has also adopted this label.[41] It is noteworthy that the earliest examples of organometallic complexes to display B–H–M bonding, namely [**Tp***Ru(R)(1,5-COD)] (R = H, Me; COD = cyclooctadiene)[42] and [{$Et_2B(pzMe_2)_2$}Mo(η^3-C_3H_5)$(CO)_2$],[43,44] both contain pyrazole-based Scorpionates (**Figure 1.5**). Interactions of this type are of significant importance in the chemistry of **Tm**, where they are deemed to be implicit in the formation of metallaboratranes.[33,45,46]

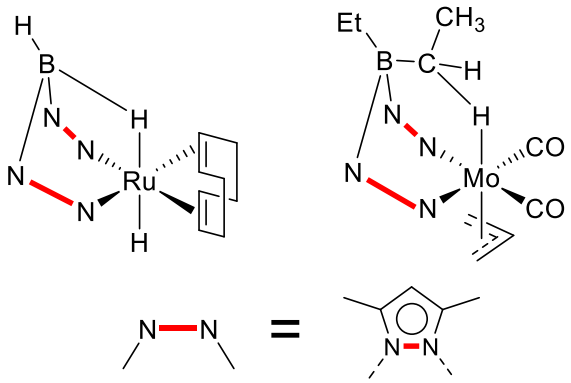

Figure 1.5. Early examples of complexes exhibiting agnostic interactions with Scorpionates.

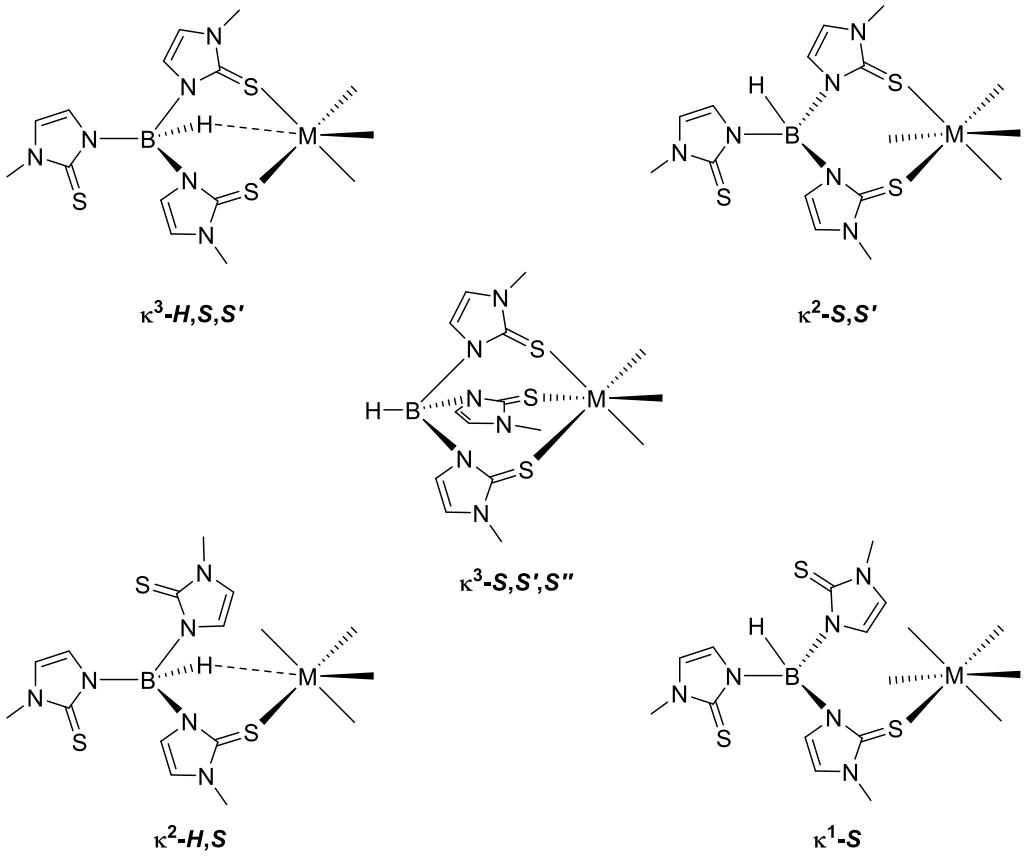

Figure 1.6. Variable binding modes of the **Tm** ligand.

The **Tm** ligand backbone contains one more atom per heterocyclic arm than **Tp**, making the overall structure less rigid and more accommodating when coordinated to a metal ion. This coordinative flexibility may be observed through the variable coordination behaviour which **Tm** exhibits, which includes bonding *via* monodentate (κ^1-*S*), bidentate (κ^2-*S*,*S*′ or κ^1-*S*,*H*), and tridentate (κ^3-*S*,*S*′,*S*″ or κ^3-*S*,*S*′,*H*) modes (**Figure 1.6**).[47,48]

Through the incorporation of this additional atom into the ligand backbone, the cage-structure which forms in **Tm** metal complexes contains eight membered chelate rings, where **Tp** (and **Tp***) form six membered chelate rings. Due to the inherent rigidity of the latter cage structure adopted by **Tp** complexes, it is quite common to find the heterocycle parallel to the nominal H-B-M axis. This is something which **Tm** ligands will very rarely exhibit.[49] Furthermore, warping of the **Tm** ligand in the solid state produces a simpler C_3 symmetry, compared to C_{3v} symmetry for **Tp** (and **Tp***) complexes (**Figure 1.7**).[7,50,51]

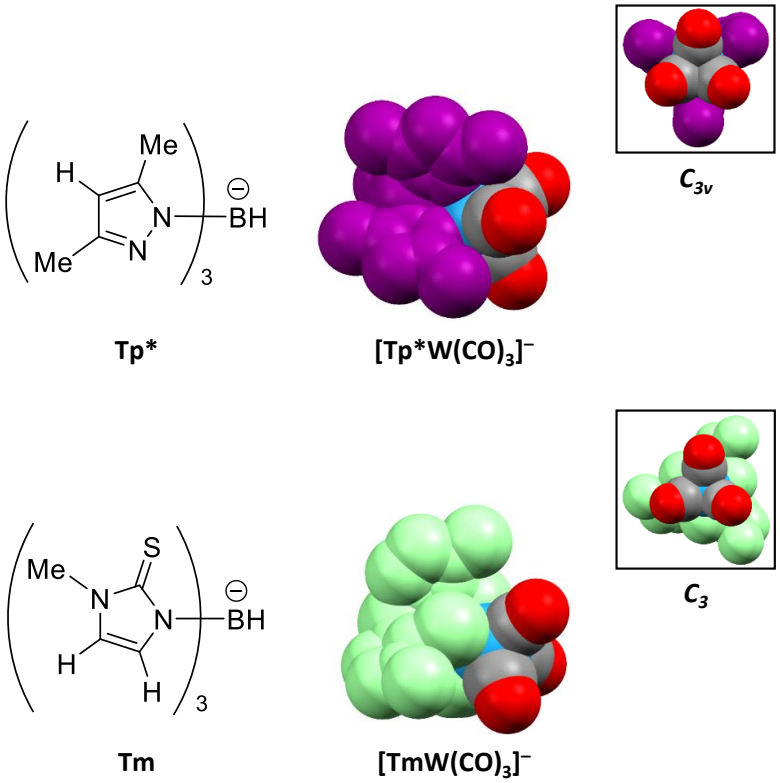

Figure 1.7. *Top*: Space-filling model of the **Tp*** ligand (magenta) bound to a {W(CO)$_3$} fragment, displaying C_{3v} crystallographic symmetry. *Bottom*: Space-filling model of the **Tm** ligand (green) bound to a {W(CO)$_3$} fragment, displaying C_3 crystallographic symmetry.

Aside from **Tp** serving as an [N$_3$] donor and **Tm** as a [S$_3$] donor, there are many other differences which may be noted about these two classes of ligands. Unlike complexes

of **Tp**, materials ligated with **Tm** tend to contain electron-rich, low-valent transition metals,[23] and display a greater susceptibility to oxidation: something which will be briefly discussed in later chapters. Also, by recalling the analogy that N-donors are harder that S-donors, this simple principle was affirmed when the reactivities of these two ligand systems were directly compared. The best manifestation of this phenomena, which shows that **Tp** exerts a stronger field strength that **Tm**, has been exemplified through the studies of the iron complexes [Fe(**Tm**)$_2$][52] and [Fe(**Tp**)$_2$].[53]

The *exo*-CH_3 groups on the **Tm** heterocycle point outwards, away from the metal ion; thereby allowing any incoming reactant greater access to the metal centre than with **Tp** or **Tp***. However, where bulky R-substituents (e.g. *t*Bu, Ph) are bound to the heterocyclic backbone of **Tm** (**Figure 1.8**),[**] as is the case in much of the work championed by Parkin,[54–57] these bulky variants of **Tm** afford several discontinuities between their predicted and observed reactivities during metal-binding studies.

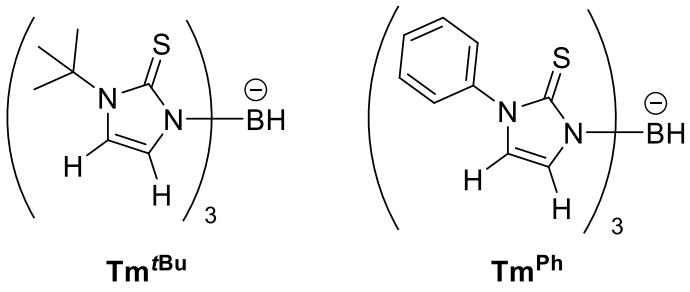

Tm$^{t\mathbf{Bu}}$ **Tm**$^{\mathbf{Ph}}$

Figure 1.8. *Left*: Molecular structure of **Tm**$^{t\mathbf{Bu}}$. *Right*: Molecular structure of **Tm**$^{\mathbf{Ph}}$.

For instance, there have been results published surrounding the formation of **Tm**$^{t\mathbf{Bu}}$ complexes of gallium[58] and indium[59] which show that these species are more than capable of forming sandwich-type complexes. Conversely, it has been established that **Tp**$^{t\mathbf{Bu}}$ complexes of gallium[60] and indium[61] are almost ideal for supporting mono-valent complexes consisting of only one coordinatively bound **Tp**$^{t\mathbf{Bu}}$ ligand. Prior to these types of comparative studies, transposition of the data which was obtained for **Tp** onto **Tm** was attempted on numerous occasions. However, the differences which are listed above serve as strong evidence for each ligand to be treated independently of one another, and that any direct comparison between the two may not be as consonant as initially thought.

[**] In many texts, the R-group bound to the heterocyclic N-atom on the **Tm** ligand backbone is denoted using the notation: **Tm**$^{\mathbf{R}}$. For example, **Tm**$^{\mathbf{Me}}$, **Tm**$^{t\mathbf{Bu}}$, **Tm**$^{\mathbf{Ph}}$, etc. In principle, this type of notation may be applied to any Scorpionate ligand, but, as discussed earlier in the chapter, there remains no consensus on the matter.

Our interests in soft Scorpionate ligands lie with their use in early transition metal alkyne complexes. Based on conventional Hard-Soft Acid-Base (HSAB) theory it would be trivial to assign the softer transition metals as preferred binding partners for **Tm**. However, in our work thus-far it has been our aim to form **Tm** complexes with harder, early transition metals; with particular focus on the use of those in group 6 of the periodic table. At a first glance this might appear to be a difficult undertaking, but this is not a new concept. For instance, Stone exploited the face-capping nature of singly-deboronated *ortho*-carboranes, considered to be isolobal with cyclopentadienyl ligands, to form tungsten-alkyne complexes (**Figure 1.9**) some thirty-years prior to the writing of this report.[62]

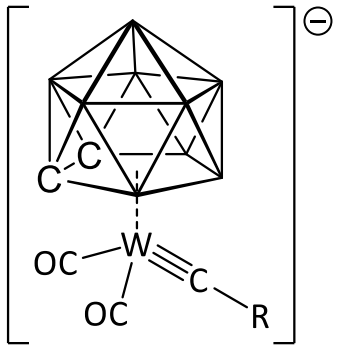

Figure 1.9. Example of a tungsten-alkyne complex formed by Stone. Each unlabelled vertex on the carborane cage bears a {BH} fragment. Hydrogen atoms have been omitted for clarity.

Furthermore, many recent publications have highlighted the broad utility of soft Scorpionates in the formation of propargylidyne, tricarbido, and metallacarbyne species, much of which will be discussed in detail in later chapters. However, some of the more significant milestones in soft Scorpionate chemistry involving group 6 transition metals have been included in the following paragraphs.

The first examples of **Tm** group 6 organometallic complexes, [**Tm**Mo(CO)$_2$(η-C$_3$H$_5$)] and [**Tm**WI(CO)$_3$], were reported in 2001 by Reglinski and co-workers (**Scheme 1.2**).[63] By utilising easily accessible [M(CO)$_3$(NCMe)$_3$] (M = Mo, W) starting materials, these complexes were combined with Na[**Tm**] at elevated temperatures in order to purportedly form Na[**Tm**M(CO)$_3$] salts. Although these particular salts were not isolated during this study, the analogous pyrazole-based Scorpionate salts of this type have been formed and successfully utilised to form numerous molybdenum and tungsten complexes.[1,44] Through the addition of allylic halides and iodine, the Na[**Tm**M(CO)$_3$] intermediates were converted

into the desired materials, where both were found to bear a **Tm** ligand in the κ^3-*S*,*S*′,*S*″ bonding mode.

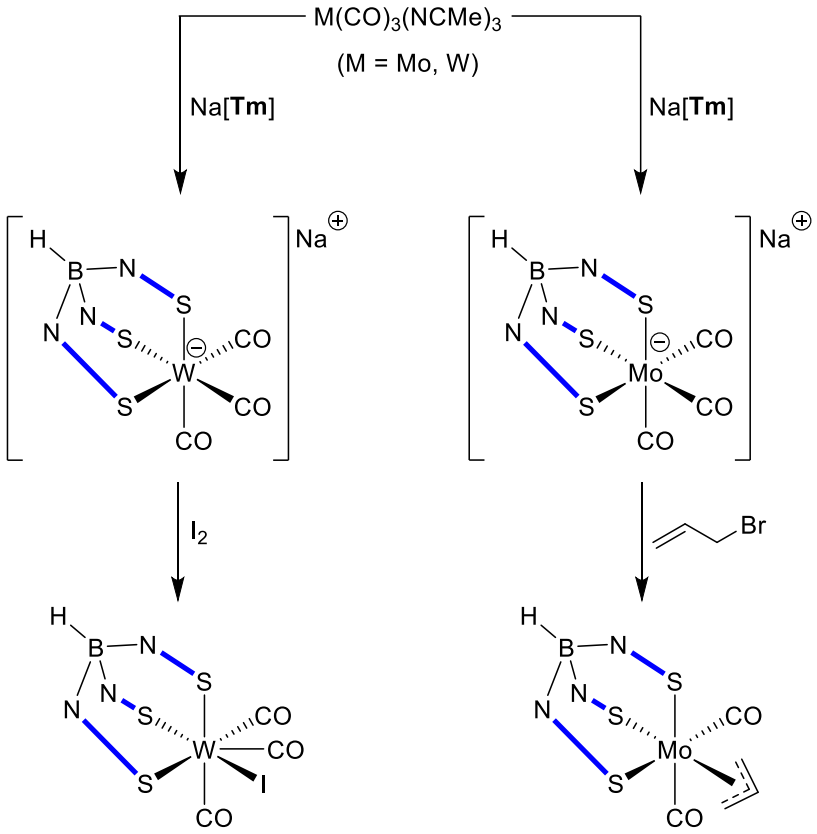

Scheme 1.2. Synthesis of [**Tm**WI(CO)$_3$] and [**Tm**Mo(CO)$_2$(η-C$_3$H$_5$)].

More recently, various tungsten and molybdenum alkylidyne (carbyne) complexes bearing poly(methimazolyl)borate ligands have been prepared by Hill and co-workers. Such complexes were initially targeted due to the belief that alkylidyne complexes co-ligated with the **Tm** ligand may be prone to hydrogen migrations, similar to those observed in the formation of a transannular dative (polar covalent, Z-type[64], M→B) bond, a characteristic feature in metallaboratranes (**Scheme 1.3**).[65]

However, unlike in the case of metallaboratrane formation, there was a likelihood that the hydrogen atom would either: migrate to the alkylidyne ligand, thereby forming an alkylidene; or, undergo α-addition to the alkylidyne carbon, much like the reports made by Stone during his work into alkylidyne hydroboration.[66–70]

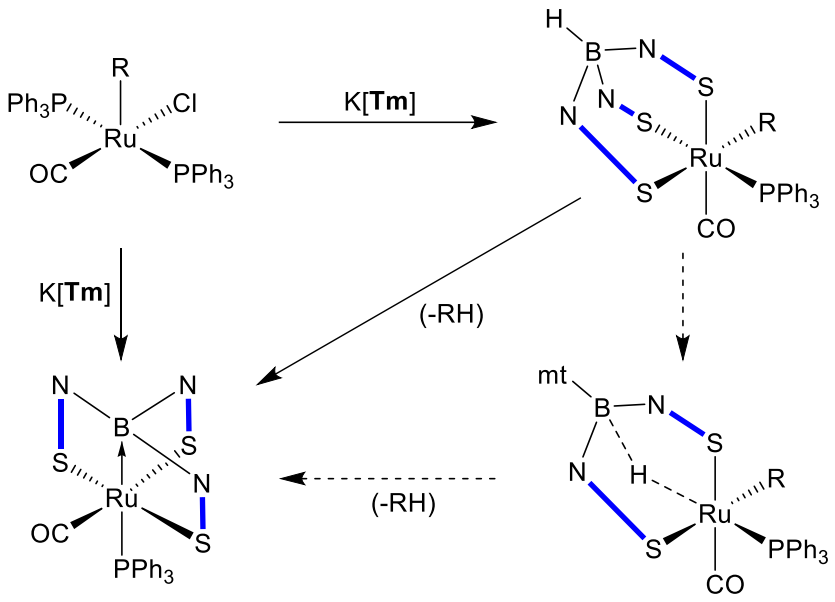

Scheme 1.3. Hydrogen migration leading to the formation of the first metallaboratrane (R = $HC{=}CH_2$,

Although the desired activation of the borohydride hydrogen atom was not observed in the initial study by Hill and co-workers, in their second publication on the topic of organometallic complexes co-ligated with poly(methimazolyl)borate ligands they were more successful.[71] Amongst other similar complexes, a thiocarbamoyl (thiocarboxamide) molybdenum complex bearing the **Bm** ligand was formed through the reactions of molybdenum salt Na[**Bm**$Mo(CO)_3$] and Me_2NCSCl, as well as the reaction of [$Mo(\eta^2$-$SCNMe_2)Cl(CO)_2$(tmeda)] (tmeda = tetramethylenediamine) with Na[**Bm**]. The resulting [**Bm**$Mo(\eta^2$-$SCNMe_2)(CO)_2$] complex was shown to contain an agostic B–H–Mo interaction, unequivocally resolved through single-crystal X-ray crystallography.

Further curios have been reported using poly(methimazolyl)borate ligands to form molybdenum stannyl complexes.[72,73] Such complexes were prepared through two complimentary strategies involving the oxidative addition of either [**Bm**$SnMe_2$] or [**Tm**$SnPh_3$] to various molybdenum(0) precursors, or *via* reactions of halostannanes with the salts Na[$Mo(CO)_3\{H_\chi B(mt)_{4-\chi}\}$] ($\chi$ = 1, 2; mt = methimazolyl).

Finally, and most recently, in work which will be further described in Chapter 3, various Scorpionate ligands have been utilised in the preparation of anthracenyl-carbyne species.[74,75] With the inclusion of polycyclic aromatic hydrocarbons into conjugated carbyne frameworks, there is a possibility that the complexes which are formed may contain notable electro- photo- and chemi-luminescent properties.[76,77]

From the information which has been detailed in the previous paragraphs, it is obvious that there has been, and there remains to be, an avid interest in the organometallic and coordination chemistry surrounding soft Scorpionate ligands. However, what might be less obvious is the ever-growing field of soft (and hard) Scorpionate ligands and their incorporation with main-group elements from the p-block. For those interested in this topic, readers are directed to a comprehensive 2015 review published by Reglinski and Spicer.[78] However, a few notable examples have been selected for discussion below.

Of the group 14 elements, it is arguable that tin provides some of the most interesting complexes with **Tm**. A series of tin complexes with the empirical formulae [Sn(**Tm**)Cl_2R], [Sn(**Tm**)R_2Cl], and [Sn(**Tm**)R_3] were prepared through the combination of K[**Tm**] with [$RSnCl_3$], [R_2SnCl_2], or [R_3SnCl], respectively.[79] Of all the various compounds which were formed, the tricyclohexyl-variant [Sn(**Tm**)Cy_3] was shown contain the first crystallographically resolved κ^1-**Tm** ligand (**Figure 1.10**).

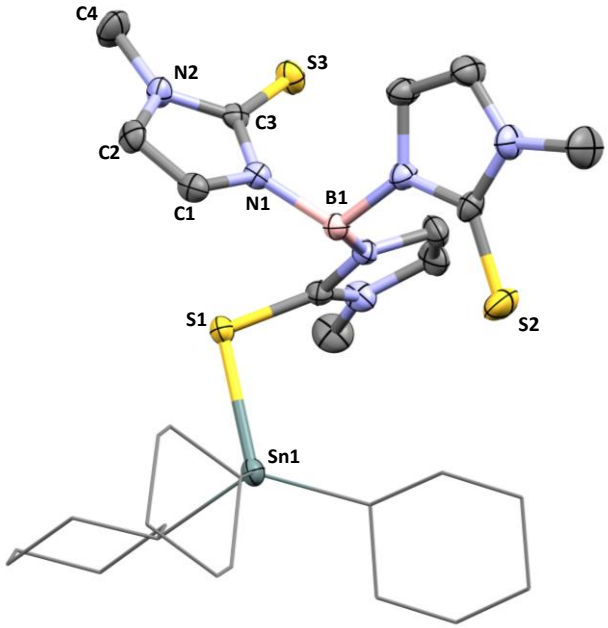

Figure 1.10. Single-crystal X-ray diffraction structure of [Sn(**Tm**)Cy_3][79] (50% displacement ellipsoids) with selected atom labels. Solvent molecules and hydrogen atoms omitted for clarity. CCDC reference number 171597.

A phenyl analogue of the form [Sn(**Tm**)Ph_3] was also prepared in a separate study by Lloyd and co-workers, which also displayed the κ^1-**Tm** binding mode.[80,81] Although Sn(IV) complexes are generally four-coordinate, the mixed alkyl-/aryl- and chloro-tin species of the

type [$R_nSnCl_{(4-n)}$] have the ability to expand their coordination numbers to five and six, depending on the substituents bound to the tin atom.

Purely alkyl-/aryl-tin complexes show no tendency to expand past coordination numbers of four. However, as the R-groups are substituted for chloride ligands, chloro-tin complexes display an increasing propensity towards forming six coordinate complexes due to the increased Lewis acidity of the tin centre, invoked by the surrounding electronegative chloro-ligands. In the case of **Tp** chemistry, this phenomena was exploited in order to form the first example of a six coordinate tin species, [Sn(**Tp**)Me_3], through the reaction of K[**Tp**] and [Me_3SnCl].[82,83]

Examples of **Tm** compounds formed with members of group 15 of the periodic table are known for phosphorus, arsenic, antimony, and bismuth. Within this series there is a marked difference between the reactivities observed between its lightest (P) and heaviest (Bi) congeners. In the case of the former, phosphorus does not exhibit any coordination chemistry with **Tm**, something which may be thought of as atypical amongst the **Tm** chemistry discussed previously. Nevertheless, variants of the **Tm** ligand have been successfully reacted with some phosphorus compounds. For example, reaction of $\mathbf{Tm^{Ph}}$ with PI_3 results in the formation of an unprecedented monocationic heterocyclic species (**Figure 1.11**).

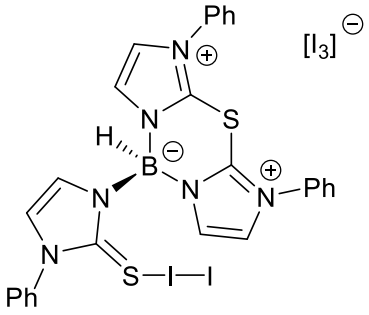

Figure 1.11. The novel heterocycle formed from the reaction of $\mathbf{Tm^{Ph}}$ with PI_3.

It was speculated that such a process may occur through the degradation of PI_3 into iodine and the triiodide anion. Having noted that Crossley and co-workers had previously reported that the **Tm** ligand scaffold may be predisposed towards the intramolecular formation of polycyclic rings,[84] Reglinski and co-workers made dedicated efforts to expand this area of chemistry. The initial step of the heterocycle-forming process is thought to involve coordination of an electrophilic species to one of the methimazole thione groups.

Recalling the work carried out into the S-alkylation of **Tm**,[85] in which it was established that two thione moieties of **Tm** are oriented *syn* with respect to the B–H bond, and the third methimazole ring is oriented away from the others, it was assumed that this arrangement may once again be true for this system. Using this assumption, it was possible to suggest a feasible three-step ring-closure mechanism (**Scheme 1.4**). Once formed, any remaining I_2 coordinates to the remaining unreacted thione moiety, and the $[I_3]^-$ acts as a suitable counterion to stabilise the formally monocationic species.

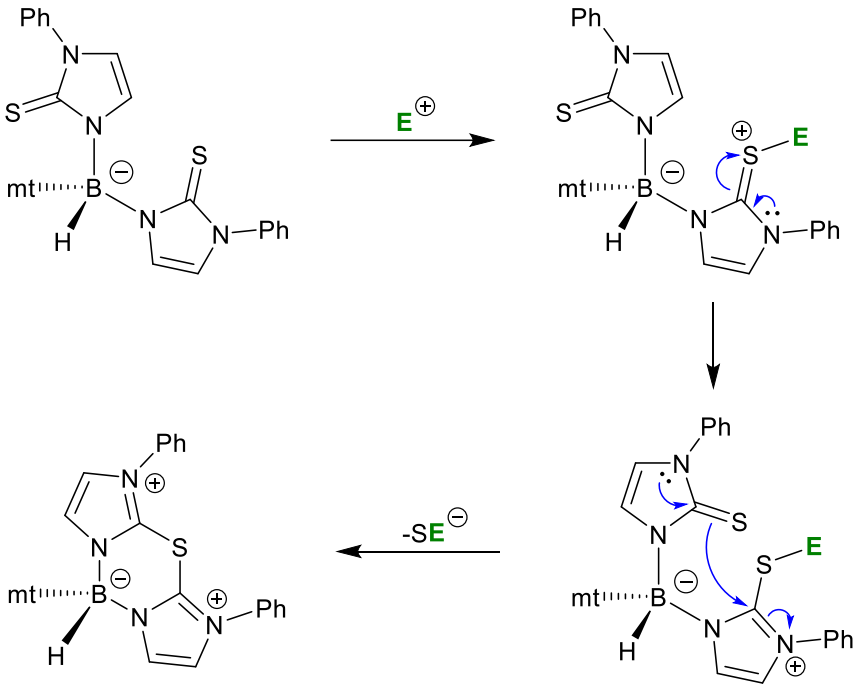

Scheme 1.4. Proposed cyclisation mechanism for **Tm^{Ph}** (E = I; mt = methimazolyl). Counterion omitted for clarity.

The **Tm** chemistry of bismuth, the heaviest of the selected congeners from group 15, could not be any more different to that of phosphorus. Out of all the elements which have been successfully combined with **Tm**, bismuth complexes were some of the first to be prepared. In the first report of its kind,[86] bismuth was specifically selected by experimenters due to its large charge (+3) and its relatively large cation radius in the hope that a combination of these factors would aid in the binding of multiple **Tm** ligands. In doing so, this would potentially allow them to display many of the variable binding modes which have been previously described for **Tm**.

However, the results obtained from these studies were far from straightforward. The combination of three equivalents of Na[**Tm**] with $BiCl_3$ produced a bulk solid with the

spectral characteristics consistent with those of [**Tm**$_2$BiCl], but once structurally analysed *via* single crystal X-ray diffraction the dimeric **Tm** complex [Bi(**Tm**)Cl(μ_2-Cl)]$_2$ was shown to be present. Intrigued by the differences indicated above, an empirical approach was chosen to resolve the ambiguity which existed in this newly formed material. The addition of two equivalents of Na[**Tp**] to the bulk "[**Tm**$_2$BiCl]" solid afforded the highly unusual and unprecedented mixed-Scorpionate salt [**Tm**$_2$Bi][**Tp**$_2$Na]. Later, studies focussed on the preparation of organobismuth complexes bearing the larger **Tm**$^{t\mathbf{Bu}}$ ligand. This larger variant of **Tm** was selected due to its increased ability to stabilise alkylbismuth complexes. Through this additional stability, **Tm**$^{t\mathbf{Bu}}$ was successfully utilised to form the analogous complex [Bi(**Tm**$^{t\mathbf{Bu}}$)Cl(μ_2-Cl)]$_2$, as well as [(Me$_2$Bi)$_3$(**Tm**$^{t\mathbf{Bu}}$)$_2$][Me$_2$BiCl$_2$].[87] The latter complex was characterised *via* single crystal X-ray diffraction and was shown to contain the first example of a **Tm**$^{t\mathbf{Bu}}$ complex with M$_3$(μ_3-η^1:η^1:η^1-L)$_2$ structure (**Figure 1.12**).

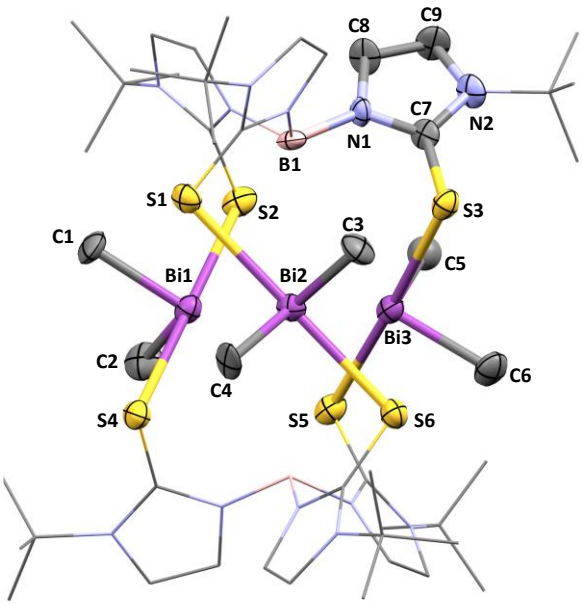

Figure 1.12. Single-crystal X-ray diffraction structure of [(Me$_2$Bi)$_3$(**Tm**$^{t\mathbf{Bu}}$)$_2$][Me$_2$BiCl$_2$][87] 50% displacement ellipsoids) with selected atom labels. Solvent molecules and hydrogen atoms omitted for clarity. CCDC reference number 236753.

For those researchers whose interests span further than just pure synthetic organometallic chemistry, many were quick to realise the potential this new homologue of soft Scorpionates may possess, and how they may be utilised in various applied roles. For example, it was quickly realised that soft Scorpionates may have potential use in modelling various bioinorganic systems.

In the same way that relevant **Tp** complexes have been successfully used to model the active-sites of zinc enzymes in hard, nitrogen-rich environments,[88,89] **Tm** has been utilised to model similar zinc enzymes, but instead in soft, sulfur-rich environments; as well as other bioinorganic systems.[90] It is noteworthy that the use of alkyne-decorated molybdenum sites by nitrogenase enzymes may have some overlap with our current work.[91]

Other uses for **Tm** complexes have been widely speculated. By exploiting the C_3 symmetry of such complexes, and their resulting atropisomerism caused by the restricted rotation about the three-dimensional cage-structure (**Figure 1.13**) they may find uses in asymmetric catalysis[50,92] in a similar manner to BINAP[93–95] and BINOL[93,96,97] which also display atropisomerism. However, it should be noted that at the time of preparing this report this type of application has not been described in literature.

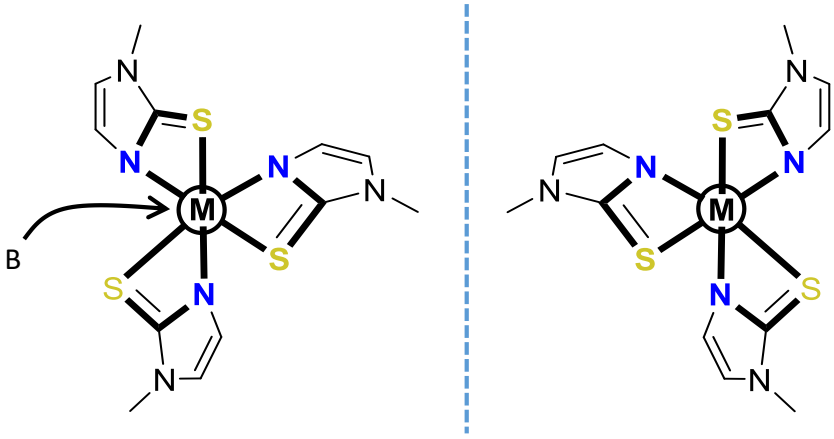

Figure 1.13. Due to the restricted rotation around the M-B-H axis caused by the cage-like structure of **Tm**, two atropisomers are formed. Viewed down the M-B-H axis; B-H eclipsed by the metal centre.

More recently, Scorpionates have been widely used in the progression of technetium chemistry, where they have been investigated for their ability to act as new diagnostic radiopharmaceuticals as imaging agents.[98] Furthermore, interest in the coordinative properties of certain Scorpionate complexes has led to the formation of surface-mounted molecular gears and motors,[99] as well as other surface-related studies using soft Scorpionate ligands, such as **Tm**, to chemisorb onto gold and silver surfaces.[100]

1.3 *N*-*t*butyl-5-mercaptotetrazole-based Ligand Systems

Compared to the work which has been carried out on the **Tm** and **Bm** ligand systems, the study of *N*-*tert*-butyl-5-mercaptotetrazole-based ligands such as **Htt** and **Hbt**

are only in their infancy. Inspired by the report by Cao and co-workers that the compound $Na[H_2B(tt^{Me})_2]$ (tt^{Me} = *N-methyl*-5-mercaptotetrazol-1-yl) had been successfully reacted with nickel acetate to form $[Ni\{\kappa^2\text{-}H,S,S'\text{-}H_2B(tt^{Me})_2\}_2]$,[101] Hill and co-workers were quick to recall Rabinovic's earlier reports of the near-isostructural complex $[Ni\{\kappa^2\text{-}H,S,S'\text{-}H_2B(mt^{Me})_2\}_2]$.[102,103] In turn, this led to Hill commencing efforts to form the previously documented, but rarely utilised, *N-tert*-butyl-5-mercaptotetrazole heterocycle, and subsequently form the pro-ligand salts $Na[H_2B(tt^{tBu})_2]$ and $Na[HB(tt^{tBu})_3]$ (tt^{tBu} = *N-t-butyl*-5-mercaptotetrazol-1-yl); Na[**Hbt**] and Na[**Htt**], respectively.[104] Preparation of the heterocyclic starting material was carried out in good yields by reacting sodium azide with *tert*-butylisothiocyanate in refluxing ethanol, as per the previous independent reports by Quast[105] and Aïssa.[106] Once isolated, and much like **Bm** and **Tm**, the heterocycle was added in stoichiometric quantities along with sodium borohydride and the mixture heated in refluxing THF or xylene to afford Na[**Hbt**] or Na[**Htt**], respectively (**Scheme 1.5**).

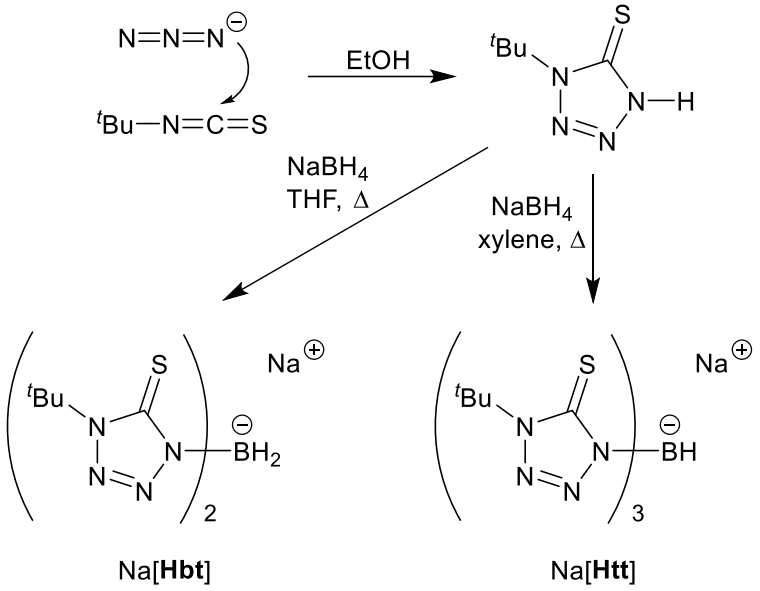

Scheme 1.5. Preparation of Na[**Hbt**] and Na[**Htt**].

In a similar manner to the synthesis of the first metallaboratrane, which utilised the **Tm** ligand in order to form the characteristic transannular M→B bond, pro-ligands **Hbt** and **Htt** have been used to form double- (diptych) and triple-buttressed (triptych) ruthenium metallaboratranes (ruthenaboratranes), respectively. In turn, these serve as the first examples of mercaptotetrazolyl-supported metallaboratranes. Reaction of $[RuCl(Ph)(CO)(PPh_3)_2]$[107] with Na[**Htt**] in either THF or CH_2Cl_2 affords the ruthenaboratrane $[Ru(CO)(PPh_3)(\mathbf{Htt})]$ *(Ru→B)*, where the Scorpionate adopts a κ^4-(*B,S,S',S''*) binding mode (**Scheme 1.6**).

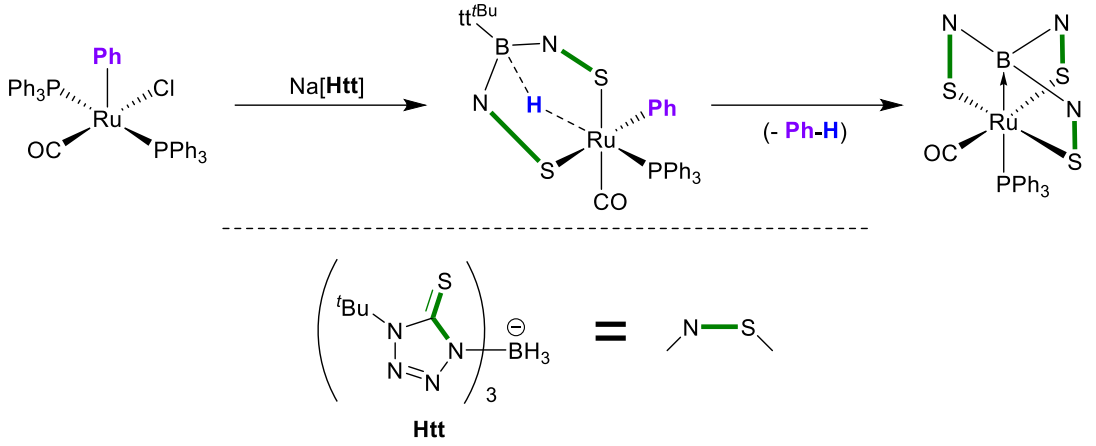

Scheme 1.6. Preparation of [Ru(CO)(PPh_3)(κ^4-*B*,*S*,*S*′,*S*″-**Htt**)] (tt^{tBu} = *N*-*tert*-butyl-5-mercaptotetrazol-1-yl)

Of all the metallaboratrane complexes which have been formed the majority of them are of the triptych variety. However, amongst this concise library of complexes, a small number of diptych metallaboratranes are known, and in some notable circumstances even form preferentially when a third bridging heterocycle is available. The first report of a diptych metallaboratrane serves as an exemplar of this type of behaviour, since Vaska's complex [IrCl(CO)(PPh_3}$_2$] was combined with Na[**Bm**] and Na[**Tm**] and both mixtures afforded the same diptych metallaboratrane: [IrH(CO)(PPh_3){κ^3-*B*,*S*,*S*′-BR'(mt)$_2$}] (R' = H or mt, depending on whether the reaction mixture contained Na[**Bm**] or Na[**Tm**], respectively; mt = methimazolyl).[108,109]

Through work carried out by Parkin and co-workers, the bulkier **Tm**^{tBu} and **Tm**^{Ph} pro-ligands have been successfully used to replicate these observations. By once again employing Vaska's complex [IrCl(CO)(PPh_3}$_2$], it was combined with M[**Tm**^{tBu}] (M = Tl, K) and Li[**Tm**^{Ph}] to form analogous iridaboratranes, which similarly featured either a pendant hydride or mt^R arm.[54]

Aside from the fact that diptych metallaboratrane structures are a rarity, there are other reasons for their continued investigation. For instance, triptych metallaboratranes contain *tricyclo*-[3.3.3.0] cage-like structures which severely inhibits the freedom of the boron atom. However, where diptych metallaboratranes form, the cage-like structure which they adopt may be described as a *bicyclo*-[3.3.0] arrangement. Crucially, if the metal-boron M→B interaction were to be sufficiently weak, this may allow the boron atom to dissociate in a

hemilabile fashion and participate in intermolecular bonding processes. Hence, this area of work remains to be of great interest to many researchers.

Using the **Hbt** pro-ligand, Hill and co-workers have recently been able to form two new examples of diptych metallaboratranes built around an iridium and a ruthenium centre. The former complex was prepared through the combination of Vaska's complex with Na[**Hbt**] in CH_2Cl_2 to afford [IrH(CO)(PPh_3){κ^3-*B*,*S*,*S*′-**Hbt**}] in modest yields. The complex was successfully characterised *via* single-crystal X-ray diffraction as well as through conventional spectroscopic techniques.

The ruthenaboratrane complex [Ru(CO)(PPh_3)$_2${κ^3-*B*,*S*,*S*′-**Hbt**}] was also prepared as well as the intermediate complex [Ru(Ph)(CO)(PPh_3){κ^3-*H*,*S*,*S*′-**Hbt**}]. Through hydride migration onto the phenyl substituent, thereby forming benzene which is eliminated from the complex, the intermediate is converted in to the ruthenaboratrane complex over a period of twenty-four hours.

1.4 Chapter 1 - References

1. Trofimenko, S., *Chem. Rev.*, **1993**, *93*, 943.
2. Curtis, M. D., Shiu, K. B., Butler, W. M., *Organometallics*, **1983**, *2*, 1475.
3. Curtis, M. D., Shiu, K. B., Butler, W. M., *J. Am. Chem. Soc.*, **1986**, *108*, 1550.
4. Reglinski, J., Garner, M., Cassidy, I. D., Slavin, P. A., Spicer, M. D., Armstrong, D. R., *J. Chem. Soc., Dalton Trans.*, **1999**, *13*, 2119.
5. Trofimenko, S., *J. Am. Chem. Soc.*, **1966**, *88*, 1842.
6. Trofimenko, S., *Polyhedron*, **2004**, *23*, 197.
7. Schwalbe, M., Andrikopoulos, P. C., Armstrong, D. R., Reglinski, J., Spicer, M. D., *Eur. J. Inorg. Chem.*, **2007**, *10*, 1351.
8. Smith, J. M., *Comments on Inorganic Chemistry*, **2008**, *29*, 189.
9. Riordan, C. G., *Coord. Chem. Rev.*, **2010**, *254*, 1815.
10. Ge, P., Haggerty, B. S., Rheingold, A. L., Riordan, C. G., *J. Am. Chem. Soc.*, **1994**, *116*, 8406.
11. Riordan, C. G., Ge, P., Ohernberg, C., Liaw, W.-F., *Inorg. Synth.*, **1998**, *32*, 108.
12. Chiou, S.-J., Ge, P., Riordan, C. G., Liable-Sands, L. M., Rheingold, A. L., *Chem. Commun.*, **1999**, 159.
13. Ruth, K., Tüllmann, S., Vitze, H., Bolte, M., Lerner, H.-W., Holthausen, M. C., Wagner, M., *Chem. Eur. J.*, **2008**, *14*, 6754.
14. Blake, A. J., Schröder, M., *Advances in Inorganic Chemistry*, **1990**, *35*, 1.
15. Bailey, B. J., Lanfranchi, M., Marchiò, L., Parsons, S., *Inorg. Chem.*, **2001**, *40*, 5030.
16. Owen, G. R., Gould, P. H., Charmant, J. P. H., Hamilton, A., Saithong, S., *Dalton Trans.*, **2010**, *39*, 392.
17. Silva, R. M., Gwengo, C., Lindeman, S. V., Smith, M. D., Gardinier, J. R., *Inorg. Chem.*, **2006**, *45*, 10998.
18. Silva, R. M., Gwengo, C., Lindeman, S. V., Smith, M. D., Long, G. J., Grandjean, F., Gardinier, J. R., *Inorg. Chem.*, **2008**, *47*, 7233.
19. Dyson, G., Hamilton, A., Mitchell, B., Owen, G. R., *Dalton Trans.*, **2009**, *31*, 6120.
20. Imran, M., Neumann, B., Stammler, H.-G., Monkowius, U., Ertl, M., Mitzel, N. W., *Dalton Trans.*, **2013**, *42*, 15785.
21. Cammi, R., Gennari, M., Giannetto, M., Lanfranchi, M., Marchiò, L., Mori, G., Paiola, C., Pellinghelli, M., A., *Inorg. Chem.*, **2005**, *44*, 4333.
22. Minoura, M., Landry, V. K., Melnick, J. G., Pang, K., Marchiò, Parkin, G., *Chem. Commun.*, **2006**, 3990.
23. Spicer, M. D., Reglinski, J., *Eur. J. Inorg. Chem.*, **2009**, *12*, 1553.
24. Kitajima, N., Moro-oka, Y., *Chem. Rev.*, **1994**, *94*, 737.
25. Tolman, W. B., *J. Biol. Inorg. Chem.*, **2006**, *11*, 261.

26. Han, R., Looney, A., McNeill, K., Parkin, G., Rheingold, A. L., Haggerty, B. S., *J. Biol. Inorg. Chem.*, **1993**, *49*, 105.

27. Vahrenkamp, H., *Acc. Chem. Res.*, **1999**, *32*, 589.

28. Parkin, G., *Chem. Commun.*, **2000**, 1971.

29. Parkin, G., *Chem. Rev.*, **2004**, *104*, 699.

30. Parkin, G., *New. J. Chem.*, **2007**, *31*, 1996.

31. Young, C. G., Wedd, A. G., *Chem. Commun.*, **1997**, 1251.

32. Garner, M., Armstrong, D. R., Reglinski, J., Smith, W. E., Wilson, R., McKillop, J. H., *Bioorganic & Medicinal Chemistry Letters*, **1994**, *4*, 1357.

33. Hill, A. F., Owen, G. R., White, A. J. P., Williams, D. J., *Angew. Chem. Int. Ed.*, **1999**, *38*, 2759.

34. Kimblin, C., Bridgewater, B. M., Churchill, D. G., Parkin, G., *Chem. Commun.*, **1999**, 2301.

35. Santini, C., Lobbia, G. G., Pettinari, C., Pellei, M., Valle, G., Calogero, S., *Inorg. Chem.*, **1998,** *37*, 890.

36. Soares, L. F., Silva, R. M., Doriguetto, A. C., Ellena, J., Mascarenhas, Y. P., Castellano, E. E., *J. Braz. Chem. Soc.*, **2004**, *15*, 695.

37. Soares, L. F., Silva, R. M., *Inorg. Synth.*, **2002**, *33*, 199.

38. Maria, L., Paulo, A., Santos, I. C., Kurz, P., Spingler, B., Alberto, R., *J. Am. Chem. Soc.*, **2006**, *128*, 14590.

39. Kimblin, C., Bridgewater, B. M., Hascall, T., Parkin, G., *J. Chem. Soc., Dalton Trans.*, **2000**, 891.

40. Kimblin, C., Hascall. T., Parkin, G., *Inorg. Chem.*, **1997**, *36*, 5680.

41. Brammer, L., *Dalton Trans.*, **2003**, 3145.

42. Albers, M. O., Crosby, S. F. A., Liles, D. C., Robinson, D. J., Shaver, A., Singleton, E., *Organometallics*, **1987**, *6*, 2014.

43. Cotton, F. A., LaCour, T., Stainislowski, A. G., *J. Am. Chem. Soc.*, **1974**, *96*, 754.

44. Trofimenko, S., *Inorg. Chem.*, **1970**, *9*, 2493.

45. Foreman, M. R. St.-J., Hill, A. F., Owen, G. R., White, A. J. P., Williams, D. J., *Organometallics*, **2003**, *22*, 4446.

46. Foreman, M. R. St.-J., Hill, A. F., White, A. J. P., Williams, D. J., *Organometallics*, **2004**, *23*, 913.

47. Dodds, C. A., Garner, M., Reglinski, J., Spicer, M. D., *Inorg. Chem.*, **2006**, *45*, 2733.

48. Nuss, G., Ozwirk, A., Harum, B. N., Saischek, G., Belaj, F., Mösch-Zanetti, N. C., *Eur. J. Inorg. Chem.*, **2012**, 4701.

49. Steel, G., Rajasekharan-Nair, R., Stepek, I. A., Kennedy, A. R., Reglinski, J., Spicer, M. D., *Eur. J. Inorg. Chem.*, **2016**, 2409.

50. Bailey, P. J., Dawson, A., McCormack, C., Moggach, S. A., Oswald, I. D. H., Parsons, S., Rankin, D. W. H., Turner, A., *Inorg. Chem.*, **2005**, *44*, 8884.

51. Bailey, P. J., McCormack, C., Parsons, S., Rudolphi, F., Perucha, A. S., Wood, P., *Dalton Trans.*, **2007**, 476.

52. Garner, M., Lewinski, K., Pattek-Janczk, A., Reglinski, J., Sieklucka, B., Spicer, M. D., Szaleniec, M., *Dalton Trans.*, **2003**, 1181.

53. Jesson, J. P., Trofimenko, S., Eaton, D. R., *J. Am. Chem. Soc.*, **1967**, *89*, 3158.

54. Landry, V. K., Melnick, J. G., Buccella, D., Pang, K., Ulichny, J. C., Parkin, G., *Inorg. Chem.*, **2006**, *45*, 2588.

55. Figueroa, J. S., Melnick, J. G., Parkin, G., *Inorg. Chem.*, **2006**, *45*, 7056.

56. Pang, K., Quan, S. M., Parkin, G., *Chem. Commun.*, **2006**, 5015.

57. Pang, K., Tanski, J. M., Parkin, G., *Chem. Commun.*, **2008**, 1008.

58. Yurkerwich, K., Buccella, D., Melnick, J. G., Parkin, G., *Chem, Commun.*, **2008**, 3305.

59. Yurkerwich, K., Buccella, D., Melnick, J. G., Parkin, G., *Chem. Sci.*, **2010**, *1*, 210.

60. Kuchta, M. C., Bonanno, J. B., Parkin, G., *J. Am. Chem. Soc.*, **1996**, *118*, 10914.

61. Reger, D. L., *Coord. Chem. Rev.*, **1996**, *147*, 571.

62. Stone, F. G. A., *Advances in Organometallic Chemistry*, **1990**, *31*, 53.

63. Garner, M., Lehmann, M.-A., Reglinski, J., Spicer, M. D., *Organometallics*, **2001**, *20*, 5233.

64. Green, M. L. H., *J. Organometallic Chem.*, **1995**, *500*, 127.

65. Foreman, M. R. St.-J., Hill, A. F., White, A. J. P., Williams, D. J., *Organometallics*, **2003**, *22*, 3831.

66. Barratt, D., Davies, S. J., Elliott, G. P., Howard, J. A. K., Lewis, D. B., Stone, F. G. A., *J. Organometallic Chem.*, **1987**, *325*, 185.

67. Wadepohl, H., Elliott, G. P., Pritzkow, H., Stone, F. G. A., Wolf, A., *J. Organometallic Chem.*, **1994**, *482*, 243.

68. Carriedo, G. A., Elliott, G. P., Howard, J. A. K., Lewis, D. B., Stone, F. G. A., *J. Am. Chem. Soc., Chem. Commun.*, **1984**, 1585.

69. Stone, F. G. A., *Advances in Organometallic Chemistry*, **1990**, *31*, 53.

70. Brew, S. A., Stone, F. G. A., *Advances in Organometallic Chemistry*, **1993**, *35*, 135.

71. Foreman, M. R. St.-J., Hill, A. F., Tshabang, N., White, A. J. P., Williams, D. J., *Organometallics*, **2003**, *22*, 5593.

72. Foreman, M. R. St.-J., Hill, A. F., Smith, M. K., Tshabang, N., *Organometallics*, **2005**, *24*, 5224.

73. Foreman, M. R. St.-J., Hill, A. F., Smith, M. K., Tshabang, N., *Organometallics*, **2006**, *25*, 1528.

74. Frogley, B. J., Hill, A. F., Welsh, S. S., *Dalton Trans.*, **2021**, *50*, 15502.

75. Frogley, B. J., Hill, A. F., Welsh, S. S., *Chem. Commun.*, **2021**, *57*, 13353.

76. Bowen, E. J., Mikiewicz, E., *Nature,* **1947**, *159*, 706.

77. Slodek, A., Filapek, M., Schab-Balcerzak, E., Grucela, M., Kotowicz, S., Janeczek, H., Smolarek, K., Mackowski, S., Malecki, J. G., Jedrzejowska, A., Szafraniec-Gorol, G., Chrobok, A., Marcol, B., Krompiec, S., Matussek, M., *Eur. J. Org. Chem.*, **2016**, 4020.

78. Reglinski, J., Spicer, M. D., *Coord. Chem. Rev.*, **2015**, *297-298*, 181.

79. Santini, C., Pellei, M., Lobbia, G. G., Pettinari, C., Drozdov, A., Troyanov, S., *Inorg. Chim. Acta*, **2001**, *325*, 20.

80. Lloyd, N. C., Nicholson, B. K., Wilkins, A.L., Thomson, R., *Chemistry in New Zealand*, **2002**, *66*, 53.

81. Hill, A. F., Smith, M. K., *Chem. Commun.*, **2005**, 1920.

82. Nicholson, B. K., *J. Organometallic Chem.*, **1984**, *265*, 153.

83. Lee, S. K., Nicholson, B. K., *J. Organometallic Chem.*, **1986**, *309*, 257.

84. Crossley, I. R., Hill. A. F., Humphrey, E. R., Smith, M. K., Tshabang, N., Willis, A. C., *Chem. Commun.*, **2004**, 1878.

85. Rajasekharan-Nair, R., Moore, D., Chalmers, K., Wallace, D., Diamond, L. M., Darby, L., Armstrong, D. R., Reglinski, J., Spicer, M. D., *Chem. Eur. J.*, **2013**, *19*, 2487.

86. Reglinski, J., Spicer, M. D., Garner, M., Kennedy, A. R., *J. Am. Chem. Soc.*, **1999**, *121*, 2317.

87. Boa, M., Hayashi, T., Shimada, S., *Dalton Trans.*, **2004**, 2055.

88. Vahrenkamp, H., *Acc. Chem. Res.*, **1999**, *32*, 589.

89. Parkin, G., *Chem. Rev.*, **2004**, *104*, 699.

90. Reglinski, J., Spicer, M. D., *Current Bioactive Compounds*, **2009**, *5*, 264.

91. Pombeiro, A. J. L., Richards, R. L., *Coord. Chem. Rev.*, **1990**, *104*, 13.

92. Bailey, P. J., McCormack, C., Parsons, S., Rudolphi, F., Perucha, A. S., Wood, P., *Dalton Trans.*, **2007**, 476.

93. Rosini, C., Franzini, L., Raffaelli, A., Salvadori, P., *Synthesis*, **1992**, *6*, 503.

94. Noyori, R., Kitamura, M., *Modern Synthetic Methods*, **1989**, 115.

95. Noyori, R., Ohkuma, T., *Angew. Chem. Int. Ed.*, **2001**, *40*, 40.

96. Pu, L., *Chem. Rev.*, **1998**, *98*, 2405.

97. Shibasaki, M., Sasai, H., Arai, T., *Angew. Chem. Int. Ed. Engl.*, **1997**, *36*, 1236.

98. Martini, P., Pasqali, M., Boschi, A., Uccelli, L., Giganti, M., Duatti, A., *Molecules*, **2018**, *23*, 2039.

99. Kammerer, C., Rapenne, G., *Eur. J. Inorg. Chem.*, **2016**, 2214.

100. Wallace, D., Quinn, E. J., Armstrong, D. R., Reglinski, J., Spicer, M. D., Smith, W. E., *Inorg. Chem.*, **2010**, *49*, 1420.

101. Wang, Y.-L., Cao, R., Bi, W.-H., *Polyhedron*, **2005**, *24*, 585.

102. Alvarez, H. M., Krawiec, M., Donovan-Merkert, B. T., Fouzi, M., Rabinovich, D., *Inorg. Chem.*, **2001**, *40*, 5736.

103. Cammi, R., Lanfranchi, M., Marchiò, L., Mora, C., Paiola, C., Pellinghelli, A., *Inorg. Chem.*, **2003**, *42*, 1769.

104. Hill, A. F., Schwich, T., Xiong, Y., *Dalton Trans.*, **2019**, *48*, 2367.

105. Quast, H., Bieber, L., *Chem. Ber.*, **1981**, *114*, 3253.

106. Aïssa, C., *J. Org. Chem.*, **2006**, *71*, 360.

107. Bohle, D. S., Clark, G. R., Rickard, C. E. F., Roper, W. R., Wright, L. J., *J. Organometallic Chem.*, **1988**, *358*, 411.

108. Crossley, I. R., Hill, A. F., Willis, A. C., *Organometallics*, **2005**, *24*, 1062.

109. Crossley, I. R., Hill, A. F., Willis, A. C., *Organometallics*, **2010**, *29*, 326.

CHAPTER 2.

PROPARGYLIDYNE & TRICARBIDO COMPLEXES

2.1 Introduction to Propargylidyne Complexes

Organometallic propargylidynes, [$L_nM(\equiv CC\equiv CR)$], are a particular class of transition metal complexes which are characterized by a {C_3} chain of sp hybridized carbon atoms.[1,2] The chain begins with a metal-carbon (M≡C) triple bond, and the remaining carbon bonds alternate between carbon-carbon single and triple bonds. Within the field of organometallic chemistry, there is a particular interest in these types of complexes, given that their unique chemical and electronic structures have the potential to afford characteristics normally only observed in conjugated organic systems. Furthermore, these complexes contain multiple reactive sites, and through semi-generalisable synthetic routes they may be further functionalised to prepare more intricate examples. Where the terminal 'R' group is substituted for another metal centre, this forms a sub-set of propargylidyne complexes named *tricarbido* complexes; molecules which undoubtedly conjure thoughts of molecular wires and molecular electronics. In this Chapter, the chemistry of tungsten- and molybdenum-based propargylidyne and tricarbido complexes shall be discussed, including insights into their reactivity and electrochemical properties.

2.2 Background and Scope

In the most general sense, the field of organometallic chemistry is reliant on the chemical interactions of metallic and non-metallic fragments. Amongst the non-metallic fragments available to synthetic chemists, carbon is undoubtedly the most studied element of them all. A cursory search on any scientific database will reveal a plethora of carbon-based structures, many of which will display carbon atoms in several intramolecular bonding modes (e.g. sp, sp^2 and sp^3 hybridised forms) which afford unique 1-, 2- and 3-dimensional molecular structures.[3–6]

Given the inherent chemical flexibility of carbon, it is not surprising that this work is primarily concerned with the installation of sp hybridised carbon atoms on tungsten and molybdenum centres to form a particular class of polyyne complex: propargylidynes, [$L_nM(\equiv CC\equiv CR)$]. These complexes contain an alternating {C_3} chain of sp hybridised carbon atoms, beginning with a metal-carbon (M≡C) triple bond and terminating at a carbon-carbon (C–R) single bond. As a result of the conjugated nature of the polyyne chain, these types of materials have been pursued in the search for their potential application in molecular

electronics, spurred on by their purported optoelectronic properties (e.g. MLCT, IMCT, NLO, etc.).[7–9]

A comprehensive review on the topic of transition metal complexes containing all-carbon (C_χ; $\chi < 60$) ligands was published in 2004 by Bruce and Low,[10] which highlighted the far-reaching scope and rapid progress which this field had by then undergone over the past several decades. Furthermore, it went on to note that polyyne species containing odd-numbered carbon chains (χ = 1, 3, 5, etc.) were far rarer than polyynes formed with even-numbered carbon chains (χ = 2, 4, 6, etc.). This, in part, may be traced back to the lack of appropriate organic-based starting materials (e.g. molecules containing preformed {C_3} alkylidyne fragments) which would be required to successfully form organometallic complexes with odd-numbered polyyne chains. However, an inherent lack of stability in complexes containing odd-numbered chains might also be a factor to consider when taking account of their scarcity.

Several different bonding descriptions exist for organometallic polyyne complexes; these different bonding modes are summarized in **Scheme 2.1**. Amongst them, bonding modes **A**-**C** are most commonly encountered in polyynes with evenly numbered carbon chains. Furthermore, **A** is the most prevalent of all the five different bonding modes. By comparison, the few examples of chains containing an odd number of carbon atoms tend to adopt cumulenic[11] (**D**) or, more commonly, alkynyl-carbyne (**E**) bonding modes.

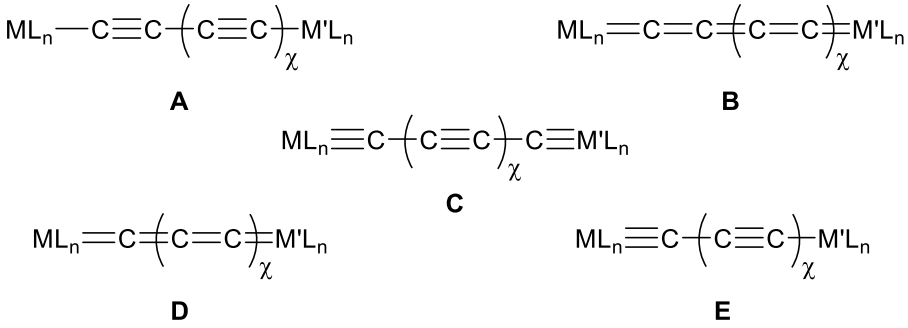

Scheme 2.1. Bonding descriptions of extended bimetallic polyyne complexes.

The presence of metal-carbon multiple bonds, as found in bonding modes **D** and **E**, has inspired interest in these types of complexes and their potential optoelectronic characteristics. Although there is significant impetus for the production and characterisation

of these types of complexes, the few current synthetic routes which are utilised lack generalisability: something which has retarded development of this field.

Irrespective of the synthetic challenges which exist when attempting to form organometallic polyyne complexes with odd numbered carbon chains, the synthetic routes which exist have been greatly improved upon since 1973 when the first carbyne was formed by E. O. Fischer.[12] This has allowed for the preparation of various extended chain (e.g. $\{C_3\}$, $\{C_5\}$, $\{C_{10}\}$, etc.) complexes which previously were not accessible.[1,13,14] Given that the principal focus of the work in this chapter relates to propargylidynes and tricarbido complexes (**Scheme 2.2**), the synthetic routes to these complexes will be discussed in detail, and routes to other organometallic polyyne complexes shall be disregarded.

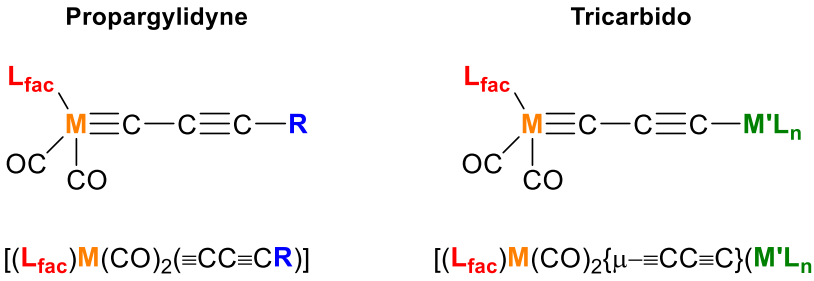

Scheme 2.2. Typical structures and general linear formulae of propargylidyne (*left*) and tricarbido (*right*)

2.3 Propargylidyne Complexes

Propargylidyne complexes, $[L_nM(\equiv CC\equiv CR)]$ (R = alkyl, aryl, or non-metal heteroatom), are characterized by the presence of a conjugated $\{C_3\}$ sp hybridised carbon chain, which begins with a metal-carbon (M≡C) triple bond and terminates with a C-R single bond. In contrast to some of the original transition metal carbyne complexes, which contained π-basic (positively mesomeric, $\boldsymbol{M}^{+}$, NR_2, SR, *etc.*) substituents to aid in stabilizing the formation of the metal-carbon triple bond, propargylidynes contain a weakly π-acidic (negatively mesomeric, $\boldsymbol{M}^{-}$) alkynyl chain. This in turn leads to the expectation that the propargylidyne metal-carbon triple bond may suffer from a slightly higher degree of destabilization compared to classical carbynes, and therefore, might be more susceptible to chemical attack.

2.3.1 Synthesis of Propargylidyne Complexes

During efforts to try and form the bromo-alkylidene complex $[Cr(CO)_5\{=CBr(Ph)\}]$ *via* the reaction between $[Cr(CO)_5\{=C(OMe)Ph\}]$ and BBr_3 at low temperature, it was discovered by Fischer and Kreis that the material which had been formed was not the intended product, but in fact was the seminal chromium carbyne complex $[Cr(CO)_4(\equiv CPh)Br]$.[12] It was soon recognized that the addition of a boron trihalide induced an alkoxide abstraction reaction, which thereby allowed for the formation of the metal-carbon triple bond. A range of carbyne complexes was soon developed using this newly discovered method, and it was later improved upon and extended to form the first propargylidyne complexes.

By starting from the tungsten alkynylcarbene complexes $[W(CO)_5\{=C(OEt)C\equiv CPh\}X]$ (X = Cl, Br, I), it was possible to similarly effect alkoxide abstraction *via* reaction with a boron trihalide to form the corresponding phenylpropargylidynes $[W(CO)_4(\equiv CC\equiv CPh)X]$ (X = Cl, Br, I) in low to moderate yields (30-60%) (**Scheme 2.3**).[15]

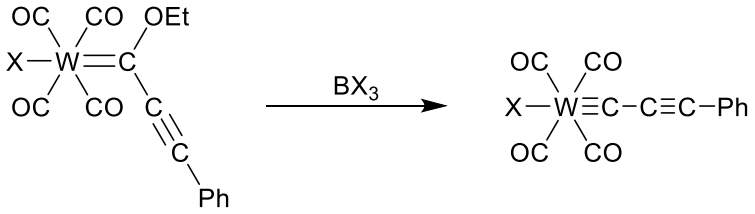

Scheme 2.3. Synthesis of the first reported propargylidyne complex (X = Cl, Br, I).

Much as this proved to be a tremendous discovery in the field of organometallic polyyne chemistry, further work in this field was regrettably hindered due to the thermal- and aerobic-instabilities these complexes displayed. Retrospectively, this can be easily rationalised, given that we now understand that the carbyne ligand is a very strong π-acidic substituent and this will weaken the retrodonation of electron density from the metal centre to the surrounding carbonyl ligands. As a result, this greatly increases ligand lability, and causes the complexes to rapidly degrade when exposed to temperatures above –40°C or aerobic atmospheres.

Although the formation of propargylidyne complexes remains challenging, the synthetic procedures used to generate them have been greatly improved. A 'one-pot' procedure, oxide abstraction carbyne synthesis, was developed by F. G. A. Stone and co-workers and has been widely utilised to form thermally stable tungsten and molybdenum propargylidyne complexes in high yields.[16] Conveniently, this synthetic route uses simple and relatively inexpensive $[M(CO)_6]$ (M = W, Mo) starting materials which, when treated with alkynyl lithium species (LiC≡CR), leads to the *in situ* generation of an intermediate acylate complex of the form $Li[M(CO)_5\{=C(O)C{\equiv}CR\}]$. As long as this species is not exposed to temperatures above 0°C for longer than 10 minutes, it can be readily transformed into a tetracarbonyl propargylidyne intermediate *via* treatment with trifluoroacetic anhydride at -78°C, before being carefully warmed to room temperature, thereby stimulating the liberation of one carbonyl ligand to give $[M(O_2CCF_3)(CO)_4(\equiv CC{\equiv}CR)]$. Finally, with the addition of an effective donor ligand to the tetracarbonyl intermediate at low temperature, this results in the loss of two further carbonyl ligands after being slowly warmed to room temperature. By utilising the loss of these two carbonyl ligands, Stone was able to conveniently add bidentate ligands to form propargylidynes of the form $[M(O_2CCF_3)(CO)_2L_2(\equiv CC{\equiv}CR)]$.

In lieu of using trifluoroacetic anhydride as an alkoxide abstraction agent, many other reagents have been employed throughout literature over the past fifty years: triel-group trihalides (B[12,15], Al[17], Ga[18]), $SOCl_2$, $OCCl_2$, various oxalyl halides,[19] and Ph_3PBr_2,.[20] However, the use of trifluoracetic anhydride, and in turn the formation of the metal-bound trifluoroacetate ligand, tends to be the method of choice due to its high yields and ability to be displaced with the addition of anionic, facially capping tridentate ligands (L_{fac}) such as **Tp**, **Tp***, Cp and **Tm** to produce neutral complexes of the form $[(L_{fac})M(CO)_2(\equiv CC{\equiv}CR)]$ (**Scheme 2.4**).

It is noteworthy that the route through which facially capping ligands are incorporated into propargylidyne complexes was improved upon by H. Fischer, as prior to his 2002 methodology,[21] not all anionic, tridentate ligand systems could be incorporated by the more traditional Stone protocol. In order to install an anionic, facially capping ligand using Stone's synthetic route, an initial complex bearing a bidentate ligand system was first isolated, before a more strongly chelating tridentate ligand was subsequently added, though this was not always successful. For example, unsuccessful attempts were made by Stone and co-workers to convert the propargylidyne complex $[M(O_2CCF_3)(CO)_2(tmen)(\equiv CC{\equiv}C^tBu)]$

(M = W, Mo; tmen = *N,N,N',N'*-tetramethylethylene-diamine), which contained the bidentate tmen ligand, into [(Cp)M(CO)$_2$(≡CC≡C^{t}Bu)] (M = W, Mo) *via* treatment with Na[Cp]·DME (DME = 1,2-dimethoxyethane).

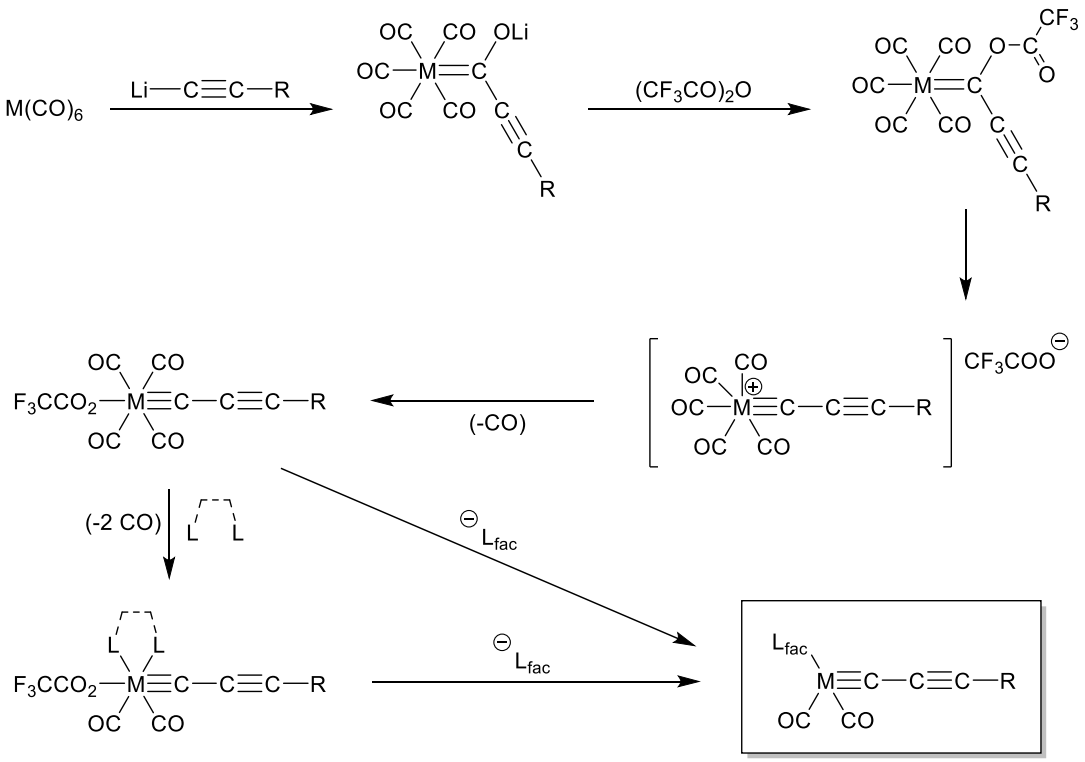

Scheme 2.4. General synthesis of propargylidyne complexes (M = Mo, W).

Ultimately, this conversion was shown not to be possible, since the coordinated tmen ligands were too strongly bound to the metal centre. However, the conversion was subsequently shown to be possible if the bidentate bipy (2,2'-bipyridyl) or two py (pyridine) ligands were installed instead of tmen.[16] These types of problems were overcome by negating the need to isolate the [M(O$_2$CCF$_3$)(CO)$_2$L$_2$(≡CC≡CR)] complex before adding the facially capping bidentate ligand, by simply treating the tetracarbonyl intermediate [M(O$_2$CCF$_3$)(CO)$_4$(≡CC≡CR)] *in situ* with the facially capping ligand (L$_{fac}$) instead to produce the desired [(L$_{fac}$)M(CO)$_2$(≡CC≡CR)] complexes directly.

The oxide abstraction protocol has largely been adopted as the preferred synthetic method to produce propargylidynes of the form [(L$_{fac}$)M(CO)$_2$(≡CC≡CR)] (M = W, Mo). This topic was reviewed by R. Manzano in 2018,[1] including a comprehensive list of previously reported propargylidyne complexes formed *via* the alkoxide abstraction route. In the first instance, readers are directed to Manzano's work for all relevant complexes which were

formed prior to 2018. However, a summary of the work published in the field of propargylidyne and tricarbido chemistry since 2018 and up until 2022 has been summarized in **Section 2.5**.

2.3.2 Bonding in Propargylidyne Complexes

Much like the bonding descriptions which have been descried numerous times for organometallic carbyne complexes,[22–26] a direct analogy to propargylidynes can also be made. Over the past fifty years, two distinct organometallic carbyne bonding classes have emerged: Schrock-type[27] and Fischer-type.[23] In the former, the carbyne substituent may be described as an anionic $\{CR^{3-}\}$ fragment bound to a metal centre to form a high valent complex. Meanwhile, in Fischer-type carbynes, the carbyne substituent is viewed as a cationic $\{CR^{+}\}$ two-electron donor fragment, such that the assigned oxidation state of the metal centre is reduced by one unit.[23] Furthermore, the carbyne (M≡C) ligand in Schrock-type carbynes typically exhibits nucleophilic reactivity, when in Fischer-carbynes the carbyne ligand tends to display electrophilic behaviour.[28]

The two families of carbyne also tend to differ in the nature of their ancillary ligands, with Schrock-type carbynes typically being ligated by anionic or π-donor ligands, while the vast majority of Fischer-type carbynes carry π-acidic co-ligands. However, it is noted that ambiguities are frequently encountered when attempting to apply these rigid specifications to the vast library of carbyne complexes. These bonding schemes may be interpreted as extremes of a spectrum, and the bonding descriptions of most carbyne and propargylidyne complexes may fall somewhere in between these two representations.

For Fischer-type complexes, such as those found therein this Chapter, the bonding may be best described by the effective σ-donation of the lone pair of electrons located in the sp hybridised orbital of the $\{CR^{+}\}$ fragment to the metal centre, and two retrodative π-back donation interactions from the metal centre into two vacant p-orbitals on the carbyne carbon atom (**Scheme 2.5**). These three simultaneous interactions form the metal-carbon triple bond, by analogy with conventional carbonyl bonding.

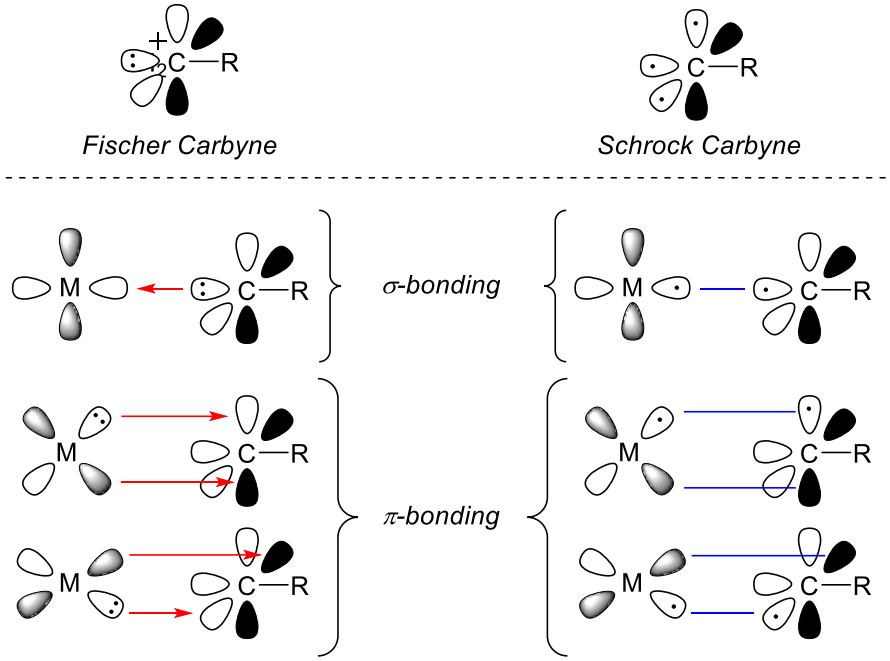

Scheme 2.5. Fischer (*left*) and Schrock (*right*) bonding descriptions of carbyne complexes.

2.4 Tricarbido Complexes

Tricarbidos are a sub-class of propargylidyne complexes which contain a $\{C_3\}$ linkage between two metal centres. Complexes of this type may be formed *via* post-synthetic modification of propargylidyne complexes, or through multi-step organometallic processes; i.e. *via* a ($\{C_4\}$ – $\{C_1\}$) approach, a ($\{C_2\}$ + $\{C_1\}$) approach, or by *in situ* desilylation and metalation of suitable silylpropargylidynes. Examples of these types of reactions have been discussed below, but emphasis has been placed on the latter desilylation and metalation approach, which has been solely used in this work to form mixed bimetallic tricarbido complexes.

The first reported tricarbido complex, $[Cp^*(NO)(PPh_3)Re(\mu\text{-}C{=}C{=}C)Mn(CO)_2Cp][BF_4]$, was prepared by J. A. Gladysz and co-workers through the initial formation of a rhenium-manganese bimetallic carbene complex $[Cp^*(NO)(PPh_3)Re(\mu\text{-}C{\equiv}C\text{–}C(OMe))Mn(CO)_2Cp]$, and subsequent treatment of this complex with BF_3, acting as an alkoxide abstraction agent (**Scheme 2.6**).[29]

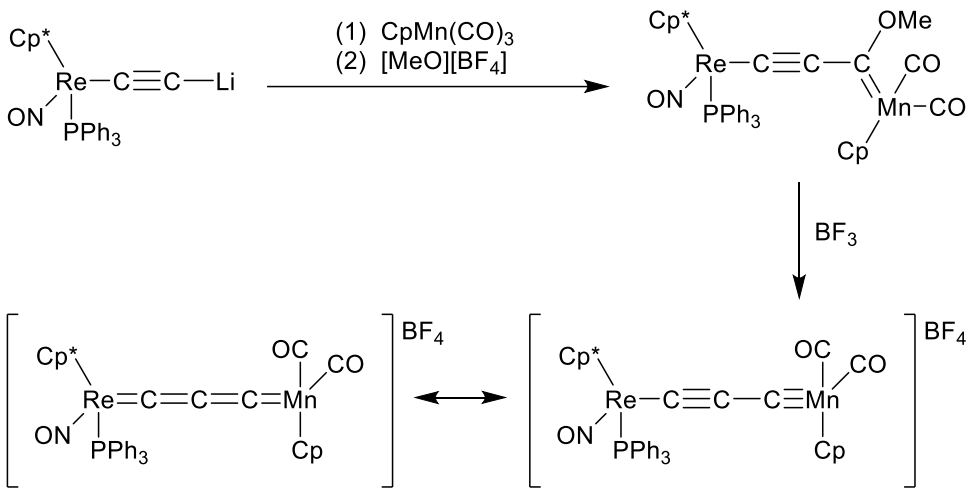

Scheme 2.6. Formation of the first reported tricarbido complex.

Later, crystallographic studies would reveal that the tricarbido segment of the complex [Cp*(NO)(PPh$_3$)Re{μ-C≡C–COMe}Mn(CO)$_2$Cp] would in fact be best described in the cumulenic form {Re=C=C=C=Mn}, as opposed to the expected alkynyl-carbyne bonding motif {Re–C≡C–C≡Mn}.[30] Gladysz would later prove to be successful in his endeavours to form a tricarbido complex in the alkynyl-carbyne form, through use of the alkyne metathesis catalyst [W$_2$(O^{t}Bu)$_6$] and its ability to cleave the alkynyl bond in a ({C$_4$} – {C$_1$}) approach, to afford the complex [Cp*(NO)(PPh$_3$)Re{μ-C≡C–C}W(O^{t}Bu)$_3$] from [Cp*Re(NO)(PPh$_3$)(C≡C–C≡C–R)] (R = H, Me).[31]

A range of tungsten and molybdenum tricarbido complexes containing alkynyl-carbyne bonding motifs were formed by a ({C$_2$} + {C$_1$}) approach, developed by J. L. Templeton.[32] By utilising the chlorocarbyne complex [**Tp***Mo(CO)$_2$(≡CCl)] which was first reported by Lalor and co-workers,[33] Templeton was able to successfully react this with the anionic molybdenum vinylidene complex [**Tp***Mo(CO)$_2$(=C=CH$_2$)]$^-$ to yield the bimetallic bridged complex [**Tp***Mo(CO)$_2${μ-C–CH$_2$–C}Mo(CO)$_2$**Tp***]. *In situ* double deprotonation of this complex using two equivalents of KO^{t}Bu affords a dianionic intermediate, [**Tp***Mo(CO)$_2${μ-C=C=C}Mo(CO)$_2$**Tp***]$^{2-}$, which upon exposure to atmospheric oxygen gives the tricarbido complex [**Tp***Mo(O)$_2${μ-≡CC≡C}Mo(CO)$_2$**Tp***] featuring the alkynyl-carbyne bonding motif. A range of complexes of the type [**Tp***M^1(O)$_2${μ-≡CC≡C}M^2(CO)$_2$**Tp***] (M = Mo, W; M^1:M^2 = Mo:Mo, W:Mo, Mo:W) were formed through substitution of Lalor's molybdenum chlorocarbyne with the analogous tungsten chlorocarbyne, which when combined with the oxidation of the crude reaction mixture led to a range of products being formed (**Scheme 2.7**).

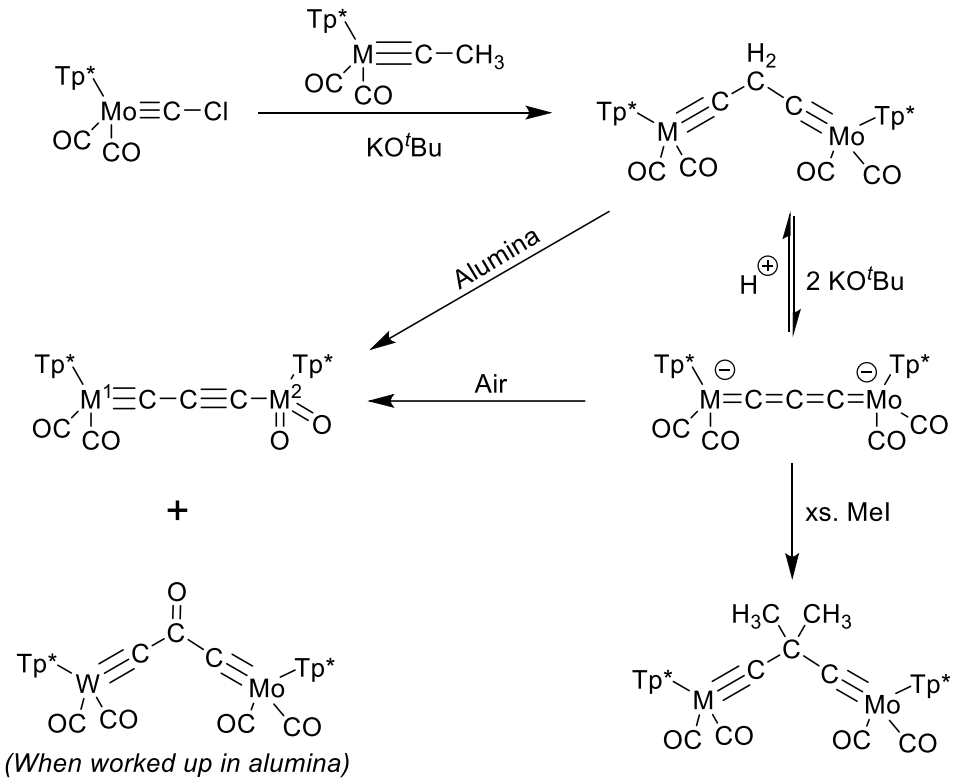

Scheme 2.7. Formation of mixed-metal propargylidyne complexes (M = Mo, W; M^1:M^2 = Mo:Mo, W:Mo, Mo:W.

Silylpropargylidynes, $[L_nM(\equiv CC\equiv CSiR_3)]$, have been shown to be a highly useful starting point for the preparation of bimetallic tricarbido species. The pre-formed nature of the alkynyl-carbyne $\{C_3\}$ fragment in these complexes removes much of the complexity associated with the inclusion of a second metal centre. Following H. Fischer's initial studies into the preparation of molybdenum and tungsten silylpropargylidyne complexes,[21,34] it was found that the addition of TBAF†† could effectively desilylate the terminal trimethylsilyl group. Desilylation with TBAF was found to either afford *in situ* the terminal parent propargylidyne complex $[L_nM(\equiv CC\equiv CH)]$, due to the inherently wet TBAF[35] and protic solvents, or its conjugate base $[L_nM(\equiv CC\equiv C)]^-$ (**Scheme 2.8**), though neither could be isolated as such.

If the latter is formed in the presence of an appropriate metal species, it was shown that a range of bi- and multi-metallic complexes could be formed through halide metathesis.[36–42]

†† The $[^nBu_4N][F]$ ('TBAF') is a commercially available 1.0 mol L^{-1} solution in THF, containing *ca.* 5% w/w water.

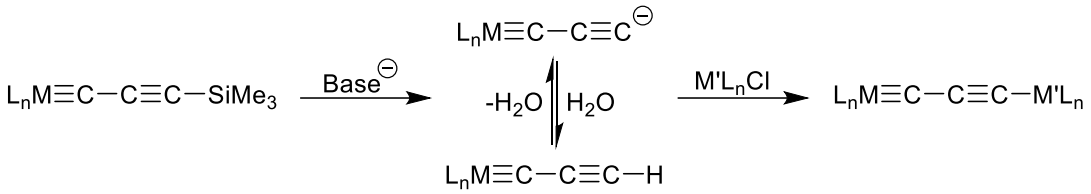

Scheme 2.8. General reaction for the protodesilylation of trimethylsilylpropargylidynes to afford tricarbido complexes through halide metathesis.

2.5 Recent Advances in Propargylidyne and Tricarbido Chemistry

Between 2018 – 2022, only a few papers have been published on the topics of propargylidyne and tricarbido complexes and these have been summarized below.

2.5.1 Preparation of the First Selenolatopropargylidyne

In mid-2018, during research being carried out on the silylpropargylidyne complex [**Tp***W(CO)$_2$(≡CC≡CSiMe$_3$)], it was noted that while bimetallic tricarbido species of the type [**Tp***W(CO)$_2${μ-CC≡C}(ML$_n$)] (M = Ru,[36,43] Rh,[38] Ir,[39] Hg[#],[44] Au[37,43]) were well documented, none of the examples which had been previously reported contained a main group element in the place of 'M', with the exception of silicon.[45] Hence, work commenced to prepare and isolate the first example of a selenolatopropargylidyne complex, [**Tp***W(CO)$_2$(≡CC≡CSeR)]. This avenue of research was bolstered by the discovery of the highly reactive intermediate salt [^{n}Bu$_4$N][**Tp***W(CO)$_2$(≡CC≡C–Se)] which could be trapped by reaction with [RuCl(PPh$_3$)$_2$(η-C$_5$H$_5$)].[40]

In an attempt to form the target complex [**Tp***W(CO)$_2$(≡CC≡CSePh)] an equimolar mixture containing the complex [**Tp***W(CO)$_2$(≡CC≡CSiMe$_3$)] and diphenyl diselenide was treated with one equivalent of TBAF in a solution of THF. After allowing the reaction mixture to stir for two hours, purification *via* column chromatography afforded two major products (**Scheme 2.9**).

Complexes featuring M = Hg exist as bis(tricarbido)mercurial complexes of the form [{Tp*W(CO)$_2$(μ-C–C≡C)}$_2$Hg].

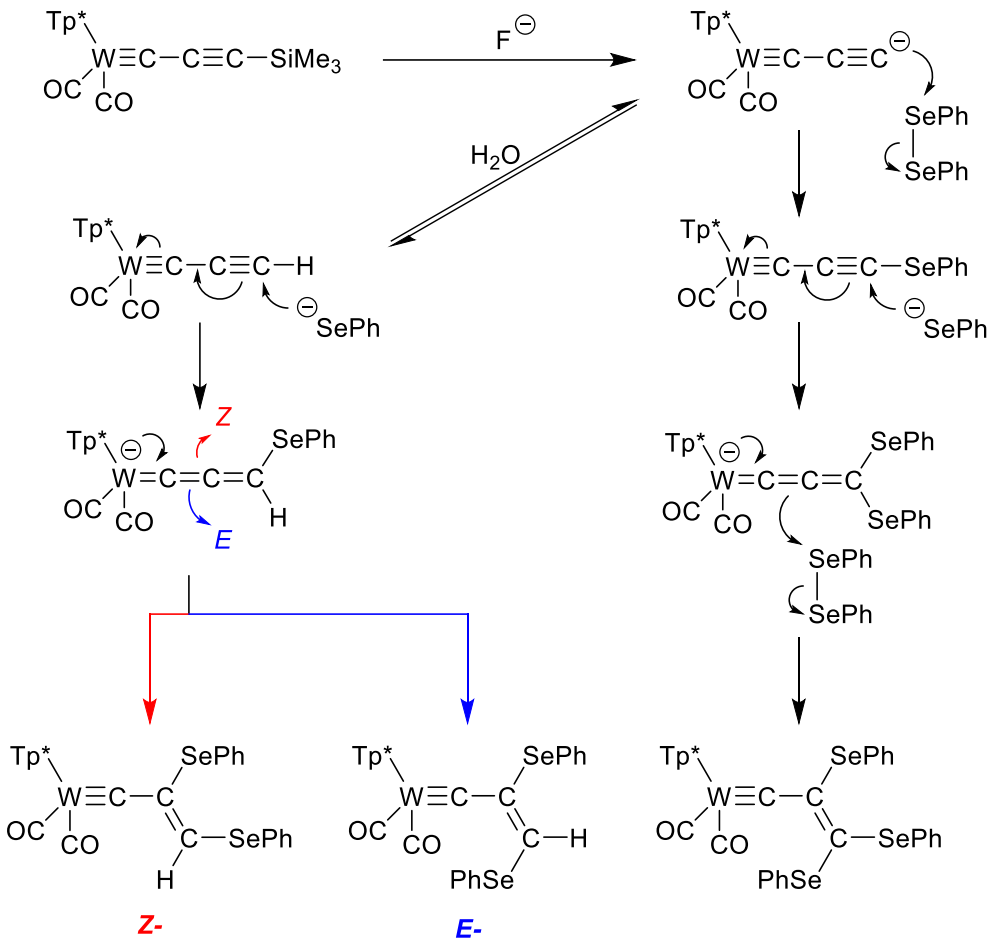

Scheme 2.9. Formation of various phenylselenato-functionalised alkylidyne complexes through the protodesilylation of [**Tp***W(CO)$_2$(≡CC≡CSiMe$_3$)].

Sadly, neither one proved to be the target material. Even although it was previously shown that this type of approach was successful for the formation of the selenolatocarbyne [**Tp***Mo(CO)$_2$(≡CSePh)],[46] it was unambiguously shown that the reaction had formed two regioisomers of the bis(phenylselenato)allylidyne complex, *E*- and *Z*-[**Tp***W(CO)$_2${≡C–C(SePh)=CH(SePh)}], as well as the tris(phenylselenato)derivative [**Tp***W(CO)$_2${≡C–C(SePh)=C(SePh)$_2$}] as the minor product.

These complexes were inadvertently formed due to the generation of the strongly nucleophilic PhSe$^-$ species which could install itself on multiple locations of the desilylated intermediates. To avoid this, diphenyl diselenide was substituted for PhSeCl with the hope that the comparatively unreactive Cl$^-$ conjugate nucleophile would not interfere with the reaction. Using PhSeCl, the selenatopropargylidyne complex [**Tp***W(CO)$_2$(≡CC≡CSePh)]

was successfully formed in low yield, along with the regioisomer *E*-[**Tp***W(CO)$_2$(≡C–C(SePh)=C(SePh)–C≡C–C≡)W(CO)$_2$**Tp***] (**Scheme 2.10**).

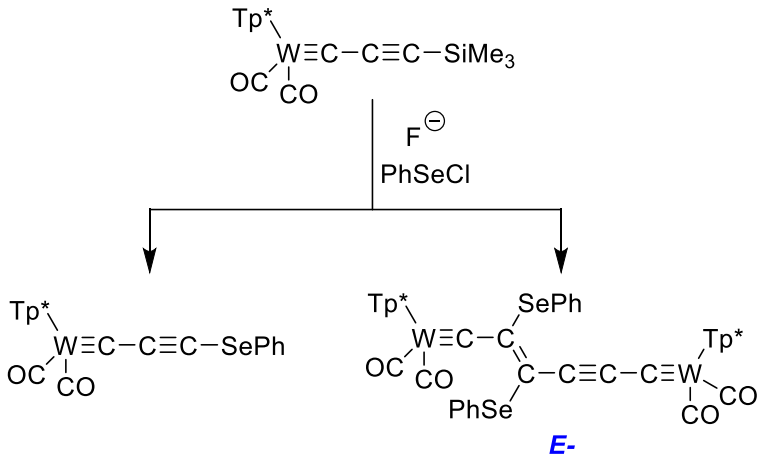

Scheme 2.10. Fluorodesilylation of [**Tp***W(CO)$_2$(≡CC≡CSiMe$_3$)] in the presence of PhSeCl.

The former target complex proved to be highly unstable in the solid state and in solution, with samples decomposing over a few hours even when stored under strict anaerobic conditions at low temperature. Unfortunately, this occluded full spectral characterisation of this previously unreported complex.

2.5.2 A New *Pseudo*-Sonogashira ({C$_2$} + {C$_1$}) Route to Forming Propargylidynes

Early in 2019, R. Manzano described in detail a *pseudo*-Sonogashira cross coupling protocol for the ({C$_2$} + {C$_1$}) approach to forming a range of propargylidynes, some of which were unobtainable through previously reported routes.[2] M. I. Bruce and co-workers had previously developed an alternative, albeit similar, ({C$_2$} + {C$_1$}) approach which involved the coupling of Lalor's molybdenum bromocarbyne complex [**Tp***Mo(CO)$_2$(≡CBr)] with the alkynylgold species [Au(C≡CC$_6$F$_5$)(PPh$_3$)] in the presence of a palladium(0) catalyst and copper(I) iodide to form the propargylidyne complex [**Tp***Mo(CO)$_2$(≡CC≡CC$_6$F$_5$)] (**Scheme 2.11**).[47] It is not fully understood why the addition of the cuprous salt is required in this process, as gold sp or sp^2 carbon bonds are known to spontaneously transmetallate to palladium(II).[48,49]

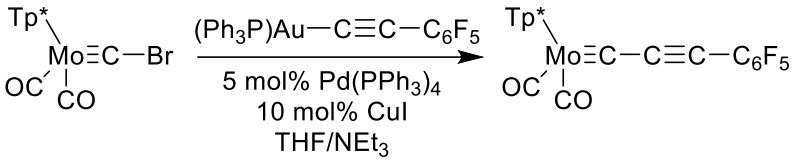

Scheme 2.11. Formation of [**Tp***Mo(CO)$_2${≡CC≡C(C$_6$F$_5$)}].

Manzano's approach was stated to involve two intersecting catalytic cycles, the first of which being the conventional palladium(0/II) regime, consisting of C–X oxidative addition, transmetallation, and reductive elimination, ultimately leading to C–C bond formation. The second intersecting cycle is known to be based on conventional Sonogashira copper chemistry, but it is less well defined. It is thought to involve the formation of an alkynylcopper species through the π-coordination/deprotonation of the terminal alkyne. This generates the nucleophilic alkynylcopper reagent for transmetallation to palladium and regeneration of cuprous bromide. As a proof of concept, these conditions were applied to the reaction between [**Tp***W(CO)$_2$(≡CBr)] and 3,3-dimethyl-1-butyne in order to successfully form the previously unreported propargylidyne complex [**Tp***W(CO)$_2$(≡CC≡CCMe$_3$)] (**Scheme 2.12**) in excellent yields.

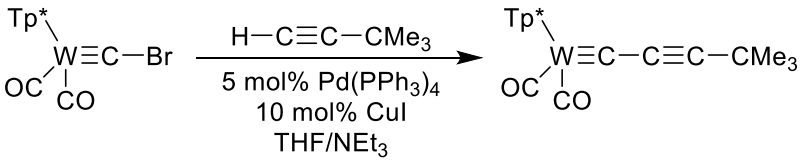

Scheme 2.12. Coupling of [**Tp***W(CO)$_2$(≡CBr)] with 3,3-dimethyl-1-butyne.

In order to probe the generalizability of these conditions, several reactions were carried out aiming to target new propargylidyne complexes containing mesomerically-active (***M***$^+$, ***M***$^-$) terminal substituents. As briefly mentioned in the introduction to this Chapter, there is significant interest in the formation of propargylidyne complexes as they may exhibit noteworthy electronic communication properties. Therefore, the incorporation of such substituents may prove to be of great utility, but prior synthetic routes which predominantly use alkynyl lithium reagents in the preparation of propargylidynes are not compatible with the incorporation of many mesomerically-active substituents.

It proved possible to prepare two tungsten propargylidyne complexes of the form [**Tp***W(CO)$_2$(≡CC≡CC$_6$H$_4$R-4)] (R = NH$_2$, NO$_2$) which, crucially, contained terminal nitrogen-directing groups (**Scheme 2.13**).

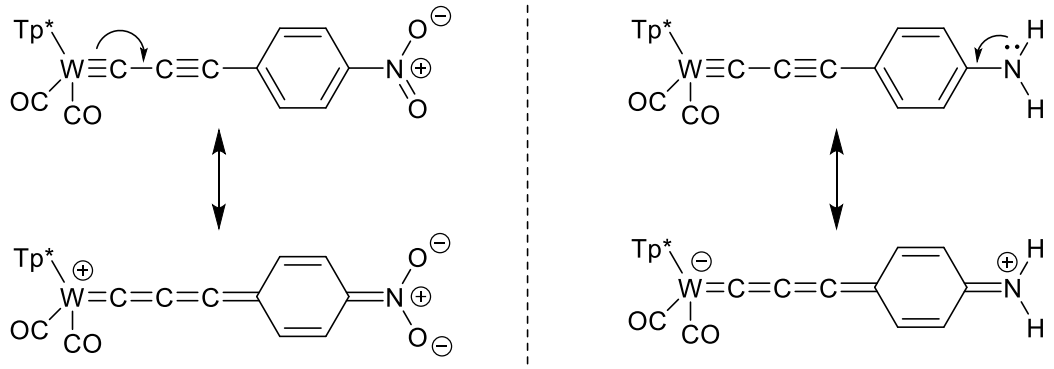

Scheme 2.13. Canonical forms of [**Tp***W(CO)$_2$(≡CC≡CC$_6$H$_4$R-4)] (R = NH$_2$, NO$_2$) displaying opposing mesomeric effects.

Some main group elements were also found to be easily incorporated into propargylidyne complexes using this cross-coupling methodology. The tungsten propargylidynes [**Tp***W(CO)$_2$(≡CC≡CAPh$_3$)] (A = C, Si, Ge) were successfully formed and characterized *via* single crystal X-ray crystallography (**Figure 2.1**).

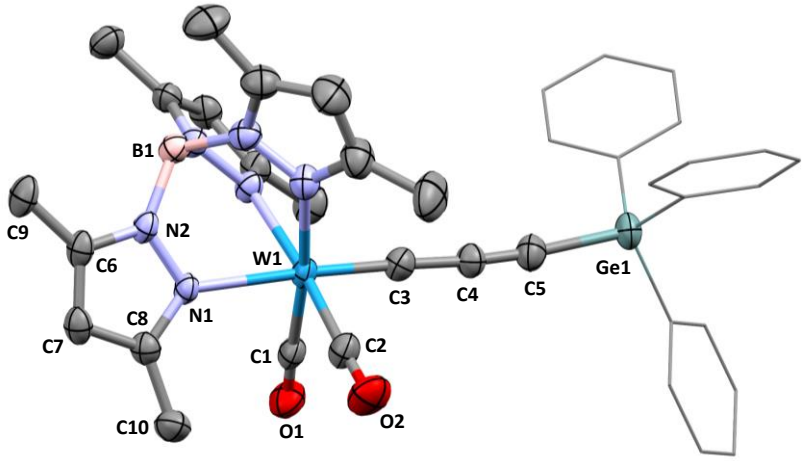

Figure 2.1. Single-crystal X-ray diffraction structure of [**Tp***W(CO)$_2$(≡CC≡CGePh$_3$)] (50% displacement ellipsoids) with selected atom labels.

2.5.3 Installation of Si, Sn, Pb, P, and As at Propargylidyne Termini

Although several synthetic routes exist for the preparation of propargylidyne complexes, many do not facilitate the incorporation of main-group elements at the terminus of the {C$_3$} carbon chain. For example, the ubiquitous oxide abstraction synthetic pathway is intolerant of the electrophilic reagents required to install a main group element, due to the

need for harsh alkoxide abstracting agents (TFAA, $SOCl_2$, etc.) and the inherently unstable thermolabile intermediates which they produce.

Silylpropargylidynes pose as a very promising set of complexes which bear a preformed {C_3} alkynyl fragment, and thereby serve as excellent candidates for postsynthetic modification protocols. Typically, modification of these scaffolds takes place *via* an *in situ* fluorodesilylation (refer to **Section 2.5.1**) in order to install a metallic or electrophilic fragment at the terminus of the {C_3} alkynyl chain. One shortcoming of this approach is it is not compatible with the use of fluorophilic reagents, due to the overwhelming likelihood of a reaction occurring between the electrophilic species and the fluoride anion, or adventitious water.

Hypothetically, the parent propargylidynes [(L_{fac})M(CO)$_2$(≡CC≡CH)] (M = W, Mo; L_{fac} = **Tp**, **Tp***, **Tm**, **Htt**) could serve as an excellent way to avoid this synthetic bottleneck if they were isolable in a state free from these other reactive species. However, to date, these complexes have not been isolated through this route, and therefore cannot be utilised.

Furthermore, depending on the desired main group element which is to be installed, the palladium catalysed cross coupling route which was discussed in **Section 2.5.2** is somewhat variously effective. The conditions used were effective for the formation of complexes of the type [**Tp***W(CO)$_2$(≡CC≡CAPh$_3$)] (A = C, Si, Ge), but failed for the installation of tin (A = Sn).[2] Instead, during the preparation of the stannylpropargylidyne complex, it was found that it exhibited a higher degree of reactivity towards the palladium catalyst compared to the other main group propargylidyne complexes such that the complex underwent a ({C_1} + {C_2} + {C_1}} cross coupling reaction to form the {C_4}-bridged dimetallahexatriyne complex [**Tp***W(CO)$_2${μ-≡CC≡CC≡}(CO)$_2$W**Tp***].[14]

It is noteworthy that the complex [**Tp***W(CO)$_2${μ-CC≡CC≡}(CO)$_2$W**Tp***] has previously been prepared in a ({C_2} + {C_2}) approach by Templeton and co-workers, whereby the oxidation of [**Tp***W(CO)$_2$(=C=CH$_2$)][Li] with ferrocenium, iodine, or nitrobenzene first affords the {C_4} bridged species [**Tp***W(CO)$_2${μ-C–CH$_2$–CH$_2$–C≡}(CO)$_2$W**Tp***] which may be oxidized and promoted to undergo a twofold net dihydrogen removal to form the desired complex [**Tp***W(CO)$_2${μ-≡CC≡CC≡}(CO)$_2$W**Tp***] (**Scheme 2.14**).[50]

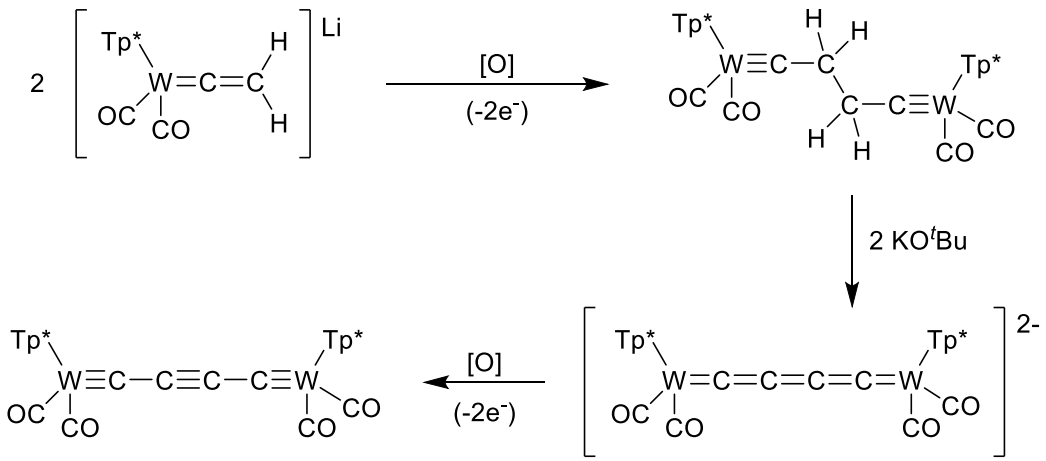

Scheme 2.14. Templeton's route to the {C_4}-bridged bimetallic complex [**Tp***W(CO)$_2${μ-≡CC≡CC≡}(CO)$_2$W**Tp***].

In lieu of a reliable synthetic route for the preparation of main group terminally functionalised propargylidyne complexes, the 2020 report by A. F. Hill and co-workers is significant as they were able to form examples of propargylidyne complexes bearing silicon, tin, lead, phosphorus, and arsenic termini.[51]

In an earlier report, the mercury bis(tricarbido) complex [Hg{C≡CC≡W(CO)$_2$**Tp***}$_2$] was found to form when [**Tp***W(CO)$_2$(≡CC≡CSiMe$_3$)] underwent fluorodesilylation in the presence of $HgCl_2$.[44] When exploring the reactivity of this complex, it was found that the addition of two equivalents of *n*-butyllithium in a solution of THF promoted the loss of ^{n}Bu$_2$Hg[§§] and the clean formation of [**Tp***W(CO)$_2$(≡CC≡CLi)]. While maintaining this solution at low temperature, it is possible to add main group reagents of the form ClAPh$_3$ (A = Si, Sn, Pb) or chlorodiphenylphosphine followed by BH$_3$·SMe$_2$ to afford a range of tetrel and pnictogen functionalised propargylidynes (**Scheme 2.15**).

In an alternative synthetic route, it was also found that the generation of a poorly defined silver-functionalised propargylidyne, of gross composition [Ag$_2${C≡CC≡W(CO)$_2$**Tp***}][NO$_3$], could be achieved through the addition of silver nitrate to an ethanolic solution of [**Tp***W(CO)$_2$(≡CC≡CSiMe$_3$)]. Subsequent treatment with ClAPh$_2$ (A = P, As) reagents allowed for the generation of phosphino- and arsino-propargylidyne complexes [**Tp***W(CO)$_2$(≡CC≡CPPh$_2$)] and [**Tp***W(CO)$_2$(≡CC≡CAsPh$_2$)], respectively (**Scheme 2.16**).

§§ CAUTION: Alkyl mercury reagents, such as ^{n}Bu$_2$Hg (CAS Registry No: 629-35-6), are extremely toxic and should be handled with the utmost care.

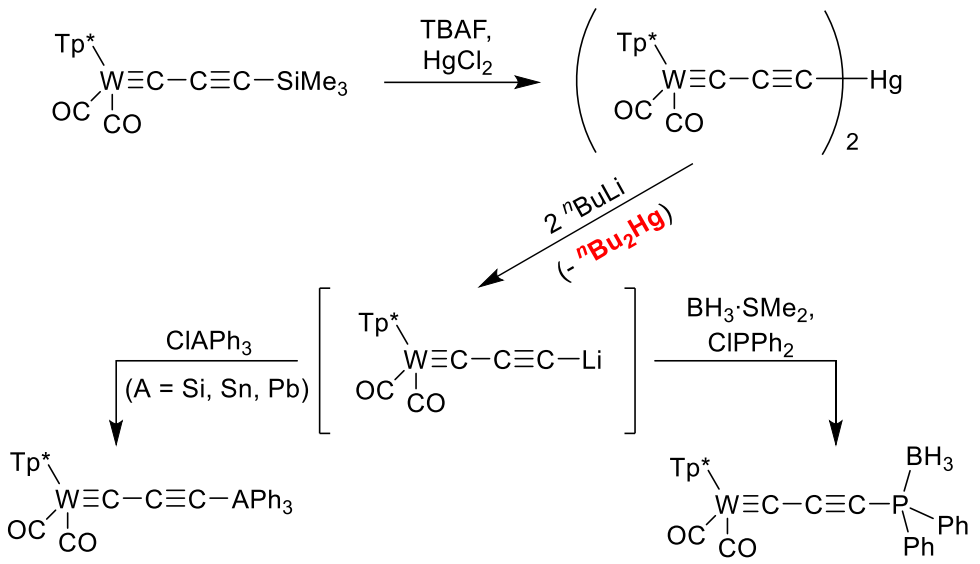

Scheme 2.15. Formation of various tetrel- and pnictogen-functionalised tungsten propargylidyne complexes.

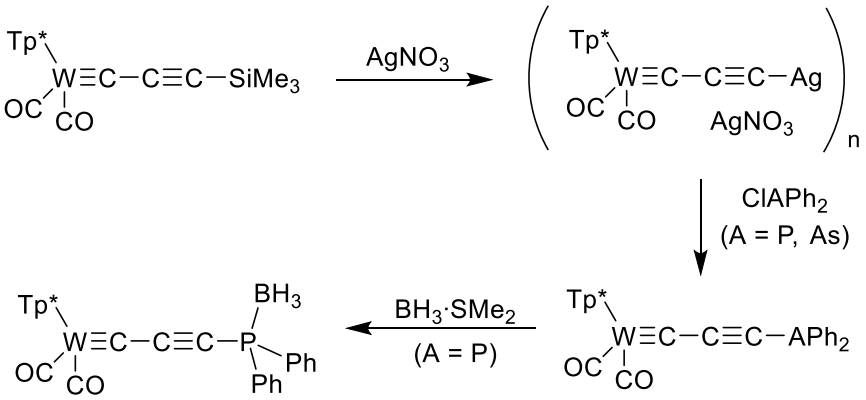

Scheme 2.16. Formation of arsino- and phosphinopropargylidynes.

2.5.4 Polycyclic Aromatic Hydrocarbon Propargylidynes

Polycyclic aromatic hydrocarbon (PAH) functionalised organometallic carbyne species have been the subject of some interest in recent years, given that the incorporation of already optoelectronically active functionality into such complexes may in turn enhance their optical and electronic properties. Much of the chemistry surrounding these types of complexes shall be discussed in detail in **Chapter 3**, but a short summary of PAH-functionalised propargylidyne complexes and their chemistries has been collated in the following paragraphs.

Hill and co-workers were able to report the synthesis of the first examples of bis- and poly(propargylidyne) complexes assembled around benzyl, anthracenyl and pyrenyl PAH cores. Alkynylsilanes featuring PAHs have become easily accessible through the Sonogashira coupling of sp^2-C halides and terminal acetylenes,[52] and hence an extensive library of such compounds are now known (**Figure 2.2**).

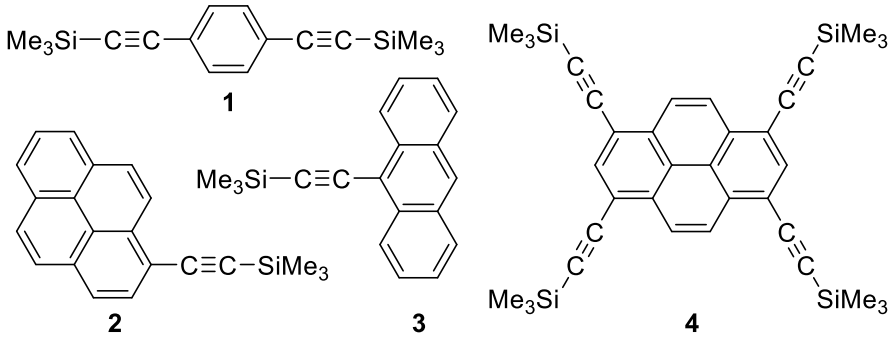

Figure 2.2. Examples of alkynylsilanes featuring various PAHs: **1** = 1,4-bis((trimethylsilyl)ethynyl)benzene; **2** = 1-((trimethylsilyl)ethynyl)pyrene; **3** = 9-((trimethylsilyl)ethynyl)anthracene; **4** = 1,3,6,8-tetrakis((trimethylsilyl)ethynyl)pyrene.

Prior to propargylidyne complex formation, alkynylsilanes must undergo desilylation. However, it is known that parent PAH alkynyl compounds rapidly undergo decomposition (polymerization) reactions, leading to intractable product mixtures. To avoid this during propargylidyne formation, fluorodesilylation of the compounds noted above were carried out *in situ*, and the parent species immediately reacted with the complex [**Tp***W(CO)$_2$(≡CBr)]. Each reaction was carried out *via* a *pseudo*-Sonogashira protocol in order to form a library of tungsten propargylidyne complexes, many of which incorporate two or more propargylidyne moieties (**Scheme 2.17**).

Although many PAH systems are known to display intense fluorescence upon irradiation with UV light, it was noted that all of the PAH propargylidyne complexes which had been formed in this study were non-emissive: purportedly as a result of quenching by the tungsten metal centres. So formidable are the quenching mechanisms, that even when the propargylidyne chains were extended from a {C_3} to a {C_5} fragment, thereby forming a rarely encountered pentadiynylidyne complex,[14] still no fluorescence emission was observed.

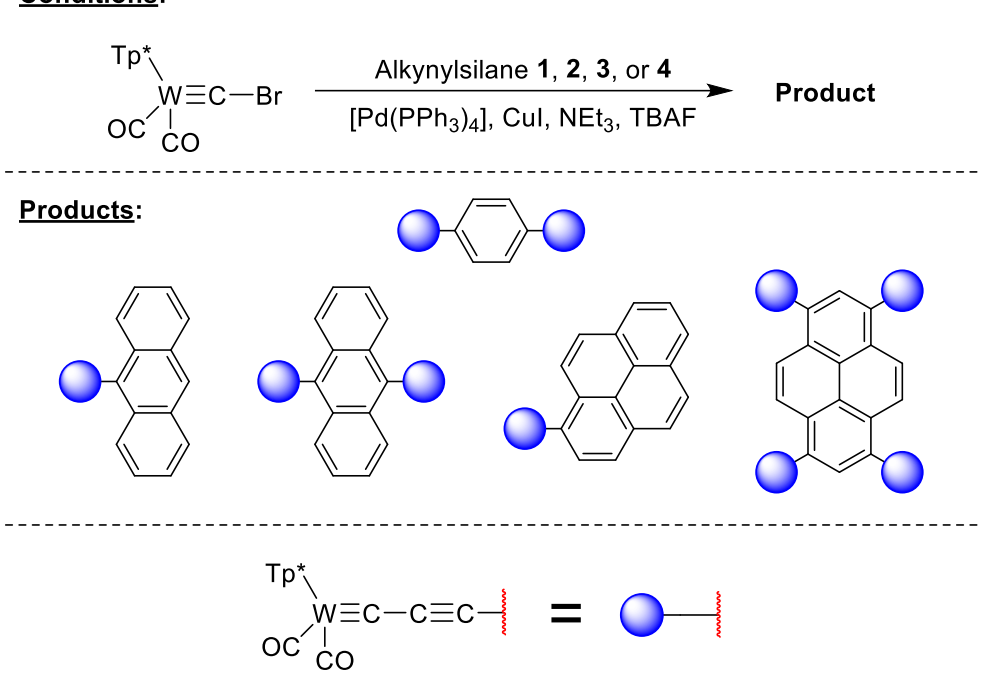

Scheme 2.17. Preparation of various tungsten propargylidyne complexes arranged around PAH cores.

2.6 Results & Discussion: Routes to Propargylidyne and Tricarbido Complexes

2.6.1 Summary of Spectral Features – Chapter 2 Complexes

Comp. No.	Metal Centre	Ligand	Liquid IR (cm^{-1})		$^{13}C\{^1H\}$ NMR							
			ν_{BH}	ν_{CO}	$M\equiv C^{\alpha}$ (ppm)	$^1J_{MC}$ (Hz)	C^{β} (ppm)	$^2J_{MC}$ (Hz)	C^{γ} (ppm)	$^3J_{MC}$ (Hz)	M(CO) (ppm)	$^1J_{MC}$ (Hz)
2.1	W	**Tm**	2436	1981, 1893	249.9	–	170.2	–	82.5	–	224.8, 219.7	–
2.2	Mo	**Tm**	–	1995, 1915	257.5	–	113.8	–	77.9	–	227.7, 222.7	–
2.3	W	**Tm**	2436	1980, 1892	251.0	202.7	80.9	–	53.6	–	224.9, 219.6	168.9, 161.3
2.4	W	**Tm**	2434	1975, 1886	251.7	–	97.9	–	85.8	–	224.7, 219.8	–
2.5	W	**Tm**	2412	1979, 1890	246.8	–	107.3	–	74.8	–	225.4, 220.6	–
2.6	W	**Tm**	2472	2050, 1990	186.5	–	126.6	–	110.9	–	203.3, 198.9	–
2.7	W	**Tm**	2434	1965, 1877	–	–	–	–	–	–	–	–
2.8 *	W	**Tm**	–	1973, 1940, 1863	253.7	–	128.5	–	134.8	–	226.6, 222.3	–

Unless otherwise indicated, $^{13}C\{^1H\}$ NMR data measured in $CDCl_3$. | Liquid IR spectra measured in CH_2Cl_2. | * NMR data measured in CD_2Cl_2

Table 2.1. Summary of selected spectral data for the complexes detailed in Chapter 2.

2.6.2 Synthesis of [TmM(CO)$_2$(≡CC≡CSiMe$_3$)] (M = Mo, W)

The general synthetic route employed to form the new tungsten and molybdenum silylpropargylidynes of the form [**Tm**M(CO)$_2$(≡CC≡CSiMe$_3$)] (M = Mo, W) involved the acylate oxide abstraction protocol: much like all of the other propargylidynes and organometallic carbyne complexes discussed in this work. In order to form the first key intermediate in this protocol, the alkynyl lithium species [LiC≡CSiMe$_3$], a THF solution of ethynyltrimethylsilane was treated with *n*-butyllithium at low temperature. To assure that all of the starting material had indeed been converted into the alkynyl lithium species, the mixture was first stirred continuously at low temperature for a period of ten minutes, before being removed from the dry-ice/acetone slush bath and warmed to ambient temperature for ten minutes. It is advised that care be taken during this step, as excessive heating may lead to reaction mixture degradation.

Formation of the second key intermediate, the acylate species Li[M(CO)$_5${=C(O)C≡C(SiMe$_3$)}] (M = W, Mo), was induced *via* the addition of the relevant metal hexacarbonyl complex into the alkynyl lithium solution at low temperature. Once again, in order to achieve full conversion, the mixture was removed from the slush bath after fifteen minutes and warmed in ambient air for a period of one hour. Although this may appear to be an extended period to allow a less-than-stable intermediate to warm to relatively elevated temperatures, no negative consequences were noted due to this part of the synthetic procedure, and good to excellent yields were obtained of both molybdenum and tungsten complexes.

As discussed in **Section 2.3.1** of this Chapter, the addition of trifluoroacetic anhydride at low temperature causes the tetracarbonyl complex [M(O$_2$CCF$_3$)(CO)$_4$(≡CC≡CSiMe$_3$)] (M = W, Mo) to form after the mixture is removed from the slush bath and allowed to warm. During this process, as the reaction mixture approaches 0°C, small bubbles of carbon monoxide gas can be observed to form. The reaction mixture is re-cooled once the liberation of carbon monoxide has visibly halted and the pro-ligand Na[**Tm**] subsequently added. By keeping the flask in the slush bath overnight and allowing the dry-ice to slowly sublime, the reaction mixture gradually warmed to room temperature, thereby affording the slow formation of the crude product mixture.

In order to extract the target material, two different purification methods were employed: (i) precipitating out the material *via* the addition of petroleum spirit (40-60°C), and (ii) *via* silica-gel column chromatography. Once the mixture was concentrated to dryness, it was subjected to crude purification by filtration through a short plug of diatomaceous earth and eluted with CH_2Cl_2 to remove a viscous insoluble residue which commonly forms in these reactions. The filtrate from this process was once again concentrated to dryness and dissolved in a minimal volume of CH_2Cl_2. A large volume of petroleum spirit (40-60°C) was rapidly added to this solution, causing the immediate formation of a pink/red precipitate, which was isolated *via* vacuum filtration, washed with more petroleum spirit (40-60°C) and *n*-pentane, and finally air dried.

In order to obtain a spectroscopically pure sample of the desired target material, further purification was required. The precipitate was subjected to silica-gel column chromatography, eluting with a 2% (v/v) mixture of THF in CH_2Cl_2. This afforded a major red band on the column which was collected and concentrated to dryness to afford the complexes [**Tm**$W(CO)_2(\equiv CC\equiv CSiMe_3)$] (**2.1**) and [**Tm**$Mo(CO)_2(\equiv CC\equiv CSiMe_3)$] (**2.2**) (**Scheme 2.18**) as purple and red powders, respectively.

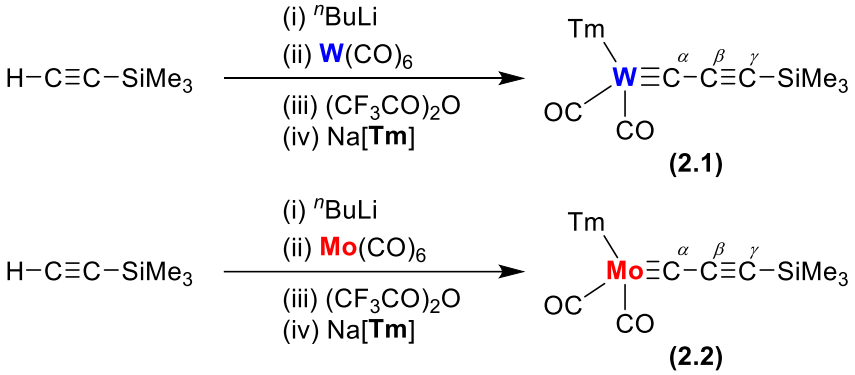

Scheme 2.18. Preparation of complex **2.1** and complex **2.2**.

Spectroscopically, both complexes display two equally intense carbonyl ν_{CO} bands when analysed *via* solution infrared spectroscopy in CH_2Cl_2. For the [**Tm**$Mo(CO)_2(\equiv CC\equiv CSiMe_3)$] complex, the carbonyl absorptions are detected at ν_{CO} 1978 and 1890 cm^{-1}, whereas for the [**Tm**$W(CO)_2(\equiv CC\equiv CSiMe_3)$] complex they are detected at ν_{CO} 1981 and 1893 cm^{-1}.

Analysis by ^{1}H NMR spectroscopy reveals a conveniently similar spectra for both complexes. Expectedly, the terminal $SiMe_3$ group displays a sharp singlet at approximately δ_H 0.15 ppm. Of the remaining signals, all can be attributed to the **Tm** ligand. Each *exo*-CH_3 group on the **Tm** ligand are chemically distinct in the ^{1}H NMR spectra for these complexes, owed to the atropisomerism enforced by the chiral cage structure that **Tm** has when facially bound to a metal centre (see **Chapter 1**). Finally, the heterocyclic C–*H* hydrogen atoms of the methimazole rings appear as several signals in the region δ_H 6.95 - 6.75 ppm.

Although both complexes contain a boron atom as part of the **Tm** ligand, the $^{11}B\{^{1}H\}$ NMR signals which are recorded for these types of complexes tend to be an uninformative diagnostic tool. For example, for the complexes [**Tm**W(CO)$_2$(≡CC≡CSiMe$_3$)] and [**Tm**Mo(CO)$_2$(≡CC≡CSiMe$_3$)] the boron nuclei resonances were detected in the $^{11}B\{^{1}H\}$ NMR spectra at δ_B -1.75 and -1.72 ppm, respectively. Being remote from the metal centre, the boron nuclei are not usefully responsive to changes in the metal and ligands of interest. Hence, this spectroscopic technique shall not be discussed in the remainder of this Chapter, but $^{11}B\{^{1}H\}$ NMR data have been included for all complexes (wherever possible) in the Experimental section.

The gross composition of both complexes was interrogated by ESI mass spectrometry and revealed a molecular ion $[M+H]^+$ as the base peak at m/z 701.0662 for the complex [**Tm**W(CO)$_2$(≡CC≡CSiMe$_3$)], and a molecular ion $[M+H]^+$ peak at m/z 615.0183 for the complex [**Tm**Mo(CO)$_2$(≡CC≡CSiMe$_3$)]. Furthermore, elemental analysis substantiated the composition and bulk purity of these samples.

Both complexes were subjected to $^{13}C\{^{1}H\}$ NMR spectroscopic analysis, but only the [**Tm**W(CO)$_2$(≡CC≡CSiMe$_3$)] complex was successfully analysed, even after several attempts. The molybdenum analogue displayed some instability in common halogenated solvents and at higher concentrations required for $^{13}C\{^{1}H\}$ NMR spectral analysis, whereby the complex precipitated out of solution over a period of one hour. Hence, only the $^{13}C\{^{1}H\}$ NMR spectroscopic data for [**Tm**W(CO)$_2$(≡CC≡CSiMe$_3$)] shall be discussed, though data for the molybdenum variant would be expected to be similar. When recorded in a solution of CD_2Cl_2, the carbyne carbon (W≡C$^{\alpha}$) is arguably the most conspicuous feature in the $^{13}C\{^{1}H\}$ NMR spectrum as it is the most downfield signal, being detected at δ_C 249.9 ppm, as a result of the deshielding behaviour of the neighbouring tungsten atom (**Figure 2.3**) and

paramagnetic contributions to the shielding tensor due to the small HOMO-LUMO gap for carbyne complexes.

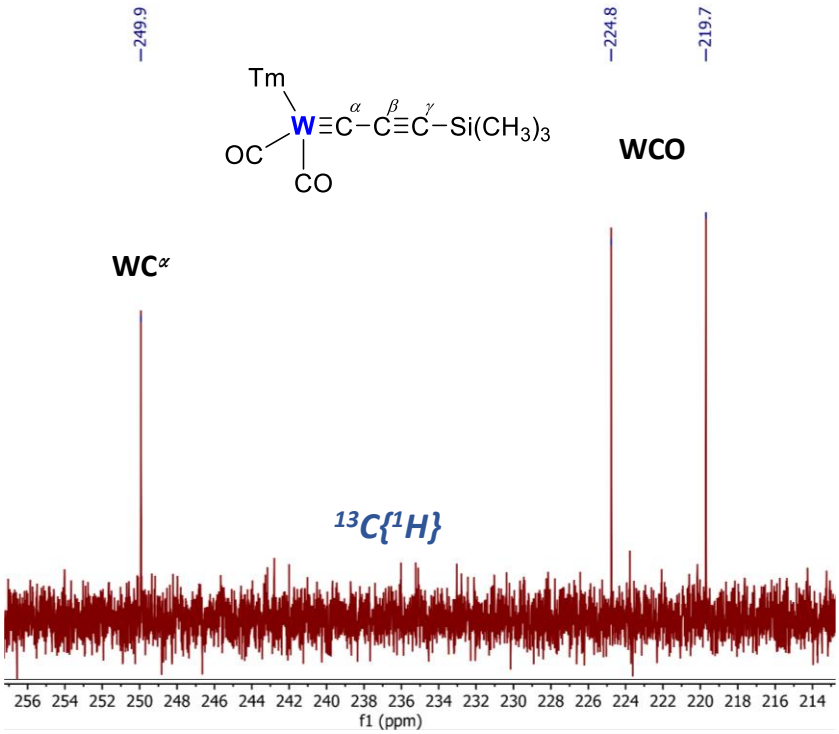

Figure 2.3. Segment of the $^{13}C\{^{1}H\}$ NMR spectrum of [**Tm**W(CO)$_2$(≡CC≡CSiMe$_3$)].

The chirality resulting from the C_3-TmW cage leads to the diastereotopic carbonyl carbons (WCO) being detected as independently resolved signals at δ_C 224.8 and 219.7 ppm. The remaining two carbons of the propargylidyne chain, C^{β} and C^{γ}, were also detected at δ_C 170.2 and 82.5 ppm, respectively: the former of which being unambiguously assigned through the use of 2D ^{13}C-^{1}H HMBC NMR spectroscopy (**Figure 2.4**).

Crystals suitable for structural determination of the complex [**Tm**W(CO)$_2$(≡CC≡CSiMe$_3$)] were grown *via* vapour diffusion of petroleum spirit (40-60°C) into a CH_2Cl_2 solution at 4°C, and were found to be of monoclinic symmetry and space group Cc (No. 9) (**Figure 2.5**).

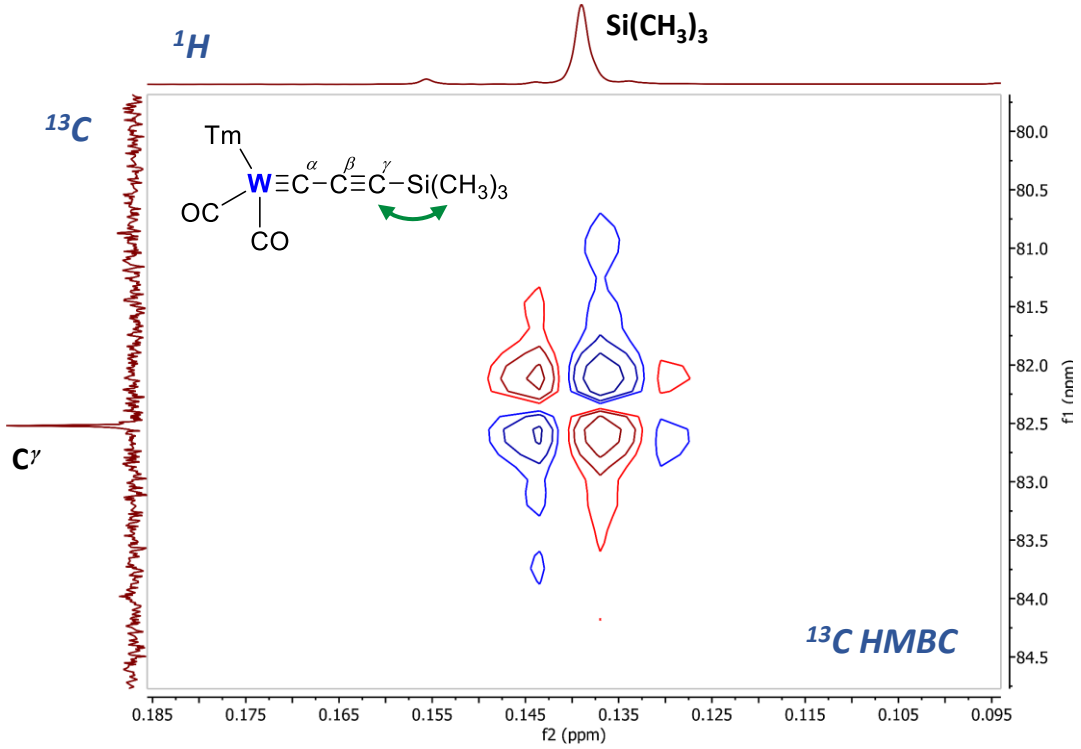

Figure 2.4. ^{13}C-^1H HMBC spectrum of [**Tm**W(CO)$_2$(≡CC≡CSiMe$_3$)], displaying the correlation between the (^{13}C) C$^\gamma$ and (^1H) SiCH$_3$ signals.

Aside from allowing for conclusive structural determination, the data for [**Tm**W(CO)$_2$(≡CC≡CSiMe$_3$)] do not yield any significantly different features from the previously reported **Tp**-ligated tungsten silylpropargylidyne complex.[41]

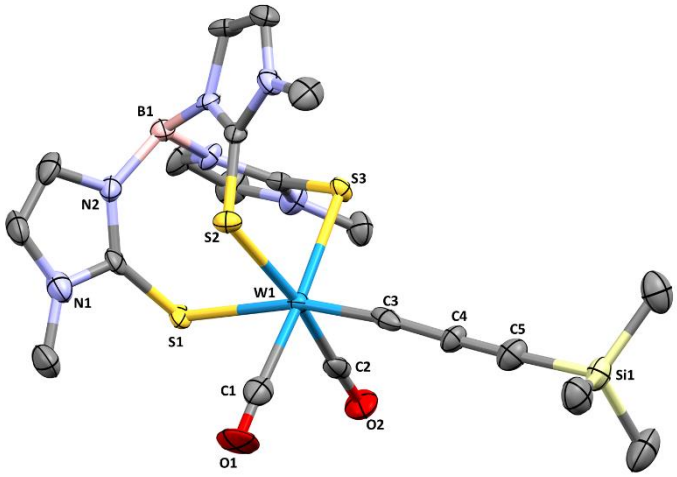

Figure 2.5. Molecular structure of [**Tm**W(CO)$_2$(≡CC≡CSiMe$_3$)] (**2.1**) in a crystal (50% displacement ellipsoids) with selected atom labels. Solvent molecules and hydrogen atoms omitted for clarity. Selected bond lengths (Å) and angles (°): W1–C1 2.034(12), W1–C2 1.999(16), W1–S1 2.636(2), W1–S2 2.511(3), W1–S3 2.566(2), W1–C3 1.838(12), C3–C4 1.380(16), C4–C5 1.217(15), C5–Si1 1.848(11); W1–C3–C4 172.4(8), C3–C4–C5 177.5(11).

In a characteristic manner, the propargylidyne segment shows only minor deviation from the 180° bond angle expected for a chain of sp hybridised carbon atoms. Furthermore, the bond lengths along the propargylidyne segment closely coincide with similar species. Unfortunately, crystals of [**Tm**Mo(CO)$_2$(≡CC≡CSiMe$_3$)] suitable for structural determination were not successfully acquired.

2.6.3 Synthesis of [TmW(CO)$_2$(≡CC≡CSi^{i}Pr$_3$)]

Following the observation that the tungsten-based trimethylsilyl propargylidynes appeared to be more stable in solution, which thereby allowed for easier characterisation, another tungsten silylpropargylidyne complex was pursued. In a manner analogous to the silylpropargylidyes prepared beforehand, the bulkier ethynyltriisopropylsilane was first treated with *n*-butyllithium in a THF solution to form the corresponding alkynyl lithium species LiC≡CSi^{i}Pr$_3$ at low temperature. Subsequent addition of [W(CO)$_6$] at low temperature afforded the acylate species Li[W(CO)$_5${=C(O)C≡CSi^{i}Pr$_3$}] which was successfully converted into the unstable tetracarbonyl intermediate [W(O$_2$CCF$_3$)(CO)$_4$(≡CC≡CSi^{i}Pr$_3$)] through treatment with trifluoroacetic anhydride. Na[**Tm**] was added to the reaction mixture at low temperature, which was then allowed to slowly warm to room temperature overnight. Purification by flash chromatography on silica gel eluting with CH_2Cl_2 afforded a major red band which was collected and concentrated to dryness to afford the complex [**Tm**W(CO)$_2$(≡CC≡CSi^{i}Pr$_3$)] (**2.3**) (**Scheme 2.19**) as a pink/red powder.

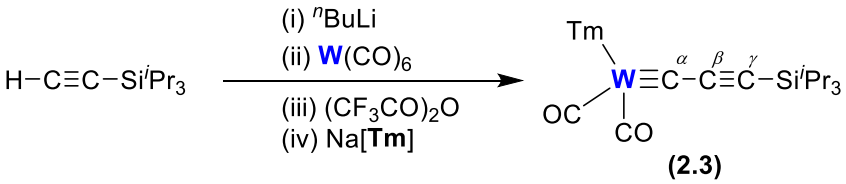

Scheme 2.19. Preparation of complex **2.3**.

As anticipated, analysis of this complex by solution infrared spectroscopy revealed two carbonyl bands of equal intensity, appearing at ν_{CO} 1980 and 1892 cm^{-1}, analogous to the previous trimethylsilyl-derivative. Additionally, a weak signal at 2436 cm^{-1} was observed and assigned as the ν_{BH} stretch of the B–H bond located on the **Tm** ligand.

Analysis by ^{1}H NMR revealed a pattern of signals similar to those of the trimethylsilyl-analogue. The terminal {Si(^{i}Pr)$_3$} group is detected as a sharp singlet at approximately δ_H 1.03 ppm and serves to be the most distinguishing feature in the ^{1}H NMR spectrum. Each *exo*-CH_3 group on the **Tm** ligand is individually resolved, appearing in the region of δ_H 3.77-3.57 ppm. Finally, the remaining proton signals may be assigned to the heterocyclic C–*H* hydrogen atoms of the methimazole rings and are detected as several overlapping signals in the region δ_H 6.88-6.76 ppm.

The gross composition of the complex [**Tm**W(CO)$_2$(≡CC≡CSi^{i}Pr$_3$)] was confirmed by ESI mass spectrometry and revealed a molecular ion $[M+H]^+$ as base peak at m/z 785.2 and the bulk composition was supported by elemental analysis.

The ^{13}C{^{1}H} NMR spectrum of [**Tm**W(CO)$_2$(≡CC≡CSi^{i}Pr$_3$)] ($CDCl_3$) featured the carbyne carbon (W≡C$^{\alpha}$) which was detected at δ_C 251.0 ppm with ^{183}W (I = ½, 14.3%) satellites measured with a $^{1}J_{WC}$ coupling constant of 202.7 Hz (**Figure 2.6**).

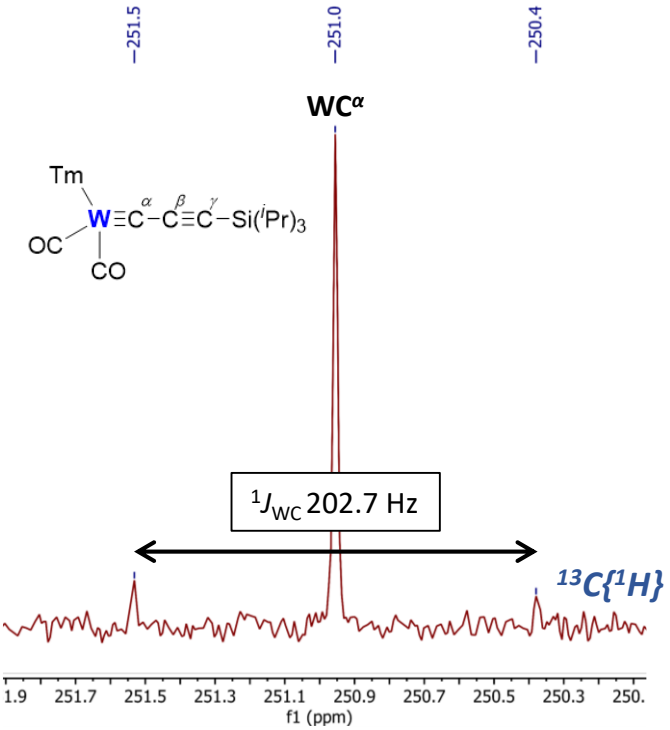

Figure 2.6. Segment of the ^{13}C{^{1}H} NMR spectrum of [**Tm**W(CO)$_2$(≡CC≡CSi^{i}Pr$_3$)] (**2.3**).

Attempts to acquire crystals suitable for structural determination were abandoned after several attempts. Although this complex serves to be notable, and further expands the list of known tungsten silylpropargylidyne complexes featuring the **Tm** ligand, no further

chemistry carried out in this body of work utilises this complex. Instead, the more easily desilylated complex [**Tm**W(CO)$_2$(≡CC≡CSiMe$_3$)] was deemed more useful as a preformed {C$_3$} fragment in the preparation of tricarbido complexes.

2.6.4 Synthesis of [TmW(CO)$_2$(≡CC≡CR)] (R = ^{t}Bu, Ph)

Propargylidyne complexes featuring alkyl- and aryl-termini were formed by the addition of [W(CO)$_6$] to the appropriate alkynyl lithium reagent [LiC≡CR] (R = ^{t}Bu, Ph) at low temperature. Successive warming and cooling of the reaction mixture was carried out to ensure full conversion of the starting materials, then the mixture was treated carefully with trifluoroacetic anhydride to form the intermediate tetracarbonyl complexes [W(O$_2$CCF$_3$)(CO)$_4$(≡CC≡CR)] (R = ^{t}Bu, Ph). Careful warming of the reaction mixture in ambient air promoted the liberation of carbon monoxide gas, which subsided after approximately 45 minutes. Following the addition of Na[**Tm**] at low temperature, the reaction mixtures were allowed to slowly warm to room temperature overnight, thereby forming the crude product mixtures containing the target materials.

In both instances, a spectroscopically pure sample of both complexes was obtained by silica-gel column chromatography, eluting with a 2% (v/v) mixture of THF in CH_2Cl_2. This afforded in both cases a major red band which was collected to afford the complexes [**Tm**W(CO)$_2$(≡CC≡C^{t}Bu)] (**2.4**) and [**Tm**W(CO)$_2$(≡CC≡CPh)] (**2.5**) (**Scheme 2.20**) as orange/peach and red/brown powders, respectively.

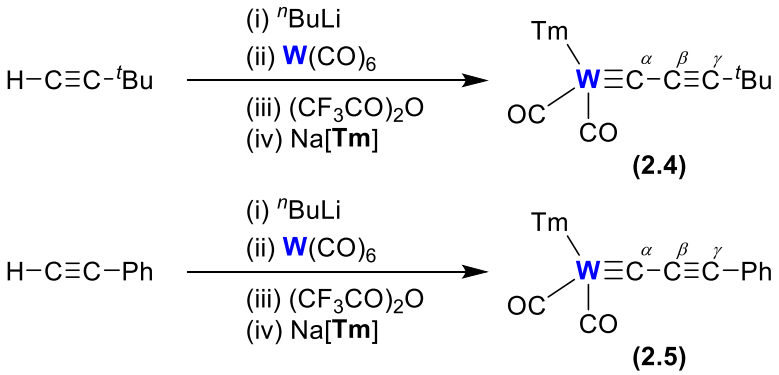

Scheme 2.20. Preparation of complex **2.4** and complex **2.5**.

The former complex had been obtained previously and less conveniently *via* a two-step sequence from pre-isolated [W(O$_2$CCF$_3$)(CO)$_2$(tmen)-(≡CC≡C^{t}Bu)] and Na[**Tm**] in refluxing THF for 8 hours.

Both complexes displayed comparable carbonyl bands when analysed *via* infrared spectroscopy as CH_2Cl_2 solutions. Two equally intense ν_{CO} bands were observed, indicating that the carbonyl ligands were approximately 90° apart. For the [**Tm**W(CO)$_2$(≡CC≡C^{t}Bu)] complex, the carbonyl ligands were detected at ν_{CO} 1975 and 1886 cm^{-1}, whereas for the [**Tm**W(CO)$_2$(≡CC≡CPh)] complex they were detected to slightly higher wavenumbers at ν_{CO} 1978 and 1890 cm^{-1}.

Analysis of the [**Tm**W(CO)$_2$(≡CC≡C^{t}Bu)] complex by ^{1}H NMR spectroscopy reveals the *tert*-butyl group as a singlet at δ_H 1.20 ppm, along with all the individually resolved *exo*-CH_3 groups on the **Tm** ligand in the range δ_H 3.77 – 3.58 ppm. Finally, the heterocyclic C–*H* hydrogen atoms of the methimazole rings appear as several signals in the region δ_H 6.91 - 6.77 ppm. Analysis of the [**Tm**W(CO)$_2$(≡CC≡CPh)] complex by ^{1}H NMR spectroscopy reveals the phenyl C–*H* hydrogen atoms as a range of signals between δ_H 7.45 – 7.27 ppm, along with all the individually resolved *exo*-CH_3 groups on the **Tm** ligand in the range δ_H 3.75 – 3.56 ppm. Finally, the cyclic alkene C–*H* hydrogen atoms of the methimazole rings appear as several signals in the region δ_H 6.94 - 6.81 ppm. The gross composition of both complexes was confirmed by ESI mass spectrometry and elemental analysis.

The ^{13}C{^{1}H} NMR spectra for both [**Tm**W(CO)$_2$(≡CC≡C^{t}Bu)] and [**Tm**W(CO)$_2$(≡CC≡CPh)] were successfully recorded. Optimal solubility for the former complex was found to be in $CDCl_3$, whereas when $CDCl_3$ was used for the latter complex it was found to rapidly precipitate out of solution requiring CD_2Cl_2 to be used such that direct comparison cannot be made. However, in general terms, the spectra for each complex bear similar features. The carbyne carbon resonance (W≡C$^\alpha$) for the complex [**Tm**W(CO)$_2$(≡CC≡C^{t}Bu)] was identified at δ_C 251.7 ppm with the remaining carbon atoms on the alkylidyne chain, C$^\beta$ and C$^\gamma$, being detected at 97.9 and 85.8 ppm, respectively. Furthermore, the two diastereotopic carbonyl ligands were detected at δ_C 224.7 and 219.8 ppm. Likewise, the complex [TmW(CO)$_2${≡CC≡CPh}] afforded signals at δ_C 246.8, 107.3, and 74.8 ppm, corresponding to the C$^\alpha$, C$^\beta$, and C$^\gamma$ atoms of the alkylidyne chain, respectively, and carbonyl resonances at δ_C 225.4 and 220.6 ppm.

Crystals suitable for structural determination were grown by vapour diffusion of petroleum spirit (40-60°C) in to saturated CH_2Cl_2 solutions containing the respective complex at 4°C. Crystals of the complex [**Tm**W(CO)$_2$(≡CC≡C^{t}Bu)] (**Figure 2.7**) were found

to comprise of the $P2_1/c$ (No. 14) space group, much like that of the previously reported data, but also afforded a better quality data set and more precise structural model.

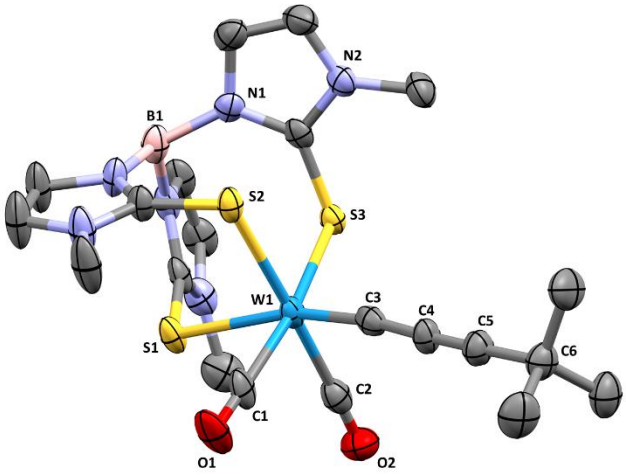

Figure 2.7. Molecular structure of [**Tm**W(CO)$_2$(≡CC≡C*t*Bu)] (**2.4**) (50% displacement ellipsoids, enantiomer generated by *P*2$_1$/c symmetry) with selected atom labels. Hydrogen atoms omitted for clarity. Selected bond lengths (Å) and angles (°): W1–C1 1994(9), W1–C2 2.020(11), W1–S1 2.633(2), W1–S2 2.575(2), W1–S3 2.5373(19), W1–C3 1.843(9), C3–C4 1.359(12), C4–C5 1.230(13), C5–C6 1.472(12); W1–C3–C4 172.7(7), C3–C4–C5 177.9(10).

The structure of this complex displayed bond lengths along the tricarbido chain consistent with those previously reported in literature.[53] Furthermore, the dihedral angle along the {C$_3$} chain was found to be 177.9(10)°, closely coinciding with the 180° dihedral angle expected for a series of sp hybridised carbon atoms.

Likewise, crystals for the complex [**Tm**W(CO)$_2$(≡CC≡CPh)] (**Figure 2.8**) formed in the monoclinic space group $P2_1/c$ (No. 14). The {C$_3$} tricarbido fragment was measured with a 178.3(6)° dihedral angle and with bond lengths consistent with other similar complexes.

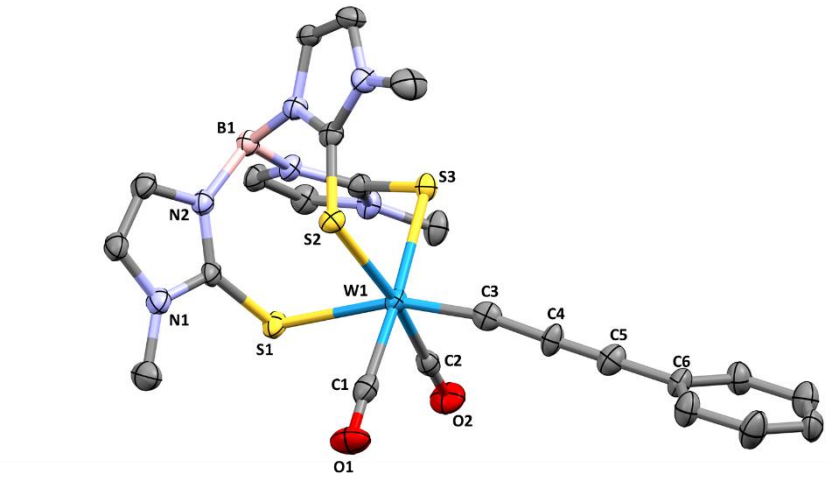

Figure 2.8. Molecular structure of [**Tm**W(CO)$_2$(≡CC≡CPh)] (**2.5**) (50% displacement ellipsoids, enantiomer generated by $P2_1/c$ symmetry) with selected atom labels. Hydrogen atoms omitted for clarity. Selected bond lengths (Å) and angles (°): W1–C1 1.999(6), W1–C2 1.992(5), W1–S1 2.6337(11), W1–S2 2.5353(11), W1–S3 2.5788(11), W1–C3 1.856(5), C3–C4 1.356(7), C4–C5 1.222(7), C5–C6 1.437(7); W1–C3–C4 168.6(4), C3–C4–C5 178.3(6).

2.6.5 Synthesis of [TmW(CO)$_2$I(≡CC≡CSiMe$_3$)][I$_3$]

Aware of the multiple reactive sites present within propargylidyne complexes, the reactivity of the complex [**Tm**W(CO)$_2$(≡CC≡CSiMe$_3$)] was explored with a view to investigating chemoselectivity. To a CH_2Cl_2 solution of [**Tm**W(CO)$_2$(≡CC≡CSiMe$_3$)], a twofold excess of elemental iodine was added at room temperature. Upon addition of iodine, the red solution underwent two successive colour changes over a period of five minutes. First from red to green, then from green to brown.

Once the reaction mixture had been concentrated to dryness, unreacted iodine was removed by ultrasonic trituration with *n*-hexane. The resulting pink supernatant fluid was carefully decanted and the washing process repeated until the supernatant fluid remained colourless. The brown powder which remained was dried under high vacuum and subjected to spectral analysis. The product was found to be soluble in halogenated solvents, allowing for the infrared spectrum to be recorded in a solution of CH_2Cl_2. Surprisingly, the *two* carbonyl ν_{CO} bands which were present in the [**Tm**W(CO)$_2$(≡CC≡CSiMe$_3$)] starting material had been retained,[***] but a clear shift from ν_{CO} 1981 and 1893 cm^{-1} in the starting complex

[***] Typically, halogenation of carbyne complexes of the form [M(CR)(CO)$_2$(L$_{fac}$)] results in complete oxidative decarbonylation, or on rare occasions to a monocarbonyl derivative.[54]

to ν_{CO} 2050 and 1990 cm^{-1} in the product was noted to be suggestive of oxidation of the metal centre.

Analysis by ^{1}H NMR revealed a similar signal pattern to that of the starting complex, albeit with a significant downfield shift applied to all signals, confirming that the silyl group remained and that the methimazolyl rings had not undergone halogenation.

The first clue as to what reaction had taken place was afforded by ESI mass spectrometry, which returned a positive match for an $[M+H]^{+}$ ion of molecular formula $C_{20}H_{25}BIN_6O_2S_3SiW$: indicating the addition of one iodine atom into the complex, however the facile ionisation of metal halides under ESI-MS conditions does not allow exclusion of the possibility of two iodo ligands.

Unequivocal structural characterisation was, however, made possible through single crystal X-ray diffractometry. Crystals suitable for structural determination (**Figure 2.9**) formed *via* vapour diffusion of petroleum spirit (40-60°C) into a saturated CH_2Cl_2 solution of the reaction precipitate at 4°C.

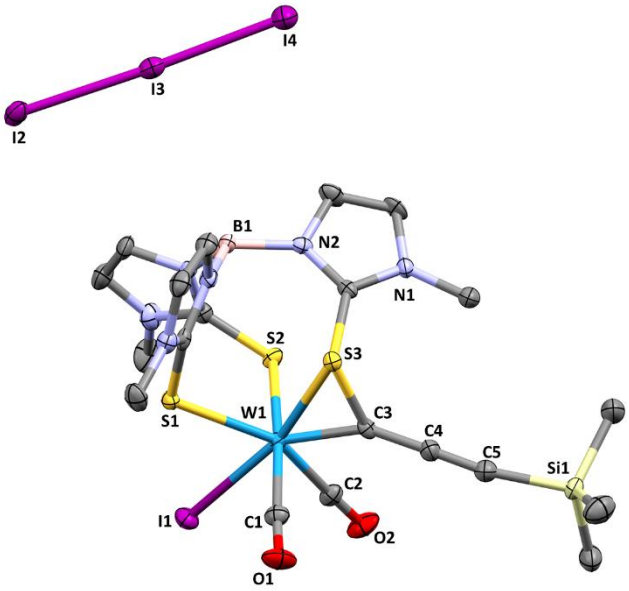

Figure 2.9. Molecular structure of [**Tm**W(CO)$_2$I(≡CC≡CSiMe$_3$)][I$_3$] (**2.6**) (50% displacement ellipsoids) with selected atom labels. Solvent molecules and hydrogen atoms omitted for clarity. Selected bond lengths (Å) and angles (°): W1–I1 2.8028(4), W1–C1 2.040(5), W1–C2 1.999(5), W1–S1 2.5568(12), W1–S2 2.5002(11), W1–S3 2.4922(11), W1–C3 1.951(4), S3–C3 1.766(5), C3–C4 1.381(6), C4–C5 1.219(7), C5–Si1 1.852(5); W1–S3–C3 51.10(14), W1–C3–C4 149.7(4), C3–C4–C5 176.8(6).

As suggested by the results obtained by high resolution mass spectrometry, the structure indeed displays the inclusion of one iodine atom coordinatively bound to the tungsten atom. The oxidative addition of the iodine atom is however accompanied by the rearrangement of the **Tm** cage, which nevertheless remains bound to tungsten *via* all three sulfur atoms. One thione donor however forms a bond to the carbyne-carbon which may be explained by the oxidation of the tungsten centre compromising retrodonation to the carbyne, thereby increasing the electrophilicity to facilitate migratory insertion. Notably, of the three W–S bond lengths, it is that of the thiolatocarbene that is shortest.

Crystals of [**Tm**W(CO)$_2$I(≡CC≡CSiMe$_3$)][I$_3$] (**2.6**) formed in the monoclinic space group P2$_1$/c (No. 14), with one equivalent of CH_2Cl_2 of solvation in the asymmetric unit. This composition and the bulk purity of the material was reflected through elemental analysis results, which were consistent with one equivalent of CH_2Cl_2. The iodine atom was found *trans* to the {C$_3$} fragment, causing the slippage of the methimazolyl arm *syn* to the {C$_3$} chain. The tungsten-sulfur bond length of the semi-bridging thione group was measured as 2.4922(11) Å, significantly shorter than the remaining tungsten-sulfur bonds. The carbyne carbon, may be described as having increased sp^2 character on account of the coordination of the semi-bridging methimazolyl thione group. This is manifested in the structure through the clear deviation of the previously near-linear W–C$^\alpha$–C$^\beta$ bond, which is now measured with a dihedral angle of 149.7(4)°. The more conventional η^2-thiolatocarbene complexes [W(CHSMe)(CO)$_2$(**Tp**)]$^+$ (W–S = 2.482 Å) and [W(CPhSMe)(CO)$_2$(Cp)]$^+$ (W–S = 2.428 Å) have slightly shorter W–S separations. The complex [Mo(SnMeCl$_2$)(CO)$_3$(**Bm**)] provides another example of a methimazolyl borate coordinating both the metal centre and an electrophilic co-ligand, in this case a dichlorostannyl ligand.

The failure of the metal oxidation to induce oxidative decarbonylation is noteworthy given that this is typically the outcome of halogenation of carbyne complexes of the form [W(≡CR)(CO)$_2$(L$_{fac}$)].[54] This may be attributed to the strong π-donor nature of the **Tm** ligand relative to other more conventional L$_{fac}$ ligands such as Cp, **Tp**, **Tp*** etc.

2.6.6 Synthesis of [TmW(CO)$_2${μ-≡CC≡C}(Au(PPh$_3$))]

Given the ease and scale at which the silylpropargylidyne complex [**Tm**W(CO)$_2$(≡CC≡CSiMe$_3$)] could be formed, it was decided that this should serve as a lead compound in the efforts towards forming **Tm**-ligated tricarbido complexes, examples of

which have not been previously reported. Prior reports have shown the **Tp** analogue of this complex to be very versatile in this regard, and a range of metal fragments (refer to **Section 2.5.1**) have been successfully added following *in situ* desilylation.

A mixture of [**Tm**W(CO)$_2$(≡CC≡CSiMe$_3$)] and [ClAu(PPh$_3$)] in CH_2Cl_2 was treated with TBAF and through a trial-and-error approach, it was noted that optimal results were obtained when TBAF was added slowly dropwise into the reaction mixture at room temperature, which in turn was stirred for 15 minutes. Longer reaction times (> 30 minutes) were found to result in the formation of intractable reaction mixtures containing unidentifiable products. Although the target complex [**Tm**W(CO)$_2${μ-≡CC≡C}(Au(PPh$_3$))] (**2.7**) (**Scheme 2.21**) proved to be unstable to silica-gel column chromatography, thin-layer chromatographic assay of the reaction mixture provided a suitable method for determining reaction progress, as the starting material complex [**Tm**W(CO)$_2$(≡CC≡CSiMe$_3$)] is visibly consumed over time.

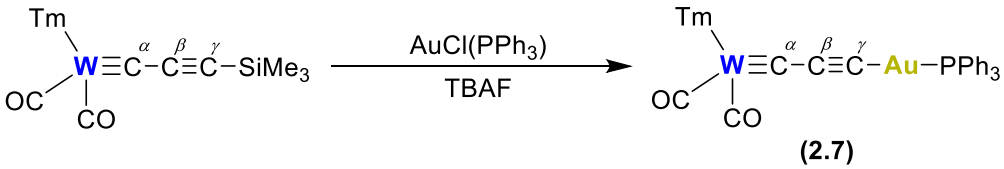

Scheme 2.21. Preparation of complex **2.7**.

After ensuring that the [**Tm**W(CO)$_2$(≡CC≡CSiMe$_3$)] complex had been consumed during the reaction, absolute ethanol was added and the mixture subjected to slow evaporation on a rotary evaporator. As the mixture was reduced in volume, this caused the target complex [**Tm**W(CO)$_2${μ-≡CC≡C}(Au(PPh$_3$))] to precipitate out of solution as an orange powder, which was subsequently isolated by filtration and washed liberally with absolute ethanol and *n*-pentane to ensure no traces of TBAF remained.

The complex [**Tm**W(CO)$_2${μ-≡CC≡C}(Au(PPh$_3$))] was found to be soluble in halogenated solvents, and was initially analysed *via* infrared spectroscopy in a solution of CH_2Cl_2. Compared to the silylpropargylidyne starting complex [**Tm**W(CO)$_2$(≡CC≡CSiMe$_3$)] (ν_{CO} 1981, 1893 cm^{-1}), the carbonyl bands recorded for the aurated complex [**Tm**W(CO)$_2${μ-≡CC≡C}(Au(PPh$_3$))] are found at lower wavenumbers: ν_{CO} 1965 and 1876 cm^{-1}, indicating an increase in the π-basicity of the tungsten centre. This may be rationalized by considering the additional electron density made available to the tungsten metal centre, as a result of the

newly installed electron rich gold centre at the opposite terminus of the conjugated {C_3} chain. In addition to the carbonyl absorbances, a weak stretching mode of the B–H bond is detectable (ν_{BH} 2434 cm^{-1}), but due to the relative isolation of this moiety on the **Tm** ligand backbone, it's value does not change between the silylpropargylidyne starting material and the aurated product.

The most diagnostic feature in the ^{1}H NMR spectrum of [**Tm**W(CO)$_2${μ-≡CC≡C}(Au(PPh$_3$))] which is implicit of product formation is the loss of the distinctive trimethylsilyl peak at δ_H 0.14 ppm found in the silylpropargylidyne starting material. Furthermore, signals corresponding to the phenyl C–H protons may now be observed in the region δ_H 7.53-7.43 ppm. All remaining signals may be attributed to the **Tm** ligand, whereby all three *exo*-CH_3 groups are independently resolved as individual peaks at δ_H 3.74, 3.72, and 3.56 ppm, and the methimazolyl heterocyclic C–H protons are detected within the range δ_H 6.85-6.76 ppm. Another source of evidence for product formation may be found in the form of $^{31}P\{^{1}H\}$ NMR spectroscopy. Direct comparison of the spectra obtained for [ClAu(PPh$_3$)] (δ_P 33.2 ppm) and [**Tm**W(CO)$_2${μ-≡CC≡C}(Au(PPh$_3$))] (δ_P 42.3 ppm) reveal a clear shift (**Figure 2.10**).

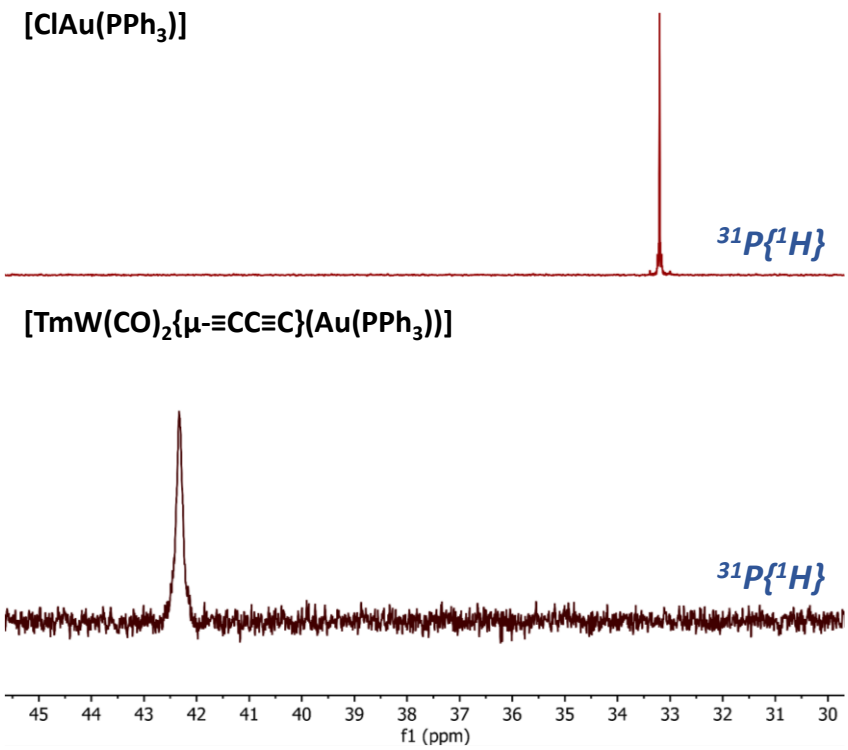

Figure 2.10. Stacked $^{31}P\{^{1}H\}$ NMR spectra of [ClAu(PPh$_3$)] and [**Tm**W(CO)$_2${μ-≡CC≡C}(Au(PPh$_3$))], displaying a clear shift of the $^{31}P\{^{1}H\}$ signal.

Although several attempts were made to record the $^{13}C\{^{1}H\}$ NMR spectrum of [**Tm**W(CO)$_2${μ-≡CC≡C}(Au(PPh$_3$))], it was found to precipitate out of common deuterated solvents over a period of one hour, and hence $^{13}C\{^{1}H\}$ NMR data remain elusive.

Given the likelihood of effective electronic communication between the tungsten and gold metal centres, the product complex was subjected to cyclic voltammetry. The complex [**Tm**W(CO)$_2${μ-≡CC≡C}(Au(PPh$_3$))] was dissolved in CH_2Cl_2 along with $[NBu_4][PF_6]$ electrolyte in a standard electrochemical cell. Using a platinum working electrode, the cyclic voltammogram of [**Tm**W(CO)$_2${μ-≡CC≡C}(Au(PPh$_3$))] was recorded at a scan rate of 100 mV s^{-1} and referenced to the ferrocene/ferrocenium redox couple (**Figure 2.11**).

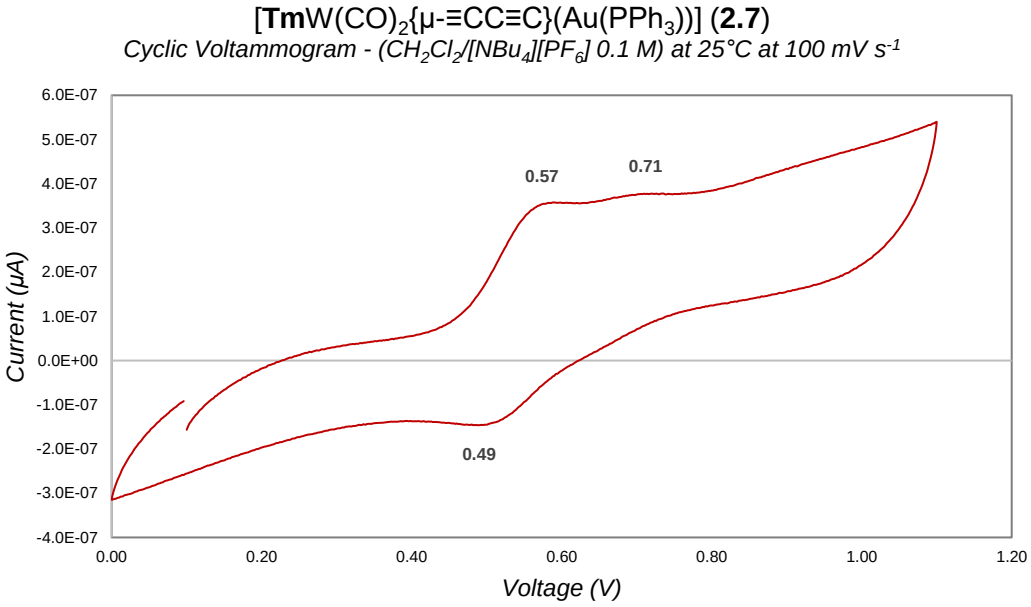

Figure 2.11. Cyclic voltammogram of the complex [**Tm**W(CO)$_2${μ-≡CC≡C}(Au(PPh$_3$))]. Referenced relative to the Ferrocene/Ferrocenium redox couple at 0.46 V *vs.* standard platinum working electrode.

The complex displays one distinct quasi-reversible redox pair, containing both an oxidation and reduction event at +0.57 V and +0.49 V, respectively. Based on these events, which may be assigned to the tungsten centre, an $E_{½}$ of +0.53 V may be calculated. Although only partly visible, a second oxidation event was detected at +0.71 V: believed to be associated with the gold centre. These assignments should only be treated as tentative, and have been made through the direct comparison of the results obtained for the complex [**Tm**W(CO)$_2${μ-CC≡C}(Rh(CO)(PPh$_3$)$_2$)] (see **Section 2.6.6**). It is noteworthy that during

the analysis of the analogous complex [**Tp**W(CO)$_2${μ-≡CC≡C}(Au(PPh$_3$))] *via* cyclic voltammetry, only two oxidation events were measured, and at markedly higher voltages (*cf.* +0.82 V and +0.89 V) compared to those measured for [**Tm**W(CO)$_2${μ-≡CC≡C}(Au(PPh$_3$))],[43] providing further evidence for the strong net donor capacity of the **Tm** *cf.* **Tp** ligands.

2.6.7 Synthesis of [TmW(CO)$_2${μ-≡CC≡C}(Rh(CO)(PPh$_3$)$_2$)]

Much like during the preparation of [**Tm**W(CO)$_2${μ-≡CC≡C}(Au(PPh$_3$))], the silylpropargylidyne complex [**Tm**W(CO)$_2$(≡CC≡CSiMe$_3$)] was once again utilised as a preformed alkylidynyl framework to form the tricarbido complex [**Tm**W(CO)$_2${μ-≡CC≡C}(Rh(CO)(PPh$_3$)$_2$)]. Under an atmosphere of argon, the complexes [**Tm**W(CO)$_2$(≡CC≡CSiMe$_3$)] and *trans*-[RhCl(CO)(PPh$_3$)$_2$] were combined in anhydrous and degassed CH_2Cl_2 and the mixture treated with TBAF. Over multiple attempts, it was noted that the slow, dropwise addition of TBAF affords the best results, whereas rapid addition tends to lead to intractable product mixtures. After stirring the mixture for 30 minutes at room temperature, absolute ethanol was added, and the crude product mixture subjected to slow evaporation on a rotary evaporator. This caused the target complex [**Tm**W(CO)$_2${μ-CC≡C}(Rh(CO)(PPh$_3$)$_2$)] (**2.8**) (**Scheme 2.22**) to precipitate out of solution as a brown powder.

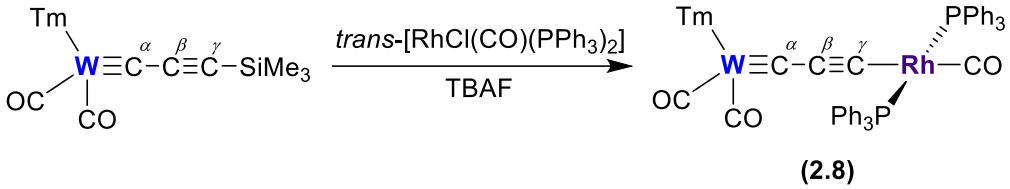

Scheme 2.22. Preparation of complex **2.8**.

Infrared spectroscopy revealed three carbonyl bands at ν_{CO} 1973, 1940, and 1863 cm^{-1} (CH_2Cl_2) which may be assigned to ν(WCO), ν(RhCO), and ν(WCO) stretching modes, respectively. These assignments may be reinforced by the observations made for the analogous **Tp**-ligated complex [**Tp**W(CO)$_2${μ-≡CC≡C}(Rh(CO)(PPh$_3$)$_2$)], which similarly displayed a triad of carbonyl stretching frequencies at ν_{CO} 1979, 1945, and 1872 cm^{-1}, corresponding to ν(WCO), ν(RhCO), and ν(WCO) stretching modes, respectively.[38] The lower value of the ν_{CO} absorption associated with the rhodium carbonyl indicates that the

increased donor strength of **Tm** *cf.* **Tp** is transmitted along the tricarbido spine to the rhodium centre.

The ^{1}H NMR spectrum (CD_2Cl_2) confirmed the desilylation process with loss of the characteristic $SiMe_3$ singlet, and the presence of phenyl signals in the region of δ_H 7.69-7.41 ppm gave a clear indication of product formation. However, it appeared that the product mixture contained additional phosphine-containing compounds, as the number of phenyl protons which were detected were in excess of those which were required. Furthermore, when the sample was analysed *via* $^{31}P\{^{1}H\}$ NMR spectroscopy, in addition to the doublet centred about δ_P 30.2 ppm which corresponded to the [**Tm**W(CO)$_2${μ-CC≡C}(Rh(CO)(PPh$_3$)$_2$)] product, a singlet was also detected at δ_P 27.3 ppm, which indicated the presence of triphenylphosphine oxide (**Figure 2.11**).

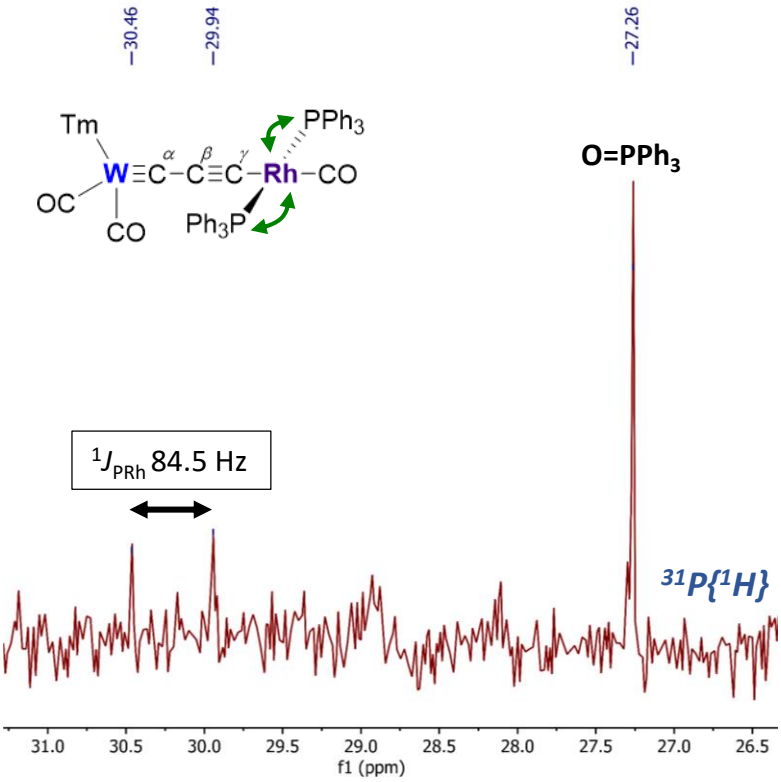

Figure 2.11. $^{31}P\{^{1}H\}$ NMR spectrum (CD_2Cl_2) of the reaction mixture containing [**Tm**W(CO)$_2${μ-≡CC≡C}(Rh(CO)(PPh$_3$)$_2$)] and triphenylphosphine oxide impurity.

All attempts to remove the triphenylphosphine impurity were exhausted, and given the small quantity of product-containing material which had been isolated spectroscopic characterisation was prioritised over continuing attempts to purify the sample.

It is noteworthy that the $^{31}P\{^{1}H\}$ NMR spectrum of the previously reported complex [**Tp**W(CO)$_2${μ-≡CC≡C}(Rh(CO)(PPh$_3$)$_2$)] also displayed a doublet centred about δ_P 32.1 ppm, albeit with a significantly larger coupling constant of $^{1}J_{PRh}$ 109 Hz (both recorded as CD_2Cl_2 solutions).

High resolution mass spectrometry revealed the desired product as the $[M]^+$ ion at m/z 1282.1, closely matching the simulated isotope pattern calculated for a complex with the formula $C_{54}H_{46}BN_6O_3P_2RhS_3W$. Regrettably, even after several attempts, satisfactory elemental microanalytical data could not be obtained. However, this is not overly surprising given that NMR data revealed the presence of additional phosphine sources in the product mixture.

The $^{13}C\{^{1}H\}$ NMR spectrum of [**Tm**W(CO)$_2${μ-≡CC≡C}(Rh(CO)(PPh$_3$)$_2$)] was recorded in CD_2Cl_2, and displayed features which were broadly similar to the analogous **Tp**-ligated complex.[38] The carbyne carbon (W≡C$^{\alpha}$) was detected at δ_C 253.7 ppm, as the most downfield signal in the spectrum. Characteristic for **Tm**-ligated complexes, the diastereotopic carbonyl (CO) ligands bound to the tungsten atom provided two resonances at δ_C 226.6 and 222.3 ppm, but the carbonyl ligand bound to the rhodium centre could not be identified in the spectrum due to insufficient signal-to-noise. Of the remaining signals detected in the $^{13}C\{^{1}H\}$ NMR spectrum, many were associated with the aromatic carbon atoms making up the PPh_3 phenyl rings, some of which appeared as virtual triplets confirming the *trans*-Rh(PPh$_3$)$_2$ geometry. However, with reference to the NMR data recorded for [**Tp**W(CO)$_2${μ-≡CC≡C}(Rh(CO)(PPh$_3$)$_2$)] (CD_2Cl_2: δ_C 258.3 C$^{\alpha}$, 128.8 C$^{\beta}$, and 133.3 C$^{\gamma}$ ppm), it was possible to identify the signals at δ_C 128.5 and 134.8 as the C$^{\beta}$ and C$^{\gamma}$ and nuclei, respectively.

Crystals of [**Tm**W(CO)$_2${μ-≡CC≡C}(Rh(CO)(PPh$_3$)$_2$)] formed in the triclinic space group P-1 (No. 2) by vapour diffusion of *n*-hexane into a saturated CH_2Cl_2 solution at 4°C (**Figure 2.12**).

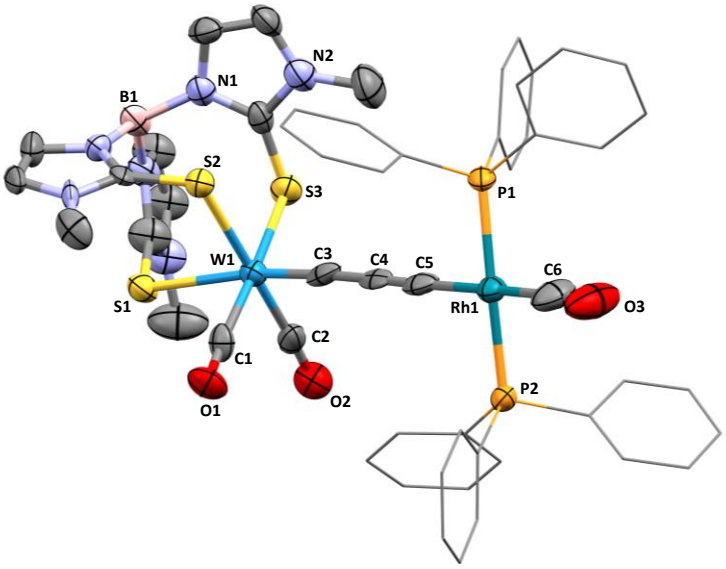

Figure 2.12. Molecular structure of [**Tm**W(CO)$_2${μ-≡CC≡C}(Rh(CO)(PPh$_3$)$_2$)] (50% displacement ellipsoids) with selected atom labels. Solvent molecules and hydrogen atoms omitted, and phenyl rings have been simplified for clarity. Selected bond lengths (Å) and angles (°): W1–C1 1.995(10), W1–C2 1.914(14), W1–S1 2.663(3), W1–S2 2.577(3), W1–S3 2.542(2), W1–C3 1.800(13), C3–C4 1.406(16), C4–C5 1.251(15), C5–Rh1 1.982(14), Rh1–C6 1.806(16), Rh1–P1 2.303(2), Rh1–P2 2.304(3); W1–C3–C4 174.9(8), C3–C4–C5 178.0(12), C4–C5–Rh1 178.4(8), C5–Rh1–P1 84.7(3), C5–Rh1–P2 91.5(3), C5–Rh1–C6 176.9(6).

Structural data shows that the bridging {C$_3$} chain displays a near-linear arrangement, with a dihedral angle of 178.0° along its length. Furthermore, the bond lengths along the chain are reflective of the alternating multiple- and single-bonds present, and do not indicate any discernible cumulenic bonding character. The tungsten carbon (W≡C$^{\alpha}$) triple bond (1.800(13) Å) is similar to the other propargylidyne complexes formed in this work. Meanwhile, the rhodium carbon bond (Rh–C$^{\gamma}$) was measured with a distance of 1.982(14) Å, which is somewhat shorter than found in the conventional alkynyl complex [Rh(C≡CPh)(CO)(PPh$_3$)$_2$] (2.039 Å) which perhaps points towards a degree of Rh-C multiple bonding.

Much like the tungsten/gold tricarbido complex discussed in **Section 2.6.5**, cyclic voltammetry was performed with [**Tm**W(CO)$_2${μ-≡CC≡C}(Rh(CO)(PPh$_3$)$_2$)] in CH_2Cl_2 with [NBu$_4$][PF$_6$] as supporting electrolyte. Using a platinum working electrode, the cyclic voltammogram of [**Tm**W(CO)$_2${μ-≡CC≡C}(Rh(CO)(PPh$_3$)$_2$)] was recorded at a scan rate of 100 mV s^{-1} and referenced to the ferrocene/ferrocenium redox couple (**Figure 2.13**).

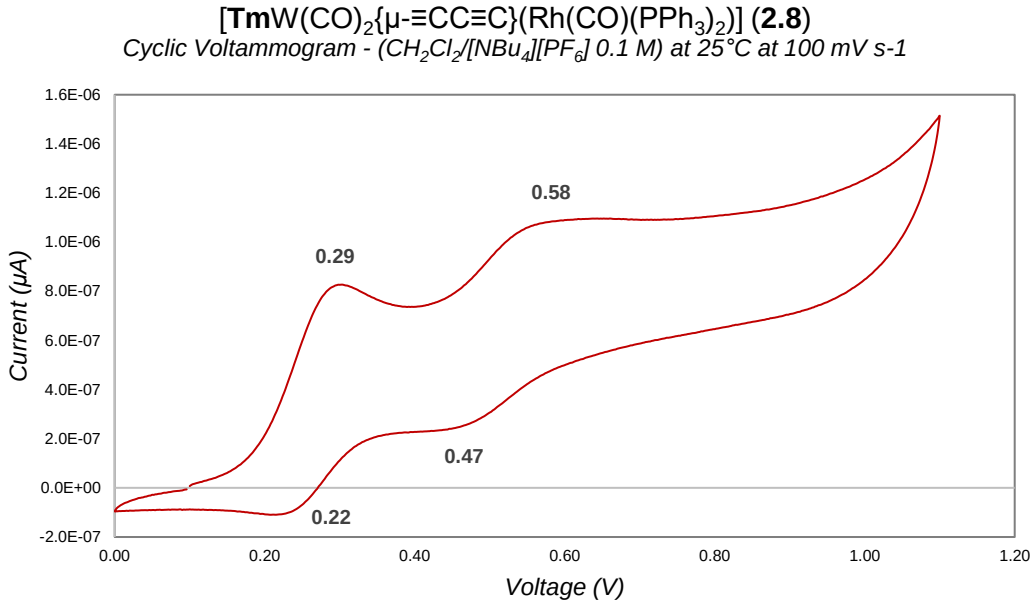

Figure 2.13. Cyclic voltammogram of the complex [**Tm**W(CO)$_2${μ-≡CC≡C}(Rh(CO)(PPh$_3$)$_2$)]. Referenced relative to the Ferrocene/Ferrocenium redox couple at 0.46 V *vs.* standard platinum working electrode.

Unlike the cyclic voltammogram for the tungsten/gold tricarbido complex, the cyclic voltammogram for [**Tm**W(CO)$_2${μ-≡CC≡C}(Rh(CO)(PPh$_3$)$_2$)] clearly shows two redox couples with $E_{½}$ values of +0.26 V and +0.53 V. Since the latter redox couple is also present in the cyclic voltammogram of the complex [**Tm**W(CO)$_2${μ-≡CC≡C}(Au(PPh$_3$))], it can be immediately assigned to events occurring at the tungsten centre. Therefore, by extension of this reasoning, the former redox couple may be assigned to events occurring at the rhodium atom. Although the analogous [**Tp**W(CO)$_2${μ-≡CC≡C}(Rh(CO)(PPh$_3$)$_2$)] complex has been previously reported, no electrochemical data have been recorded,[38] though it was shown that the rhodium centre was susceptible to oxidative addition processes.

2.6.8 Attempted Synthesis of other Tricarbido Complexes

As highlighted in **Section 2.5.1**, tricarbido complexes have been previously reported of the form [**Tp***W(CO)$_2${μ-≡CC≡C}(ML$_n$)] (M = Ru,[36,43] Rh,[38] Ir,[39] Hg,[44] Au[37,43]). Given the limited success noted above through the preparation of the complexes [**Tm**W(CO)$_2${μ-≡CC≡C}(Au(PPh$_3$))] and [**Tm**W(CO)$_2${μ-≡CC≡C}(Rh(CO)(PPh$_3$)$_2$)], efforts were made to try and mirror this series of known **Tp***-ligated complexes using the **Tm** ligand.

In a manner identical to that described for the preparation of complexes [**Tm**W(CO)$_2${μ-≡CC≡C}(Au(PPh$_3$))] and [**Tm**W(CO)$_2${μ-≡CC≡C}(Rh(CO)(PPh$_3$)$_2$)], a solution of [**Tm**W(CO)$_2$(≡CC≡CSiMe$_3$)] with an appropriate metal complex containing a metal-halogen bond was prepared at room temperature. Through the addition of various desilylating agents, a range of mixed bimetallic tricarbido complexes were synthetically targeted. To try and find a higher yielding route through which tricarbido complex formation could still be facilitated, desilylation conditions such as AgF,[55] alkali metal fluorides,[56,57] CsF,[58] K_2CO_3,[59] and Cs_2CO_3[60] were trialled in some selected examples. A summary of the reactions which were trialled are detailed in **Scheme 2.23**.

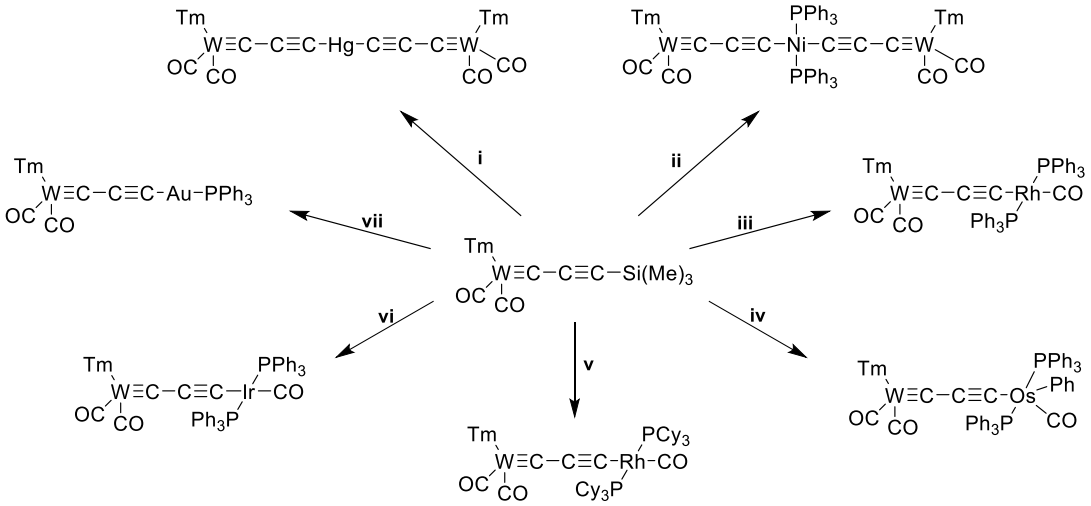

Scheme 2.23. Attempted synthesis of various bridged- and terminal-tricarbido complexes. *Conditions*: **(i)** $HgCl_2$: TBAF, CH_2Cl_2, RT, 15 min. **(ii)** $NiBr_2(PPh_3)_2$: TBAF, CH_2Cl_2, RT, 15 min; or, AgF, MeOH, RT, 16 h; or, K_2CO_3, MeOH, RT, 3 h. **(iii)** *trans*-[RhCl(CO)(PPh$_3$)$_2$]: AgF, (1:1) MeOH/THF, RT, 16 h. **(iv)** OsCl(Ph)(CO)(PPh$_3$)$_2$: TBAF, CH_2Cl_2, RT, 10 min. **(v)** *trans*-[RhCl(CO)(PCy$_3$)$_2$]: TBAF, CH_2Cl_2, RT, 15 min. **(vi)** *trans*-[IrCl(CO)(PPh$_3$)$_2$]: CsF, THF, RT, 1 h. **(vii)** AuCl(PPh$_3$): KF, (1:1) MeOH/THF, RT, 2 h; or, Cs_2CO_3, MeCN, RT, 20 h.

In addition to probing alternative synthetic routes to Au-, Ir-, and Rh-tricarbido complexes, pathways to Hg- and Ni-bridged complexes, and the Os-tricarbido complex [**Tm**W(CO)$_2${μ-≡CC≡C}(Os(Ph)(CO)(PPh$_3$)$_2$)] were also investigated. Overall, none of the reactions which were attempted afforded the desired tricarbido complex. In some reactions, [**Tm**W(CO)$_2$(≡CC≡CSiMe$_3$)] starting material was recovered, but in most cases an intractable mixture of products was obtained.

2.7 Summary

Through the oxide abstraction synthetic protocol, a library of propargylidyne complexes were formed, which feature the previously underreported **Tm** ligand. Notably, the complex [**Tm**W(CO)$_2$(≡CC≡CSiMe$_3$)] was prepared in excellent yields and on multi-gram scales. This allowed for it to serve as a lead compound in further work. Given the incorporation of the trimethylsilyl functional group, this complex served as an excellent candidate for the preparation of mixed bimetallic tricarbido complexes through an *in situ* desilylation and metalation approach.

The use of the desilylating agent TBAF was found to be effective in the removal of the trimethylsilyl functional group from the complex [**Tm**W(CO)$_2$(≡CC≡CSiMe$_3$)]. This allowed for the terminus of the {C$_3$} chain to be capped with Au- and Rh- fragments, thereby forming new **Tm**-ligated tricarbido complexes [**Tm**W(CO)$_2${μ-≡CC≡C}(Au(PPh$_3$))] and [**Tm**W(CO)$_2${μ-≡CC≡C}(Rh(CO)(PPh$_3$)$_2$)]. These tricarbido complexes represent the first examples of **Tm** ligated 'carbon wire' bimetallics. Although attempts were made to form various other tricarbidos through the use of TBAF and other previously reported desilylating agents, no other complexes of this form were successfully prepared.

2.8 Chapter 2 - References

1. Manzano, R. A., Hill, A. F., *Advance in Organometallic Chemistry*, **2019**, *72*, 103.

2. Hill, A. F., Manzano, R. A., *Dalton Trans.*, **2019**, *48*, 6596.

3. Falcao, E. H. L., Wudl, F., *J. Chem. Tech. & Biotech.*, **2007**, *82*, 524.

4. Lagow, R. J., Kampa, J. J., Wie, H.-C., Battle, S. L., Genge, J. W., Laude, D. A., Harper, C. J., Bau, R., Stevens, R. C., Haw, J. F., Munson, E., *Science*, **1995**, *267*, 362.

5. Vejpravová, J., Benito, A. M., *Nanomaterials*, **2021**, *11*, 2469.

6. Kasálková, N. S., Slepička, P., Švorčík, V., Rodríguez-Ramos, I., Al-Haik, M., *Nanomaterials*, **2021**, *11*, 2368.

7. Lang, H., *Angew. Chem. Int. Ed. Engl.*, **1994**, *33*, 547.

8. Bunz, U. H. F., *Angew. Chem. Int. Ed. Engl.*, **1996**, *35*, 969.

9. Bruce, M. I., *Coord. Chem. Rev.*, **1997**, *166*, 91.

10. Bruce, M. I., Low, P. J., *Advance in Organometallic Chemistry*, **2004**, *50*, 179.

11. Wendinger, D., Tykwinski, R. R., *Acc. Chem. Res.*, **2017**, *50*, 1468.

12. Fischer, E. O., Kreis, G., Kreiter, C. G., Mulle, J., Huttner, G., Lorenz, H., *Angew. Chem.*, **1973**, *85*, 618.

13. Hill, A. F., Manzano, R. A., *Angew. Chem. Int. Ed.*, **2019**, *58*, 15354.

14. Hill, A. F., Manzano, R. A., *Angew. Chem. Int. Ed.*, **2019**, *58*, 7357.

15. Fischer, E. O., Kalder, H. J., Kohler, F. H., *J. Organomet. Chem.*, **1974**, *81*, C23.

16. Hart, I. J., Hill, A. F., Stone, F. G. A., *J. Chem. Soc., Dalton Trans.*, **1989**, *2*, 2261.

17. Fischer, E. O., Hollfelder, H., Friedrich, P., Kreissl, F. R., Huttner, G., *Angew. Chem. Int. Ed. Engl.*, **1977**, *16*, 401.

18. Fischer, E. O., Walz, S., Wagner, W. R., *J. Organomet. Chem.*, **1977**, *134*, C37.

19. McDermott, G. A., Dorries, A. M., Mayr, A., *Organometallics*, **2002**, *6*, 925.

20. Fischer, H., Fischer, E. O., *J. Organomet. Chem.,* **1974**, *69*, C1.

21. Schwenzer, B., Schleu, J., Burzlaff, N., Karl, C., Fischer, H., *J. Organomet. Chem.*, **2002**, *641*, 134.

22. Reinholdt, A., Bendix, J., *Chem. Rev.*, **2022**, *122*, 830.

23. Vyboishchikov, S. F., Frenking, G., *Chem. Eur. J.*, **1998**, *4*, 1439.

24. Kim, H. P., Angelici, R. J., *Advances in Organometallic Chemistry*, **1987**, *27*, 51.

25. Mayr, A., Hoffmeister, H., *Advances in Organometallic Chemistry*, **1991**, *32*, 227.

26. Kostic, N. M., Fenske, R. F., *J. Am. Chem. Soc.,* **1981**, *103*, 4677.

27. McLain, S. J., Wood, C. D., Messerle, L. W., Schrock, R. R., Hollander, F. J., Youngs, W. J., Churchill, M. R., *J. Am. Chem. Soc.*, **1978**, *100*, 5962.

28. Nugent, W. A., Mayer, J. M., *Metal-Ligand Multiple Bonds: The Chemistry of Transition Metal Complexes Containing Oxo, Nitriddo, Inido, Alkylidene, or Alkylidyne Ligands*, Wiley – Interscience, **1988**.

29. Weng. W., Ramsden, J. A., Arif, A. M., Gladysz, J. A., *J. Am. Chem. Soc.*, **1993**, *115*, 3824.

30. Bartik, T., Weng, W., Ramsden, J. A., Szafert, S., Falloon, S. B., Arif, A. M., Gladysz, J. A., *J. Am. Chem. Soc.*, **1998**, *120*, 11071.

31. Dembinski, R., Szafert, S., Haquette, P., Lis, T., Gladysz, J. A., *Organometallics*, **1999**, *18*, 5438.

32. Woodworth, B. E., Templeton, J. L., *J. Am. Chem. Soc.*, **1996**, *118*, 7418.

33. Desmond, T., Lalor, F. J., Ferguson, G., Parvez, M., *J. Chem. Soc., Chem. Commun.*, **1983**, *8*, 457.

34. Schwenzer, B., Fischer, H., *J. Organomet. Chem.*, **2003**, *667*, 16.

35. Sun, H., DiMagno, S. G., *J. Am. Chem. Soc.*, **2005**, *127*, 2050.

36. Dewhurst, R. D., Hill, A. F., Smith, M. K., *Angew. Chem. Int. Ed.*, **2004**, *43*, 476.

37. Dewhurst, R. D., Hill, A. F., Smith, M. K., *Organometallics*, **2005**, *24*, 5576.

38. Dewhurst, R. D., Hill A. F., Willis, A. C., *Organometallics*, **2004**, *23*, 5903.

39. Dewhurst, R. D., Hill, A. F., Willis, A. C., *Organometallics*, **2004**, *23*, 1646.

40. Hill, A. F., Manzano, R. A., Sharma, M., Ward, J. S., *Organometallics*, **2015**, *34*, 361.

41. Dewhurst, R. D., Hill, A. F., Willis, A. C., *Chem. Commun.*, **2004**, *24*, 2826.

42. Frogley, B. J., Hill, A. F., Onn, C. S., *Dalton Trans.*, **2019**, *48*, 11715.

43. Bruce, M. I., Cole, M. L., Gaudio, M., Skelton, B. W., White, A. H., *J. Organomet. Chem.*, **2006**, *691*, 4601.

44. Dewhurst, R. D., Hill, A. F., Willis, A. C., *Chem, Commun,*, **2004**, *24*, 2826.

45. Hill, A. F., Manzano, R. A., Ward, J. S., *Dalton Trans.*, **2018**, *47*, 14621.

46. Cordiner, R. L., Hill, A. F., Wagler, J., *Organometallics*, **2008**, *27*, 5177.

47. Armitt, D. J., Bruce, M. I., Gaudio, M., Zaitseva, N. N., Skelton, B. W., White, A. H., le Guennic, B., Halet, J. F., Fox, M. A., Roberts, R. L., Hartl, F., Low, P. J., *Dalton Trans.*, **2008**, *47*, 6763.

48. Borren, E. S., Hill, A. F., Shang, R., Sharma, M., Willis, A. C., *J. Am. Chem. Soc.*, **2013**, *135*, 4942.

49. Delpozo, J., Carrasco, D., Pérez-Temprano, M. H., García-Melchor, M., Álvarez, R., Casares, J. A., Espinet, P., *Angew. Chem. Int. Ed.*, **2013**, *52*, 2189.

50. Woodworth, B. E., White, P. S., Templeton, J. L., *J. Am. Chem. Soc.*, **1997**, *119*, 828.

51. Manzano, R. A., Hill, A. F., Georgelin, R. L., *Chem. Commun.*, **2020**, *56*, 14597.

52. Sonogashira, K., *J. Organomet. Chem.*, **2002**, *653*, 46.

53. Mark, M. R., Hill, A. F., White, A. J. P., Williams, D. J., *Organometallics*, **2003**, *22*, 3831.

54. Filippou, A. C., Fischer, E. O., *J. Organomet. Chem.,* **1988**, *349*, 367.

55. Kim, S., Kim, B., In, J., *Synthesis*, **2009**, *12*, 1963.

56. Filatov, M. A., Cheprakov, A. V., Beletskaya, I. P., *Eur. J. Org. Chem.*, **2007**, *21*, 3468.

57. Bellina, F., Carpita, A., Mannocci, L., Rossi, R., *Eur. J. Org. Chem.*, **2004**, *12*, 2610.

58. Capani, J. S., Cochran, J. E., Liang, J., *J. Org. Chem.,* **2019**, *84*, 9378.

59. Kusaka, S. I., Dohi, S., Doi, T., Takahashi, T., *Tetrahedron Lett.*, **2003**, *44*, 8857.

60. Jiang, Z. Y., Wang, Y. G., *Tetrahedron Lett.*, **2003**, *44*, 3859.

CHAPTER 3.

PAH FUNCTIONALISED METALLOCARBYNE COMPLEXES

3.1 Introduction to Polycyclic Aromatic Hydrocarbon-containing Complexes

Polycyclic aromatic hydrocarbons (PAHs) are a homologous of organic compounds which contain a number of ring-fused conjugated carbocyclic rings.[1,2] Typically, compounds of this type exist as planar structures, but several examples of 'curved' PAH compounds have been reported in recent years.[3,4] It is widely known that, in addition to exhibiting potent carcinogenic effects,[5,6] such compounds exhibit notable optical and electronic properties, such as fluorescence emission and, under some circumstances, phosphorescent properties.[7,8] Predominantly, these physical phenomena come about due to the highly conjugated nature of the carbocyclic rings. Even in some of the simplest PAHs, such as naphthalene, its fluorescent properties are easily observed when it is dissolved in solution. As the number of ring fused carbocycles increase within a compound, the intensity of the optical properties which the compound exhibits increases significantly, thereby prompting significant interest in the application of these types of compounds in various fields, including solar cells,[9,10] organic field effect transistors,[11–14] and light emitting diodes.[15–19]

3.2 Background and Scope

Until very recently, polycyclic fused aromatic hydrocarbons bearing a single carbyne substituent were incredibly rare, with only naphthyl derivatives arising *via* the Fischer method,[20] or by treating the dichlorocarbene complexes $[M(=CCl_2)Cl_2(CO)(PPh_3)_2]$ (M = Ru, Os) with 1- or 2-naphthyllithium to furnish $[M(\equiv C(C_{10}H_7))Cl(CO)(PPh_3)_2]$.[21]

In recent years, the field has been expanded, predominantly as a result of work carried out by A. F. Hill and co-workers, with the report of a series of poly(carbyne) functionalised PAH tungsten complexes.[22] Complexes of this type were formed using an adapted Stille cross coupling protocol, featuring the stannylcarbyne $[\mathbf{Tp^*}(CO)_2W(\equiv CSnBu_3)]$[23,24] and a range of halogenated PAH compounds. Given the success observed with this preparative method, a similar reaction route was adopted herein to prepare two of the final complexes reported in this Chapter.

3.3 Results & Discussion: Routes to PAH Functionalised Metallocarbyne Complexes

Of the complexes formed within this Chapter, and in congress with the majority of the materials formed in this Thesis, the oxide abstraction protocol served as the predominant route through which many complexes were prepared.

A series of monobrominated polycyclic aromatic hydrocarbons were commercially sourced and were individually treated with *n*-butyllithium solution to afford the activated mono-lithiated species. Through the addition of either molybdenum or tungsten hexacarbonyl, followed by treatment with trifluoroacetic anhydride and the addition of either **Tm** or **Htt**, several different complexes bearing a range of polycyclic aromatic hydrocarbons were formed.

Of the remaining complexes which were not prepared *via* this route, some were accessed through the use of late common intermediates, such as the bis(γ-picoline) complex $[Br(pic)_2(CO)_2W{\equiv}C(Mes)]$.[25] Through this route, it was possible to easily access complexes functionalised with the **Bm** and **Hbt** ligands, which, in the case of the former, has proven to be a more difficult synthetic target than it's analogous tridentate homologue. In order to form the remaining complexes in this Chapter, the careful post-synthetic modification of previously formed complexes was required. In some cases, the complexes which were isolated were not the intended target materials. However, as is ever the case in the chemical sciences, serendipity can play a major role in the discovery of new materials. For some of the latter complexes in this Chapter, they serve as quintessential examples of this widely acknowledged principle, and the full details relating to each of these complexes have been included therein.

3.3.1 Summary of Spectral Features – Chapter 3 Complexes

Complex No.	Metal Centre	Ligand	Liquid IR (cm^{-1})		$^{11}B\{^1H\}$ NMR (ppm)	$^{13}C\{^1H\}$ NMR					
			ν_{BH}	ν_{CO}		$M{\equiv}C^{\alpha}$ (ppm)	$^1J_{MC}$ (Hz)	M(CO) (ppm)	$^1J_{MC}$ (Hz)	C^{β} (ppm)	$^2J_{MC}$ (Hz)
3.1	W	**Bm**	2437	1986, 1904	42.55	–	–	–	–	–	–
3.2	W	**Tm**	2431	1966, 1874	48.32	284.1	196.5	225.4, 220.9	173.7, 168.9	145.2	39.4
3.3	W	**Hbt**	–	1996, 1917	-10.25	–	–	–	–	–	–

3.4	W	**Htt**	–	1981, 1894	-2.75						
3.5	W	**Tm**	–	1971, 1880	48.38	264.2	197.4	223.7, 218.8	170.5, 163.7	155.3	49.9
3.6	W	**Tm**	2435	1970, 1879	48.44	279.5	192.6	223.8, 219.2	171.4, 165.2	146.9	41.7
3.7	Mo	**Tm**	2434	1984, 1900	48.47	290.3	–	226.5, 222.1	–	143.0	–
3.8	W	**Tm**	2435	1970, 1880	48.26	279.5	–	233.8, 219.2	–	145.3	–
3.9	Mo	**Tm**	–	1984, 1900	48.49	290.2	–	226.6, 222.1	–	141.4	–
3.10	W	**Tm**	–	1970, 1880	48.38	279.4	–	225.1, 220.8	–	141.9	–
3.11	Mo	**Tm**	2400	1984, 1901	48.56	291.8	–	228.2, 224.0	–	138.6	–
3.12	W	**Tm**	–	1969, 1880	48.34	280.0	–	224.1, 219.6	–	144.7	–
3.13	Mo	**Tm**	2399	1983, 1900	48.51	–	–	–	–	–	–
3.14	W	**Tm**	–	1969, 1879	48.38						
3.15	Mo	**Tm**	2400	1983, 1899	48.54	290.1	–	226.9, 222.4	–	142.8	–
3.16	W	**Tm**	2435	1979, 1891	-1.65						
3.17	W	**Tm**	–	1978, 1891	–	246.5	203.8	225.2, 220.0	168.9, 160.5	118.9	–
3.18	W	**Tm**	–	1978, 1891	–	247.1	–	225.1, 220.0	–	117.8	–
3.19	W	**Tm**	–	1969, 1878	–	–	–	–	–	–	–
3.20	W	**Tp***	2554	1973, 1882	40.95	271.9	187.5	224.1	165.4	160.2	44.3
3.21	W	**Tp***	2554	1974, 1883	40.69	271.9	–	224.1	–	160.2	–
3.22	W	**Tm**	2435	1969, 1880	48.48	279.5	196.2	225.1, 220.9	172.2, 165.7	141.9	40.3
3.23	W	**Tm**	2411	1972, 1884	48.28	277.4	196.2	225.0, 220.7	171.1, 164.6	142.4	40.3
3.24	W	**Tm**	–	1971, 1870	48.55	–	–	–	–	–	–
3.25	W	**Tm**	–	1972, 1884	48.45	277.5	197.4	225.0, 220.7	171.3, 165.6	142.4	40.7
3.26 *	W	**Tm**	–	1945, 1923, 1808	–	–	–	224.9, 220.2	–	–	–
3.27 *	W	**Tm**, **Tp***	–	1974, 1966, 1884	48.41	282.0, 279.3	–	227.6, 227.5, 225.4, 220.8	–	–	–
3.28 **	W, Mo	**Tm**, **Tp***	–	1987, 1970, 1903, 1884	–	249.1, 278.2	–	229.3, 229.2, 225.2, 220.5	–	145.1, 142.3	–

* $^{13}C\{^{1}H\}$ NMR data measured at -40°C. | ** $^{13}C\{^{1}H\}$ NMR data measured at -50°C. | Liquid IR spectra measured in CH_2Cl_2.

Table 3.1. Summary of selected spectral data for the complexes detailed in Chapter 3.

3.3.2 Synthesis of [(L_{fac})W(CO)$_2${≡C-(Mesityl)}] (L_{fac} = Bm, Tm, Hbt, Htt)

Carbyne complexes which serve as late common intermediates often contain moieties which may be easily displaced when in the presence of more strongly coordinating ligands. Prime examples of such complexes in the field of organometallic carbyne chemistry include those ligated with γ-picoline ligands, which when bound to a metal centre along with a sufficiently labile halogen atom may undergo ligand substitution with various Scorpionate pro-ligands. In this regard, the complex [Br(pic)$_2$(CO)$_2$W≡C(Mesityl)] (pic = γ-picoline)[25] has been previously used to form a range of Scorpionate-functionalised carbyne complexes. During the course of the work herein, the aforementioned tungsten complex was successfully reacted with all four of the main Scorpionate ligand systems used in this thesis (**Bm**, **Tm**, **Hbt** and **Htt**) to form the mesityl-functionalised complexes [**Bm**W(CO)$_2${≡C-(Mesityl)}] (**3.1**), [**Tm**W(CO)$_2${≡C-(Mesityl)}] (**3.2**), [(**Hbt**)W(CO)$_2${≡C-(Mesityl)}] (**3.3**) and [(**Htt**)W(CO)$_2${≡C-(Mesityl)}] (**3.4**) (**Scheme 3.1**).

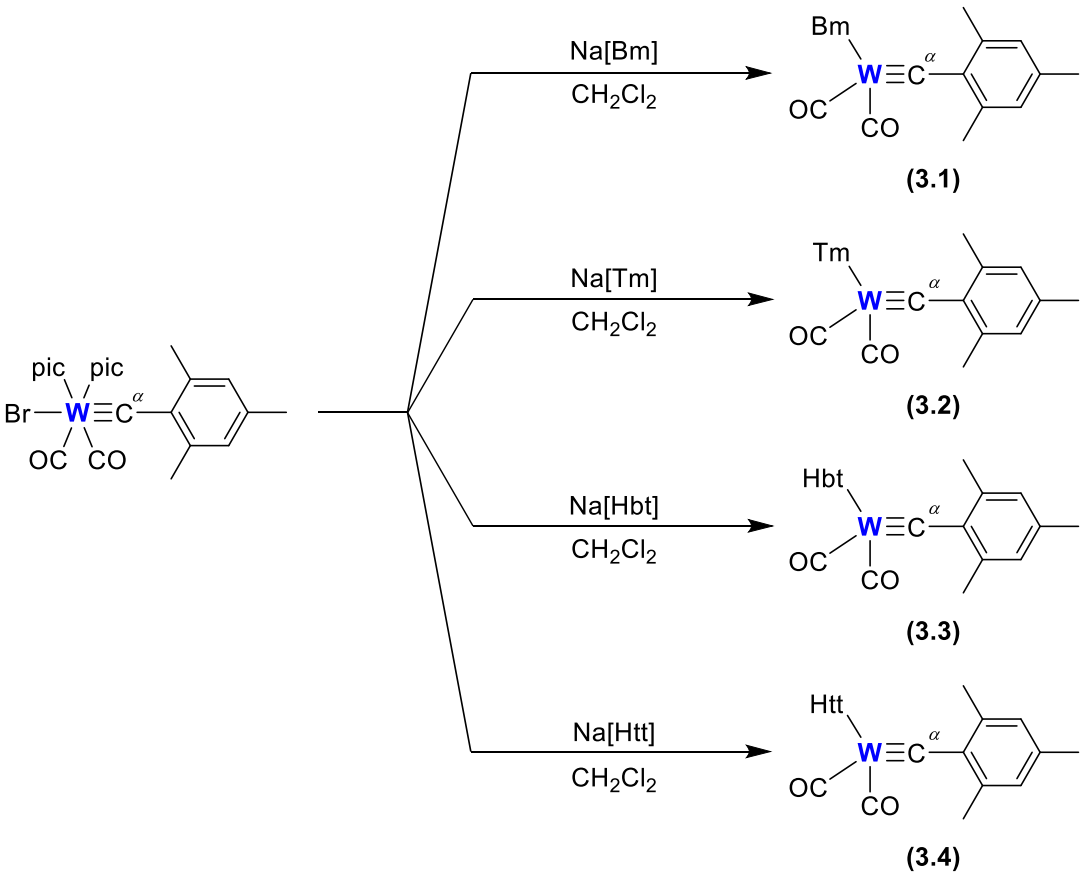

Scheme 3.1. Preparation of complexes **3.1**, **3.2**, **3.3**, and **3.4**.

All four complexes were formed through the stoichiometric addition of the relevant Scorpionate ligand to a CH_2Cl_2 solution of $[Br(pic)_2(CO)_2W{\equiv}C(Mesityl)]$ at room temperature. After a few hours of stirring, spectroscopically pure samples of complexes **3.1** and **3.2** were isolated in moderate-to-good yields *via* silica gel column chromatography, eluting with CH_2Cl_2.

The reaction mixtures containing complexes **3.3** and **3.4** required longer reaction times compared to that of complexes **3.1** and **3.2.** This may be rationalised by consideration of the bulkier nature of the **Hbt** and **Htt** pro-ligands, which are furnished with two and three *exo*-$(C(CH_3)_3)$ groups, respectively, and hence it may be inferred that longer reaction times may be necessary in order to arrange the bulkier groups about the metal centre. After 12 hours of stirring at room temperature, a spectroscopically pure sample of complex **3.3** was isolated *via* silica gel column chromatography, eluting with CH_2Cl_2. Meanwhile, in order to obtain a sample of complex **3.4** of sufficient purity for spectral characterisation, neutral alumina was used in conjunction with CH_2Cl_2 eluent.

All samples were found to exhibit an orange colour in the solid state, and did not display any appreciable decomposition over extended periods of time at room temperature. As an added precaution, complexes **3.1** – **3.4** were stored in sealed sample vials in air at -20°C, although this was not deemed to be critical to maintaining their purity. All samples were found to be readily soluble in halogenated solvents, and therefore were initially probed *via* solution infrared spectroscopy as CH_2Cl_2 solutions. Irrespective of the Scorpionate ligand used to form the complexes, all displayed two individually resolved carbonyl bands within the region ν_{CO} 1996-1874 cm^{-1}. A weak B-H band was also detected for all complexes, with the exception of complex **3.3**, and took on typical values within the range ν_{BH} 2431-2529 cm^{-1}. It should be noted that a weak band at ν 2505 cm^{-1} was detected for complex **3.3**, but due to the noise within the baseline of the sample it cannot be stated with certainty that this band originates at the {B-H} fragment.

The ^1H NMR spectra for all complexes were recorded as $CDCl_3$ solutions at room temperature. For complex **3.1**, the spectrum which was obtained displayed an excellent signal-to-noise ratio, so much so that the three-centre two-electron B–H–W interaction which is inferred in the structure was detected as a broad signal centred at approximately δ_H -2.50 ppm. The two *exo*-CH_3 groups on the **Bm** ligand backbone were detected as a single signal at δ_H 3.56 ppm, as well as the cyclic alkene protons in the spectral range δ_H 6.76-6.70 ppm. Of the remaining signals, all correlated to the mesityl ligand. The two mesityl C–H

protons bound to the aromatic ring were detected at δ_H 6.80 ppm as a singlet, and the protons bound to the three CH_3 groups were found to be split over two signals at δ_H 2.49 and 2.17 ppm. The former was calculated to have a relative integration of six protons, and therefore could only correspond to the two CH_3 groups positioned *ortho*- to the {W≡C} carbyne fragment. Resultingly, the latter signal was assigned to the CH_3 group oriented *para*- to the {W≡C} group.

The ^{1}H NMR spectrum of complex **3.1** was also recorded as a CD_2Cl_2 solution at room temperature, and revealed and identical array of signals, including the notable B–H–W three-centre two-electron interaction.

Complex **3.2** afforded a similarly highly detailed ^{1}H NMR spectrum. In contrast to that recorded for complex **3.1**, the spectrum contained a higher degree of resolution, which was evident upon inspection of the **Tm** ligand's heterocyclic C-H proton signals in the range δ_H 6.89-6.77 ppm, which were all detected as doublets. Likewise, the three *exo*-CH_3 groups of the **Tm** ligand were individually resolved as three singlets over the range δ_H 3.77-3.62 ppm. All protons bound to the mesityl ligand were found in an identical arrangement to that of complex **3.1**.

For the complexes bearing the **Hbt** and **Htt** ligands, the ^{1}H NMR spectra tend to be much more spartan compared to their methimazolyl-based analogues. This is as a result of the bulkier *exo*-$(C(CH_3)_3)$ groups on their ligand backbones and the loss of the heterocyclic C-H protons on account of the substitution of the carbon atoms with nitrogen. Complex **3.3** afforded a clean spectrum with a detectable B–H–W agostic interaction at δ_H -2.24 ppm. The only other signal which could be assigned to the **Hbt** ligand was the singlet at δ_H 1.81 ppm, corresponding to the two *exo*-$(C(CH_3)_3)$ groups. In a pattern identical to that for complexes **3.1** and **3.2**, three signals were assigned to the mesityl ligand. The most downfield of which belonging to the ring-bound C–H protons, followed by the two CH_3 groups *cis*- to the {W≡C} carbyne, and finally the CH_3 group *trans*- to the {W≡C} fragment.

The ^{1}H NMR spectrum for complex **3.4** displayed an identical signal pattern for the mesityl ligand which has been detailed for complexes **3.1**-**3.3**. The three *exo*-$(C(CH_3)_3)$ groups on the **Htt** ligand were individually resolved as three singlets in the spectral range δ_H 1.94-1.79 ppm.

The presence of complexes **3.1**-**3.4** was partially affirmed through the use of ESI mass spectrometry. Complex **3.1** was found to afford an isotope pattern consistent with the $[M+H]^+$ ion with an m/z ratio of 611.0941, consistent with a complex ion of formula $C_{20}H_{24}BN_4O_2S_2W$. Complex **3.2** was successfully detected with a range of fragments which included $[M]^+$, $[M\text{-}CO]^+$ and $[M\text{-}2(CO)]^+$. Meanwhile, complexes **3.3** and **3.4** were detected as $[M+H]^+$ and $[M+Na]^+$ ions, respectively. The bulk purity of the samples was further reinforced with elemental microanalytical results. All complexes returned results which matched those calculated for their molecular formulae devoid of any solvation.

The $^{13}C\{^1H\}$ NMR spectra of complexes **3.1** and **3.3** could not be recorded, on account of their tendency to precipitate out of common deuterated solvents over several hours. However, the $^{13}C\{^1H\}$ NMR spectra of complexes **3.2** and **3.3** were successfully recorded at room temperature using $CDCl_3$ solutions. In general terms, the characteristic features with both spectra were found to be very similar. The most downfield signals corresponded to the carbyne carbon ($W\equiv C^{\alpha}$) nuclei and those forming the diastereotopic carbonyl ligands. Of those remaining, the signal patterns observed may be considered typical for complexes bearing this assortment of Scorpionate ligands, as well as the mesityl ligand.

Unfortunately, unequivocal structural determination of each complex could not be carried out. All attempts to form crystals suitable for structural determination were unsuccessful, even after multiple attempts.

3.3.3 Synthesis of [TmW(CO)$_2${≡C-(Thienyl)}]

Although the 2-thienyl ligand is not itself a PAH, it has been noted previously in literature that thienyl-based polymers are prone to exhibit notable electronic and optical properties;[26,27] much like those found in many of the larger PAH's. The thienyl ligand was incorporated into a **Tm** functionalised tungsten carbyne through the oxide abstraction synthetic protocol, which afforded the complex [**Tm**W(CO)$_2${≡C-(Thienyl)}] (**3.5**) (**Scheme 3.2**).

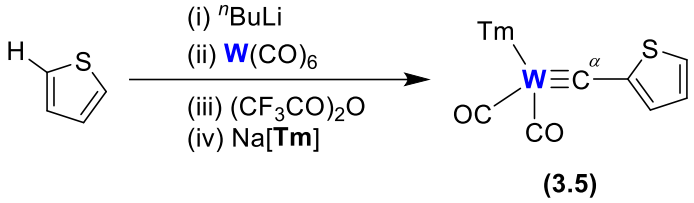

(3.5)

Scheme 3.2. Preparation of complex **3.5**.

The crude reaction mixture containing complex **3.5** was purified through the use of silica gel column chromatography. Once the reaction had been halted and concentrated to dryness, the brown residues were loaded on to a purification column using a small volume of CH_2Cl_2. Prior to this, the column was packed a mixture of 8:2 (v/v) CH_2Cl_2 and petroleum spirits (40-60 °C), and subsequently this solvent mixture was also used to elute the target complex off the column. Steady elution resulted in the development of a major red band which traversed down the column. Once collected and concentrated to dryness, it was shown that through various spectroscopic techniques that the material isolated was that of complex **3.5**. Complex **3.5** displayed good stability in the solid form, but as a precaution, was sealed in a sample vial and stored at -20 °C. Over an extended period of time (*ca.* >3 months) under these conditions, no significant decomposition of the material was noted.

Complex **3.5** was first analysed *via* infrared spectroscopy as a CH_2Cl_2 solution. This revealed two intense carbonyl bands at ν_{CO} 1970 and 1880 cm^{-1}, but the anticipated B–H vibration could not be detected.

The ^{1}H NMR spectrum of complex **3.5** was recorded in a solution of $CDCl_3$ at room temperature, and confirmed the presence of the target material. Three sets of signals could be assigned to the thienyl ligand, which had now been installed on the terminus of the metallocarbyne chain. Signals at δ_H 7.09, 6.97 and 6.79 ppm could be assigned to the thienyl ligand on account of their relative integrations of one hydrogen atom each. Of the remaining signals in the spectrum, all corresponded to the **Tm** ligand, and were found to be present in a typical manner, whereby the cyclic alkene protons located on the heterocyclic rings of **Tm** were detected as an array of signals over the spectral range δ_H 6.88-6.81 ppm, and the three *exo*-CH_3 groups were individually resolved as three singlets at δ_H 3.75, 3.71 and 3.61 ppm.

A range of ion fragments of complex **3.5** were detected using ESI mass spectrometry. Three ions of *m*/*z* 630.0175, 687.0142 and 708.9962 were found to closely correspond to the isotope patterns and values calculated for the [M-2(CO)]$^+$, [M+H]$^+$ and [M+Na]$^+$ ions of

complex **3.5**, respectively. Furthermore, elemental microanalysis returned results which further bolstered confidence in the bulk purity of the sample containing complex **3.5**, as the elemental composition values which were obtained closely matched those calculated for the title complex.

Analysis of complex **3.5** *via* $^{13}C\{^{1}H\}$ NMR spectroscopy afforded a plethora of NMR data, which included a great deal of coupling information. The $^{13}C\{^{1}H\}$ NMR spectrum was recorded as a $CDCl_3$ solution at room temperature, and aside from the presence of some minor solvent signals it was found to be of very good purity. In a characteristic manner, the most downfield signal present in the spectrum was assigned to the carbyne carbon ($W\equiv C^{\alpha}$) atom at δ_C 264.2 ppm with a single bond carbon-tungsten coupling constant of 197.4 Hz. Likewise, both carbonyl carbon atoms were found at δ_C 223.7 and 218.8 ppm with single bond carbon-tungsten coupling constants of 170.5 and 163.7 Hz, respectively. The abundance of coupling information allowed for the easy identification of the carbyne-bound thienyl carbon atom (C^{1}), which was assigned to the signal at δ_C 155.3 ppm with clear tungsten satellites coupling to a signal with a magnitude of 49.9 Hz. The remaining thienyl carbon atoms were detected over the spectral range δ_C 128.1-125.5 ppm. Of the remaining signals, all could be assigned to the **Tm** ligand.

Attempts to form crystals suitable for unequivocal structural determination proved unsuccessful, even after several repeated attempts. Hence, single crystal X-ray diffraction data for complex **3.5** remains to be elusive.

3.3.4 Synthesis of [TmM(CO)$_2${≡C-(1-Naphthyl)}] (M = Mo, W)

In the series of mono-brominated PAH precursors which were utilised in this Chapter, 2-bromonaphthalene served to be the smallest within the series. Two metallocarbyne complexes bearing the 2-naphthyl ligand were successfully prepared about tungsten and molybdenum centres: [**Tm**W(CO)$_2${≡C-(1-Naphthyl)}] (**3.6**) and [**Tm**Mo(CO)$_2${≡C-(1-Naphthyl)}] (**3.7**) (**Scheme 3.3**).

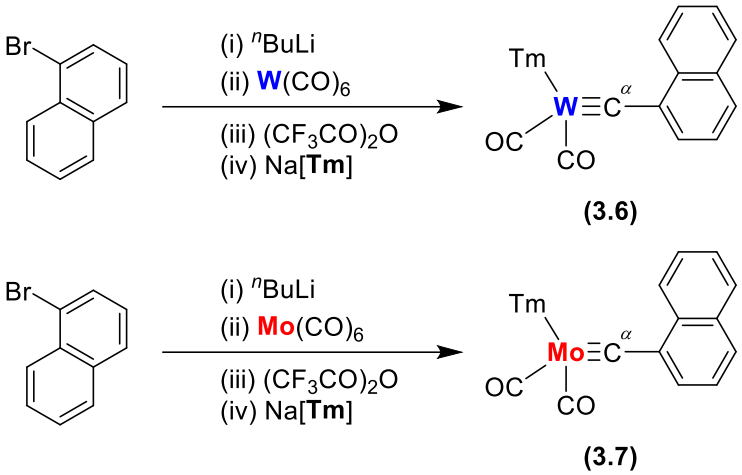

Scheme 3.3. Preparation of complexes **3.6** and **3.7**.

Following the preparation of the crude reaction mixtures containing complexes **3.6** and **3.7**, both were individually purified *via* silica gel column chromatography, eluting with CH_2Cl_2. In both cases, a major red band was observed to form on the column, which was then collected and concentrated to afford complex **3.6** and complex **3.7** in moderate and good yield, respectively. As expected, both complexes displayed good stability in the solid form under ambient conditions. However, in order to arrest any potential degradation processes, both samples were stored in sealed sample vials at -20 °C.

Both title complexes were found to be easily soluble in halogenated solvents. Hence, initial testing was carried out *via* infrared spectroscopy using CH_2Cl_2 solutions. The spectrum recorded for complex **3.6** was found to contain two very intense carbonyl bands at ν_{CO} 1970 and 1879 cm^{-1}. In addition to this, the weak B–H stretch associated with the bridgehead boron atom on the **Tm** ligand was also detected at ν_{BH} 2435 cm^{-1}. Similarly, the carbonyl bands for complex **3.7** were detected at ν_{CO} 1984 and 1900 cm^{-1}, alongside the weak B–H stretch at ν_{BH} 2434 cm^{-1}.

The ^1H NMR spectra for both complexes were recorded as $CDCl_3$ solutions at room temperature. In both cases, the spectra clearly displayed the incorporation of both the **Tm** ligand and the naphthyl substituent into the complexes. In the case of complex **3.6**, the signals associated with the **Tm** ligand were found to have adopted an arrangement commonly encountered in these types of complexes. Each *exo*-CH_3 group was identifiable in the spectrum at approximately δ_H 3.7 ppm, albeit with two signals closely overlapping at δ_H 3.64 ppm. The cyclic alkene protons on the backbone of **Tm** were found to be completely resolved and neatly grouped over the spectral range δ_H 6.91-6.82 ppm. All of the remaining

signals were assigned to the naphthyl ligand, which took on values between δ_H 7.51-7.30 ppm, with the exception of one signal which was shifted downfield to δ_H 8.88 ppm. Conveniently, the spectrum obtained for complex **3.7** afforded a similar arrangement of signals when analysed *via* ^{1}H NMR spectroscopy.

Both samples were analysed using ESI mass spectrometry, and were found to produce a number of complex ions. Complex **3.6** was detected as $[M+H]^+$ and $[M+Na]^+$ ions, with isotope patterns consistent with complexes of the formulae $C_{25}H_{24}BN_6O_2S_3W$ and $C_{25}H_{23}BN_6NaO_2S_3W$, respectively. Meanwhile, complex **3.7** afforded a single identifiable fragment, which was identified as the $[M+Na]^+$ ion of formula $C_{25}H_{23}BMoN_6NaO_2S_3$. The bulk purity of the samples containing complexes **3.6** and **3.7** were tested through elemental microanalysis. The elemental composition of complex **3.6** was found to closely match values calculated for the complex without solvation. However, the results for complex **3.7** were found to be more agreeable once one equivalent of THF had been included.

As far as reasonably practicable, efforts were made to individually assign each carbon atom located on the PAH ring within the $^{13}C\{^1H\}$ NMR spectra of all complexes herein. Assignments were made with the help of 2D ^{13}C NMR experiments (*e.g.* ^{13}C-^1H HMBC, ^{13}C-^1H HSQC) commonly encountered in literature. For complex **3.6**, the majority of the ring-bound PAH carbon atoms were detected in the spectral range δ_C 133-124 ppm. However, one outlying signal at δ_C 146.9 ppm was unequivocally assigned as the PAH carbon atom bound to the carbyne chain (*i.e.* WC^{β}) since tungsten satellites flanked this signal, and were calculated to have a two-bond carbon-tungsten coupling of approximately 42 Hz. Coupling information was also extracted for the signals correlated to the carbyne carbon ($W{\equiv}C^{\alpha}$) (δ_C 279.5 ppm) and the two diastereotopic carbonyl ligands (δ_C 223.8 and 219.2 ppm).

A similar signal pattern for complex **3.7** was found upon inspection of its $^{13}C\{^1H\}$ NMR spectrum. Most of the napthyl-carbon atoms produced signals clustered around δ_C 133-124 ppm, and once again the WC^{β} carbon atom was easily identifiable due to its noticeable downfield shift (δ_C 143.0 ppm), relative to all the other PAH carbon signals. Since complex **3.7** contained an NMR silent molybdenum centre, no coupling information could be extracted from the spectrum.

For both complexes, attempts to form crystals suitable for unequivocal structural determination proved unsuccessful, even after several repeated attempts. Hence, single crystal X-ray diffraction data for complexes **3.6** and **3.7** remain to be elusive.

3.3.5 Synthesis of [TmM(CO)$_2${≡C-(9-Phenanthryl)}] (M = Mo, W)

The addition of another six-membered aromatic ring to naphthalene affords a thrice ring-fused structure. When one of these three rings is positioned out of linearity of the other two, this affords the PAH phenanthrene. In order to incorporate this phenanthrene into a Scorpionate-functionalised metallocarbyne, the mono-halogenated variant, 9-bromophenanthrene, was used in the oxide abstraction synthetic protocol to prepare the complexes [**Tm**W(CO)$_2${≡C-(9-Phenanthryl)}] (**3.8**) and [TmMo(CO)$_2${≡C-(9-Phenanthryl)}] (**3.9**) (**Scheme 3.4**).

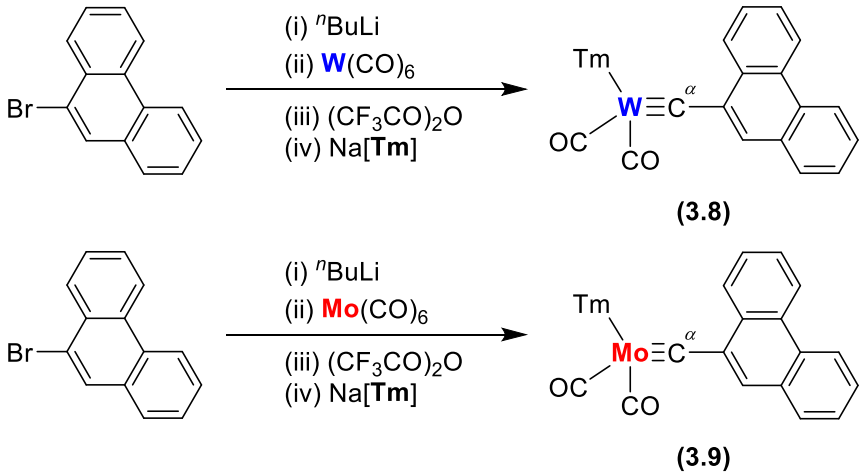

Scheme 3.4. Preparation of complexes **3.8** and **3.9**.

A sample of complex **3.8** suitable for spectral characterisation was isolated through the use of silica gel column chromatography. The crude reaction mixture containing complex **3.8** was concentrated to dryness and the resulting residues were extracted with a small volume of CH_2Cl_2 and loaded onto a purification column. The column was continuously eluted with CH_2Cl_2, which led to a major red band developing from the baseline of the silica gel. Subsequent isolation and concentration of this band afforded complex **3.8** as a red powder in moderate yield.

Similarly, a suitable sample of complex **3.9** was isolated following silica gel column chromatography. A CH_2Cl_2 solution containing the residues of the crude reaction mixture were loaded onto the column, and in order to separate out the target complex, a 4:1 (v/v) mixture of CH_2Cl_2/petroleum spirit (40-60 °C) was used to elute the column. Two red bands were observed to traverse down the column, the second of which to be collected was found

to contain complex **3.9**. Concentration of this sample to dryness afforded complex **3.9** as a red powder in low yield.

Solution infrared spectroscopy of both complexes afforded very similar spectra. In both cases, the most conspicuous features were the two carbonyl ligands, detected at ν_{CO} 1970 and 1880 cm^{-1} for complex **3.8**, and ν_{CO} 1984 and 1900 cm^{-1} for complex **3.9**. Furthermore, the B–H bond within each complex was detected in both samples, and corresponded to stretches at ν_{BH} 2435 and 2434 cm^{-1} for complex **3.8** and complex **3.9**, respectively.

The ^{1}H NMR spectra of complexes **3.8** and **3.9** were measured as $CDCl_3$ solutions at room temperature. For complex **3.8**, all of the most downfield signals in the range δ_H 9.04-7.49 ppm were assigned to the phenanthryl ligand. The heterocyclic C-H protons bound to the backbone of the **Tm** ligand were detected as several signals over the range δ_H 6.92-6.83 ppm and, finally, the three *exo*-CH_3 groups were individually resolved as three singlets at δ_H 3.83, 3.66 and 3.65 ppm. In a trend which will be repeated throughout this Chapter, both complexes were found to afford closely matching signal patterns. As a result of this, the spectral details for complex **3.9** will not be discussed in detail, in order to avoid repetitive descriptions.

ESI mass spectrometry was used to analyse samples of complexes **3.8** and **3.9**. Complex **3.8** was confirmed to be present within the sample as a complex ion of formula $C_{29}H_{25}BN_6O_2S_3W$, and was found to closely coincide with the isotope pattern calculated for a $[M - e^-]^+$ fragment of complex **3.8**. Complex **3.9** was successfully detected as a $[M+Na]^+$ ion, which matched the isotope pattern of a complex with the formula $C_{29}H_{25}BMoN_6NaO_2S_3$. Furthermore, elemental microanalysis of both samples returned results which could be easily matched to both complexes.

The $^{13}C\{^{1}H\}$ NMR spectrum of complex **3.8** was recorded as a $CDCl_3$ solution at room temperature. Although the signals within the spectrum displayed good signal-to-noise ratios, no tungsten satellites were detected for any of the suitable signals, and no coupling information could be extracted. The most downfield signal at δ_C 279.5 ppm was assigned to the carbyne carbon ($W{\equiv}C^{\alpha}$), and the carbon atoms associated with the carbonyl ligands were individually detected nearby at δ_C 223.8 and 219.2 ppm. The signals associated with the phenanthryl ligand were found over the spectral range δ_C 132-123 ppm, just downfield of the heterocyclic C-H protons on the backbone of the **Tm** ligand, which were detected over

the range δ_C 129-120 ppm. The only outlying signal which could be assigned to the phenanthryl ligand was that at δ_C 145.3 ppm, which was assigned to the atoms bound to the carbyne carbon (WC^{β}). The spectrum which was obtained for complex **3.9** displayed a similar arrangement of signals. As a result, to avoid repetitive descriptions, the intrinsic details for complex **3.9** will not be discussed.

3.3.6 Synthesis of [TmM(CO)$_2${≡C-(9-Anthracenyl)}] (M = Mo, W)

Much like phenanthrene, anthracene contains three ring-fused six-membered rings. However, a linear arrangement is adopted in the case of anthracene. The mono-brominated PAH compound 9-bromoanthracene was used to form two metallocarbyne complexes, assembled around tungsten and molybdenum centres: [**Tm**W(CO)$_2${≡C-(9-Anthracenyl)}] (**3.10**) and [**Tm**Mo(CO)$_2${≡C-(9-Anthracenyl)}] (**3.11**) (**Scheme 3.5**).

Samples of both complexes **3.10** and **3.11** were isolated following purification *via* silica gel column chromatography. The reaction mixtures containing the respective title complexes were concentrated to dryness and the resulting residues were extracted with a small volume of CH_2Cl_2. The solvated residues were loaded onto the columns and continuously eluted with CH_2Cl_2, thereby allowing complexes **3.10** and **3.11** to be isolated in low-to-moderate yields as brown and black/brown powders, respectively. Both samples were found to be air stable in the solid form, and hence were stored in sealed sample vials under an aerobic atmosphere. However, in order to arrest any potential degradation processes, both samples were stored at -20 °C.

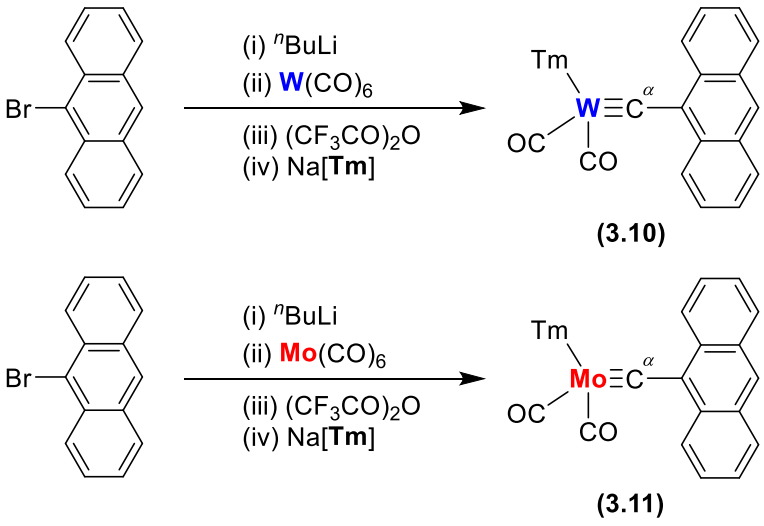

Scheme 3.5. Preparation of complexes **3.10** and **3.11**.

Both complexes were found to be readily soluble in halogenated solvents, and hence were initially analysed using infrared spectroscopy as CH_2Cl_2 solutions. In the case of complex **3.10**, the only noteworthy features which were detected in the spectrum related to the two carbonyl ligands, which were detected at ν_{CO} 1970 and 1880 cm^{-1}. Meanwhile, for complex **3.11**, in addition to the carbonyl ligands being detected at ν_{CO} 1984 and 1901 cm^{-1}, the B–H stretch of the **Tm** ligand was detected at ν_{BH} 2400 cm^{-1}.

The ^1H NMR spectra of both complexes **3.10** and **3.11** were successfully recorded as $CDCl_3$ solutions at room temperature. Although the intricate details of which differ from those recorded for the phenanthryl-ligated complexes which were discussed in the previous section, the features within these spectra are very similar. Hence, in order to avoid repetitive descriptions, a full analysis of the spectra recorded for complexes **3.10** and **3.11** has been omitted. Instead, readers are directed to the preceding section relating to complexes **3.8** and **3.9**, as well as the Experimental section.

Samples isolated containing complexes **3.10** and **3.11** was partially assured through ESI mass spectrometry. A complex ion, calculated to closely match the isotope pattern for a complex of formula $C_{29}H_{25}BN_6NaO_2S_3W$, was found to correspond to the $[M+Na]^+$ fragment for complex **3.10**. An analogous ion was detected for complex **3.11** which closely matched the simulated isotope pattern for a complex with the formula $C_{29}H_{25}BMoN_6NaO_2S_3$.

The $^{13}C\{^1H\}$ NMR spectra which were recorded for both complexes were found to contain a similar arrangement of signals. Hence, in order to avoid repetitive descriptions, only the details pertaining to complex **3.10** have been included below. The $^{13}C\{^1H\}$ NMR spectrum of complex **3.10** was recorded as a $CDCl_3$ solution at room temperature. Although a good signal-to-noise ratio was obtained, no coupling data could be extracted from the spectrum. Expectedly, the most downfield signal at δ_C 279.4 ppm was assigned to the carbyne carbon ($W{\equiv}C^{\alpha}$), and both carbonyl carbon atoms were detected as individually resolved signals at δ_C 225.1 and 220.8 ppm. With reference to the previously synthesised PAH metallocarbyne complexes, the carbon atom within the anthracenyl ligand which is bound directly to the carbyne carbon (*i.e.* WC^{β}) was found to be clearly segregated from the rest. While the majority of the anthracenyl carbon atoms were detected over the spectral range δ_C 133-125 ppm, the atom bound the carbyne carbon was detected further downfield at δ_C 141.9 ppm.

3.3.7 Synthesis of [TmM(CO)$_2${≡C-(1-Pyrenyl)}] (M = Mo, W)

Pyrene is a PAH consisting of four ring-fused six-membered rings, arranged in a diamond configuration. By using the mono-halogenated derivative 1-bromopyrene, it is possible to synthesise the complexes [**Tm**W(CO)$_2${≡C-(1-Pyrenyl)}] (**3.12**) and [**Tm**Mo(CO)$_2${≡C-(1-Pyrenyl)}] (**3.13**) (**Scheme 3.6**) through the previously described oxide abstraction protocol.

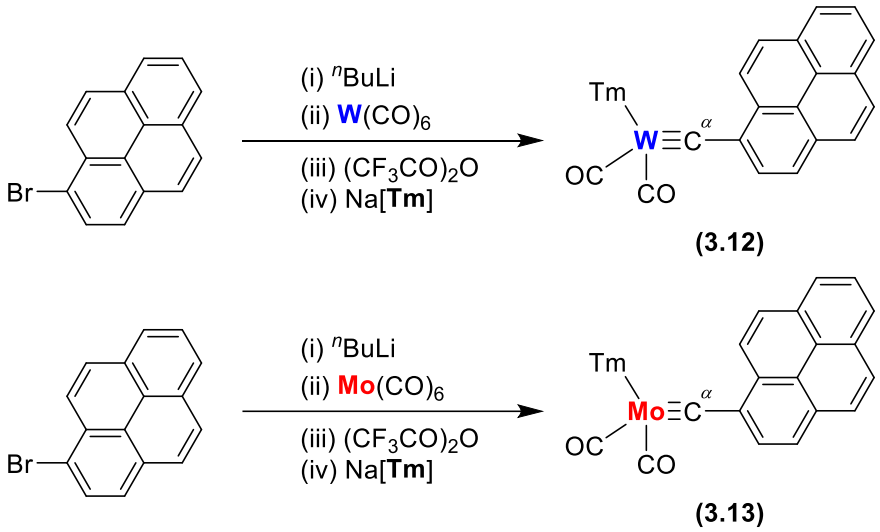

Scheme 3.6. Preparation of complexes **3.12** and **3.13**.

Both complexes **3.12** and **3.13** were isolated from their respective reaction mixtures following purification *via* silica gel column chromatography. When each column was continuously eluted with a 2:1 (v/v) mixture of CH_2Cl_2 and petroleum spirit (40-60 °C), an orange/brown band developed from the baseline. Once collected and concentrated to dryness to afford brown powders, it was proven through spectroscopic analysis that these samples consisted of complexes **3.12** and **3.13**. While in the solid form, both samples were stable under aerobic conditions. However, in order to arrest any potential degradation, both samples were stored in sealed vials at -20 °C.

Solution infrared spectroscopy was initially used to analyse both complexes, given the ease at which they dissolved in CH_2Cl_2. The spectrum recorded for complex **3.12** displayed two carbonyl bands at ν_{CO} 1969 and 1880 cm^{-1}, and likewise these functional groups were also detected for complex **3.13** at ν_{CO} 1983 and 1900 cm^{-1}. However, the B–H stretch of the **Tm** ligand in complex **3.13** was also detected at ν_{BH} 2399 cm^{-1}.

The ^{1}H NMR spectra of both complexes were recorded as $CDCl_3$ solutions at room temperature. Complex **3.12** afforded a spectrum which clearly displayed the incorporation of the **Tm** ligand and the pyrenyl PAH in the complex. The latter was detected as several signals over the spectral range δ_H 8.14-7.92 ppm, with another signal occurring further downfield at δ_H 9.12 ppm. All remaining signals were assigned to the **Tm** ligand, whereby the heterocyclic C-H protons were detected as a series of signals over the spectral range δ_H 6.92-6.83 ppm, and the three *exo*-CH_3 groups as three singlets at δ_H 3.83, 3.68 and 3.67 ppm. A similar arrangement of signals were observed in the spectrum of complex **3.13**. The only appreciable difference (aside from the chemical shifts) which may be noted is the coalescence of the two most upfield signals corresponding to the *exo*-CH_3 groups. Generally, this is a feature which is commonly encountered, and is not implicit of any underlying intramolecular interactions within complex **3.13**.

Results from ESI mass spectrometry was successfully used to detect complex **3.12** as two separate ion fragments corresponding to complexes of the formulae $C_{31}H_{26}BN_6O_2S_3W$ and $C_{30}H_{25}BN_6OS_3W$, thereby matching those expected for the $[M+H]^+$ and $[M-CO]^+$ ions of this complex. Two ion fragments were also successfully identified for complex **3.13**, which were shown to closely match the isotope patterns associated with $[M-2(CO)]^+$ and $[M+Na]^+$ fragments. Regrettably, the bulk purity of complex **3.12** could not be ensured, as an agreeable elemental microanalysis result could not be obtained. Similarly, complex **3.13** returned results which partially matched the calculated elemental composition values, but could not be matched for all; even with the inclusion of solvent molecules.

The $^{13}C\{^{1}H\}$ NMR spectrum of complex **3.12** was successfully recorded as a $CDCl_3$ solution at room temperature. However, an analogous spectrum of complex **3.13** could not be recorded due to its tendency to precipitate out of common deuterated solvents over several hours. Although this did not directly impact the recording of the ^{1}H NMR spectrum of this complex, the significantly longer analysis time required ^{13}C NMR rendered this technique unusable. Based on the trend observed in the preceding pairs of complexes, it can be speculated that the spectra for both these complexes will appear to be very similar.

The signals within the $^{13}C\{^{1}H\}$ NMR spectrum of complex **3.12** displayed a signal pattern which has been typical amongst the other PAH-functionalised metallocarbyne complexes formed in this Chapter. Unfortunately, the signal-to-noise ratio within the spectrum was not sufficiently high enough for coupling information to be measured. The carbyne carbon ($W{\equiv}C^{\alpha}$) was assigned to the most downfield signal in the spectrum at δ_C

280.0 ppm. between this signal and the three thionyl carbon signals at approximately δ_C 160 ppm, the two carbonyl carbon atoms were detected individually at δ_C 224.1 and 219.6 ppm. Based on the trends observed in the complexes described previously in this Chapter, the pyrenyl carbon atom tethered to the carbyne chain (*i.e.* C^{β}) was assigned as the signal at δ_C 144.7 ppm. The remaining pyrenyl signals were detected in a cluster over the spectral range δ_C 132-124 ppm, immediately downfield of the heterocyclic carbon atoms which were detected as two clusters of signals at approximately δ_C 123 and 120 ppm. Finally, the *exo*-CH_3 groups on the **Tm** ligand were each individually detected at δ_C 35.0, 34.9 and 34.3 ppm.

Although multiple attempts were made to form crystals suitable for unequivocal structural determination *via* single crystal X-ray diffraction, none were successfully acquired. Hence, the crystallographic structure and associated parameters of complexes **3.12** and **3.13** remain elusive.

3.3.8 Synthesis of [TmM(CO)$_2${≡C-(3-Perylenyl)}] (M = Mo, W)

One of the largest PAHs used in this study was the compound perylene. As the number of ring-fused aromatic rings in a structure increases, so does the propensity for the complex to display exaggerated optical and electronic properties. In the context of PAHs, this is normally observed by way of optical fluorescence and, rarely, phosphorescence. Certainly, most of the PAHs and halogenated PAHs used in this study which had a minimum of three ring-fused aromatic rings displayed some sort of fluorescence when irradiated with UV light. Resultingly, perylene and its mono-brominated derivative 3-bromoperylene afforded some of the most intense fluorescence when in the solid form and in solution. However, when 3-bromoperylene was used to form the metallocarbyne complexes [**Tm**W(CO)$_2${≡C-(3-Perylenyl)}] (**3.14**) and [**Tm**Mo(CO)$_2${≡C-(3-Perylenyl)}] (**3.15**) (**Scheme 3.7**), it was found that all fluorescence had been quenched, presumably due to the presence of the heavy metal centres facilitating alternative non-radiative decay pathways.

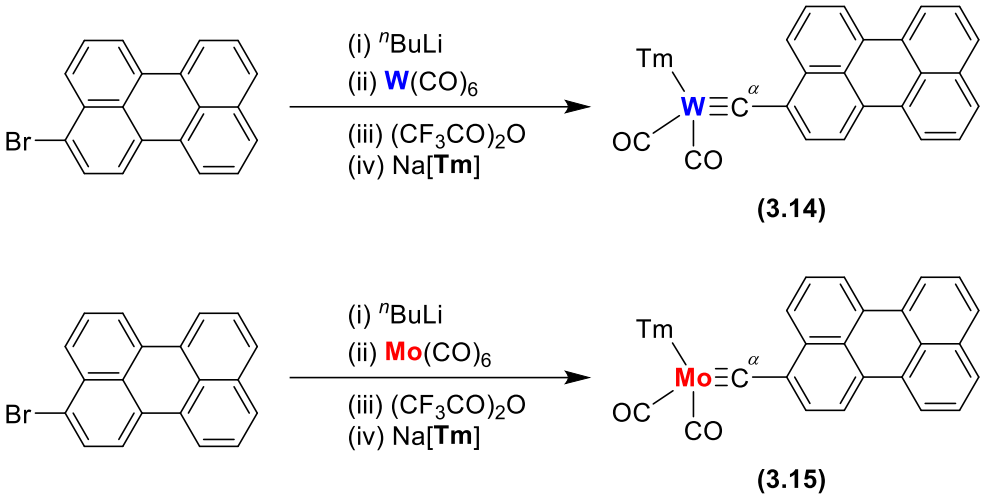

Scheme 3.7. Preparation of complexes **3.14** and **3.15**.

A spectroscopically pure sample of complex **3.14** was isolated following two sequential purification processes. Initially, the crude reaction mixture was concentrated to dryness, the resulting residues were extracted with a small volume of CH_2Cl_2 and loaded onto a silica gel column. As the column was eluted with CH_2Cl_2, several differently coloured bands developed from the baseline, some of which were fluorescent under UV light. Among those which displayed no fluorescent properties was the major dark band which eluted from the baseline and eventually split into three closely associated segments. By shining a bright white light through the column, it was possible to clearly distinguish these segments from one another and hence each band was successfully collected individually. Testing revealed that the central (major) segment which had been collected contained complex **3.14**, albeit in a slightly contaminated form. Hence, for the purposes of obtaining a spectroscopically pure sample of complex **3.14**, the material from the middle segment was once again subjected to silica gel column chromatography, eluting with CH_2Cl_2. Collection of the major brown/red band afforded complex **3.14** in low yield.

A similar purification method was used to isolate a spectroscopically pure sample of complex **3.15**, whereby two sequential purification steps were required to remove contaminants. Complex **3.15** was isolated in a marginally higher yield than that of complex **3.14**, but it should be emphasised that the overall conversion was still low. Both complexes **3.14** and **3.15** displayed good stability in the solid form, but as a precaution were stored in sealed sample vials at -20 °C. Even after an extended period of time, minimal degradation was noted under these conditions.

Complexes **3.14** and **3.15** were found to be readily soluble in halogenated solvents, and were initially analysed *via* infrared spectroscopy as CH_2Cl_2 solutions. This revealed two carbonyl bands for complex **3.14** at ν_{CO} 1969 and 1879 cm^{-1}. Likewise, two carbonyl bands were also detected for complex **3.15** at ν_{CO} 1983 and 1899 cm^{-1}. However, the {B–H} fragment of the **Tm** ligand in complex **3.15** was also detected through its weak vibration at ν_{BH} 2400 cm^{-1}.

The ^1H NMR spectra of both complexes were recorded as $CDCl_3$ solutions at room temperature. Much like many of the PAH ligated complexes which were previously prepared in this Chapter, the array of signals which were recorded for complexes **3.14** and **3.15** were typical for materials of this type. In the case of complex **3.14**, the most downfield signals over the spectral range δ_H 8.75-7.41 ppm were assigned to the perylenyl protons. All the remaining signals within the spectrum originated from the **Tm** ligand. A very similar signal pattern was recorded in the ^1H NMR spectrum of complex **3.15**, and hence, the full details of which have been omitted in order to avoid repetitive descriptions.

Complex **3.14** was successfully detected through the use of ESI mass spectrometry. A single complex ion fragment with m/z 855.1039 was calculated to closely match the simulated isotope pattern for a complex with the formula $C_{35}H_{28}BN_6O_2S_3W$. This was found to be a match for the $[M+H]^+$ ion of complex **3.14**. Similarly, complex **3.15** was also detected as a $[M+H]^+$ ion, which corresponded to a complex with the formulae $C_{35}H_{28}BMoN_6O_2S_3$. The bulk purity of the samples containing complexes **3.14** and **3.15** were assured through elemental microanalytical results, which were found to coincide with the elemental composition values calculated for both complexes.

The $^{13}C\{^1H\}$ NMR spectra for both complexes were successfully recorded as $CDCl_3$ solutions at room temperature. Due to the broadly similar arrangement of signals which were detected in both cases, only the details pertaining to complex **3.14** will be discussed below. The most downfield signal in the $^{13}C\{^1H\}$ NMR spectrum of complex **3.14** was recorded at δ_C 279.2 ppm, and was assigned to the carbyne carbon ($W{\equiv}C^{\alpha}$). The signal-to-noise ratio within the spectrum was sufficient enough to allow for coupling information to be extracted, and the carbyne carbon was measured to have a one-bond tungsten-carbon coupling constant of approximately 194 Hz. Likewise, the one-bond tungsten-carbon coupling constants associated with the two carbonyl ligands were calculated to be approximately 171 and 165 Hz for the signals at δ_C 223.9 and 219.4 ppm, respectively. The majority of the signals associated with the perylenyl ligand were found over the spectral range δ_C 135-126

ppm. However, one further signal which was appreciably downfield of this could also be assigned to the perylenyl ligand due to its clear coupling to the tungsten centre through a two-bond interaction with a magnitude of approximately 43 Hz. Hence, the signal at δ_C 159.2 ppm was confidently assigned as the perylenyl carbon atom directly bound to the carbyne atom (*i.e.* WC^{β}). All of the carbon atoms contained with the **Tm** ligand were accounted for with the help of 2D ^{13}C NMR experiments, which were particularly useful in the assignment of the cyclic alkene carbon atoms which displayed some overlap with perylenyl signals.

Although multiple attempts were made to form crystals suitable for unequivocal structural determination *via* single crystal X-ray diffraction, none were successfully acquired. Hence, the crystallographic structure and associated parameters of complexes **3.14** and **3.15** remain elusive.

3.3.9 Synthesis of [TmW(CO)$_2${≡CC≡C-R)}] (R = 3-Phenanthryl, 9-Anthracenyl, 1-Pyrenyl)

Given the broad utility of mono-halogenated PAH compounds, further derivatisation of three PAH starting materials was carried out in an attempt to increase the intensity of any optoelectronic processes which may have been present. Recalling work which was carried out in Chapter 2 of this Thesis, the addition of a conjugated, linear {C_3} fragment was successfully carried out to effectively functionalise the compounds 9-bromophenanthrene, 9-bromoanthracene and 1-bromophrene with an ethynyl chain. Once isolated, these three PAH derivatives were used to form the tungsten complexes [**Tm**W(CO)$_2${≡CC≡C-(3-Phenanthryl)] (**3.16**), [**Tm**W(CO)$_2${≡CC≡C-(9-Anthracenyl)}] (**3.17**) and [**Tm**W(CO)$_2${≡CC≡C-(1-Pyrenyl)}] (**3.18**) (**Scheme 3.8**) in low to moderate yields.

The parent ethynyl-functionalised compounds 9-ethynylphenanthrene, 9-ethynylanthracene and 1-ethynylpyrene were formed through the desilylation of their trimethylsilyl-functionalised sources using various literature procedures. Once formed, a protocol analogous to that used in Chapter 2 to form propargylidyne complexes was utilised, whereby the three aforementioned compounds were treated with ^{n}BuLi at low temperature, and the successive addition of [W(CO)$_6$], trifluoroacetic anhydride and Na[**Tm**].

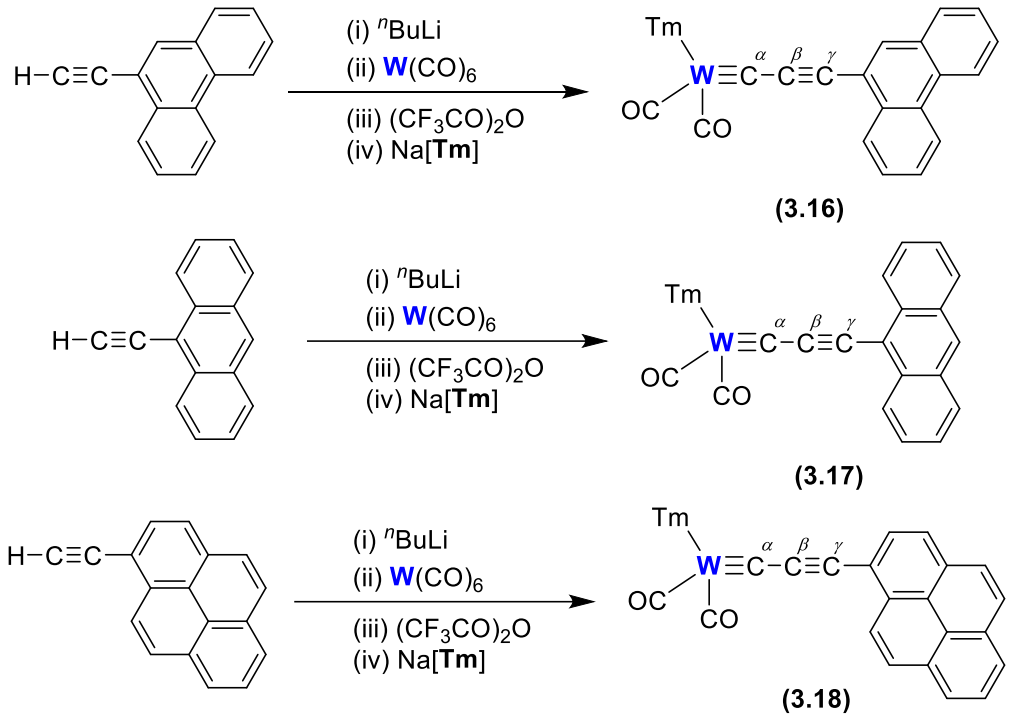

Scheme 3.8. Preparation of complexes **3.16**, **3.17** and **3.18**.

In order to isolate spectroscopically pure samples of complexes **3.16**, **3.17**, and **3.18**, silica gel column chromatography was used to purify the respective crude product mixtures. Once isolated, samples of each complex were stored in the solid form in sealed sample vials at -20 °C. Under these conditions, minimal degradation was noted, even after extended periods of time.

Complexes **3.16**, **3.17** and **3.18** were found to be readily soluble in halogenated solvents. Hence, the infrared spectra of complexes **3.16** and **3.17** were recorded as CH_2Cl_2 solutions. Unfortunately, due to the small quantity of complex **3.18** which was isolated, analysis *via* other spectroscopic techniques were prioritised over solution infrared spectroscopy, and as a result it was not recorded. Within the solution infrared spectra of complexes **3.16** and **3.17**, the most conspicuous features present were the two equally intense carbonyl bands at ν_{CO} 1979 and 1891 cm^{-1} for complex **3.16**, and ν_{CO} 1978 and 1891 cm^{-1} for complex **3.17**. Given the similarities observed between these two complexes, it is speculated that the liquid infrared spectrum of complex **3.18** would also return a similar result. In addition to the carbonyl ligands, the B–H stretch originating from the bridgehead {BH} fragment of the **Tm** ligand could be assigned in the spectrum of complex **3.16** at ν_{BH} 2435 cm^{-1}.

The ^{1}H NMR spectra of all three complexes were recorded as $CDCl_3$ solutions at room temperature, and afforded results which confirmed the inclusion of both the **Tm** ligand and each respective PAH termini. By visually comparing each ^{1}H NMR spectrum, it is evident that they are broadly similar, and the major differences between them are as a result of the changing PAH being used. With reference to the signals corresponding to the protons located on the **Tm** ligand (*i.e.* the cyclic alkene C–H protons and those on the *exo*-CH_3 groups), the spectral ranges over which these were detected were remarkably similar for all three complexes. Hence, in order to avoid repetitive descriptions, only the details pertaining to complex **3.16** have been discussed below. For further information on complexes **3.17** and **3.18**, readers are directed to the relevant Experimental section and spectra detailed in the Supplementary Information.

Complex **3.16** afforded a ^{1}H NMR spectrum which clearly displayed the presence of the target material, with only minor impurities being present. In a typical manner, the most downfield signals in the spectrum were assigned to the aromatic protons bound to the phenanthryl ligand, which were detected over the spectral range δ_H 8.64-7.54 ppm. The cyclic alkene protons located on the **Tm** ligand backbone were detected as a series of signals over the spectral range δ_H 6.91-6.79 ppm. Finally, the three *exo*-CH_3 groups of the **Tm** ligand could be easily identified due to their isolated nature, and therefore were assigned to the three singlets at δ_H 3.82, 3.78 and 3.62 ppm.

ESI mass spectrometry fortified our assumptions that the materials which had been isolated did indeed contain the three target complexes. Complex **3.16** was detected as a $[M+H]^+$ molecular ion with an isotope pattern which closely matched that calculated for a complex with the formula $C_{31}H_{26}BN_6O_2S_3W$. Both complexes **3.17** and **3.18** were detected as $[M+Na]^+$ ions which had the formulae $C_{31}H_{25}BN_6NaO_2S_3W$ and $C_{33}H_{25}BN_6NaO_2S_3W$, respectively. To prove the bulk purity of these samples, elemental microanalysis was also recorded for all three complexes. Regrettably, only the results for complex **3.16** were found to be in reasonable agreement with the elemental composition values calculated for the complex. Even after numerous attempts, agreeable elemental microanalytical results could not be obtained for complexes **3.17** and **3.18**.

The ^{13}C{^{1}H} NMR spectra for all three complexes were successfully recorded as $CDCl_3$ solutions at room temperature, and much like the ^{1}H NMR spectra which were discussed earlier, the three complexes shared many common features, with the main differences originating from the variation of the PAH groups. For full details relating to each

complex, readers are directed to the Experimental section and the Supplementary Information. However, the key features in the spectra of each complex have been summarised below.

The most downfield signals in the $^{13}C\{^{1}H\}$ NMR spectra of each complex were assigned to the carbyne carbon ($W\equiv C^{\alpha}$) and were detected at δ_C 247.1, 246.5 and 247.0 ppm for complexes **3.16**, **3.17** and **3.18**, respectively. For complexes **3.16** and **3.17**, the signal to noise ratio of the signals within the spectra were found to be sufficient enough to allow for coupling data to be extracted. Hence, to coincide with these chemical shifts, a one-bond tungsten-carbon coupling constant of approximately 204 Hz was detected for complexes **3.16** and **3.17**. The two carbonyl ligands which are bound to the tungsten centre in each complex were all independently detected as two signals at approximately δ_C 225 and 220 ppm for all complexes. Again, for complexes **3.16** and **3.17**, a one-bond tungsten-carbon coupling constant was recorded alongside both of their respective carbonyl carbon signals. For both of these complexes, the magnitude of these coupling constants were found to be approximately 169 and 160 Hz for the signals at δ_C 225 and 220 ppm, respectively. Unlike any of the other complexes which were formed in this Chapter, complexes **3.16, 3.17** and **3.18** are the only species which contain a linear $\{C_3\}$ sp hybridised chain of conjugated carbon atoms. Although the carbyne carbon ($W\equiv C^{\alpha}$) atoms have already been assigned, the remaining two carbon atoms (*i.e.* WC^{β} and WC^{γ}) still need to be discussed. The assignment of the relevant signals within each $^{13}C\{^{1}H\}$ NMR spectrum was aided with reference to the results obtained for the propargylidyne and tricarbido complexes formed in Chapter 2 of this Thesis, as well as 2D ^{13}C NMR experiments. For all three complexes, the WC^{β} carbon atom was detected within the approximate spectral range δ_C 112-119 ppm. In the case of complex **3.16** coupling data was successfully extracted, and a two-bond tungsten-carbon coupling constant with a magnitude of approximately 60 Hz was calculated for this signal. Additionally, a three-bond tungsten-carbon coupling constant with a magnitude of approximately 8 Hz was miraculously detected to coincide with the signal at δ_C 73 ppm in the $^{13}C\{^{1}H\}$ NMR spectrum of complex **3.16**. This unequivocally identified this signal as the WC^{γ} carbon atom. Although complexes **3.17** and **3.18** were devoid of coupling information for their respective WC^{γ} signals, they were found to be in close agreement, since they were also detected at approximately δ_C 73 ppm.

Attempts to grow crystals suitable for single crystal X-ray diffraction studies were attempted on several occasions, using a range of typical crystallisation solvent mixtures

through the low-temperature vapour diffusion technique. Although attempts proved to be futile in the cases of complexes **3.17** and **3.18**, single crystal X-ray diffraction data for complex **3.16** was successfully recorded (**Figure 3.1**) after a crystal was grown *via* the vapour diffusion of toluene into a CH_2Cl_2 solution of complex **3.16** at 4 °C.

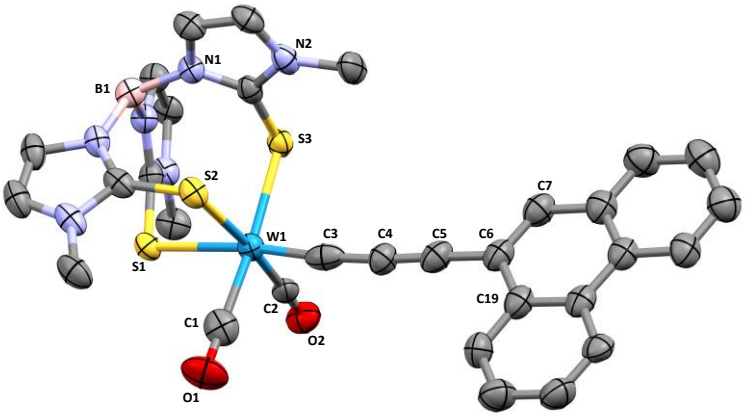

Figure 3.1. Molecular structure of **3.16** (50% displacement ellipsoids) with selected atom labels. Solvent molecules and hydrogen atoms omitted for clarity. Selected bond lengths (Å) and angles (°): W1–C1 1.992(7), W1–C2 1.984(6), W1–S1 2.6677(12), W1–S2 2.5726(13), W1–S3 2.5374(12), W1–C3 1.835(7), C3–C4 1.360(9), C4–C5 1.226(8), C5–C6 1.422(8); W1–C3–C4 172.8(5), C3–C4–C5 174.6(6), C4–C5–C6 178.9(7).

As anticipated, the $\{C_3\}$ chain shows little deviation for the 180° dihedral angle associated with sp hybridised carbon atoms. Furthermore, the bonds linking the three carbon atoms in the $\{C_3\}$ chain display a crystallographically significant change in their bond distances in accordance with the alkynyl-alkyl bonding motif. Much like many of the other complexes formed in this work, the tungsten centre displays a *pseudo*-octahedral geometry, which allows for the incorporation of the **Tm** ligand, two carbonyl ligands, and the PAH functionalised propargylidynyl ligand.

3.3.10 Synthesis of Tp*(CO)$_2$W{≡C(1-(1,2,4,5-dehydro[2.2]paracyclophane)} and [Tp*(CO)$_2$W≡C]$_2$-{1,9/10-(1,2,4,5-dehydro[2.2]paracyclophane)}

As the readily available stocks of PAH compounds were either exhausted or successfully utilised in the preparation of the aforementioned complexes, a local search for more exotic PAH and aromatic compounds was conducted. During this search, a small quantity of cyclophane species were unearthed which were deemed to be potentially valuable additions to our work, given the presence of halogenated groups within their structures. For

those not familiar with cyclophane chemistry, they may be defined as a homologous of organic compounds which feature at least two aromatic rings tethered together by aliphatic linkers (**Figure 3.2**).

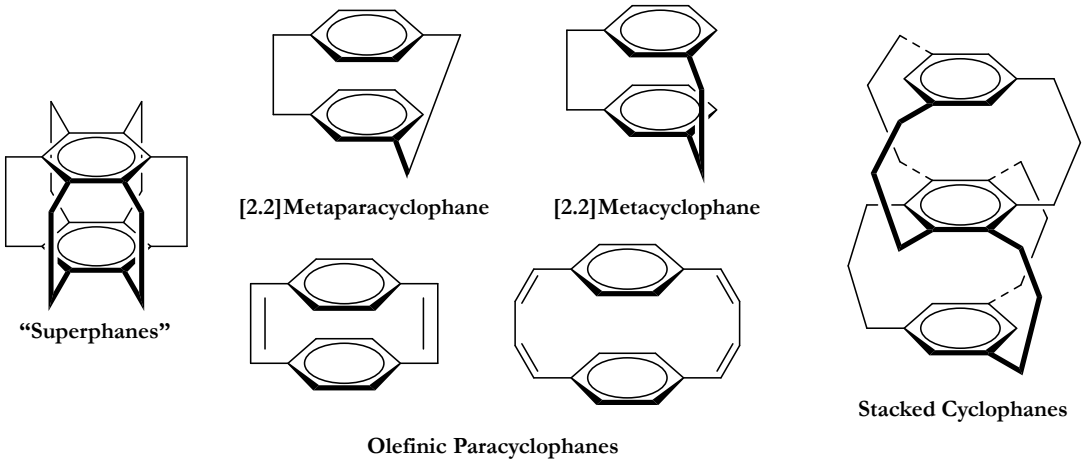

Figure 3.2. Various examples of cyclophane structures which have been reported in literature.

One of the first cyclophanes to be synthesised was [2.2]paracyclophane, which was prepared by Brown and Farthing in 1949,[28] and later investigated scrupulously by Cram and co-workers from 1951 onwards.[29–32]

The first reported preparation of [2.2]paracyclophane involved the high temperature pyrolysis of *para*-xylene, which formed the highly unstable intermediate *para*-xylylene. When in dilute mixtures, an intermolecular 1,6-cycloaddition reaction would take place to afford the desired [2.2]paracyclophane product. However, in concentrated solutions of *para*-xylylene, a condensation polymerisation reaction would take place, thereby removing the vast majority of the activated species required to form [2.2]paracyclophane (**Scheme 3.9**).[28,32,33]

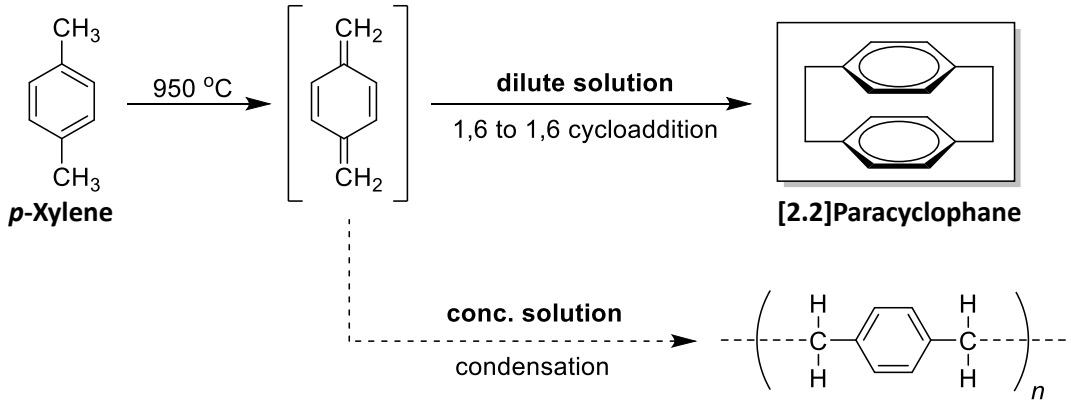

Scheme 3.9. Formation of [2.2]paracyclophane through the high temperature pyrolysis of *para*-xylene.

From this reaction, it was believed that extreme conditions were required to overcome the significant ring strain present in [2.2]paracyclophane. However, further refinements on the synthetic routes towards cyclophanes has allowed for the development of several reaction routes which utilise relatively mild conditions. One of the most convenient routes was developed by Winberg and co-workers,[34,35] and involved the 1,6-Hoffmann elimination of *para*-methylbenzyltrimethylammonium hydroxide (**Scheme 3.10**) in order to produce [2.2]paracyclophane in low yields.##

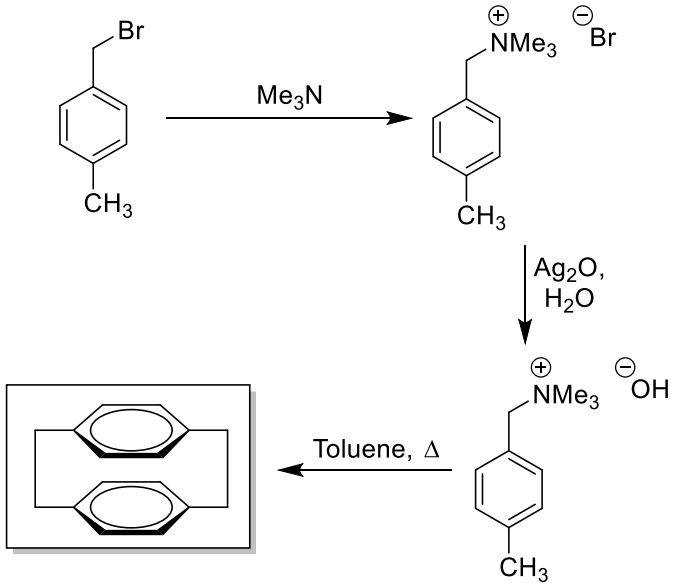

Scheme 3.10. Preparation of [2.2]paracyclophane.

Much of the interest in [2.2]paracyclophane can be traced back to its uncommon structural features, which differ greatly from other aromatic compounds. For example, when the distance between the planes of the two aromatic rings is compared with other π-π stacked systems, such as graphite, it is found that the aromatic rings of [2.2]paracyclophane are significantly closer together (**Figure 3.3**).

Although this reaction allowed for the preparation of [2.2]paracyclophane from conveniently available starting materials, did not require excessively high reaction temperatures, nor any complex experimental setups, it was noted that the polymerisation of unstable intermediate species remained as an issue. If was found that the addition of a polymerisation inhibitor such as MeHQ (4-methoxyphenol) improved the overall yield of [2.2]paracyclophane.

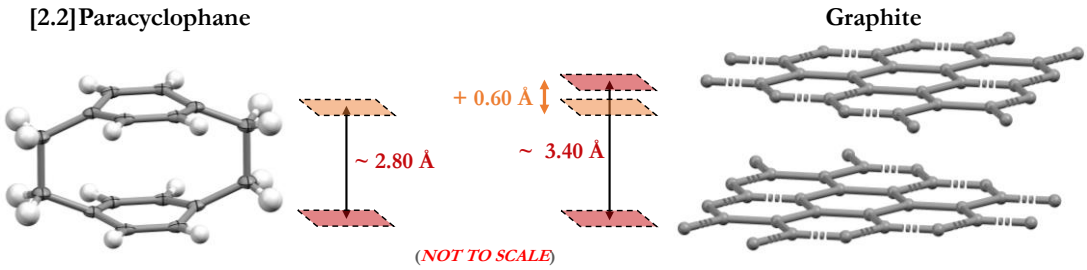

Figure 3.3. Comparison of the distance between the two aromatic rings in [2.2]paracyclophane and two planes of graphite.

It is trivial to account for this difference, as the aliphatic linkers within [2.2]paracyclophane enforce a closely packed arrangement of the aromatic rings. However, this also impacts upon the geometries of the sp^2 hybridised carbon atoms bound to the linkers, which suffer from a distinct deviation from linearity into either boat- or chair-like conformations (depending on the cyclophane in question) (**Figure 3.4**).

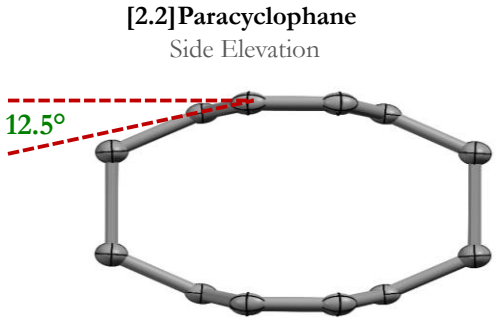

Figure 3.4. Visualization of the steric strain within [2.2]paracyclophane.

The first organometallic complex of [2.2]paracyclophane (a metallocyclophane) was formed in 1960 and featured a tricarbonyl chromium centre with the [2.2]paracyclophane coordinated in a η^6 manner through one of the C_6H_4 rings (**Scheme 3.11**).[36]

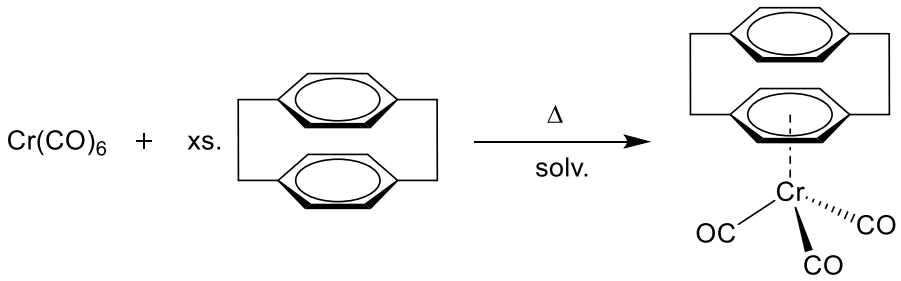

Scheme 3.11. Preparation of the first reported metallocyclophane complex.

Although the structure of this complex was somewhat open to speculation at the time, a single crystal X-ray diffraction image of the complex was successfully recorded some eighteen years after its initial preparation.[37]

The metallocyclophanes prepared in the course of this work featured the doubly dehydrogenated variant of [2.2]paracyclophane, 1,2,4,5-dehydro[2.2]paracyclophane. The compounds 1-bromo-1,2,4,5-dehydro[2.2]paracyclophane and 1,9/10-dibromo-1,2,4,5-dehydro[2.2]paracyclophane§§§ were selected due to their labile halogen groups, and were subsequently reacted with one and two equivalents of the tungsten stannyl carbyne [**Tp***$(CO)_2W{\equiv}C(SnBu_3)$], respectively. Through a modified Stille coupling reaction, the complexes [**Tp***$(CO)_2W\{{\equiv}C$(1-(1,2,4,5-dehydro[2.2]paracyclophane)}] (**3.19**) and [**Tp***$(CO)_2W{\equiv}C]_2$-{1,9/10-(1,2,4,5-dehydro[2.2]paracyclophane)} (**3.20**) were formed in moderate-to-good yields (**Scheme 3.12**).

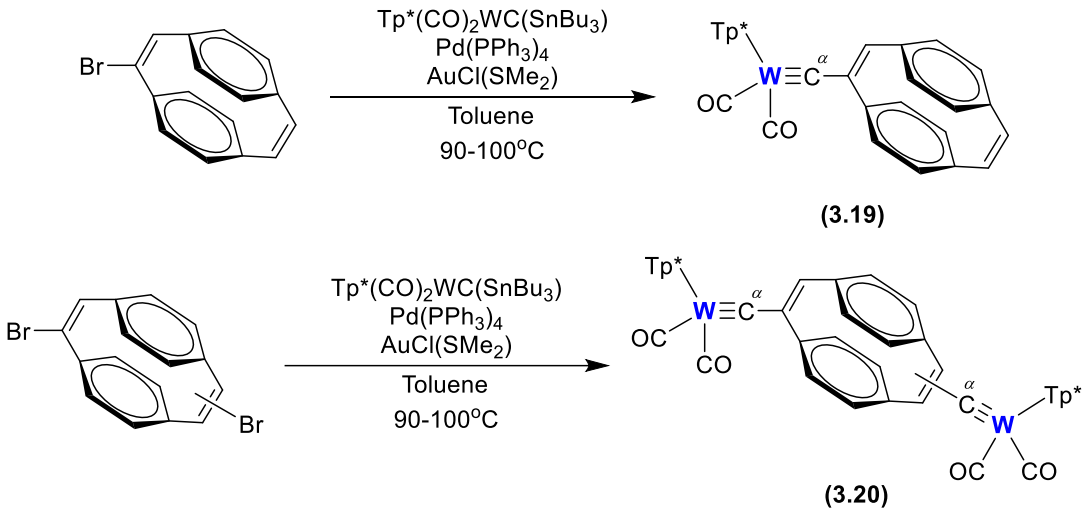

Scheme 3.12. Preparation of complexes **3.19** and **3.20**.

The respective reaction mixtures containing complexes **3.19** and **3.20** were concentrated to dryness and extracted with a small volume of toluene. These residues were subsequently used to isolate both complexes *via* silica gel column chromatography, eluting with toluene. In both cases, a major red band developed from the silica gel baseline, which

§§§This compound, derived from [2.2]paracyclophane, is believed to contain a mixture of dibrominated products (based on $^{13}C\{^1H\}$ NMR). The isomers present in this mixture are also referred to as (2*E*,5*E*)-2,5-dibromo-1,4(1,4)-dibenzenacyclohexaphane-2,5-diene and (2*E*,5*E*)-2,6-dibromo-1,4(1,4)-dibenzenacyclohexaphane-2,5-diene. It is implied through the use of the name 1,9/10-dibromo-1,2,4,5-dehydro[2.2]-paracyclophane (above) that the mixture consists of approximately equal amounts of both isomers.

was collected, and concentrated to dryness in order to isolate samples of complexes **3.19** and **3.20** as a pink and red powder, respectively.

Although toluene was used to successfully separate the target materials from any unreacted starting materials or impurities during column chromatography, complexes **3.19** and **3.20** were also found to be readily soluble in halogenated solvents. Hence, one of the first spectroscopic tests which both complexes were subjected to was solution infrared spectroscopy. Both samples were loaded as CH_2Cl_2 solutions and afforded remarkably similar spectral features. The most noticeable of which were the two carbonyl bands which were detected at approximately ν_{CO} 1973 and 1882 cm^{-1} for both complexes. Additionally, the {B–H} fragment located on the **Tm** ligand was also detected as a weak stretch at ν_{BH} 2554 cm^{-1} in both spectra.

The ^1H NMR spectra for both complexes **3.19** and **3.20** were recorded as $CDCl_3$ solutions at room temperature. For complex **3.19**, the olefinic C–H protons were found to be the most downfield signals in the spectrum, with the isolated C–H group being detected at δ_H 7.49 ppm, and the two unsubstituted C–H protons being detected as a single signal at δ_H 7.19 ppm. A small cluster of signals over the spectral range δ_H 6.60-6.48 ppm was assigned to the hydrogen atoms located on the two C_6H_4 rings, thereby leaving the remaining signals to be attributed to the **Tp*** ligand. In a manner typical of the **Tp*** ligand, the pyrazolyl C–H groups were detected as two singlets at δ_H 5.90 and 5.78 ppm, in a 2:1 ratio, respectively. Furthermore, the three *exo*-($C(CH_3)_3$) groups of the **Tp*** ligand were detected as a series of four singlets at approximately δ_H 2.5 ppm, in their typical 6:3:6:3 ratio.

The ^1H NMR spectrum of complex **3.20** displayed many of the features which were observed for complex **3.19**. However, the spectrum was able to conclusively confirm the presence of two **Tp*** ligands in the complex, due to the doubling of the pyrazolyl hydrogen atoms and *exo*-($C(CH_3)_3$) hydrogen atom signals. Furthermore, the integration of the signal at δ_H 7.48 ppm, which was assigned to the olefinic hydrogen atoms, clearly showed the loss of one hydrogen atom.

Both complexes **3.19** and **3.20** were analysed *via* ESI mass spectrometry, which ultimately confirmed the presence of both species in the materials which had been isolated using column chromatography. Complex **3.19** was detected as a $[M+H]^+$ complex ion which had an isotope pattern which closely matched the formula $C_{34}H_{33}BN_6O_2W$. Likewise, complex **3.20** was also detected as a $[M+H]^+$ ion, corresponding to a complex with the

formula $C_{52}H_{55}B_2N_{12}O_4W_2$. Furthermore, a $[M+Na]^+$ complex ion with the formula $C_{52}H_{54}B_2N_{12}NaO_4W_2$ was also identified. The bulk composition of both complexes was affirmed through elemental microanalysis, albeit with the inclusion of a small quantity of toluene in each sample.

The $^{13}C\{^1H\}$ NMR spectra of complexes **3.19** and **3.20** were recorded as $CDCl_3$ solutions at room temperature. For complex **3.19**, the carbyne carbon ($W\equiv C^{\alpha}$) atom was detected at δ_C 271.9 ppm, making it the most downfield signal in the spectrum. To coincide with this, a one-bond tungsten-carbon coupling constant was recorded with a magnitude of approximately 188 Hz. The carbon atoms located on the tungsten-bound carbonyl groups were detected as a single signal at δ_C 224.1 ppm with a one-bond tungsten-carbon coupling constant of 165 Hz. Unlike all of the **Tm** ligated complexes prepared in this work, analogous complexes ligated with **Tp*** have a higher degree of symmetry about their metal centres. This is enforced by the rigid cage-like structure which the **Tp*** ligand forms when it coordinates to a metal centre through its three nitrogen donor groups. The high signal intensity also allowed for the easy identification of the carbon atom bound to the carbyne carbon (*i.e.* WC^{β}), given the presence of tungsten satellites on the signal at δ_C 160.2 ppm which had a magnitude of approximately 44 Hz. The data recorded for complex **3.20** was noted to be similar to that described above, albeit devoid of coupling information.

Although multiple attempts were made to form crystals suitable for unequivocal structural determination *via* single crystal X-ray diffraction, none were successfully acquired. Hence, the crystallographic structures and associated parameters of complexes **3.19** and **3.20** remain elusive.

3.3.11 Synthesis of [Tm(CO)$_2$W{≡C(9-[10-phenyl-anthracenyl])}]

All of the complexes which will be described in the remainder of this Chapter relate to anthracenyl-functionalised complexes akin to complex **3.10**. A range of complexes were formed through the use of pre- and post-synthetic modifications of the PAH starting materials and some of the complexes which have been detailed therein.

A sample of 9-bromo-10-phenylanthracene, formed from 9,10-dibromoanthracene *via* a literature procedure,[38] was successfully used in the oxide abstraction protocol to form complex **3.21** in good yield (**Scheme 3.13**).

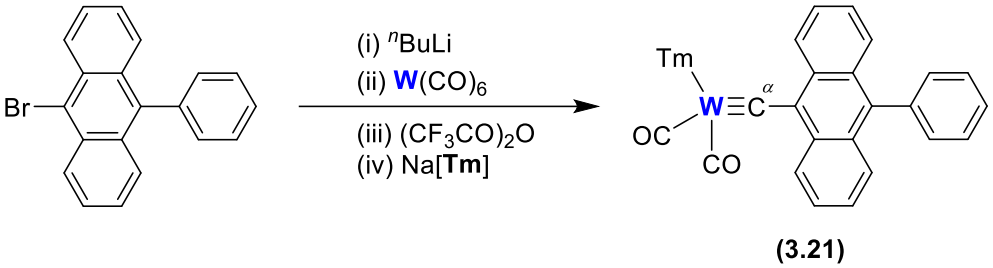

(3.21)

Scheme 3.13. Preparation of complex **3.21**.

Complex **3.21** was extracted from the crude reaction mixture through the use of silica gel column chromatography. The crude reaction mixture was concentrated to dryness and the residues loaded onto the column using a small volume of CH_2Cl_2. Elution with CH_2Cl_2 caused a number of bands to develop from the baseline, the most prominent of which being brown in colour. This band was collected and concentrated to dryness under high vacuum, and was shown through the following spectroscopic techniques to be a pure sample of complex **3.21**. The material which had been isolated showed good stability under aerobic conditions, but some degradation was noted over several hours when complex **3.21** was dissolved in halogenated and deuterated solvents. As a precaution, the material which had been isolated was stored in the solid form in a sealed sample vial at -20 °C.

Generally, complex **3.21** was found to be readily soluble in halogenated solvents, and thus was initially probed *via* liquid infrared spectroscopy as a CH_2Cl_2 solution. The two carbonyl ligands bound to the tungsten centre afforded the most recognisable features in the spectrum, as two equally intense bands at ν_{CO} 1969 and 1880 cm^{-1}. It is notable that for the related complex **3.10**, the carbonyl stretching frequencies had almost identical values. Therefore, it can be assumed that the inclusion of the phenyl ring at the 10-position of the anthracenyl ligand does not significantly change the electronic structure about the tungsten metal centre. In addition to the two carbonyl ligands, a series of very weak bands were noted at approximately 2400 cm^{-1}. Bands within this region of the spectrum are typically indicative of the B–H group at the bridgehead of the **Tm** ligand. Hence, the most intense peak within this cluster of signals was assigned to the B–H vibration at ν_{BH} 2435 cm^{-1}.

The ^{1}H NMR spectrum of complex **3.21** was recorded at room temperature as a $CDCl_3$ solution. Without carrying out any major scrutiny of the spectrum, it is trivial to see the inclusion of the phenyl group at the 10-position of the anthracenyl ligand. With reference to the analogous spectrum which was recorded for complex **3.10**, the proton in the 10-position on the anthracenyl ligand produces a singlet at δ_H 8.36 ppm ($CDCl_3$, 25 °C). This

signal is clearly absent in the spectrum of complex **3.21**, and without any further analysis, it may be concluded that this has been successfully substituted with the desired phenyl group. A more detailed analysis of the ^{1}H NMR spectrum of complex **3.21** reveals the detection of the phenyl group as a cluster of signals centred at approximately δ_H 7.52 ppm, equating to five hydrogen atoms. With the exemption of the cyclic alkene protons bound to the backbone of the **Tm** ligand, which were detected over the spectral range δ_H 6.93-6.84 ppm, the remaining signals in the downfield region of the spectrum could be assigned as anthracenyl-bound protons. As is typical for complexes ligated with the **Tm** ligand, the *exo*-CH_3 groups it contains were detected as three individually resolved singlets at δ_H 3.89, 3.69 and 3.58 ppm.

ESI mass spectrometry afforded results consistent with the formation of complex **3.21** as $[M]^+$ and $[M\text{-}(CO)]^+$ ion fragments. These fragments were found to closely match the isotope patterns simulated for complex ions of the formulae $C_{35}H_{29}BN_6O_2S_3W$ and $C_{34}H_{29}BN_6OS_3W$, respectively. The bulk purity of the material containing complex **3.21** was tested *via* elemental microanalysis and returned results which were in good agreement for those calculated for the title complex.

The $^{13}C\{^{1}H\}$ NMR spectrum of complex **3.21** was recorded as a $CDCl_3$ solution at room temperature. The most downfield signal in the spectrum was recorded at δ_C 279.5 ppm and was assigned to the carbyne carbon ($W{\equiv}C^{\alpha}$). The location of this signal is almost identical to that found in the related complex **3.10**, in which the carbyne carbon was detected at δ_C 279.4 ppm. Although tungsten satellites were not detected in the spectrum of complex **3.10**, coupling information was successfully measured in the spectrum of complex **3.21**, whereby a one-bond tungsten-carbon coupling constant of approximately 196 Hz was calculated for the carbyne carbon. Furthermore, the two carbonyl carbon atoms which were detected at δ_C 225.1 and 220.9 ppm were also found to have one-bond tungsten-carbon coupling constants of approximately 172 and 166 Hz, respectively. The similarities found in the signal patterns of complexes **3.10** and **3.21** continue throughout the remainder of the spectrum of complex **3.21** with the exception of the signals attributed to the phenyl-substituent. These were detected as an array of signals over the (broad) spectral range of δ_C 140-125 ppm, and were not individually assigned due to the difficulties faced in discerning these from the signals arising from the anthracenyl carbon atoms.

Although multiple attempts were made to form crystals suitable for unequivocal structural determination *via* single crystal X-ray diffraction, none were successfully acquired.

Hence, the crystallographic structures and associated parameters of complex **3.21** remain elusive.

3.3.12 Synthesis of [TmW(CO)$_2${≡C(9-[10-bromo-anthracenyl])}]

A literature search of the dibrominated compound 9,10-dibromoanthracene was found to contain information relating to the novel ways in which the compound undergoes lithiation *via* treatment with alkyl lithium reagents. Notably, it was found that the compound effectively undergoes selective monolithiation,[39,40] which thereby renders the unsubstituted bromide group to potentially partake in post-synthetic modification procedures. Attempts to do this shall be discussed in the following sections, and how such studies let to the serendipitous preparation of two novel complexes which were the subject of two papers published in 2021.[41,42]

Complex **3.22** was prepared through the monolithiation of 9,10-dibromoanthracene with ^{n}BuLi in a THF solution at low temperature, and the sequential addition of [W(CO)$_6$], trifluoroacetic anhydride, and finally Na[**Tm**] (**Scheme 3.14**).

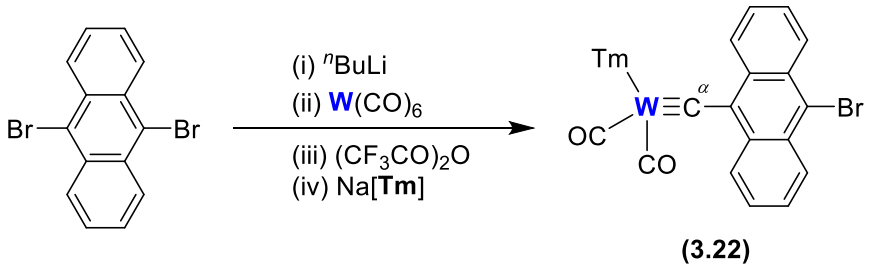

Scheme 3.14. Preparation of complex **3.22**.

Once the crude reaction mixture which contained complex **3.22** had been concentrated to dryness, the residues were extracted with a small volume of CH_2Cl_2. These were subjected to chromatographic purification *via* silica gel column chromatography. As the column was eluted with CH_2Cl_2 a major brown band developed from the baseline and traversed down the column. This was collected, concentrated to dryness under high vacuum, and was shown through the following spectroscopic analysis to be an almost entirely pure sample of complex **3.22**. In the solid form, complex **3.22** was found to be stable under ambient conditions over extended periods of time. However, in order to avoid any potential degradation processes which could take place, the sample was stored in a sealed vial at -20 °C. Complex **3.22** was found to be readily soluble in halogenated solvents, and was initially

tested *via* infrared spectroscopy as a CH_2Cl_2 solution. As anticipated, two carbonyl bands of equal intensity were detected at ν_{CO} 1972 and 1884 cm^{-1}, as well as a B–H stretch at ν_{BH} 2411 cm^{-1}, thereby confirming the presence of the **Tm** ligand.

The ^1H NMR spectrum of complex **3.22** was recorded as a $CDCl_3$ solution at room temperature. By comparison of the relative integrations of all the anthracenyl proton signals, it was trivial to confirm the inclusion of the brominated anthracenyl ligand, which is festooned with a total of eight hydrogen atoms. These signals were detected as an array of two doublets at δ_H 9.34 and 8.49 ppm, as well as a multiplet (bearing some similarity to two triplets) at approximately δ_H 7.53 ppm. All of the remaining signals in the spectrum could be attributed to the **Tm** ligand, whereby the cyclic alkene protons located on the methimazolyl rings were detected over the spectral range δ_H 6.91-6.83 ppm, leaving the three *exo*-CH_3 groups of the **Tm** ligand to be detected as three individually resolved singlets at δ_H 3.87, 3.67 and 3.52 ppm.

The presence of the title complex was confirmed through ESI mass spectrometry, which revealed a number of ion fragments of complex **3.22**. Due to the inclusion of the bromide group at the 10-position of the anthracenyl ligand, the ions which were identified contained a mixture of ^{79}Br and ^{81}Br. In the Experimental section, attempts have been made to clearly identify these using the following notation: *e.g.* $[M(^{79}Br)]^+$ and $[M(^{81}Br)]^+$. A total of four complex ions were identified, two of which had isotope patterns which closely matched those calculated for complexes with the formula $C_{29}H_{25}BBrN_6O_2S_3W$, and thereby matched the $[M]^+$ ion of complex **3.22** and contained both isotopes of bromine. Two further ions, identified as $[M\text{-}2(CO)\text{-}2H]^+$ fragments of complex **3.22**, were found with the formula $C_{27}H_{23}BBrN_6S_3W$, once again bearing both isotopes of bromine. The bulk purity of the sample containing complex **3.22** was fortified through elemental microanalysis. Results revealed a good match with the elemental composition values calculated for complex **3.22** without the inclusion of solvent impurities.

When complex **3.22** was subjected to $^{13}C\{^1H\}$ NMR spectroscopy as a $CDCl_3$ solution at room temperature, the spectrum which was obtained displayed an excellent signal to noise ratio, so much so that it allowed for coupling data to be recorded for various signals throughout the spectrum. The most downfield signal in the spectrum was detected at δ_C 277.4 ppm with a one-bond tungsten-carbon coupling constant of approximately 196 Hz. The two carbonyl carbon atoms were individually detected at δ_C 225.0 and 220.7ppm with one-bond tungsten-carbon coupling constants of approximately 171 and 165 Hz,

respectively. Further to this, the anthracenyl carbon atom bound to the carbyne carbon (*i.e.* WC^{β}) was detected with a two-bond tungsten-carbon coupling constant of approximately 40 Hz at δ_C 142.4 ppm. All of the remaining anthracenyl carbon atoms were detected over the approximate spectral range δ_C 133-121 ppm. All six cyclic alkene carbon atoms located within the methimazolyl rings were independently detected as two signal clusters at approximately δ_C 123 and 120 ppm, along with all three thione carbon atoms at δ_C 159 ppm. Finally, the three *exo*-CH_3 carbon atoms were detected as the most upfield signals in the spectrum at δ_C 34.9 and 34.8 ppm (with two signals overlapping in the former).

Unequivocal structural determination of complex **3.22** was made possible through the use of single crystal X-ray diffraction (**Figure 3.5**). Crystals suitable for structural determination were grown by vapour diffusion of petroleum spirits (40-60°C) into a concentrated CH_2Cl_2 solution of complex **3.22** at 4°C.

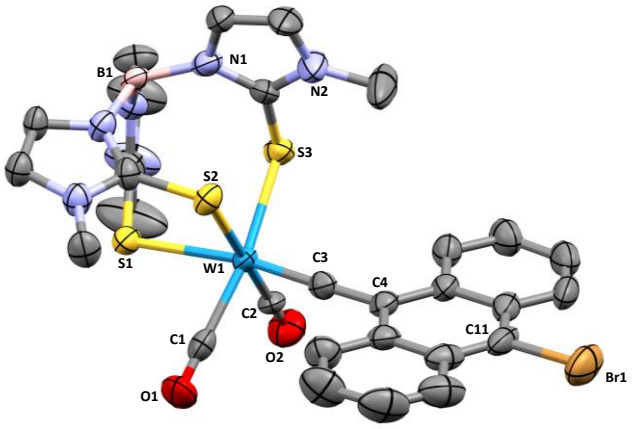

Figure 3.5. Molecular structure of **3.22** (50% displacement ellipsoids) with selected atom labels. Solvent molecules and hydrogen atoms omitted for clarity. Selected bond lengths (Å) and angles (°): W1–C1 2.033(9), W1–C2 2.025(9), W1–S1 2.655(2), W1–S2 2.567(2), W1–S3 2.525(2), W1–C3 1.837(9), C3–C4 1.441(12), C11–Br1 1.922(9); W1–C3–C4 178.6(7).

3.3.13 Synthesis of [TmW(CO)$_2${SC(9-[10-bromo-anthracenyl])}]

Much like in the post-synthetic modification procedures used to prepare thiocarbamoyl (thiocarboxyamide) complexes of molybdenum aminocarbynes,[43] attempts were made to install a bridging sulfur atom over the metallocarbyne bond found in complex **3.22**. Given the conjugated nature of complex **3.22**, it was speculated that the incorporation of a bridging sulfur atom might afford novel optical and electronic properties, on account of

the differing coordination modes (*via* resonance forms) through which the sulfur atom can coordinate to the metal centre (**Scheme 3.15**).

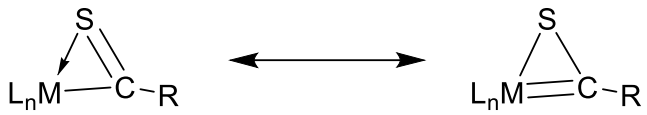

Scheme 3.15. Resonance forms of metal-bound bridging sulfur atoms in organometallic complexes.

A sample of complex **3.22** was dispersed in THF, treated with an excess of elemental sulfur and heated at reflux overnight. Once the crude reaction mixture was cooled to room temperature and concentrated to dryness, the residues were extracted with CH_2Cl_2 and purified *via* silica gel column chromatography, eluting with further CH_2Cl_2. Although a colour change was not immediately noted in the reaction mixture upon cooling due to its dark nature, a distinctive major green band quickly developed on the purification column. This was selectively collected and concentrated to dryness under high vacuum to afford a sample of complex **3.23** in low yield (**Scheme 3.16**).

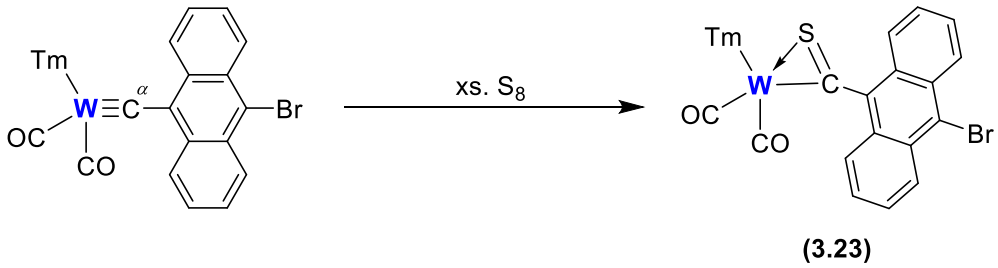

Scheme 3.16. Preparation of complex **3.23**.

The material which was isolated from the column was initially tested *via* infrared spectroscopy as a CH_2Cl_2 solution. Although the baseline of the spectrum which was recorded was relatively poor, two distinctive carbonyl signals could still be easily assigned at ν_{CO} 1971 and 1870 cm^{-1}. Despite the clear colour change which had been noted during the purification process, the results from the liquid infrared spectrum did not conclusively indicate the addition of a bridging sulfur atom. By comparison to the carbonyl bands of complex **3.22** (*ca.* ν_{CO} 1972 and 1884 cm^{-1}), only a minor deviation from these values was noted.

The ^1H NMR spectrum of complex **3.23** was recorded as a $CDCl_3$ solution at room temperature. Although the spectrum which was recorded was once again similar to that

recorded for complex **3.22**, it contained some indications that the bridging sulfur atom had been successfully installed. Perhaps the most distinctive of which being the broadening of one of the *exo*-CH_3 signals which was found at approximately δ_H 3.8 ppm.

The most conclusive evidence which supported the formation of complex **3.23** was afforded through ESI mass spectrometry. Complex ions containing ^{79}Br and ^{81}Br were detected with isotope patterns which closely matched those calculated for those of the formula $C_{27}H_{24}BBrN_6S_4W$. This was shown to match the simulated isotope pattern [M-2(CO)] for complex **3.23**. Furthermore, the bulk composition of the material isolated during column chromatography wash shown to be pure by elemental microanalysis. The elemental composition values which were recorded for the sample closely matched those calculated for complex **3.23**.

Although complex **3.23** showed good stability in the solid form, once dissolved in halogenated or deuterated solvents, decomposition was noted over a period of several hours. Although this did not hinder the recording of the ^1H NMR spectrum, it was not possible to record a $^{13}C\{^1H\}$ NMR spectrum of complex **3.23** due to the significantly longer acquisition time which was required.

Multiple attempts were made to form crystals suitable for structural determination. However, even after trialling several different solvent mixtures in low temperature vapour diffusion crystallisation setups, single crystals were never successfully acquired.

3.3.14 Synthesis of [TmW(CO)$_2${≡C(9-[10-bromo-triptycenyl])}]

An additional six-membered ring system was successfully installed onto the anthracenyl ligand of complex **3.22** through the addition of the highly reactive cyclic alkyne benzyne. Benzyne was generated *in situ* using the Kobayashi method,[44] whereby the commercially available reagent 2-(trimethylsilyl)phenyl trifluoromethane sulfonate was treated with a stoichiometric quantity of the desilylating agent TBAT[****]. Although the resulting anionic intermediate has the potential to undergo reprotonation, the trifluoromethane sulfonyl group rapidly disassociates, thereby preferentially forming benzyne (**Scheme 3.17**).

[****] TBAT – Tetrabutylammonium difluorotriphenylsilicate. CAS Registry No.: 163931-61-1.

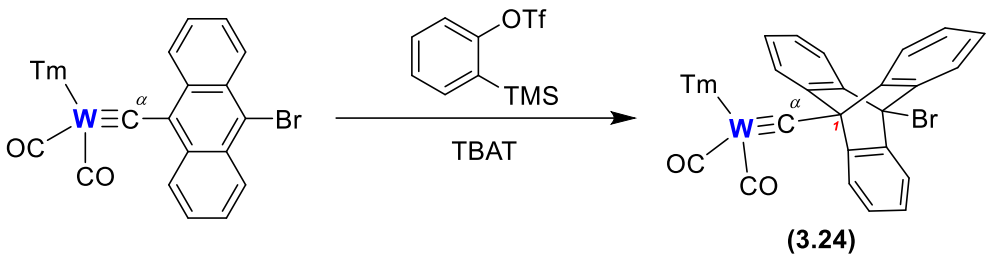

Scheme 3.17. Preparation of complex **3.24**.

A sample of complex **3.24** was isolated *via* silica gel column chromatography, eluting with CH_2Cl_2. Once the CH_2Cl_2 soluble residues had been extracted from the reaction mixture and loaded onto the column, a major brown band was observed to develop from the baseline. This was isolated, concentrated to dryness, and was later shown to be a spectroscopically pure sample of complex **3.24**. Although the assumed structure of complex **3.24** is one which proves to be notable and reasonably rare in the field of organometallic and coordination chemistry, it doesn't afford much in the way of further reaction potential. For example, the terminal bromide group which originated on the anthracenyl ligand is now rendered inaccessible to incoming reactants due to the inclusion of another ring fused $\{C_6H_4\}$ fragment, especially to reactions proceeding *via* S_N1 and S_N2 reaction mechanisms. Although, the carbonyl ligands, metal centre and metallocarbyne bond may still be accessible and subjected to further derivatisation, but such reactions were not attempted during the course of this work.

Complex **3.24** was found to be readily soluble in halogenated solvents, and hence was initially probed using infrared spectroscopy as a CH_2Cl_2 solution. As expected, the two carbonyl bands which were detected for complex **3.22** proved to be almost identical to those found in the spectrum of complex **3.24**, where they were detected at ν_{CO} 1972 and 1884 cm^{-1} in both cases.

The ^1H NMR spectrum of complex **3.24** was recorded as a $CDCl_3$ solution at room temperature, and clearly displayed the addition of another four aromatic protons in the spectrum, compared to the analogous spectrum recorded of complex **3.22**. The triptycenyl protons were detected as two doublets at δ_H 9.34 and 8.49 ppm, with the remaining signals clustered together as an array over the spectral range δ_H 7.64-7.39 ppm. The remaining signals which were detected can all be attributed to protons located on the **Tm** ligand which remained unperturbed and coordinated to the tungsten centre. The cyclic alkene protons found on the three methimazolyl rings were detected upfield of the triptycenyl signals over

the spectral range δ_H 6.92-6.84 ppm, leaving the three *exo*-CH_3 groups which were individually detected as three singlets at δ_H 3.88, 3.67 and 3.52 ppm.

ESI mass spectrometry further affirmed the formation of complex **3.24** as two complex ions, containing both ^{79}Br and ^{81}Br, of the form $[M\text{-}2(CO)+H]^+$. These were calculated to correspond to the isotope pattern simulated for the complex of formula $C_{33}H_{29}BBrN_6S_3W$. The bulk purity of the sample containing complex **3.24** was confirmed through elemental microanalysis, which returned elemental composition results closely matching those calculated for complex **3.24**.

The $^{13}C\{^1H\}$ NMR spectrum of complex **3.24** was recorded as a $CDCl_3$ solution at room temperature. The most downfield signal in the spectrum was recorded at δ_C 277.5 ppm and was assigned to the carbyne carbon atom ($W{\equiv}C^{\alpha}$). Coinciding with this signal, it was measured that the carbyne carbon had a one-bond tungsten-carbon coupling constant of approximately 197 Hz; once again displaying parallels with complex **3.22**. Both diastereotopic carbonyl carbon atoms were independently detected at δ_C 225.0 and 220.7 ppm, with a one-bond tungsten-carbon coupling constant of approximately 171 and 166 Hz, respectively. The signal corresponding to the triptycenyl carbon atom bound directly to the carbyne carbon (*i.e.* WC^{β}) was easily identifiable at δ_C 142.4 ppm, given that it also displayed tungsten satellites with a two-bond tungsten-carbon coupling constant of approximately 41 Hz. The remaining triptycenyl carbon atom signals were grouped together over the spectral range δ_C 135.4-126.2 ppm, with the exception of a signal at δ_C 121.5 ppm which bisected the cyclic alkene carbon atom signals at approximately δ_C 123 and 120 ppm.

Unfortunately, even after several attempts, crystals suitable for structural determination were not formed for complex **3.24**. Hence, the crystal structure of complex **3.24** remains to be elusive.

3.3.15 Synthesis of $[TmW(CO)_2\{{\equiv}C(9\text{-}[10\text{-bromo-anthracenyl}])\}]_2Pt$ and $[TmW(CO)_2\{{\equiv}C(9\text{-}[10\text{-bromo-anthracenyl}])\}]_2Pd$

A concerted effort was undertaken to try and substitute the terminal bromide group at the 10-position on the anthracenyl ligand in complex **3.22** to form larger conjugated structures. Given that it is possible to carry out Sonogashira cross-coupling reactions involving many of the brominated PAHs, it was postulated that a similar process involving complex **3.22** may be feasible, whereby the terminal bromide group might be substituted for

an alkyne fragment, such as phenylacetylene. However, when reactions of this type were trialled, no materials bearing extended conjugated frameworks were ever identified or isolated. During the attempted purification of such crude reaction mixtures, it was consistently noted that a thin brown/red band always developed off the baseline as the silica gel column was eluted. This band was isolated, and despite the extremely low yields which were obtained, the spectroscopic analysis of this material indicated that a product consisting of two equivalents of complex **3.22** and one palladium atom had been formed. Although this result was unexpected, it could be tentatively rationalised by assuming that the initial oxidative addition step in the Sonogashira reaction mechanism, which relied on the coordination of the bromo-anthracenyl ligand to the $[Pd(PPh_3)_4]$ catalyst, was successful, but the subsequent rearrangement and transmetallation steps were unsuccessful . As a result, the palladium metal centre was able to coordinate to another site, and effectively bridge two molecules of complex **3.22**.

Following on from this result, the reaction conditions were changed to try and selectively form the palladium complex which was implicated during these trial reactions. Furthermore, to try and better understand complexes of this type, the analogous platinum-bridged complex was also targeted. To give optimal chance of forming these complexes in more manageable yields, the palladium and platinum metal complexes which were used were selected due to their highly labile ligands, which would ultimately be lost during the reaction. As a result, complex **3.22** was treated with $[Pt(nbe)_3]$ (nbe = norbornene) and $[Pd_2(dba)_3{\cdot}CHCl_3]$ (dba = dibenzylideneacetone) to form complexes **3.25** and **3.26**, respectively, under non-forcing reaction conditions (**Scheme 3.18**).

Samples of both complexes were purified from their respective reaction mixtures using silica gel column chromatography, and were found to be suitable for spectroscopic analysis. Complex **3.25** was isolated as a brown band which developed from the baseline when eluted with 5% (v/v) THF in CH_2Cl_2. Likewise, a marginally less polar eluent mixture consisting of 4% (v/v) THF in CH_2Cl_2 was utilised to isolate complex **3.26** as a dark red/brown solution. The respective column bands containing complexes **3.25** and **3.26** were concentrated to dryness under high vacuum and were subsequently subjected to spectral characterisation.

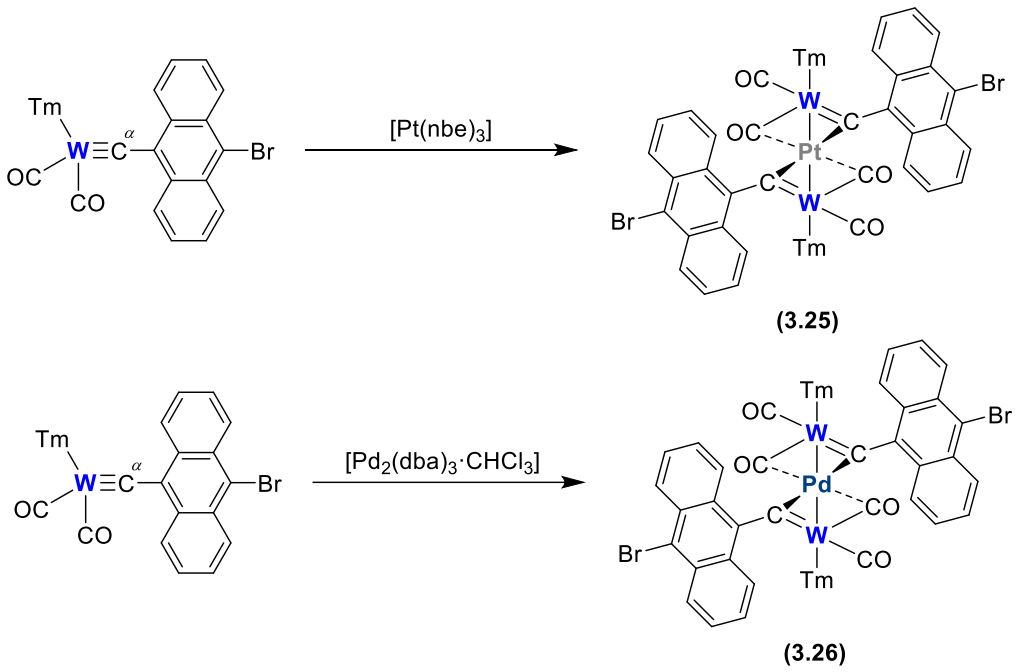

Scheme 3.18. Preparation of complex **3.25** and **3.26**.

Both title complexes were found to be soluble in halogenated solvents, and hence were initially probed *via* infrared spectroscopy as CH_2Cl_2 solutions. For both complexes, the spectra which were obtained contained identical features, which included two carbonyl bands at ν_{CO} 1949 and 1927 cm^{-1} for complex **3.25**, and ν_{CO} 1945 and 1923 cm^{-1} for complex **3.26**. Additionally, a broad band detected towards slightly lower wavenumbers was also detected, and was deemed to be characteristic of a bridging carbonyl ligand. For complexes **3.25** and **3.26**, these bridging carbonyl bands were detected at ν_{CO} 1792 and 1808 cm^{-1}, respectively.

Unfortunately, the ^{1}H NMR spectrum of complex **3.25** was not obtained, given that the complex was found to rapidly precipitate out of common deuterated solvents. However, the ^{1}H NMR spectrum of complex **3.26** was successfully recorded, albeit with moderate contamination from trace solvents and impurities such as BHT (butylated hydroxytoluene, 2,6-bis(1,1-dimethylethyl)-4-methylphenol).

ESI mass spectrometry proved to be a much more useful spectroscopic tool for the analysis of both complexes, as the results which were obtained clearly showed the presence of both target materials. Complex **3.25** was detected as a number of different complex ions on account of the two commonly encountered isotopes of bromine (^{79}Br and ^{81}Br) being detected, and the fact that two bromo-anthracenyl fragments were housed in the complex. Hence, complex ion fragments of the form $[M(^{79}Br_2)]^+$, $[M(^{79}Br, ^{81}Br)]^+$, and $[M(^{81}Br_2)]^+$ were

all identified for complex **3.25**. Likewise, analogous complex ions were also detected for complex **3.26**. For all of these ions, the data which was recorded was found to closely coincide with the isotope patterns simulated for the relevant fragments of complexes **3.25** and **3.26**. Irrespective of the relatively small quantities of both complexes which were isolated, it was possible to confirm the bulk purity of both samples through elemental microanalysis. The results for complex **3.25** closely matched the elemental composition values calculated for a complex of the formula $C_{58}H_{48}B_2Br_2N_{12}O_4PtS_6W_2$ with the inclusion of two equivalents of THF solvent, which likely remained trapped in the sample from the eluent used during column chromatography. Luckily, all traces of solvent were removed in the sample of complex **3.26** which was submitted for elemental microanalytical testing, as the results which were returned matched those calculated for a complex of the formula $C_{58}H_{48}B_2Br_2N_{12}O_4PdS_6W_2$.

Much like the recording of ^{1}H NMR spectra, which was attempted for both complexes, the recording of $^{13}C\{^{1}H\}$ NMR spectra also proved to be problematic. In the case of complex **3.25**, the persistent insolubilities it displayed in a range of deuterated solvents rendered this spectroscopic technique impossible. However, due to the slightly higher degree of stability which complex **3.26** displayed in deuterated solvents, it was possible to record some partial data for the complex. Unfortunately, the spectrum which was recorded contained poor signal-to-noise, as well as missing signals (*e.g.* the bridging carbon nuclei directly bound to the tungsten centres). Hence, for disclosure and noting, these signals have been listed in the Experimental section, but are not suitable for discussion or scrutinization.

Given the several difficulties faced when trying to record various spectroscopic datasets for complexes **3.25** and **3.26**, the prospect of analysis *via* X-ray diffraction became more heavily relied upon to conclusively prove the formation of both title complexes. For complex **3.25**, a crystal suitable for structure determination was grown by vapour diffusion of ethanol into a $CHCl_3$ solution at 4°C (**Figure 3.6**). A region of highly disordered solvent could not be adequately modelled and were removed using a solvent mask.

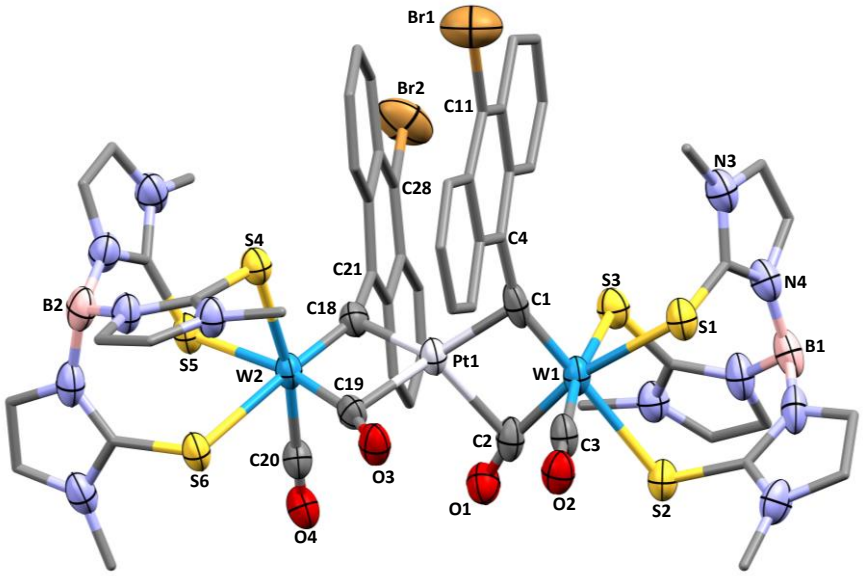

Figure 3.6. Molecular structure of **3.25** (30% displacement ellipsoids) with selected atom labels. Solvent molecules and hydrogen atoms omitted for clarity. Selected distances (Å) and angles (°): W1–Pt1 2.7208(7), W2–Pt1 2.7254(7), Pt1–C1 2.020(8), Pt1–C2 2.272(10), Pt1–C18 2.024(8), Pt1–C19 2.283(7), W1–C1 1.872(11), W1–C2 1.997(11), W2–C18 1.905(8), W2–C19 2.010(9), C1–C4 1.499(13), C18–C21 1.458(11), C11–Br1 1.901(12), C28–Br2 1.938(8), W1–Pt1–W2 166.550(18), C1–Pt1–C2 89.5(4), W1–C1–Pt1 88.6(4), W1–C1–C4 153.6(6), W1–C2–O1 166.7(8), W2–C18–Pt1 87.8(3), W2–C18–C21 152.9(6), W2–C19–O2 164.8(6).

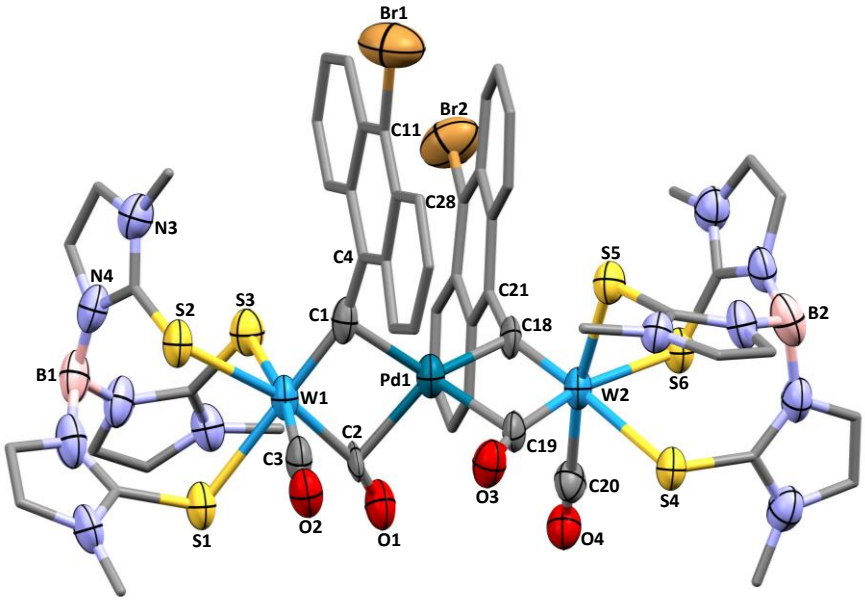

Figure 3.7. Molecular structure of **3.26** (30% displacement ellipsoids) with selected atom labels. Solvent molecules and hydrogen atoms omitted for clarity. Due to the low quality of this synchrotron data, the extensive use of restraints and the solvent mask that was required, this dataset is only included as evidence of connectivity.

Similarly, a crustal of complex **3.26** which was suitable for structural determination was grown *via* the vapour diffusion of ethanol into a $CHCl_3$ solution at 4°C (**Figure 3.7).**

3.3.16 Synthesis of [TmW(CO)$_2${μ-≡C-(9,10-anthracenyl)-C≡}M(CO)$_2$Tp*] (M = Mo, W)

Although it was concluded that the Sonogashira cross coupling approach was incompatible with complex **3.22**, materials featuring extended conjugation were still targeted through the use of alternative reaction pathways. The previously reported tin metallocarbyne complexes [**Tp***(CO)$_2$W≡C(Sn^{n}Bu$_3$)] and [**Tp***(CO)$_2$Mo≡C(Sn^{n}Bu$_3$)] were successfully utilised in conjunction with complex **3.22** to carry out modified Stille cross coupling reactions to prepare the complexes [**Tm**W(CO)$_2${μ-≡C-(9,10-anthracenyl)-C≡}W(CO)$_2$**Tp***] (**3.27**) and [**Tm**W(CO)$_2${μ-≡C-(9,10-anthracenyl)-C≡}Mo(CO)$_2$**Tp***] (**3.28**) in good yields (**Scheme 3.19**).

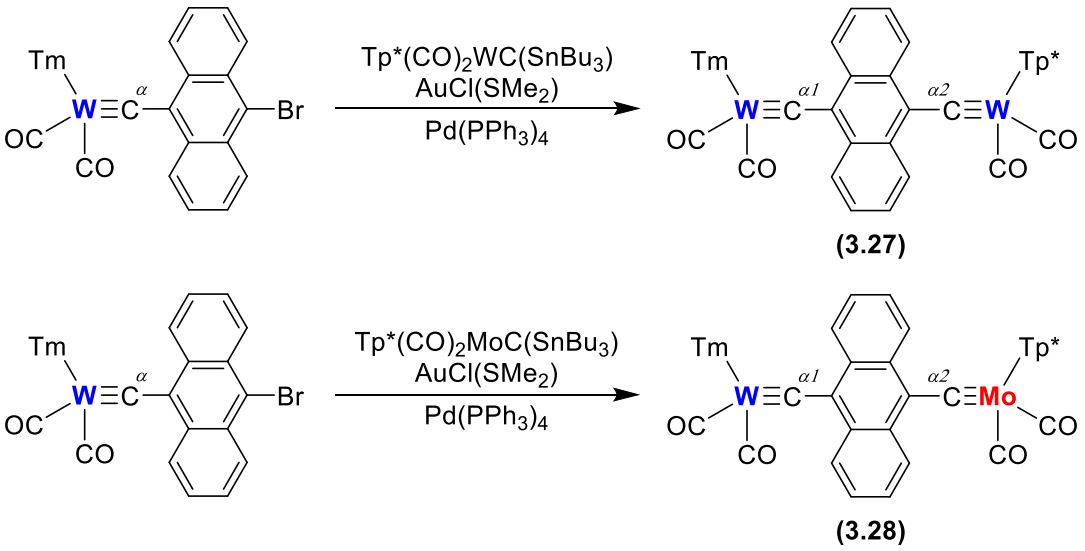

Scheme 3.19. Preparation of complex **3.27** and **3.28**.

Both complexes were isolated from their respective reaction mixtures through silica gel column chromatography, eluting with CH_2Cl_2. Both complexes were highly coloured, on account of their extended conjugated structures, and were isolated as vivid purple powders. Samples of both complexes appeared to be stable in the solid form, but were stored in sealed sample vials at -20°C in an attempt to arrest any potential degradation pathways.

Both samples were found to be readily soluble in halogenated solvents, and were initially tested *via* infrared spectroscopy as CH_2Cl_2 solutions. For complex **3.27**, a total of

three signals in the carbonyl region of the spectrum were observed at ν_{CO} 1974, 1966 and 1884 cm^{-1}. The latter signal was observed to have a notably higher intensity that the others, and it was assumed that this corresponded to two overlapping signals, thereby accounting for the four carbonyl ligands which were contained in the complex. In the case of complex **3.28**, all four carbonyl bands were independently detected at ν_{CO} 1987, 1970, 1903 and 1884 cm^{-1}.

The ^{1}H NMR spectra of both complexes were recorded as $CDCl_3$ solutions at low temperature in order to increase signal resolution. Complex **3.27** afforded a spectrum which clearly showed the incorporation of both the **Tm** and **Tp*** ligands, as well as all eight anthracenyl protons which were detected as the most downfield signals in the spectrum. A similar signal pattern was observed for complex **3.28**, and thereby confirmed the presence of both title materials.

The presence of complex **3.27** was further reinforced through the use of ESI mass spectrometry, which returned results consistent with ion fragments of the form $[M]^+$ and $[M-(CO)]^+$ being present. A single complex ion fragment was identified in the case of complex **3.28**, which was found to closely match the isotope pattern simulated for a complex of the formula $C_{47}H_{46}B_2MoN_{12}O_4W$, thereby corresponding with the $[M]^+$ ion of this complex. The bulk purity of both samples was tested through elemental microanalysis. In both cases, the results which were obtained were shown to be a close match to the those calculated.

Much like the ^{1}H NMR spectra which were recorded of these complexes, the $^{13}C\{H\}$ NMR spectra were also recorded as $CDCl_3$ solutions at low temperature. For complex **3.27**, the most downfield signals which were detected at δ_C 282.0 and 279.3 ppm corresponded to the two carbyne carbon atoms ($W{\equiv}C^{\alpha}$) found in the complex. All four carbonyl carbon atoms were independently detected as a cluster of closely associated signals at δ_C 227.6, 227.5, 225.4 and 220.8 ppm. The signals associated with the anthracenyl carbon atoms were detected as an array of signals over the approximate spectral range δ_C 142-126 ppm, and were flanked by signals corresponding to various carbon atoms located in the backbone structures of the **Tm** and **Tp*** ligand systems. A similar spectrum was also obtained for complex **3.28**, although the most downfield signal in this spectrum at δ_C 249.1 ppm corresponded to the carbyne carbon atom directly bound to the molybdenum centre ($Mo{\equiv}C^{\alpha}$). The carbyne carbon atom bound to the tungsten centre ($W{\equiv}C^{\alpha}$) was found marginally upfield of this signal, at δ_C 278.2 ppm, and in line with results typical for a carbon atom in this environment. Once again, all four carbonyl signals were independently detected at δ_C 229.3, 229.2, 225.2 and 220.5 ppm.

A crystal of complex **3.27** which was suitable for structural determination was grown *via* vapour diffusion of *n*-pentane into a CH_2Cl_2 solution at 4°C. Due to the small size of the crystal, a larger X-ray source was required in order to successfully obtain an X-ray diffraction image (**Figure 3.8**). Unfortunately, the quality of the data rendered it not useful for the study of its internal bond parameters, but it did successfully confirm the connectivity found within the complex.

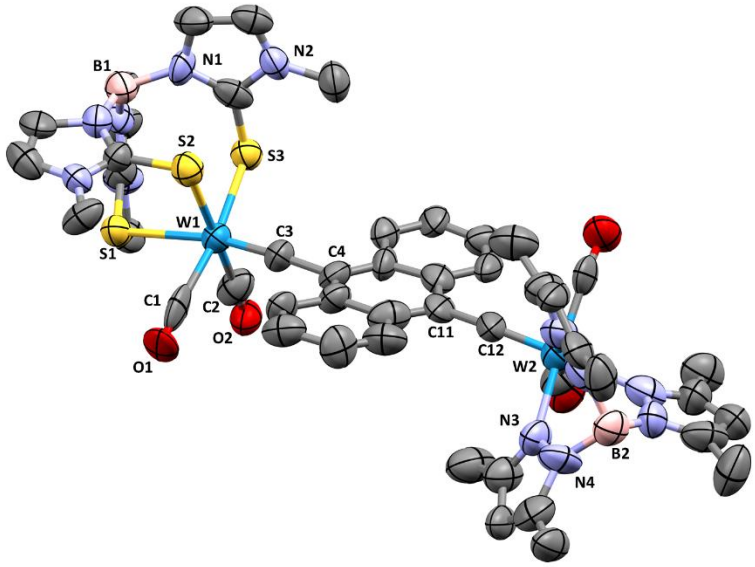

Figure 3.8. Molecular structure of **3.27** (50% displacement ellipsoids) with selected atom labels. Solvent molecules and hydrogen atoms omitted for clarity. The low quality of the acquired synchrotron data means that this structural model is included only as evidence of connectivity.

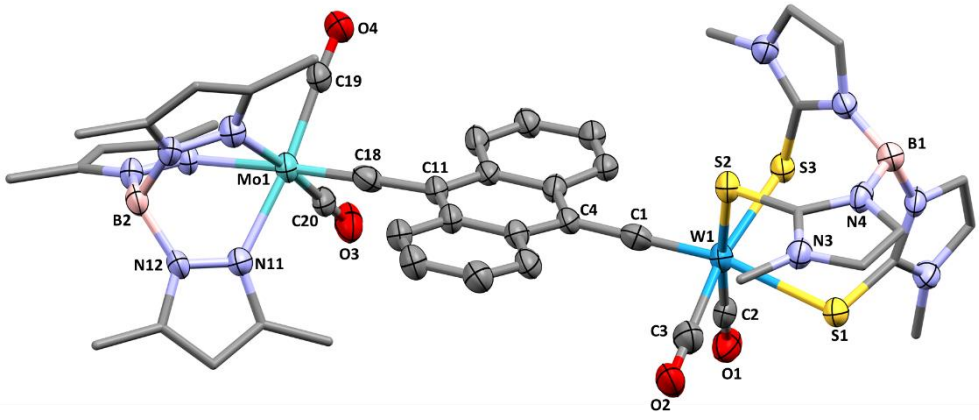

Figure 3.9. Molecular structure of **3.28** (30% displacement ellipsoids) with selected atom labels. Solvent molecules and hydrogen atoms omitted for clarity. Selected bond lengths (Å) and angles (°): W1–S3 2.540(3), W1–S2 2.546(3), W1–S1 2.652(3), W1–C1 1.817(12), Mo1–N7 2.319(9), Mo1–N9 2.224(9), Mo1–N11 2.233(8), Mo1–C18 1.796(11), C1–C4 1.456(15), C11–C18 1.478(14), C25–S3–W1 108.0(4), C29–S2–W1 104.4(4), C21–S1–W1 105.5(4), C4–C1–W1 178.6(9), C11–C18–Mo1 171.9(9).

A single crystal of complex **3.28** was grown *via* vapour diffusion of ethanol into a $CHCl_3$ solution at 4°C. In contrast to the data obtained for complex **3.27**, the structural data which was recorded was shown to be of sufficiently high quality to allow for the extraction of bond parameters (**Figure 3.9**).

3.4 Summary

Through the utilisation of the oxide abstraction synthetic protocol, a library of **Tm**-ligated tungsten and molybdenum metallocarbyne complexes were successfully formed, featuring a range of PAH (e.g. naphthyl, phenanthryl, anthracenyl, etc.) termini. Although it was initially postulated that the inclusion of optoelectronically active moieties into carbyne frameworks would lead to similarly active metallocarbynes, the complexes which were formed did not display any notable optical properties (e.g. fluorescence emission). This is undoubtedly due to the heavy metal nuclei facilitating intramolecular quenching mechanisms and resulting in optically inactive materials.

In addition to common PAHs, a select few novel complexes were prepared through alternative reaction pathways. For example, it was found that through the post-synthetic modification of the bromo-anthracenyl functionalised complex [**Tm**$W(CO)_2${≡C(9-[10-bromo-anthracenyl])}], a bromo-triptycenyl terminus can be formed through the *in situ* generation of benzyne in the reaction mixture. Furthermore, two rarely encountered cyclophane functionalised complexes were formed *via* a modified Stille coupling mechanism.

It was acknowledged that through a modified Sonogashira cross-coupling reaction, it may be possible to extend the conjugated electronic system in the complex [**Tm**$W(CO)_2${≡C(9-[10-bromo-anthracenyl])}] through the substitution of the bromo-group with suitable alkyne fragments. However, during attempts to carry out such a conversion, it was noted that the reaction did not proceed as anticipated, and instead afforded 'butterfly' complexes of the form [**Tm**$W(CO)_2${≡C(9-[10-bromo-anthracenyl])}]$_2$M (M = Pt, Pd). Subsequently, dedicated efforts led to the preparation of such complexes through more efficient routes, namely through the addition of more suitable Pt- and Pd-reagents.

Although the electronic systems within [**Tm**$W(CO)_2${≡C(9-[10-bromo-anthracenyl])}] were not successfully extended through the Sonogashira pathway, through the application of the modified Stille protocol complexes of the form [**Tm**$W(CO)_2${μ-≡C-(9,10-anthracenyl)-C≡}$M(CO)_2$**Tp***] (M = Mo, W) were prepared. Both W:W and W:Mo

variants prove to be noteworthy, due to the incorporation of both **Tm**- and **Tp***-ligand systems within the same complex. However, neither complex was found to display notable optical properties.

3.5 Chapter 3 - References

1. Harvey, R. G., *Polycyclic Aromatic Hydrocarbons*, Wiley, **1997**.
2. Miao, Q., *Polycyclic Arenes & Heteroarenes: Synthesis, Properties, and Applications*, Wiley, **2015**.
3. Wu, Y. T., Siegel, J. S., *Chem. Rev.*, **2006**, *106*, 4843.
4. Scott, L. T., *Chem. Soc. Rev.,* **2015**, *44*, 6464.
5. Keyte, I. J., Harrison, R. M., Lammel, G., *Chem. Soc. Rev.*, **2013**, *42*, 9333.
6. Kim, K. H., Jahan, S. A., Kabir, E., Brown, R. J. C., *Environ. Int.*, **2013**, *60*, 71.
7. Anthony, J. E., *Chem. Rev.*, **2006**, *106*, 5028.
8. Anthony, J. E., *Angew. Chem. Int. Ed.*, **2008**, *47*, 452.
9. Tremblay, N. J., Gorodetsky, A. A., Cox, M. P., Schiros, T., Kim, B., Steiner, R., Bullard, Z., Sattler, A., So, W. Y., Itoh, Y., Toney, M. F., Ogasawara, H., Ramirez, A. P., Kymissis, I., Steigerwald, M. L., Nuckolls, C., *ChemPhysChem.*, **2010**, *11*, 799.
10. Xiao, S., Kang, S. J., Wu, Y., Ahn, S., Kim, J. B., Loo, Y. L., Siegrist, T., Steigerwald, M. L., Li, H., Nuckolls, C., *Chem. Sci.*, **2013**, *4*, 2018.
11. Zhan, X., Zhang, J., Tang, S., Lin, Y., Zhao, M., Yang, J., Zhang, H. L., Peng, Q., Yu, G., Li, Z., *Chem. Commun.*, **2015**, *51*, 7156.
12. Li, C., Wang, Y., Zhang, T., Zheng, B., Xu, J., Miao, Q., *Chem. Asian. J.*, **2019**, *14*, 1676.
13. Wu, J., Pisula, W., Mullen, K., *Chem., Rev.*, **2007**, *107*, 718.
14. Liu, G., Xiao, C., Negri, F., Li, Y., Wang, Z., *Angew. Chem. Int. Ed.*, **2020**, *59*, 2008.
15. Tang, C. W., Vanslyke, S. A., *Appl. Phys. Lett.*, **1998**, *51*, 913.
16. Wu, K. C., Ku, P. J., Lin, C. S., Shih, H. T., Wu, F. I., Huang, M. J., Lin, J. J., Chen, I. C., Cheng, C. H., *Adv. Funct. Mater.*, **2008**, *18*, 67.
17. Orner, K. M., Ku, S. Y., Wong, K. T., Bard, A. J., *Angew. Chem. Int. Ed.*, **2009**, *48*, 9300.
18. Lee, K. H., Park, J. K., Seo, J. H., Park, S. W., Kim, Y. S., Kim, Y. K., Yoon, S. S., *J. Mater. Chem.*, **2011**, *21*, 13640.
19. Xiao, J., Liu, S., Liu, Y., Ji, L., Liu, X., Zhang, H., Sun, X., Zhang, Q., *Chem. Asian J.*, **2012**, *7*, 561.
20. Schoch, T. K., Main, A. D., Burton, R. D., Lucia, L. A., Robinson, E. A., Schanze, K. S., McElwee-White, L., *Inorg. Chem.*, **1996**, *35*, 7769.
21. Baker, L. J., Clark, G. R., Rickard, C. E. F., Roper, W. R., Woodgate, S. D., Wright, L. J., *J. Organomet. Chem.*, **1998**, *551*, 247.
22. Frogley, B. J., Hill, A. F., Seitz, A., *Chem. Commun.*, **2020**, *56*, 3265.
23. Borren, E. S., Hill, A. F., Shang, R., Sharma, M., Willis, A. C., *J. Am. Chem. Soc.*, **2013**, *135*, 4942.
24. Reinholdt, A., Bendix, J., Hill, A. F., Manzano, R. A., *Dalton Trans.*, **2018**, *47*, 14893.
25. Hill, A. F., Malget, J. M., White, A. J. P., Williams, D. J., *Eur. J. Inorg. Chem.*, **2004**, 818.

26. Roncali, J., *Chem. Rev.*, **1992**, *92*, 711.

27. Snook, G. A., Kao, P., Best, A. S., *J. Power Sources*, **2011**, *196*, 1.

28. Brown, C., Farthing, A. C., *Nature*, **1949**, *164*, 915.

29. Reich, H. J., Cram, D. J., *J. Am. Chem. Soc.*, **1969**, *91*, 3517.

30. Cram, D. J., Allinger, N. L., *J. Am. Chem. Soc.,* **1955**, *77*, 6289.

31. Reich, H. J., Cram, D. J., *J. Am. Chem. Soc.*, **1969**, *91*, 3527.

32. Cram, D. J., Steinberg, H., *J. Am. Chem. Soc.,* **1951**, *73*, 5691.

33. Cram, D. J., Cram, J. M., *Acc. Chem. Res.*, **1971**, *4*, 204.

34. Winberg, H. E., Fawcett, F. S., Mochel, W. E., Theobald, C. W., *J. Am. Chem. Soc.*, **1960**, *82*, 1428.

35. Winberg, H. E., Fawcett, F. S., *Org. Synth.*, **1962**, *42*, 83.

36. Cram, D. J., Wilkinson, D. I., *J. Am. Chem. Soc.*, **1960**, *82*, 5721.

37. Kai, Y., Yasuoka, N., Kasai, N., *Acta Cryst. B*, **1978**, *34*, 2840.

38. Hu, J. Y., Pu, Y. J., Yamashita, Y., Satoh, F., Kawata, S., Katagiri, H., Sasabe, H., Kido, J., *J. Mater. Chem. C*, **2013**, *1*, 3871.

39. Stern, D., Finkelmeier, N., Stalke, D., *Chem. Commun.*, **2011**, *47*, 2113.

40. Stern, D., Finkelmeier, N., Meindl, K., Henn, J., Stalke, D., *Angew. Chem. Int. Ed.*, **2010**, *49*, 6869.

41. Frogley, B. J., Hill, A. F., Welsh, S. S., *Chem. Commun.*, **2021**, *57*, 13353.

42. Frogley, B. J., Hill, A. F., Welsh, S. S., *Dalton Trans.*, **2021**, *50*, 15502.

43. Foreman, M. R. St.-J., Hill, A. F., Tshabang, N., White, A. J. P., Williams, D. J., *Organometallics*, **2003**, *22*, 5593.

44. Himeshima, Y., Sonoda, T., Kobayashi, H., *Chem. Lett.*, **1983**, *12*, 1211.

CHAPTER 4.

AMINOCARBYNE COMPLEXES

4.1 Introduction

Transition metal aminocarbynes (aminoalkylidynes), $[L_nM{\equiv}C{-}NR_2]$, much like their carbyne (alkylidyne) predecessors, have been underpinned as a prominent field within organometallic chemistry. Materials of this type have been the subject of tenacious interest over the past several decades, predominantly spurred on by the search for their purportedly unique opto-electronic properties, which ultimately may be harnessed in organometallic non-linear optical materials.[1–4]

4.2 Background and Scope

Soon after the initial report by E. O. Fischer and co-workers of the first metal-carbyne species in 1973,[2,3] the first organometallic aminocarbyne complex was also reported.[1] By utilising the same chemical strategy which had led them to their initial seminal discovery, they were able to treat the complex $[(CO)_5W\{{=}C(NEt_2)(OEt)\}]$ with BX_3 (X = Br, I) in a solution of *n*-pentane to form the tetracarbonyl aminocarbyne complex $[X(CO)_4W\{{\equiv}CN(Et_2)\}]$ (X = Br, I) (**Scheme 4.1**).

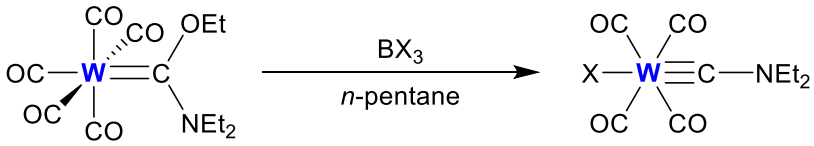

Scheme 4.1. Formation of the first aminocarbyne complex (X = Br, I).

Merely one year later, the synthetic routes towards organometallic aminocarbyne complexes were yet again expanded and improved upon by Richards, Pombeiro and co-workers with their one-step synthesis of aminocarbyne complexes featuring group 6 transition metals. Through the β-protonation of electron-rich tungsten and molybdenum complexes ligated with isocyanides, it was found that dicationic bis-aminocarbyne complexes of the type *trans*-$[(dppe)_2M\{{\equiv}C{-}N(H)(Me)\}_2][BF_4]_2$ (M = Mo, W; dppe = $Ph_2P(CH_2)_2PPh_2$) could be formed (**Scheme 4.2**).[5] Furthermore, the reactivity of these complexes was tentatively explored *via* the addition of alkylating- and reducing-agents, resulting in the mono-alkylation or mono-protonation of the nitrogen-atom, respectively.

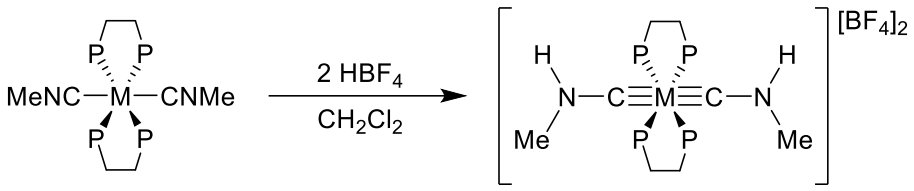

Scheme 4.2. Aminocarbyne formation *via* the protonation of isocyanides (M = Mo, W).

The isonitrile ligands bound to the *trans*-[(dppe)$_2$M(CNMe)$_2$] (M = Mo, W) starting materials used in the reaction detailed above are known to receive very strong π-back donation from the metal centre, which results in the build-up of electron density on the isonitrile ligands. This effect becomes evident upon review of the C–N–Me dihedral angle in the crystal structure of this complex, which shows a deviation of approximately 25° from the expected 180° dihedral angle for isonitrile ligands.[6] Overall, the bending of the nitrogen atom out of linearity renders it more susceptible to attack from electrophiles, thereby allowing for the formation of carbyne-like species.

Although similarities exist between the aminocarbyne and carbyne fragments, the incorporation of the amino substituent induces a unique effect on the structure and reactivity of such species. Hence, the bonding description for organometallic aminocarbynes cannot be adequately described without the inclusion of the 2-azavinylidene resonance form (**Scheme 4.3**).

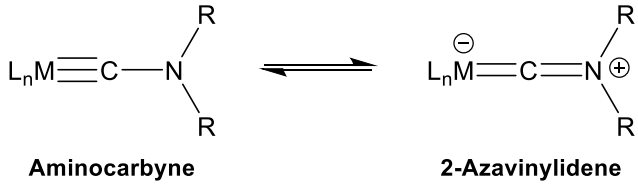

Scheme 4.3. Aminocarbyne and 2-azavinylidene canonical resonance forms.

The lone pair on the nitrogen atom competes with the retrodative bonding from the metal centre for one of the empty p-orbitals on the interstitial carbon atom. This delocalization of electron density along the aminocarbyne fragment has a pertinent effect, manifested by a clear weakening of the metal-carbon triple bond; something which may be crystallographically detected in many complexes upon review of the elongated M≡C and contracted C–N bonds. Furthermore, the reactivity of aminocarbyne complexes appears to

be sluggish when compared to that of their carbyne analogues; thereby further emphasising the contribution of the 2-azavinylidene resonance form, and the stabilising effect it infers.

Aminocarbynes may be further categorized depending on the level of substitution on the nitrogen atom. Where the aminocarbyne ligand bears two alkyl- or aryl-groups (C–NR^1R^2), these may be classified as tertiary aminocarbynes. Likewise, secondary (C–NR^1H) and primary (C–NH_2) aminocarbynes may be formed bearing one or two hydrogen atoms, respectively (**Figure 4.1**).

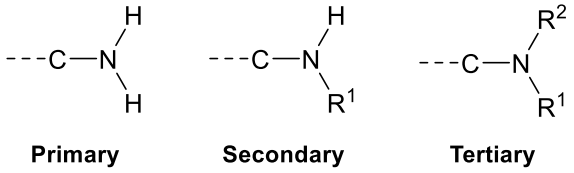

Figure 4.1. Primary, secondary, and tertiary aminocarbyne fragments.

Throughout the work carried out herein, complexes featuring predominantly tertiary aminocarbyne fragments have been formed around tungsten and molybdenum centres. Much like the common theme throughout all Chapters of this report, the complexes that have been formed feature the soft Scorpionate ligands **Tm**[7] and **Htt**,[8] which act as tridentate, facially capping ligands (L_{fac}) (**Figure 4.2**).

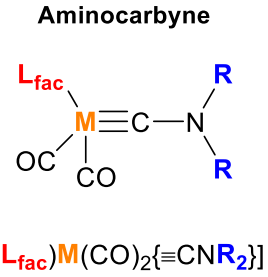

Figure 4.2. Typical structure and linear formulae of aminocarbynes formed in this work.

Although many combinations of metals, ligands, and simple amino fragments were synthetically targeted, not all combinations were successfully reacted in order to form their respective target materials. However, out of all the complexes which were isolated, the majority contain the **Htt** ligand; something which serves as a novelty, given the rarity of this ligand throughout literature. Many analogues of the complexes prepared herein have been

previously reported in literature, and include many examples bearing Cp,[9–11] Cp*,[11] **Tp**[12] and **Tp***[10,13,14] facially capping ligands. Hence, the expansion of this field through the use of the chemically divergent homologous of soft Scorpionate ligands, such as **Tm** and **Htt**, is not without precedent.

4.3 Synthesis of Group 6 Aminocarbyne Complexes

4.3.1 Preparation from Isocyanide Ligands

Isocyanide (C≡NR) ligands are widely used throughout both organic[15] and organometallic[16] chemistry, on account of the vast library of known examples and ability to undergo electronic modulation through alteration of the terminal R-group and subsequent coordination to a transition metal centre in several different bonding modes (**Scheme 4.4**).[17,18]

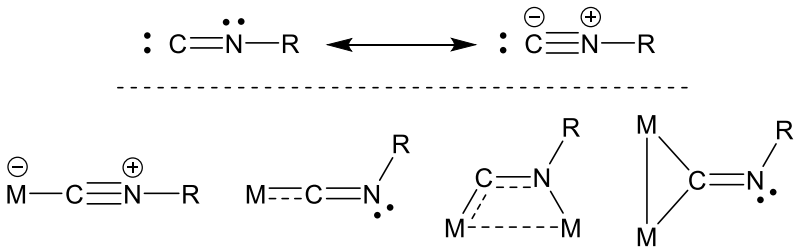

Scheme 4.4. (*Top*) Two of the highest contributing resonance forms of isocyanide ligands. (*Bottom*) Examples of isocyanide binding modes to metal centres.

Upon coordination to a metal centre, isocyanide ligands may become activated in one of two ways, depending on the electronic properties of the coordination site. Ultimately, depending on the activation regime adopted by the isocyanide ligand, reactivity may be directed towards either the carbon atom, or the nitrogen atom, thereby allowing them to form two separate classes of complexes.

If an incoming isocyanide ligand binds to an efficient Lewis acidic site primarily through a σ-donor interaction (i.e. with no appreciable π-electron interactions), the isocyanide ligand becomes activated towards nucleophilic addition at the coordinated carbon atom (M–C$^{\alpha}$NR). Through the addition of protic nucleophiles (NuH), this provides a route to forming aminocarbene species: something which will not be discussed in detail throughout

this Chapter. Conversely, in cases where the free coordination site is situated on a low-valent, electron-rich transition metal centre, which exhibits a high π-electron releasing ability, the isocyanide ligands become activated towards electrophilic attack at the nitrogen atom, which in turn allows for the formation of aminocarbyne complexes (**Scheme 4.5**).[17]

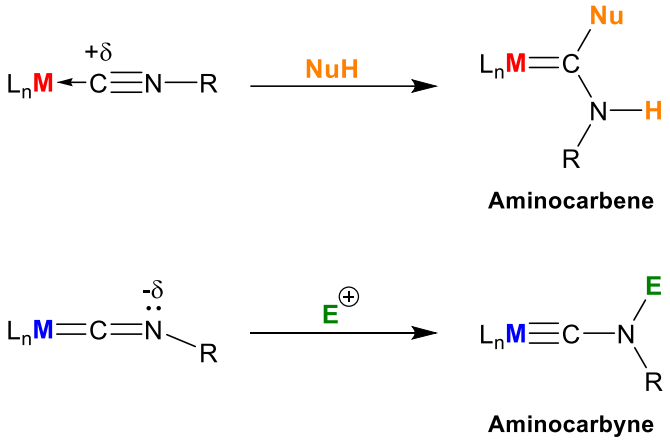

Scheme 4.5. Formation of aminocarbene and aminocarbyne complexes through the addition of protic nucleophiles (NuH) and electrophiles (E^+), respectively.

It has been shown that the use of platinum or palladium metal centres in middle or high oxidation states allows for the formation of aminocarbene species.[19] By comparison, to invoke the electrophilic addition process and form aminocarbyne complexes, typically, low-valent metals such as rhenium, molybdenum, or tungsten are normally utilised. To highlight some of the examples of aminocarbyne complexes which have been prepared through this synthetic route, some select examples from literature have been detailed in the following paragraphs.

The dinitrogen ligated complex *trans*-[ReCl(N_2)(dppe)$_2$] (dppe = $Ph_2P(CH_2)_2PPh_2$) has been shown to undergo ligand substitution with isocyanides to prepare Re(I) complexes of the form *trans*-[ReCl(dppe)$_2${≡C-NR}] (R = alkyl, or aryl) (**Scheme 4.6**).[20,21]

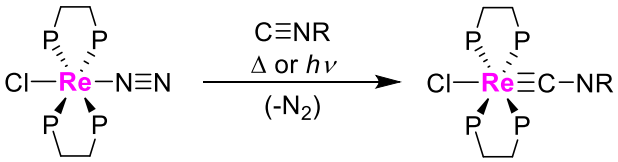

Scheme 4.6. Formation of *trans*-[ReCl(dppe)$_2${≡C-NR}] through substitution by isocyanide.

Similarly, analogous complexes assembled around molybdenum and tungsten centres have also been formed.[22] It is noteworthy that the reaction between isocyanides and *trans*-[MCl(N$_2$)(dppe)$_2$] (M = Mo, W) occurs in a reasonably facile manner compared to that of isocyanides with the aforementioned dinitrogen rhenium complex. In the case of the latter, longer heating times, or photochemical irradiation is required to labilise the dinitrogen ligand.[21]

Moreover, tungsten and molybdenum piano-stool aminocarbyne complexes, akin to those prepared in this report (albeit *via* different routes), can be accessed through the alkylation of the monoanionic complexes [Cp^{R}M(CO)$_2$(CNEt)]$^-$ with [Et$_3$O][BF$_4$] in order to form complexes of the type [Cp^{R}M(CO)$_2${≡CNEt$_2$}] (M = Mo, W; Cp^R = Cp, Cp*) (**Scheme 4.7**).[23,24]

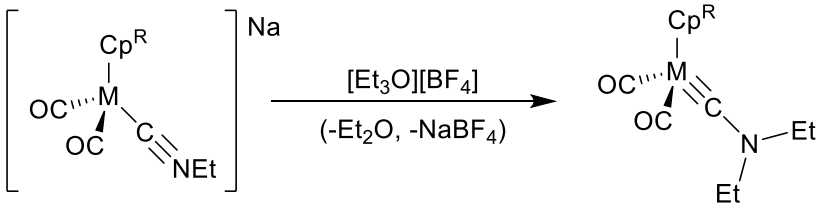

Scheme 4.7. Formation of [Cp^{R}M(CO)$_2${≡CNEt$_2$}] (M = Mo, W; Cp^R = Cp, Cp*).

Electron rich complexes bearing both isocyanide and Scorpionate ligands have been previously utilised to form aminocarbyne complexes using a similar alkylation strategy to that outlined above. For example, the **Tp*** ligated complex [**Tp***Mo(CO)$_2${≡C-NRMe}] has been successfully prepared *via* the methylation of the monoanionic precursor [**Tp***Mo(CO)$_2$(C≡NR)]$^-$ (R = Me, Ph) through the addition of methyl iodide (**Scheme 4.8**).[25]

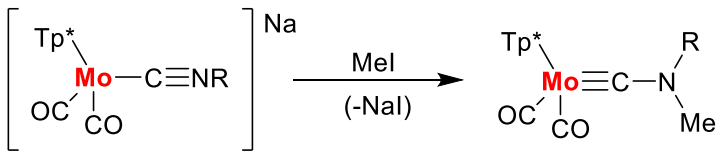

Scheme 4.8. Formation of [**Tp***Mo(CO)$_2$(C≡NR^1)] (R^1 = Me, Ph).

It is noteworthy that while this procedure works well for the molybdenum complex bearing the methyl isocyanide ligand, it is not a generalisable synthetic route. When the same reaction was attempted using the *tert*-butyl isocyanide functionalised complex, a mixture of

products was formed. Although the desired molybdenum aminocarbyne complex [**Tp***Mo(CO)$_2${≡CN(ᵗBu)(Me)}] was successfully isolated from the complex mixture, the other two complexes which were isolated displayed alkylation of the isocyanide carbon atom, or alkylation of one of the carbonyl carbon atoms, thereby forming complexes with a semi-bridging motif (**Scheme 4.9**).

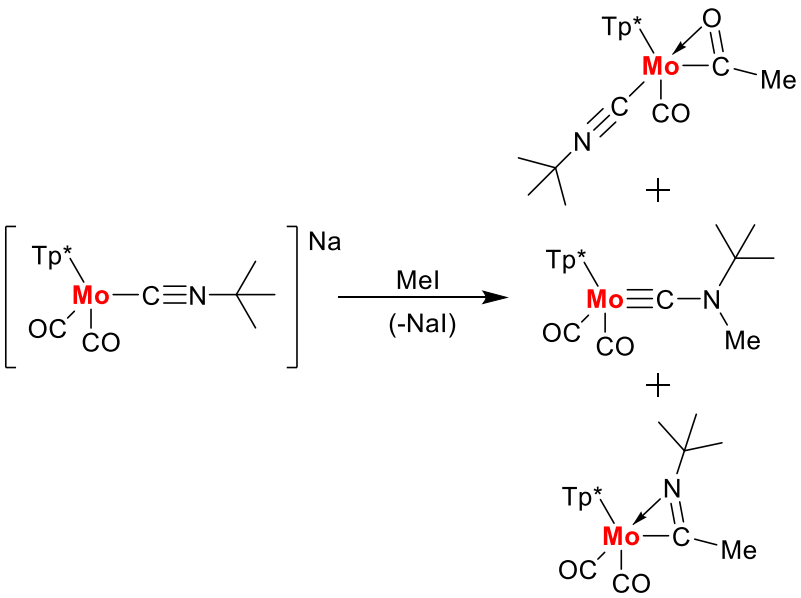

Scheme 4.9. Methylation of [**Tp***Mo(CO)$_2$(C≡N(ᵗBu)]⁻, resulting in the formation of [**Tp***Mo(CO)$_2${≡CN(ᵗBu)(Me)}] and two other isomeric products.

4.3.2 Preparation from Carbonyl Ligands

Given the inexpensive and readily available nature of group 6 metal hexacarbonyl complexes, they serve to be excellent starting materials for the preparation of aminocarbyne complexes. The most common synthetic process which utilises these starting materials is the ubiquitous oxide abstraction reaction protocol, which serves to be omnipresent throughout the work herein. The oxide abstraction process to forming group 6 aminocarbyne complexes has been discussed in detail in **Section 4.4.1**. However, in the following paragraphs, some select examples from literature have been included to describe this process and to provide further insight into the chemical and physical properties of aminocarbyne complexes prepared *via* this route, as well as others derived from various carbonyl chemistries.

Examples of aminocarbyne complexes formed from chromium, molybdenum, and tungsten hexacarbonyl have all been noted in literature. Typically, chromium complexes

bearing carbyne or aminocarbyne ligands exhibit significantly greater thermal sensitivities compared to their molybdenum and tungsten analogues. However, this is not always the case. The monocationic chromium aminocarbyne complex $[Cr(CO)_5\{\equiv CNMe_2\}][BF_4]$ may be formed through the sequential treatment of $[Cr(CO)_6]$ with lithium dimethylamide, $[Et_3O][BF_4]$, and BF_3 at low temperature (**Scheme 4.10**) and serves to be an exemplar of this type of behaviour.[26,27]

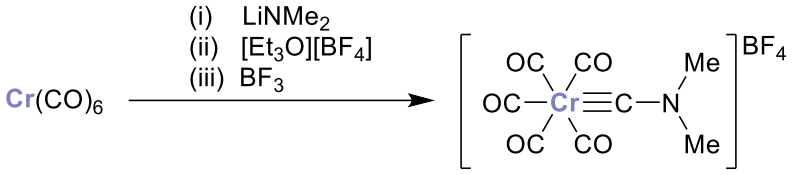

Scheme 4.10. Formation of $[Cr(CO)_5\{\equiv CNMe_2\}][BF_4]$.

Even when stored under an argon atmosphere at low temperature, the tungsten and molybdenum complexes of the form $[M(CO)_5\{\equiv CNMe_2\}][BF_4]$ (M = Mo, W) decompose *via* the liberation of carbon monoxide over a period of hours. Whereas, the analogous $[Cr(CO)_5\{\equiv CNMe_2\}][BF_4]$ complex appears to be more resistant towards decomposition, given that under identical conditions the complex decomposes over a period of months. This may be rationalised with reference to the lower electronegativity of the chromium centre, compared to that of molybdenum or tungsten, which ensures that sufficient electron density is labilised from the metal centre to partake in π-back donation to the carbonyl ligands. Although this synergic bonding model weakens the carbonyl C–O bond, the M–C interactions of the carbonyl ligands are strengthened, thereby ensuring degradation processes are significantly stunted.

E. O. Fischer and co-workers were able to sufficiently stabilise the diethylamino-substituted variant of the aforementioned tungsten complex through substitution of the $[BF_4]^-$ counterion with $[SbX_6]^-$ (X = F, Cl).[28] Compared to the $[BF_4]^-$ ion, $[SbX_6]^-$ (X = F, Cl) exhibits even greater non-coordinative behaviour. This has a stabilising effect on the $[W(CO)_5\{\equiv CNEt_2\}]^+$ cation as a result of the increased electron density about the complex, which would otherwise be committed in the ionic interaction with the counterion. Subsequently, crystals suitable for structural analysis were successfully formed of the complex $[W(CO)_5\{\equiv CNEt_2\}][SbCl_6]$ (**Figure 4.3**).

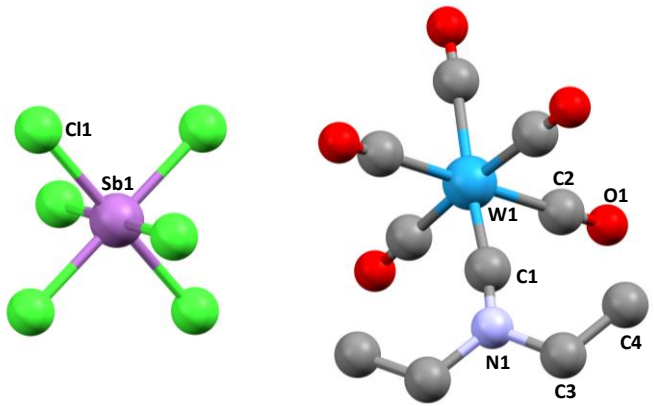

Figure 4.3. Molecular structure of $[W(CO)_5\{\equiv CNEt_2\}][SbCl_6]$ with selected atom labels. Hydrogen atoms have been omitted for clarity. CCDC reference number 1111634.

Through modification of the synthetic route to forming complexes of the type $[M(CO)_5\{\equiv CNR_2\}][BF_4]$ (M = Cr, Mo, W; R = alkyl), as detailed above in **Scheme 4.10**, it is possible to prepare tetracarbonyl complexes of the form $[XM(CO)_4\{\equiv CNR_2\}]$ (M = Cr, Mo, W; X = Cl, Br, I) through various routes (**Scheme 4.11**).[1,28,29]

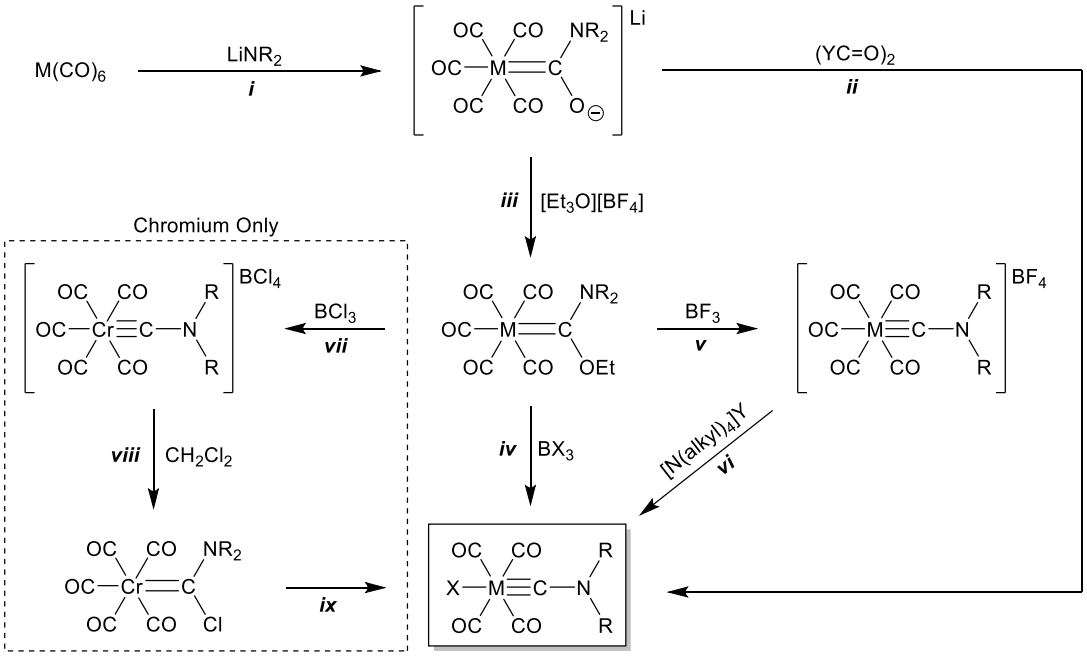

Scheme 4.11. Routes to forming $[XM(CO)_4\{\equiv CNR_2\}]$ (M = Cr, Mo, W; X = Cl, Br, I). (***i***) M = Cr, Mo, W; R = Me, Et, ^{i}Pr. (***ii***) M = Cr, W; R = ^{i}Pr; Y = Cl, Br. (***iii***) M = Cr, Mo, W; R = Me, Et, ^{i}Pr. (***iv***) M = Cr, R = Et; M = W, R = Me or Et; X = Cl, Br, I. (***v***) M = Mo, W; R = Et. (***vi***) M = Mo; R = Et; alkyl = Et, ^{n}Bu; Y = Br, I, SCN. (***vii***) M = Cr; R = Me, Et, piperidine. (***viii***) R = Me, Et, pyrrolidine. (***ix***) R = Me, Et, pyrrolidine, Ph.

The most simplistic of these may be carried out through the formation of the desired iminoacyl complex (*path* ***i***) and subsequent treatment with an oxalyl halide (*path* ***ii***) which leads directly to the desired [XM(CO)$_4${≡CNR$_2$}] complex. Otherwise, generation of the highly versatile pentacarbonyl intermediate [M(CO)$_5${=C(NR$_2$)(OEt)}] from the iminoacyl complex (*path* ***iii***) allows for several other synthetic routes. Once isolated, the [XM(CO)$_4${≡CNR$_2$}] complex may then be utilised in a large range of synthetic protocols,[30] almost all of which involve ligand substitution. For example, the addition of γ-picoline†††† to [XCr(CO)$_4${≡CN^{i}Pr$_2$}] affords the bis(γ-picoline) complex [X(pic)$_2$Cr(CO)$_2${≡CN^{i}Pr$_2$}].[31] The two picoline ligands increase the relative electron density on the chromium metal centre and thereby increases the stability of the complex. Nonetheless, the two γ-picoline ligands can be easily substituted when a stronger chelating ligand is added. If a tridentate ligand is added, both γ-picoline ligands and the metal-bound halogen atom may be substituted. Examples of complexes which have been prepared through this route include those ligated with Cp, Cp*, and **Tp*** (**Scheme 4.12**).[31]

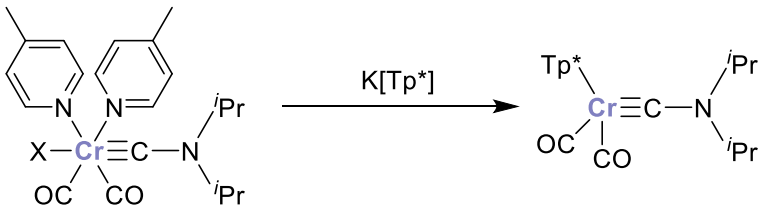

Scheme 4.12. γ-Picoline ligand substitution with **Tp*** to form [**Tp***Cr(CO)$_2${≡CN^{i}Pr$_2$}].

Late common-intermediates such as the bis(γ-picoline) complex [X(pic)$_2$Cr (CO)$_2${≡CN^{i}Pr$_2$}] offer a simple way to incorporate a range of alternative ligand systems. The **Tm**-ligated tungsten analogue of the complex formed in **Scheme 4.12** has also been prepared using another such intermediate, [BrW(CO)$_3$(PPh$_3$){≡CN^{i}Pr$_2$}] (**Scheme 4.13**), and further highlights the utility of these types of complexes.[32]

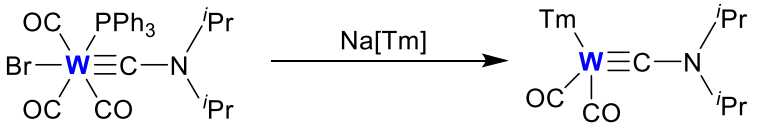

Scheme 4.13. Formation of [**Tm**W(CO)$_2${≡CN^{i}Pr$_2$}] *via* ligand substitution.

†††† Also referred to as 4-methylpyridine, 4-picoline, or 4-C$_5$H$_4$N-Me. CAS Registry No.: 108-89-4.

4.4 Results & Discussion: Routes to Tm & Htt Ligated Aminocarbyne Complexes

4.4.1 General Reaction Procedure

Much like the protocols used to prepare the majority of the carbyne and propargylidyne complexes detailed in this report, the oxide abstraction synthetic protocol (**Scheme 4.14**) using metal hexacarbonyl starting materials was once again applied here in order to form a range of aminocarbyne complexes. To avoid repetitive descriptions, a general overview of the synthetic method has been provided here, and in the following sections descriptions relating to the isolation and purification of specific target complexes have been provided, as well as a discussion on their notable spectral features.

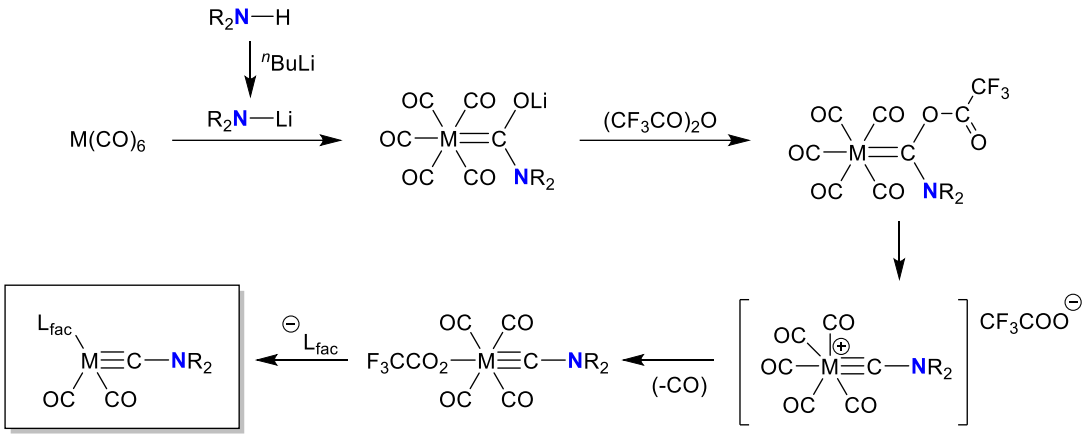

Scheme 4.14. Formation of aminocarbyne complexes through the Fischer-Mayr synthetic protocol. (M = Mo, W; R = alkyl, aryl; L_{fac} = **Tm**, **Htt**)

In order to successfully form the lithiated acylate species $Li[M(CO)_5\{=C(O)(NR_2)\}]$ (M = W, Mo), the majority of the commercially available secondary amines which were utilised in this study were first dispersed in THF solutions and treated with *n*-butyllithium at low temperature.### The lithiated mixtures were briefly warmed in ambient air for up to 15 minutes, before once again being re-cooled in a dry-ice/acetone slush bath, thereby ensuring good conversion to the lithiated amide. Addition of the relevant metal hexacarbonyl was carried out at low temperature and the mixtures subsequently warmed in ambient air.

The exception to this is lithium diisopropylamide, which was commercially sourced as a 2.0 mol L^{-1} solution in THF.

The addition of trifluoroacetic anhydride at low temperature caused the tetracarbonyl complexes $[M(CO_2CF_3)(CO)_4\{\equiv CN(R_2)\}]$ (M = W, Mo; R = alkyl, aryl) to form after the mixtures were removed from the slush bath and warmed in ambient air. As the reaction mixtures approached 0°C, small bubbles of carbon monoxide gas were often observed to rise through the centre of the continuously stirred mixtures, which were re-cooled only once the liberation of carbon monoxide had visibly halted. The appropriate pro-ligand (Na[**Tm**] or Na[**Htt**]) was subsequently added and the reaction mixtures stirred overnight. The reactions gradually warmed to room temperature, thereby affording the slow formation of the crude product mixtures.

A range of simple, chiral, and tethered secondary amines were used to form a total of thirteen previously unknown complexes in this work. For the simple amines, full combinatorial analysis was attempted with molybdenum and tungsten metal centres, and the Scorpionate ligands **Tm** and **Htt**. A summary of the reactions carried out, and their outcomes, are summarised in **Table 4.1**. Full combinatorial studies were not carried out for the chiral or secondary amines detailed below due to their increased costs and smaller quantities supplied from commercial sources.

Secondary Amine	Metal Centre	Ligand	Reaction Attempted (Y/N)	Successful/Unsuccessful	Complex No.
Diethylamine	Mo	**Tm**	Y	Successful	**4.1**
		Htt	Y	Successful	**4.3**
	W	**Tm**	Y	Unsuccessful	–
		Htt	Y	Successful	**4.2**
Diisopropylamine	Mo	**Tm**	Y	Unsuccessful	–
		Htt	Y	Successful	**4.5**
	W	**Tm**	Y	Unsuccessful	–
		Htt	Y	Successful	**4.4**
Diphenylamine	Mo	**Tm**	Y	Successful	**4.7**
		Htt	Y	Unsuccessful	–
	W	**Tm**	Y	Successful	**4.6**
		Htt	Y	Successful	**4.8**
(*R*)-(+)-α,4-dimethylbenzylamine	Mo	**Tm**	N	–	–
		Htt	N	–	–
	W	**Tm**	Y	Successful	**4.9**
		Htt	N	–	–
(+)-bis[(*R*)-1-phenylethyl]amine	Mo	**Tm**	N	–	–
		Htt	N	–	–
	W	**Tm**	N	–	–
		Htt	Y	Successful	**4.10**
N,*N*'-diphenylbenzidine	Mo	**Tm**	N	–	–
		Htt	N	–	–
	W	**Tm**	Y	Successful	**4.11**
		Htt	Y	Successful	**4.12, 4.13**

Table 4.1. Summary of reaction combinations attempted with various secondary amines.

4.4.2 Summary of Spectral Features – Chapter 4 Complexes

Complex No.	Metal Centre	Ligand	Liquid IR (cm^{-1})		$^{11}B\{^1H\}$ NMR (ppm)	$^{13}C\{^1H\}$ NMR			
			ν_{BH}	ν_{CO}		M≡C$^{\alpha}$ (ppm)	$^1J_{MC}$ (Hz)	M(CO) (ppm)	$^1J_{MC}$ (Hz)
4.1	Mo	**Tm**	–	1944, 1845	-1.54	256.2*	–	229.9*, 225.1*	–
4.2	W	**Htt**	2530	1946, 1847	-2.80	250.3	216.5	222.3, 217.8	173.3, 173.2
4.3	Mo	**Htt**	2519	1959, 1864	-2.66	256.7	–	226.5, 222.9	–
4.4	W	**Htt**	2526	1944, 1845	-2.74	249.7	217.8	224.2, 217.8	172.2, 176.5
4.5	Mo	**Htt**	2516	1958, 1862	-2.63	257.4	–	228.3, 223.4	–
4.6	W	**Tm**	–	1952, 1853	-1.59	238.8	230.7	224.0, 219.7	171.9, 167.5
4.7	Mo	**Tm**	–	1966, 1871	-1.44	243.0	–	227.6, 223.5	–
4.8	W	**Htt**	2528	1966, 1871	-2.69	240.2	229.6	220.3, 216.3	172.9, 168.9
4.9 ‡	W	**Tm**	–	1932, 1830	–	248.7*	–	227.1*, 226.2*, 220.9*, 220.1*	–
4.10	W	**Htt**	2528	1947, 1850	-2.58	246.3*	–	223.1*, 220.4*	–
4.11	W	**Tm**	–	1953, 1854	-1.64	238.6	–	224.2, 219.8	–
4.12	W	**Htt**	2528	1966, 1871	-2.40	240.1	229.4	220.4, 216.4	173.3, 168.9
4.13	W	**Htt**	2528	1967, 1871	-2.48	239.7	230.0	220.4, 216.3	173.3, 168.9

NMR Spectra measured in $CDCl_3$. | Liquid IR spectra measured in CH_2Cl_2. | * Measured at -40°C. | ‡ Diastereomers present.

Table 4.2. Summary of selected spectral data for the complexes detailed in Chapter 4.

4.4.3 Synthesis of [TmMo(CO)$_2${≡CN(Et$_2$)}]

Following the synthetic procedure used to generate the crude reaction mixture containing complex **4.1**, the contents of the reaction vessel were concentrated to dryness and the residues subjected to chromatographic purification. In order to obtain a spectroscopically pure sample, the residues were first dissolved in minimal CH_2Cl_2 and subjected to silica-gel column chromatography, eluting with a 2% (v/v) mixture of THF in CH_2Cl_2. This afforded a major orange band on the column which was collected and concentrated to dryness to afford complex **4.1** (**Scheme 4.15**) as a beige powder in low yield.

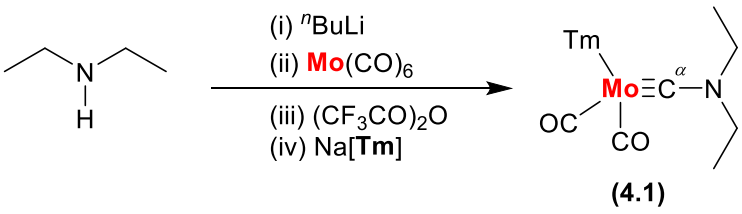

(4.1)

Scheme 4.15. Preparation of complex **4.1**.

Complex **4.1** was found to be readily soluble in halogenated solvents, so was initially probed *via* infrared spectroscopy as a CH_2Cl_2 solution. Two carbonyl bands of equal intensity were recorded at ν_{CO} 1944 and 1845 cm^{-1}. Although several other signals may be tentatively assigned (e.g. ν_{BH} at approx. 2398 cm^{-1}) from the solution infrared spectrum, sufficient spectral resolution was not maintained near the baseline to ensure the accurate detection of weak signals. Hence, the two detected carbonyl bands prove to be the most diagnostic features present in the liquid infrared spectrum of **4.1**.

Analysis by ^1H NMR spectroscopy of the title complex was carried out as a concentrated $CDCl_3$ solution, initially at approximately 25°C. At this temperature, it was noted that the signals corresponding to the *exo*-CH_3 groups and cyclic alkene protons, both located on the **Tm** ligand, had coalesced into broad signals at δ_H 3.63 and 6.78 ppm, respectively (**Figure 4.4**).

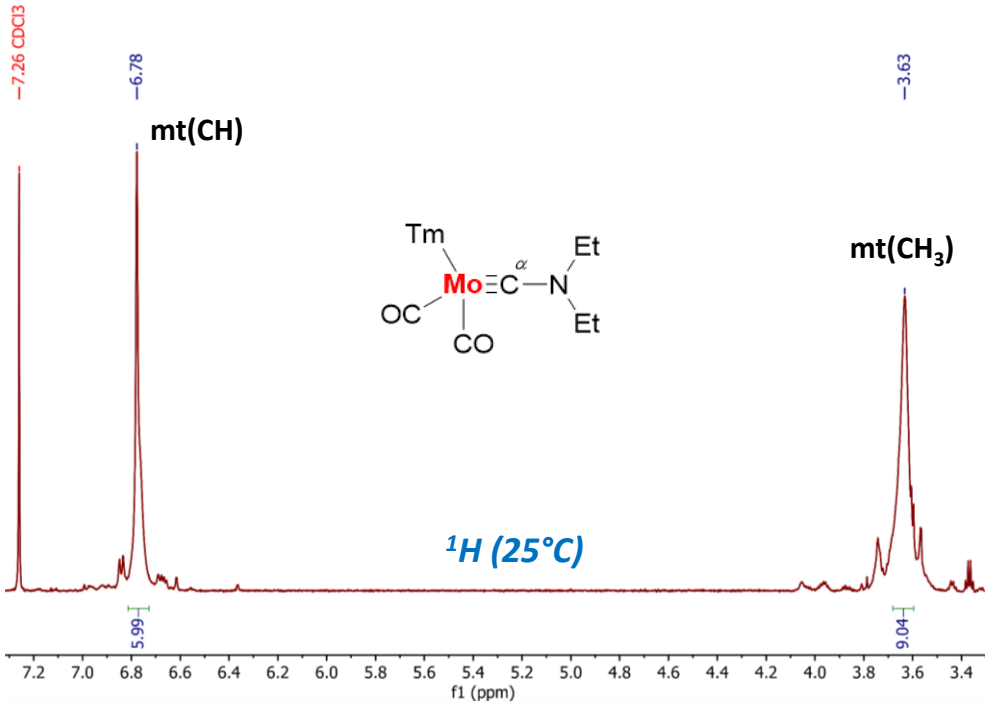

Figure 4.4. Segment of the ^1H NMR spectrum of complex **4.1**, measured at room temperature.

This observation was unusual, given that during the analysis of prior carbyne and propargylidyne complexes most had afforded ^1H NMR spectra which were resolved at room temperature. Furthermore, the signals corresponding to the -CH_2- groups of the nitrogen-bound ethyl chains were also not fully resolved, as they were detected as a multiplet in the

range δ_H 3.25-3.20 ppm. Unlike all of the other signals detected in the room temperature spectrum of **4.1**, the terminal -CH_3 groups were successfully detected and resolved as two overlapping triplets at δ_H 1.29 ppm.

To try and improve the resolution of the ^{1}H NMR spectrum, a sample of **4.1** was once again dissolved in $CDCl_3$ and subjected to variable temperature (VT) NMR spectroscopy. The sample was cooled to approximately -40°C, and the resulting ^{1}H NMR spectrum displayed a marked improvement in the resolution of all previously coalesced signals. At low temperature, the most downfield signals corresponded to the heterocyclic C-H protons on the **Tm** framework, which were detected as a set of four doublets in the range δ_H 6.82-6.75 ppm. The *exo*-CH_3 groups of the **Tm** ligand were individually resolved as three singlets at δ_H 3.69 and 3.62 ppm, with the latter marginally overlapping (**Figure 4.5**).

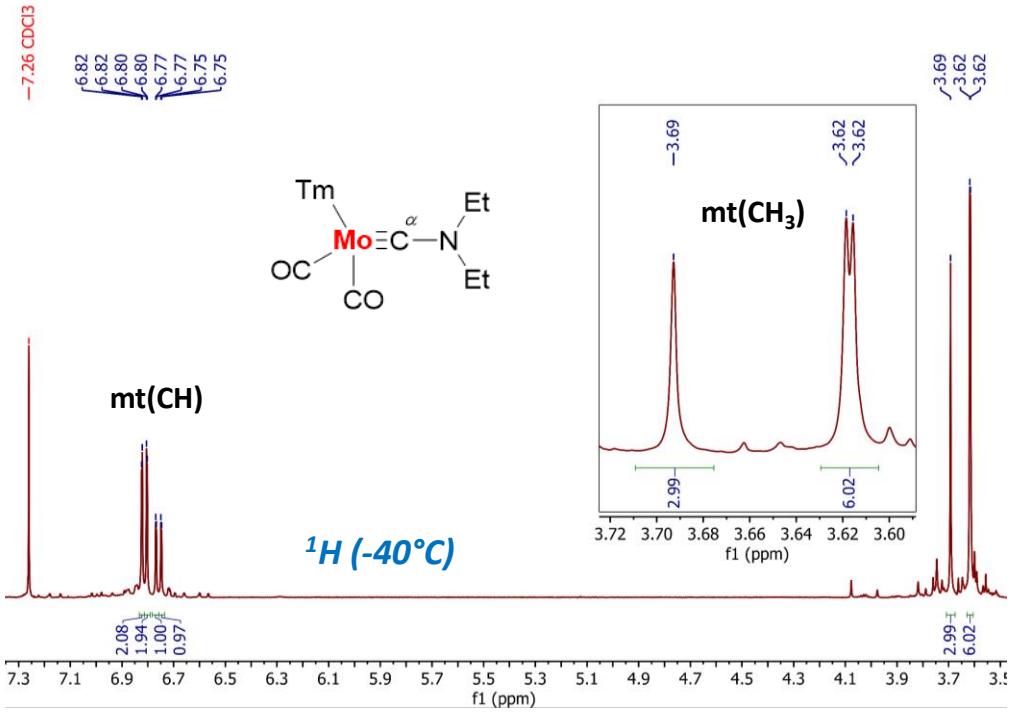

Figure 4.5. Segment of the ^{1}H NMR spectrum of complex **5.1**, measured at -40°C.

Unlike in the room temperature ^{1}H NMR spectrum, the -CH_2- groups of the nitrogen-bound ethyl chains were detected as distinct multiplets centred around approximately δ_H 3.24 and 3.19 ppm. Finally, the terminal -CH_3 groups of the ethyl chains were once again detected as two overlapping triplets at δ_H 1.27 ppm.

The gross composition of complex **4.1** was analysed initially *via* ESI mass spectrometry and revealed a molecular ion $[M\text{-}2(CO)]^+$ peak at approximately m/z 533.1 and an isotope pattern which closely matched a fragment of formula $C_{17}H_{26}BN_7S_3Mo$. Bulk purity of the sample was further affirmed through elemental microanalysis, which displayed results near identical to that calculated for the complex.

Following on from the successful recording of the ^1H NMR spectrum at low temperature, the $^{13}C\{^1H\}$ NMR spectrum of complex **4.1** was also recorded at low temperature in a solution of $CDCl_3$. The key features of complex **4.1**, namely the carbyne carbon ($Mo{\equiv}C^{\alpha}$) and the two molybdenum-bound carbonyl ligands were detected at δ_C 256.2, 229.9, and 225.1 ppm, respectively. Unfortunately, unequivocal structural determination through single crystal X-ray diffraction was not carried out, given that attempts to form crystals suitable for structural determination were unsuccessful, even after several attempts.

Electrochemical testing was carried out *via* cyclic voltammetry, whereby a CH_2Cl_2 solution of **4.1** was analysed using a standard electrochemical cell setup at room temperature (**Figure 4.6**).

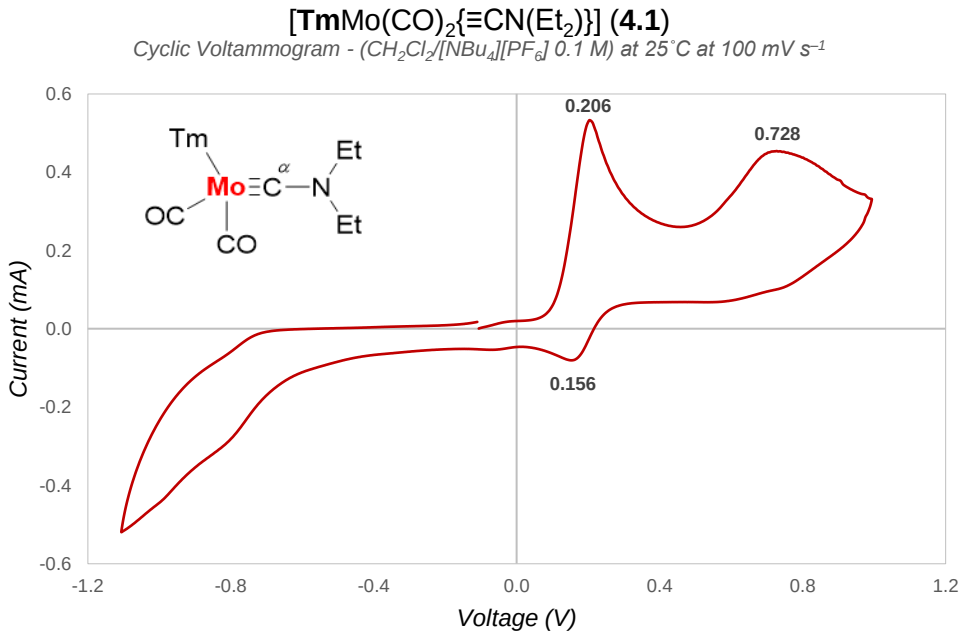

Figure 4.6. Cyclic voltammogram of complex **4.1**. Referenced relative to the Ferrocene/Ferrocenium redox couple at 0.46 V *vs.* standard calomel electrode.

Testing revealed a total of three redox events, consisting of two oxidation events at approximately 0.21 and 0.73 V, and one reduction event at 0.16 V. The redox events occurring at 0.16 V and 0.21 V are believed to be coupled in a quasi-reversible redox process. Although it is not clearly evident in the voltammogram above, a second weak reduction may be present between approximately 0.5-0.8 V, but this cannot be confirmed upon review of the data recorded thus far.

4.4.4 Synthesis of [(Htt)M(CO)$_2${≡CN(Et$_2$)}] (M = Mo, W)

Using the lesser known soft Scorpionate ligand **Htt**, the aminocarbyne complexes [(**Htt**)W(CO)$_2${≡CN(Et$_2$)}] (**4.2**) and [(**Htt**)Mo(CO)$_2${≡CN(Et$_2$)}] (**4.3**) (**Scheme 4.16**) were prepared in low-to-moderate yields.

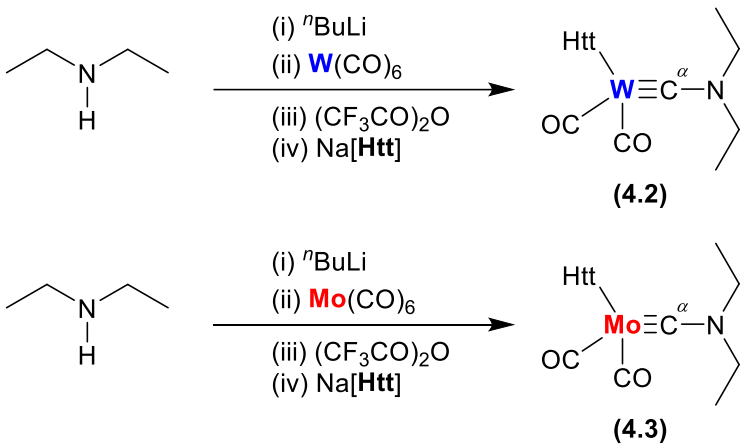

Scheme 4.16. Preparation of complexes **4.2** and **4.3**.

Once the synthetic protocols had been completed using the relevant metal hexacarbonyl starting material, the reaction mixtures were concentrated to dryness and the residues extracted with a small volume of CH_2Cl_2. In order to afford spectroscopically pure samples, the extracted residues were each subjected to silica gel column chromatography, eluting with CH_2Cl_2. In both cases, a major orange band developed and traversed through the columns, which was subsequently collected and concentrated to dryness on a rotary evaporator to afford complexes **4.2** and **4.3**.

Both materials were found to be soluble in halogenated solvents and stable under ambient conditions in the solid form. In order to arrest any degradation processes which may

have taken place, the samples were stored in sealed vials at -20°C. Under these conditions, no significant decomposition was noted over an extended period of time.

Complexes **4.2** and **4.3** were initially tested *via* infrared spectroscopy as CH_2Cl_2 solutions. The carbonyl ligands on the tungsten centre of complex **4.2** were detected in the middle of the spectral range at ν_{CO} 1946 and 1847 cm^{-1}. Also, the B-H bond of the **Htt** ligand was clearly detected at ν_{BH} 2530 cm^{-1}. Meanwhile, the carbonyl ligands bound to the molybdenum centre of complex **4.3** were detected at similar values at ν_{CO} 1959 and 1864 cm^{-1}. The B-H bond of the **Htt** ligand bound to the molybdenum centre in complex **4.3** was also clearly detected at ν_{BH} 2519 cm^{-1}, making it only slightly lower in energy compared to that recorded for complex **4.2**.

Analysis of complex **4.2** by ^1H NMR spectroscopy was carried out as a concentrated $CDCl_3$ solution, at approximately 25°C. At this temperature, all signals were individually resolved and there was no need to carry out VT NMR, like in the case of complex **4.1**. Much like in the liquid infrared spectrum, the B-H functionality was detected in the ^1H NMR spectrum, where the B-H hydrogen atom was found at δ_H 5.59 ppm as a broad signal due to the quadrupolar nature of the boron atom. Compared to complexes containing the **Tm** ligand, those ligated with **Htt** contain very few detectable protons. In complex **4.2**, the only signals in the ^1H NMR spectrum which correspond to the **Htt** ligand are those belonging to the *exo*-$C(CH_3)_3$ groups, detected as a singlet at δ_H 1.87 ppm. All remaining signals corresponded to the ethyl chains of the amino functional group. The ^1H NMR spectrum of complex **4.3** was also recorded at room temperature, without the need to carry out VT NMR. Concordantly, the *exo*-$C(CH_3)_3$ groups of the molybdenum-bound **Htt** ligand were detected at δ_H 1.87 ppm, and all remaining signals corresponded to the ethyl chains of the amino functional group.

ESI mass spectrometry of complex **4.2** revealed a molecular ion $[M+Na]^+$ peak at m/z 830.1924, which closely matched the isotope pattern calculated for a complex of the formula $C_{22}H_{38}BN_{13}NaO_2S_3W$. Likewise, the ESI mass spectrum of complex **4.3** also indicated the presence of the $[M+Na]^+$ ion, with a peak at m/z 744.148 being detected with an isotope pattern which closely matched that calculated for a complex of the formula $C_{22}H_{38}BMoN_{13}NaO_2S_3$. The bulk purity of both materials was assessed through the use of

elemental microanalysis, which afforded results that closely matched those calculated for complexes **4.2** and **4.3**.

Analysis of complex **4.2** by $^{13}C\{^{1}H\}$ NMR spectroscopy was carried out at room temperature in a concentrated solution of $CDCl_3$. A very clean spectrum was obtained, and displayed an excellent signal-to-noise ratio, thereby allowing for coupling information to also be recorded. The carbyne carbon ($W{\equiv}C^{\alpha}$) was detected at δ_C 250.3 ppm with coupling to the tungsten atom measured as around 216 Hz. Likewise, the two carbon atoms located on the carbonyl ligands were detected at δ_C 222.3 and 217.8 ppm, with associated coupling constants of 173 Hz for each. Although the coupling constants which were measured for the carbonyl ligands are in the typical range for aminocarbyne complexes of this type, the coupling of the carbyne carbon proves to be the lowest detected amongst the complexes prepared in this Chapter.

Unfortunately, unequivocal structural determination through single crystal X-ray diffraction was not carried out for either complex. Attempts to form crystals suitable for structural determination were unsuccessful, even after several attempts.

Complex **4.3** also afforded a very clean $^{13}C\{^{1}H\}$ NMR spectrum, which was recorded in $CDCl_3$ at approximately 25°C. The carbyne carbon ($Mo{\equiv}C^{\alpha}$) was detected at δ_C 256.7 ppm, and the two carbon atoms of the molybdenum-bound carbonyl ligands were found at δ_C 226.5 and 222.9 ppm. It is noteworthy that in both complexes **4.2** and **4.3**, the thione (C=S) carbon atoms on the **Htt** ligand backbone are detected as a very weak, broad, and coalesced signal, even although the signal-to-noise ratio of all signals is excellent. This is in direct contrast to complexes ligated with methimazolyl-based ligand systems, which almost always afford three individually resolved, intense C=S signals (**Figure 4.7**).§§§§

It should be noted that the $^{13}C\{^{1}H\}$ NMR spectrum of complex **4.1** was recorded at -40°C, meanwhile the spectrum of complex **4.3** was recorded at approximately 25°C. At face value, this might be assumed to be the reason for the distinct difference in resolution between these two spectra. However, given the results which have been noted throughout this work involving the use of the **Tm** ligand, it has been found that even at room temperature, it is

§§§§ This is based off the observations made during the course of this work, and this statement doesn't extend to include complexes which have been reported in literature.

more common than not to find the thione (C=S) carbon atoms to be individually resolved, as is observed for complex **4.1**

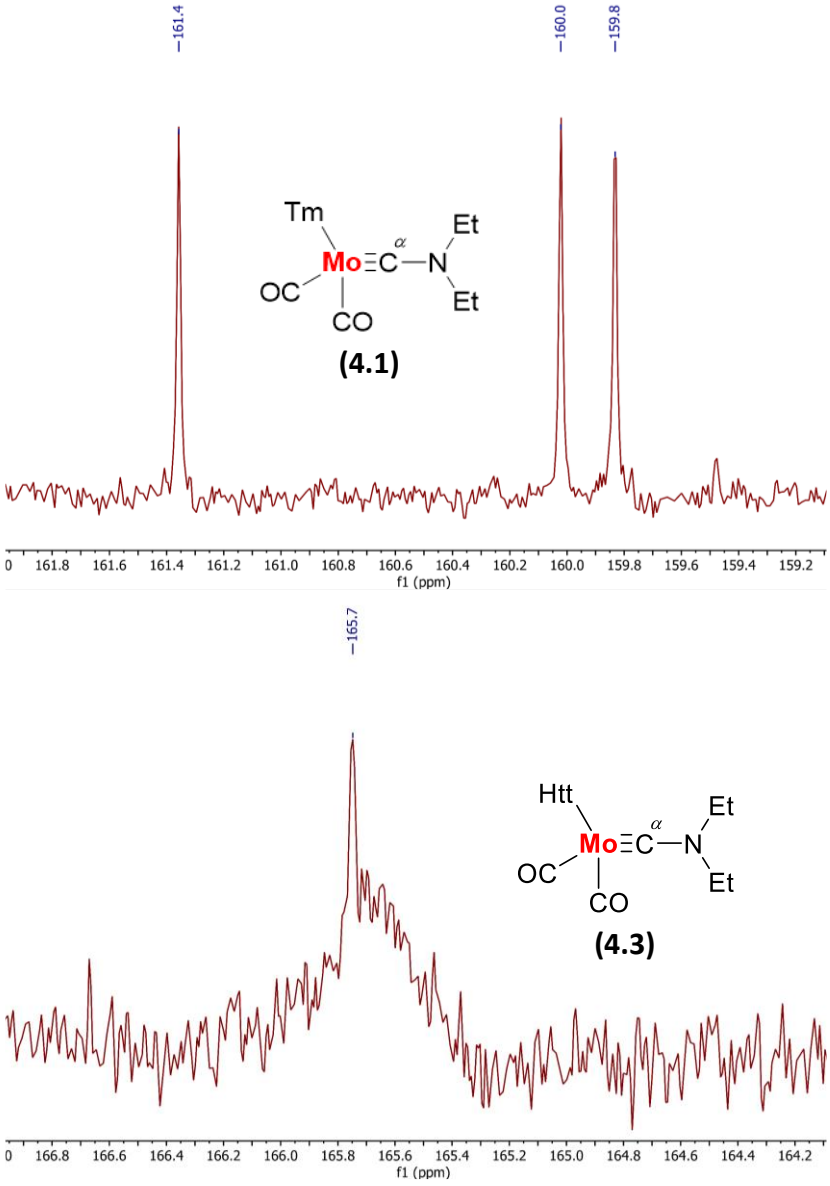

Figure 4.7. Segments of $^{13}C\{^{1}H\}$ NMR spectra ($CDCl_3$) recorded for complex **4.1** and complex **4.3**.

Both complexes were subjected to electrochemical testing as CH_2Cl_2 solutions at room temperature, using a standard electrochemical cell setup. Complex **4.2** afforded two redox couples, consisting of two oxidation events at approximately 0.42 and 0.70 V, and two reduction events at 0.33 and 0.65 V (**Figure 4.8**).

The first quasi-reversible redox couple ($E_{½}$ = 0.37 V) is of significantly greater intensity than the second at $E_{½}$ = 0.67 V, and is believed to correspond to oxidation and reduction events occurring at the tungsten centre. In the case of the latter ($E_{½}$ = 0.67 V), it is unknown where this redox couple originates.

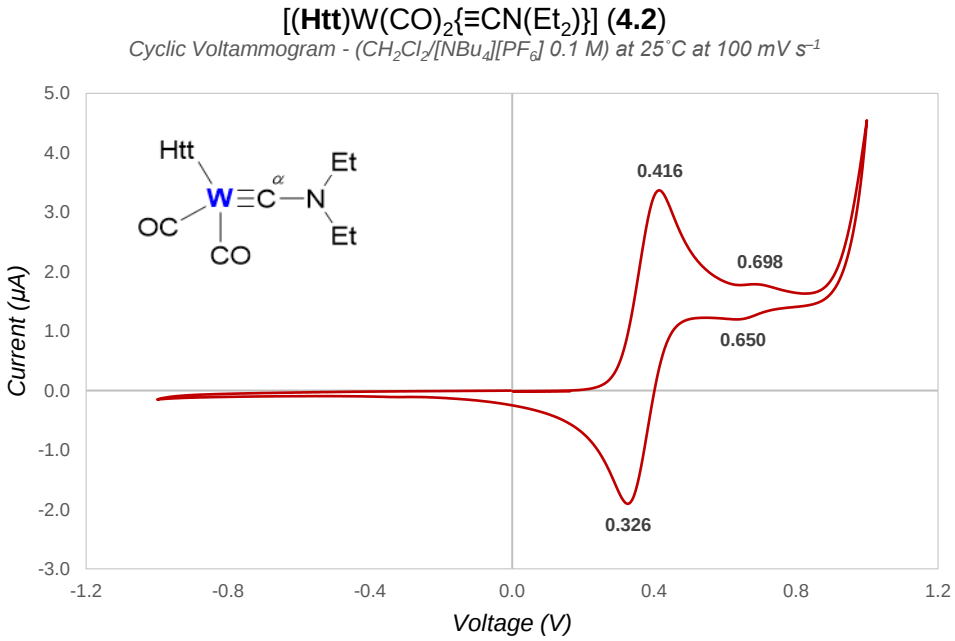

Figure 4.8. Cyclic voltammogram of complex **4.2**. Referenced relative to the Ferrocene/Ferrocenium redox couple at 0.46 V *vs.* standard calomel electrode.

Certainly, for the related **Tm** ligand system, it has been previously noted that it may exhibit non-innocent behaviour during electrochemical processes.[33,34] However, such processes are normally irreversible, and ultimately result in the decomposition of the complex. Hence, the origin of the high potential redox couple remains to be unconfirmed.

Similarly, the cyclic voltammogram recorded for complex **4.3** revealed one intense quasi-reversible redox pair ($E_{½}$ = 0.45 V) and one pair at significantly higher potential ($E_{½}$ = 0.80 V) (**Figure 4.9**). It can be noted that while the molybdenum centre undergoes reversible redox processes, much like that of the analogous tungsten complex **4.2**, marginally higher potentials are required to induce such processes (*cf.* $\Delta E_{½}$ = 0.08 V).

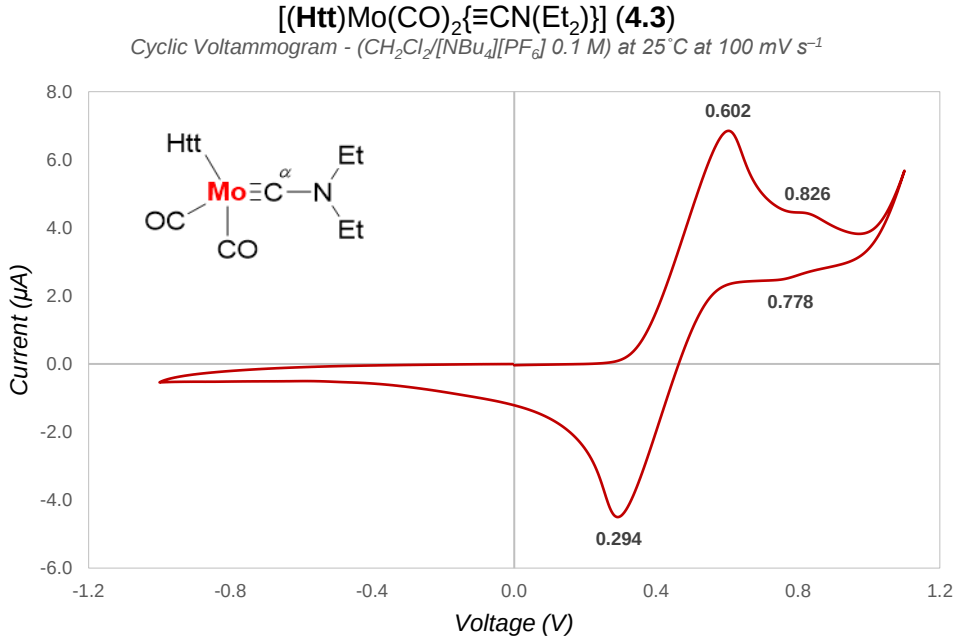

Figure 4.9. Cyclic voltammogram of complex **4.3**. Referenced relative to the Ferrocene/Ferrocenium redox couple at 0.46 V *vs.* standard calomel electrode.

4.4.5 Synthesis of [(Htt)M(CO)$_2${≡CN(ⁱPr$_2$)}] (M = Mo, W)

Unlike all other aminocarbyne complexes which were formed in this chapter, the complexes [(**Htt**)W(CO)$_2${≡CN(ⁱPr$_2$)}] (**4.4**) and [(**Htt**)Mo(CO)$_2${≡CN(ⁱPr$_2$)}] (**4.5**) were prepared through the use of a commercially available lithium reagent, lithium diisopropylamide (LDA) (**Scheme 4.17**).

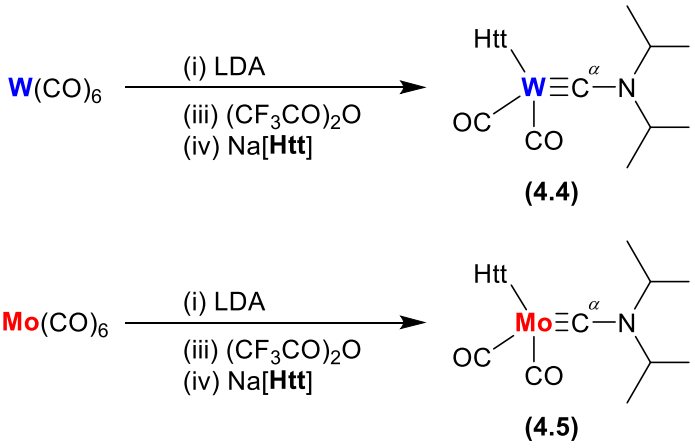

Scheme 4.17. Preparation of complexes **4.4** and **4.5**.

The red and orange/brown crude reaction mixtures containing complex **4.4** and **4.5**, respectively, were concentrated to dryness on a rotary evaporator and the residues subsequently dissolved in a minimal volume of CH_2Cl_2. In order to prepare spectroscopically pure samples of each complex, both were subjected to silica gel column chromatography, eluting with CH_2Cl_2. In both cases, a major orange band was observed to traverse down the columns, and was collected and concentrated to dryness to afford complexes **4.4** and **4.5**.

In line with the aminocarbyne analogues which had been prepared previously, complexes **4.4** and **4.5** were found to be stable in the solid form, but were stored in sealed sample vials at -20°C in order to arrest any potential degradation processes. Given the ease at which both complexes were found to dissolve in halogenated solvents, infrared spectroscopy was carried out as concentrated CH_2Cl_2 solutions. For the tungsten-containing complex **4.4**, the carbonyl ligands were detected as two independent bands at ν_{CO} 1944 and 1845 cm^{-1}. Meanwhile, for molybdenum complex **4.5**, the two carbonyl bands were found at ν_{CO} 1958 and 1862 cm^{-1}.

It was found to be possible to record ^1H NMR spectra of both samples at room temperature. Analysis of these spectra did not afford anything untoward, but did clearly show the incorporation of the **Htt** ligand and diisopropylamino groups, the latter producing a characteristic septet centred around δ_H 3.31 for complex **4.4** (**Figure 4.10**), and δ_H 3.32 for complex **4.5**.

For both complex **4.4** and **4.5**, ESI mass-spectrometry revealed molecular ion $[M+Na]^+$ peaks at m/z 858.2243 and 772.1791, respectively. These values and their accompanying isotope patterns closely coincide with complexes of the composition $C_{24}H_{42}BN_{13}NaO_2S_3W$ and $C_{24}H_{42}BMoNaN_{13}O_2S_3$, and thereby match those calculated for **4.4** and **5.5**. The bulk purity of both samples was affirmed through the use of elemental microanalysis, the results of which displayed good congruence with values calculated for both complexes.

The $^{13}C\{^1H\}$ NMR spectrum of complex **4.4** was recorded in $CDCl_3$ at room temperature, and revealed a clean spectrum with a sufficient signal-to-noise ratio to allow coupling data to be detected. The carbyne carbon ($W{\equiv}C^{\alpha}$) was detected at δ_C 249.7 ppm, with a single-bond coupling of approximately 218 Hz to the tungsten centre.

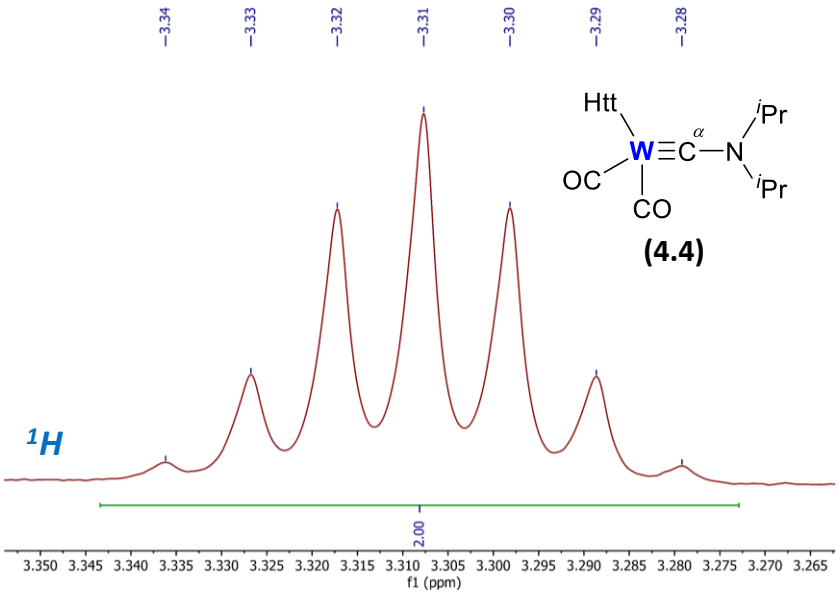

Figure 4.10. Segment of the ^{1}H NMR spectrum recorded for complex **4.4**, displaying the septet originating from the diisopropylamino group. Recorded as a $CDCl_3$ solution.

Both carbonyl ligands were independently detected at δ_C 224.2 and 217.8 ppm, with coupling constants of approximately 172 and 177 Hz, respectively. Much like in the case of complex **4.3**, a weak signal was detected at δ_C 165.0 ppm, attributed with the C=S groups of the heterocyclic rings of **Htt**. This was the only signal to display such low intensity, and the remainder of the signals associated with the **Htt** ligand and diisopropyl-groups were detected with excellent signal-to-noise ratios.

Similarly, the $^{13}C\{^{1}H\}$ NMR spectrum of complex **4.5** was recorded as a $CDCl_3$ solution at room temperature, and revealed many similar features to those detected for complex **4.4** (with the exception of coupling data due to the molybdenum centre). The carbyne carbon (Mo≡C$^{\alpha}$) atom was detected at δ_C 257.4 ppm along with both carbonyl groups at δ_C 228.3 and 223.4 ppm. A weak and somewhat broad signal at approximately δ_C 166 ppm was detected and assigned to the heterocyclic C=S moieties of the **Htt** ligand.

For complexes **4.4** and **4.5**, attempts to form crystals suitable for single-crystal X-ray diffraction were exhausted, thereby not allowing for unequivocal structural determination of both species.

Electrochemical testing was carried out *via* cyclic voltammetry, whereby CH_2Cl_2 solutions of complex **4.4** and complex **4.5** were individually analysed using a standard electrochemical cell setup at room temperature.

Both complexes were found to produce hysteresis curves which suggested one major quasi-reversible redox process and one minor redox event. In the case of complex **4.4**, two oxidation events were detected at approximately 0.53 and 0.80 V, as well as two reduction events at approximately 0.29 and 0.69 V (**Figure 4.11**).

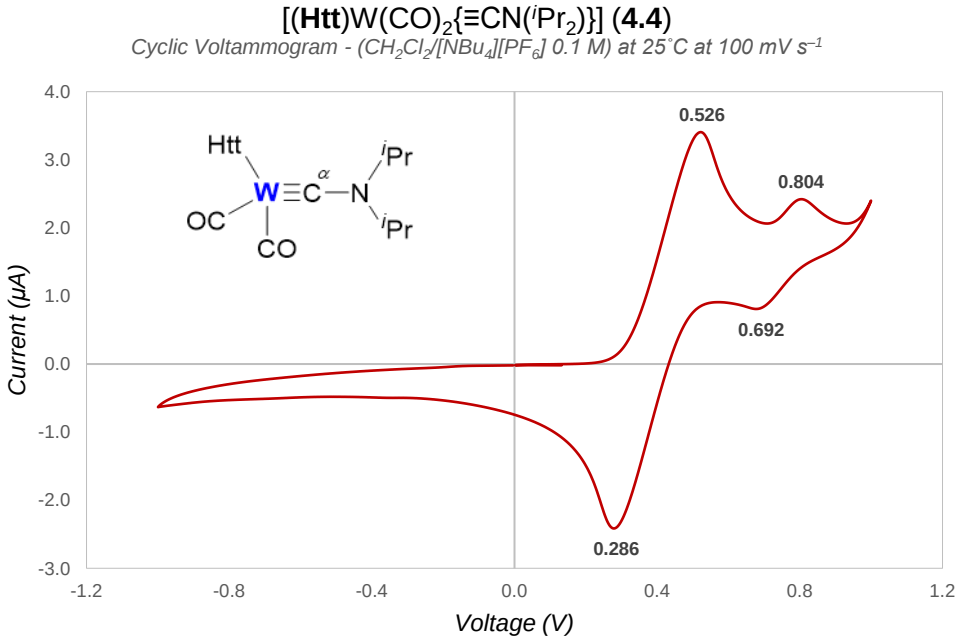

Figure 4.11. Cyclic voltammogram of complex **4.4**. Referenced relative to the Ferrocene/Ferrocenium redox couple at 0.46 V *vs.* standard calomel electrode.

Likewise, results for complex **4.5** revealed two oxidation events and two reduction events, with the major and minor processes being measured at approximately $E_{½}$ = 0.48 and 0.82 V, respectively (**Figure 4.12**).

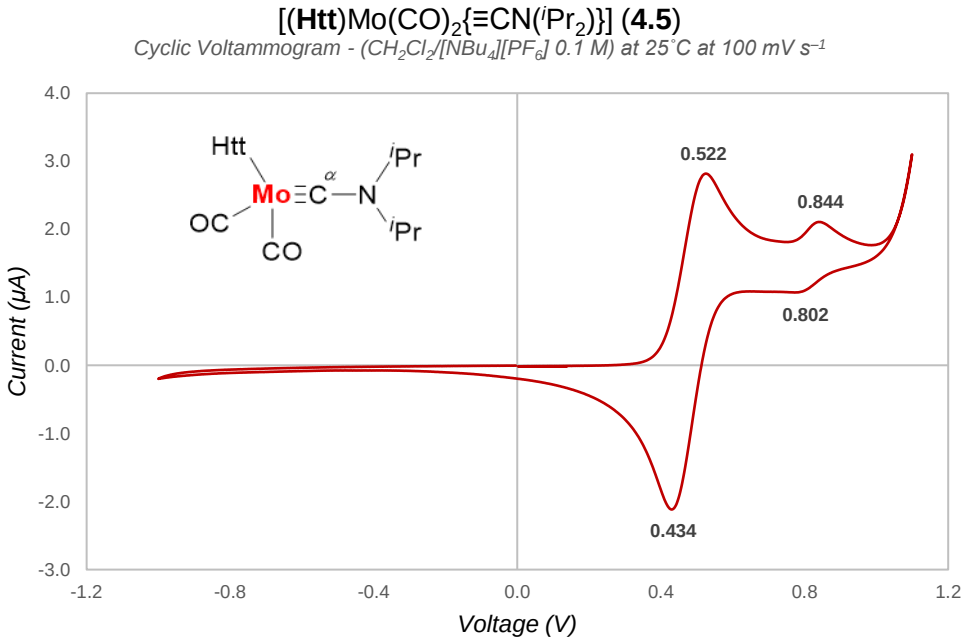

Figure 4.12. Cyclic voltammogram of complex **4.5**. Referenced relative to the Ferrocene/Ferrocenium redox couple at 0.46 V *vs.* standard calomel electrode.

4.4.6 Synthesis of [TmM(CO)$_2${≡CN(Ph$_2$)}] (M = Mo, W)

It has been noted in literature that the incorporation of diphenylamino-substituents into group 6 metallocarbyne complexes remains to be a rarity. In fact, at the time of writing of this report, the only well-defined examples of such complexes were reported by A. F. Hill and B. J. Frogley in 2018, using the **Tp*** ligand to form the molybdenum and tungsten complexes [**Tp***M(CO)$_2${≡CN(Ph$_2$)}] (M = Mo, W) (**Scheme 4.18**).[13] The number of known group 6 diphenylamino-substituted metallocarbyne complexes has now been further expanded during this work to include three further complexes which shall be discussed in the following paragraphs.

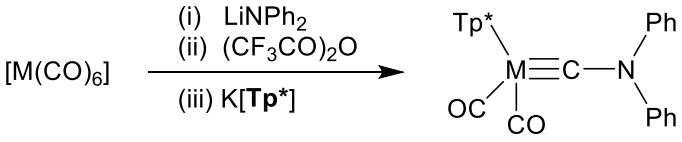

Scheme 4.18. Synthetic protocol adopted by Hill and Frogley in order to form the diphenyl-substituted aminocarbyne complexes [**Tp***M(CO)$_2${≡CN(Ph$_2$)}] (M = Mo, W).

Using the synthetic protocol outlined in **Section 4.4.1** with the **Tm** ligand system, the complexes [**Tm**W(CO)$_2${≡CN(Ph$_2$)}] (**4.6**) and [**Tm**Mo(CO)$_2${≡CN(Ph$_2$)}] (**4.7**) were formed as orange powders in moderate and low yields, respectively (**Scheme 4.19**).

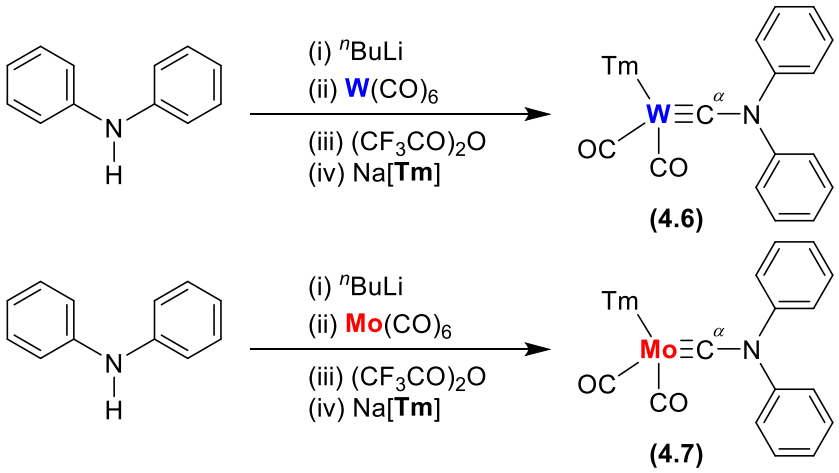

Scheme 4.19. Preparation of complexes **4.6** and **4.7**.

The respective crude reaction mixtures containing complexes **4.6** and **4.7** were concentrated to dryness on a rotary evaporator and the subsequent residues extracted with a small volume of CH_2Cl_2. All residues were purified *via* silica-gel column chromatography and, once loaded, were eluted with CH_2Cl_2. In both cases, a major orange band developed on the columns, which was collected, concentrated to dryness and finally dried thoroughly under high vacuum to afford spectroscopically pure samples of the title complexes. Although both **4.6** and **4.7** appeared to be stable under ambient conditions in the solid form, in order to arrest any potential degradation processes, the bulk samples were stored in sealed sample vials at -20°C.

Both complexes were found to be readily soluble in halogenated solvents, and hence complexes **4.6** and **4.7** were initially interrogated *via* solution infrared spectroscopy. In the case of complex **4.6**, two carbonyl bands were detected at ν_{CO} 1952 and 1853 cm^{-1} and served to be the most conspicuous signals present in the spectrum. Similarly, complex **4.7** displays two carbonyl bands at ν_{CO} 1966 and 1871 cm^{-1}. A tentative assignment of the B-H stretch may be made for complex **4.7**, and is thought to be present in the spectrum at approximately ν_{BH} 2399 cm^{-1}. However, due to the lack of intensity of the stretch, and several other nearby signals, this assignment cannot be made with certainty.

The ^{1}H NMR spectrum of complex **4.6** was recorded as a $CDCl_3$ solution at room temperature, and clearly displayed the incorporation of both the diphenylamino-substituent and the **Tm** ligand. Several multiplet signals in the range δ_H 7.5-7.0 ppm, equating to ten hydrogen atoms, were assigned as aromatic protons bound to the phenyl rings. The cyclic alkene protons located on the heterocyclic arms of the **Tm** ligand were found immediately upfield of the aromatic signals in the range δ_H 6.84-6.78 ppm, and in this case were detected as a multiplet without any discernible fine structure. In the characteristic manner for **Tm**-ligated complexes, the *exo*-CH_3 groups were individually resolved in the ^{1}H NMR spectrum as three singlets in the range δ_H 3.74-3.36 ppm.

For complex **4.7**, the ^{1}H NMR spectrum was also recorded as a $CDCl_3$ solution at room temperature. Phenyl signals equating to ten protons were detected as a series of multiplets over the approximate range δ_H 7.5-7.1 ppm. Much like the spectrum obtained for complex **4.6**, the remainder of the signals present in the spectrum can be attributed to the **Tm** ligand, and were found to be present in a comparable format to those of complex **4.6**.

The gross composition of complexes **4.6** and **4.7** was affirmed in part through the use of ESI mass spectrometry. Complex **4.6** was successfully detected as $[M]^+$, $[M\text{-}(CO)]^+$ and $[M\text{-}2(CO)]^+$ molecular ions, corresponding to species of the formulae $C_{27}H_{26}BN_7O_2S_3W$, $C_{26}H_{26}BN_7OS_3W$, and $C_{25}H_{26}BN_7S_3W$, respectively. Complex **4.7** was found to be present as $[M+Na]^+$ and $[M\text{-}2(CO)]^+$ molecular ions, with isotope patterns closely matching those calculated for species of the formulae $C_{27}H_{26}BMoN_7NaO_2S_3$ and $C_{25}H_{26}BMoN_7S_3$, respectively. Elemental microanalysis of both complexes also indicated the bulk purity of both samples, albeit with the inclusion of one equivalent of $CHCl_3$ in the case of complex **4.6**, and one equivalent of THF in the case of complex **4.7**.

The $^{13}C\{^{1}H\}$ NMR spectrum of complex **4.6** offered data commensurate with that recorded for previously synthesised **Tm**-ligated tungsten complexes from the work herein, and from the aforementioned diphenyl-substituted aminocarbyne complexes formed by Hill and Frogley. The most downfield signal was detected at δ_C 238.8 ppm and corresponded to the carbyne carbon ($W{\equiv}C^{\alpha}$). A carbon-tungsten one-bond coupling constant was also recorded for this signal, which had a magnitude of approximately 231 Hz. Both carbonyl ligands which are bound to the tungsten centre were detected as independently resolved signals at δ_C 224.0 and 219.7 ppm, each with associated coupling constants of approximately

172 and 168 Hz, respectively. Three signals were detected at approximately δ_C 159 ppm, which were assigned to the C=S moieties of the **Tm** heterocyclic backbone, as well as the cyclic alkene protons, also on the methimazole rings, in the ranges δ_C 122.8-122.6 and 119.8-199.6 ppm. Of the remaining signals, the aromatic carbon atoms of the phenyl rings were detected as several signals centred around approximately δ_C 125 ppm, and the *exo*-CH_3 groups of the **Tm** ligand were detected as three signals in the typical region of approximately δ_C 35 ppm.

Conveniently, the $^{13}C\{^1H\}$ NMR spectral data for complex **4.7** also displays much of the same signal data trends as complex **4.6**, as is typical for such analogous complexes. Of the key features which may be easily identified, the carbyne carbon (Mo≡C^{α}) was found at δ_C 243.0 ppm, and the molybdenum-bound carbonyl ligands were individually resolved as two signals at δ_C 227.6 and 223.5 ppm.

Despite several repeated attempts, crystals suitable for structural determination could not be formed for complex **4.6** or **4.7**. Therefore, unequivocal structural determination could not be carried out for either complex.

4.4.7 Synthesis of [(Htt)W(CO)$_2${≡CN(Ph$_2$)}]

Using the **Htt** ligand, both the tungsten and molybdenum diphenylamino-substituted metallocarbynes were synthetically targeted. However, only the tungsten complex [(**Htt**)W(CO)$_2${≡CN(Ph$_2$)}] (**4.8**) was successfully isolated (**Scheme 4.20**).

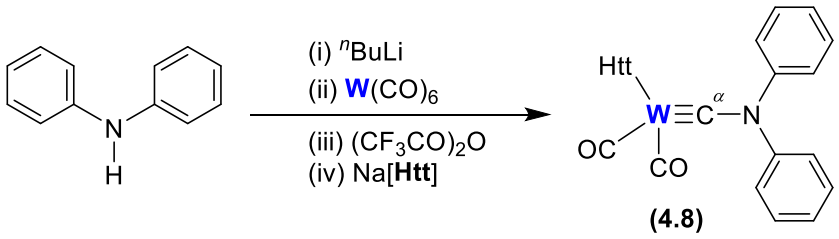

Scheme 4.20. Preparation of complex **4.8**.

Once the reaction mixture was allowed to slowly warm to room temperature overnight in the presence of Na[**Htt**], the crude products were purified by the use of silica-gel column chromatography. Once loaded onto the column, the crude product residues were

eluted with CH_2Cl_2 until the major orange band which traversed down the column was isolated, concentrated to dryness, and dried thoroughly under high vacuum. This afforded a spectroscopically pure sample of complex **4.8** in good-to-excellent yield, which was then stored in the solid form in a sealed sample vial at -20°C.

A small quantity of complex **4.8** was re-dissolved in CH_2Cl_2 and analysed *via* solution infrared spectroscopy. Two carbonyl bands were detected near the centre of the spectral range at ν_{CO} 1966 and 1871 cm^{-1}, notably with identical stretching frequencies to that of the **Tm**-ligated molybdenum aminocarbyne complex **4.7**. Furthermore, a B-H stretch was clearly detected at ν_{BH} 2528 cm^{-1}, which corresponded to the bridgehead {B-H} fragment of the **Htt** ligand.

The ^1H NMR spectrum of complex **4.8** was recorded in $CDCl_3$ at room temperature, and affirmed the presence and purity of the title complex. The ten aromatic protons located on the two nitrogen-bound phenyl rings were detected in the range δ_H 7.40-7.15 ppm as a series of multiplets devoid of any fine structure. Each *exo*-($C(CH_3)_3$) group located on the **Htt** ligand were detected as individually resolved singlets at δ_H 1.89, 1.85, and 1.67 ppm, as is expected for complexes of this type.

Through the use of ESI mass spectrometry and elemental microanalysis, the gross composition of complex **4.8** was confirmed. The mass spectrum revealed two identifiable fragments with isotope patterns closely matching complexes of formulae $C_{30}H_{38}BN_{13}O_2S_3W$ and $C_{29}H_{38}BN_{13}OS_3W$, matching $[M]^+$ and $[M\text{-}(CO)]^+$ molecular ions, respectively. No solvation of the sample was noted through elemental microanalysis, the results of which were shown to closely match calculated values for complex **4.8**.

A well resolved $^{13}C\{^1H\}$ NMR spectrum was recorded for complex **4.8** in $CDCl_3$ at room temperature. The carbyne carbon ($W{\equiv}C^{\alpha}$) signal was detected as the most downfield signal in the spectrum at δ_C 240.2 ppm, with a one-bond carbon-tungsten coupling constant of approximately 230 Hz. The two tungsten-bound carbonyl ligands were individually resolved and were detected at δ_C 220.3 and 216.3 ppm with associated one-bond coupling constants of magnitude 173 and 169 Hz, respectively. The {C=S} donor fragments on the **Htt** ligand were detected as three signals at approximately δ_C 165 ppm, and signals corresponding to the phenyl-carbon atoms were detected either side of this group. Of the

remaining signals, all corresponded to the *exo*-($C(CH_3)_3$) groups of the **Htt** ligand. Despite several repeated attempts, crystals suitable for structural determination could not be formed for complex **4.8**. Therefore, unequivocal structural determination could not be carried out for this complex.

Electrochemical data for complex **4.8** was recorded as a CH_2Cl_2 solution at room temperature (**Figure 4.13**).

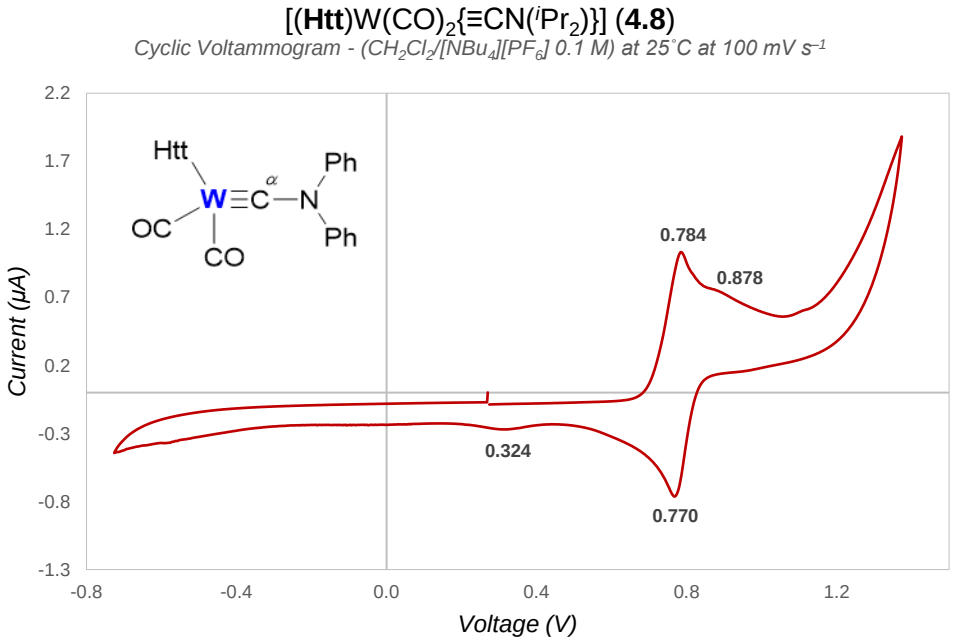

Figure 4.13. Cyclic voltammogram of complex **4.8**. Referenced relative to the Ferrocene/Ferrocenium redox couple at 0.46 V *vs.* standard calomel electrode.

One major reversible redox couple was noted with $E_{½}$ = 0.78 V, and two other redox events were tentatively assigned. One oxidation event was detected at approximately 0.88 V, and one reduction event was also measured at approximately 0.32 V. Both of these events are peculiar, given that they do not seem to be coupled, and aren't reminiscent of any other electrochemical processes detected in any other complexes.

4.4.8 Synthesis of [TmW(CO)$_2${≡C((*R*)-dimethylbenzylamine)}]

The optically active secondary amine (*R*)-(+)-*N*-α-dimethylbenzylamine was selected as a candidate to trial the incorporation of a chiral amine into group 6 metallocarbyne

complexes. In the work herein, it has been acknowledged that during the formation of carbyne-type complexes with either **Tm** or **Htt**, a mixture of isomers (atropisomers) form due to the conformational locking of the ligand cage once it is bound to a metal centre (refer to **Chapter 1**, **Section 1.2**). Under normal circumstances, this effect is not usually detectable on NMR timescales.[*****] However, when a relatively sterically encumbering, chiral group is installed on the terminus of the carbyne moiety, such as is the case with the preparation of complex **4.9** (**Scheme 4.21**), two distinct chemical environments about **Tm** are established between the atropisomeric forms. Upon review of the low temperature ^{1}H and $^{13}C\{^{1}H\}$ NMR spectral data for complex **4.9**, it is evident that this results in the doubling of many signals, indicating the presence of a diastereotopic mixture of products: these features will be highlighted in the following paragraphs. In a similar manner to complex **4.8**, both the molybdenum and tungsten analogues were synthetically targeted. However, only the tungsten complex was successfully isolated.

A spectroscopically pure sample of complex **4.9** was obtained in moderate yield following purification of the crude reaction mixture *via* silica-gel column chromatography, eluting with CH_2Cl_2. In the solid form, complex **4.9** was obtained as an orange powder which was dried under high vacuum and stored in a sealed sample vial at -20°C in order to arrest any potential degradation processes.

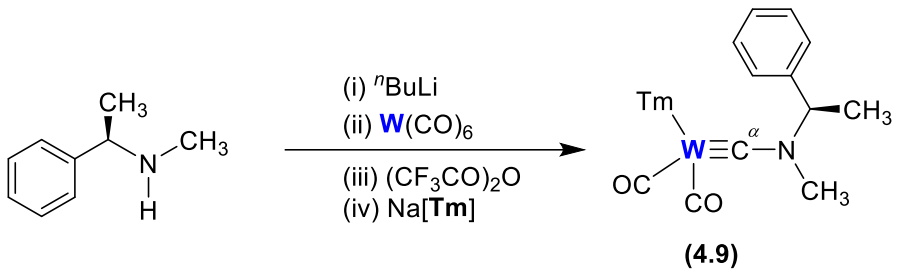

(4.9)

Scheme 4.21. Preparation of complex **4.9**.

Complex **4.9** was found to be highly soluble in halogenated solvents, and was initially interrogated *via* infrared spectroscopy in a solution of CH_2Cl_2. Two well resolved carbonyl bands were recorded at ν_{CO} 1932 and 1830 cm^{-1}. No stretching vibration indicative of the B-

[*****] When ^{1}H and $^{13}C\{^{1}H\}$ NMR spectra were recorded through the course of the studies herein, the majority of these spectra were recorded at approximately 25°C, but some selected complexes were subjected to low temperature VT NMR. In either case, no fluxionality of the ligand cage was noted, nor was any evidence of conformational preference ever indicated during these experiments.

H bond was observed in the IR spectrum, but this moiety was shown to be present through the use of $^{11}B\{^{1}H\}$ NMR spectroscopy.

A sample of complex **4.9** was dissolved in $CDCl_3$ and the ^{1}H NMR spectrum of the complex was recorded at room temperature. As expected, a clear doubling of the signals related to the **Tm** ligand and the amino substituent were observed, but the spectrum was poorly resolved (**Figure 4.14**).

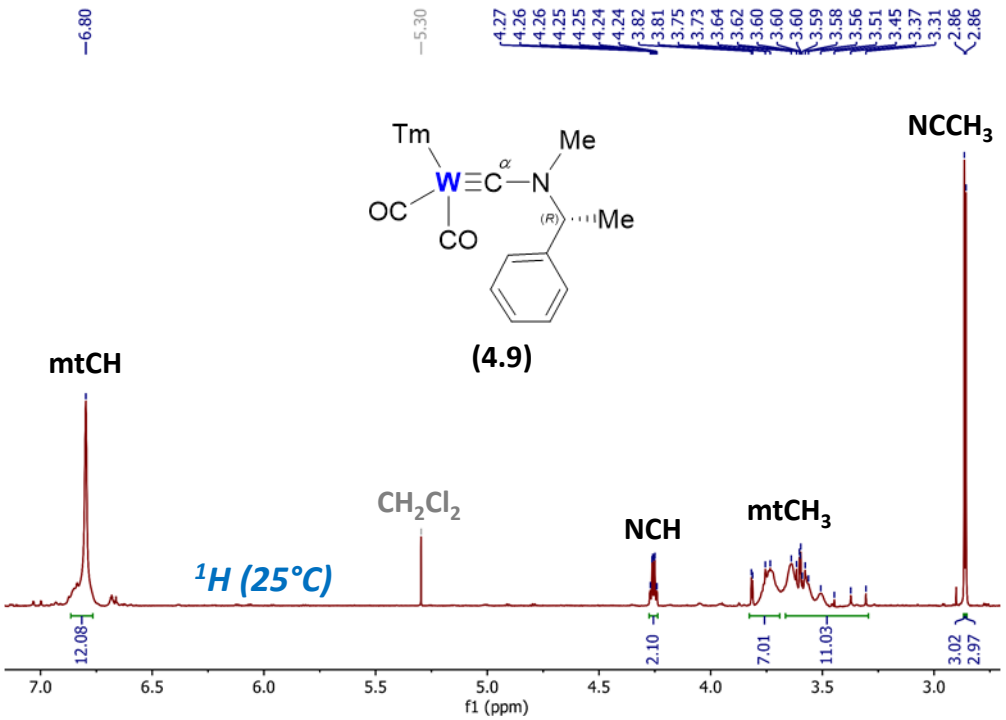

Figure 4.14. Segment of the room temperature ^{1}H NMR spectrum recorded for complex **4.9**, displaying the coalesced signals of the **Tm** ligand. Recorded as a $CDCl_3$ solution.

To try and improve the resolution, the sample was subjected to VT NMR spectroscopy, where a significant improvement was observed once cooled to -40°C (**Figure 4.15**). Upon inspection of the low temperature ^{1}H NMR spectrum, clear evidence for the presence of two cage-locked diastereomers can be observed. In this case, both diastereomers are present in equal proportions, as deduced by the identical relative intensities of the duplicated signals throughout the spectrum. The most noticeable evidence for the presence of these isomers comes with the six singlets detected in the range δ_H 4.23-3.49 ppm, all of which correspond to the *exo*-CH_3 groups of the **Tm** ligand. Based on the ^{1}H NMR spectra recorded for the **Tm**-ligated propargylidyne, metallocarbyne, and aminocarbyne complexes

reported herein, up to three singlets equating to three protons each are normally detected. The isomeric cage-locked structures of complex **4.9** forces these *exo*-CH_3 groups into differing chemical environments, thereby causing each signal to be individually resolved across the two diastereomers. Although less evident at a glance, the doubling of the remaining NMR signals can be observed upon review of their relative integrations. For example, the C–H hydrogen atom on the chiral centre of complex **4.9** is detected as a multiplet at approximately δ_H 4.21 ppm, crucially, with an integration of two protons.

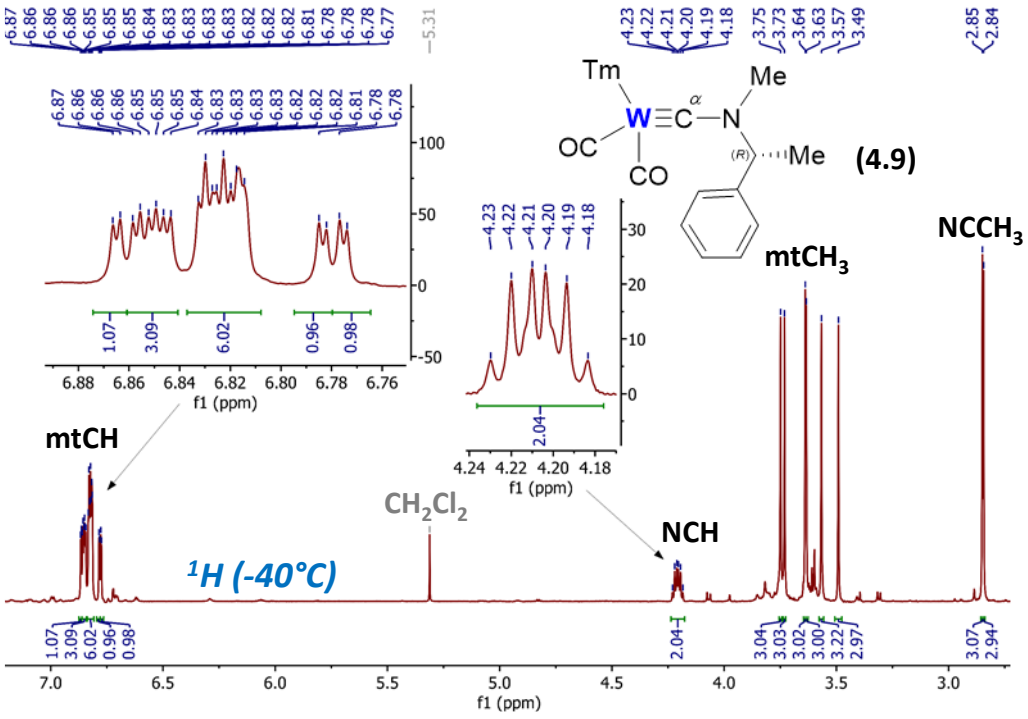

Figure 4.15. Segment of the low temperature (-40°C) ^{1}H NMR spectrum recorded for complex **4.9**, displaying well resolved and duplicated signals for the **Tm** ligand and the amino substituent. Recorded as a $CDCl_3$ solution.

In order to rule out the possibility that contaminants within the sample were the source of the duplicate signals, the bulk purity of complex **4.9** was probed. ESI mass spectrometry affirmed the presence of the title complex through the detection of two complex ions of formulae $C_{24}H_{28}BN_7NaO_2S_3W$ and $C_{24}H_{28}BN_7O_2S_3W$, calculated to match $[M+Na]^+$ and $[M]^+$ molecular ions, respectively. Elemental microanalysis also showed the sample to consist solely of complex **4.9**, albeit solvated with half an equivalent of acetone.

Complex **4.9** was analysed *via* $^{13}C\{^{1}H\}$ NMR spectroscopy as a $CDCl_3$ solution. Once again, low temperature VT NMR was employed to ensure sufficient spectral resolution was obtained. When recorded at -40°C, the most downfield signal was found to be that of the carbyne carbon (W≡C$^{\alpha}$), which was detected at δ_C 248.7 ppm as a single signal. Conversely, the two carbonyl ligands on the metal centre of each diastereomer were detected individually between the range δ_C 227.1-220.1 ppm (**Figure 4.16**).

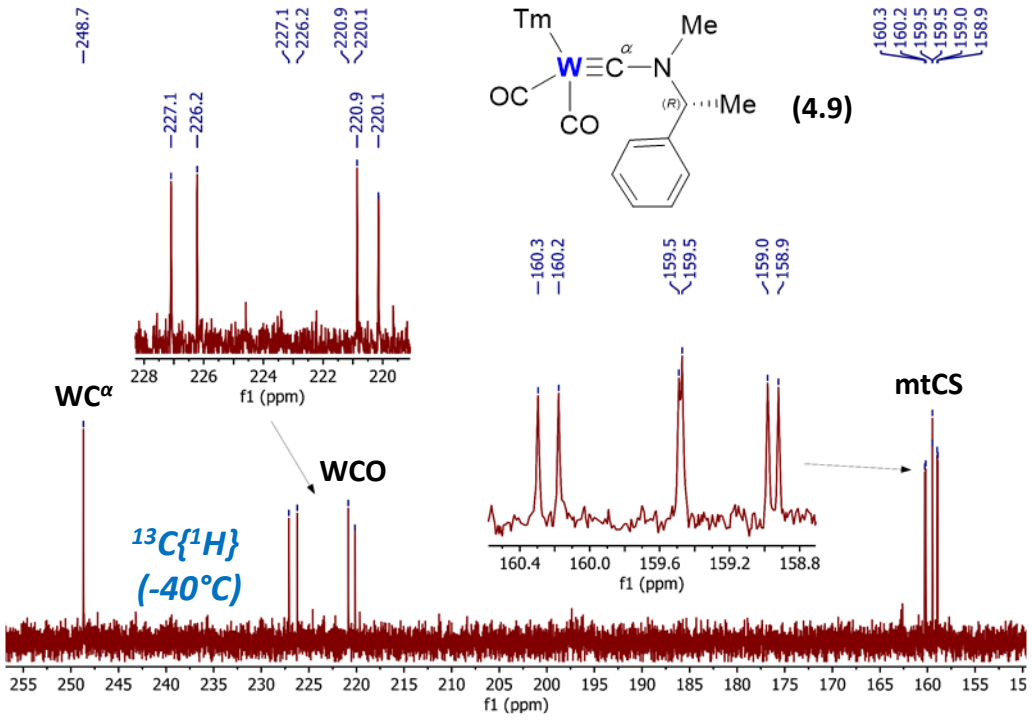

Figure 4.16. Segment of the low temperature (-40°C) $^{13}C\{^{1}H\}$ NMR spectrum recorded for complex **4.9**, displaying duplicated signals for the carbonyl ligands and the methimazolyl-thione donor groups. Recorded as a $CDCl_3$ solution.

Of the remaining signals, all were detected with apparent doubling. For example, the {C=S} thione donor fragments were detected as six signals about δ_C 159.5 ppm, and the single nitrogen-bound CH_3-group was detected as two signals at δ_C 36.3 and 36.1 ppm.

4.4.9 Synthesis of [(Htt)W(CO)$_2${≡C((*R*,*R*)-bis(1-phenylethyl)amine)}]

Following on from the successful inclusion of a chiral amine into a group 6 aminocarbyne, another chiral amine was selected to further probe these chemical systems. The doubly-enantiotopic secondary amine (+)-bis[(*R*)-1-phenylethyl]amine was successfully

used to form the **Htt**-ligated tungsten aminocarbyne complex [(**Htt**)W(CO)$_2${≡C((*R*,*R*)-bis[1-phenylethyl]amine)}] (**4.10**) in moderate yield (**Scheme 4.22**).

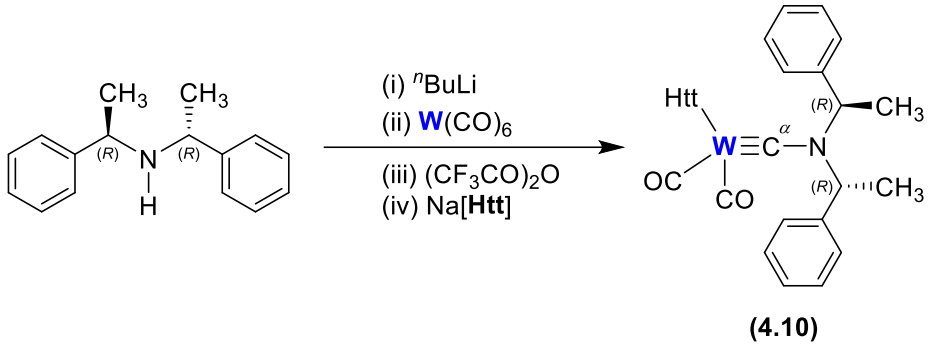

(4.10)

Scheme 4.22. Preparation of complex **4.10**.

Following the final step of the reaction procedure, where the **Htt** pro-ligand was added and stirred vigorously as the contents of the reaction vessel slowly warmed to room temperature, the resulting red mixture was concentrated to dryness on a rotary evaporator and the residues extracted with a small volume of CH_2Cl_2. A spectroscopically pure sample of complex **4.10** was obtained through purification *via* silica-gel column chromatography, eluting with CH_2Cl_2. The major orange band which traversed down the column was collected and concentrated to dryness to afford complex **4.10**.

The title complex was found to be readily soluble in halogenated solvents, and was initially probed *via* infrared spectroscopy as a CH_2Cl_2 solution. Two strong carbonyl bands were detected near the middle of the spectral range at ν_{CO} 1947 and 1850 cm^{-1}. Two shoulders to these stretches were also detected with weaker intensity and shifted to higher frequencies. These signals, observed at ν 1967 and 1880 cm^{-1}, are reminiscent of carbonyl stretches, but it cannot be stated with certainty whether they correspond to another diastereomer, unreacted starting material, or some other impurity. In addition to the carbonyl bands, a weak B–H stretching vibration was detected at ν_{BH} 2528 cm^{-1}, which served to be the last of the diagnostic signals present in the spectrum.

Complex **4.10** was analysed *via* ^{1}H NMR spectroscopy at -40°C as a $CDCl_3$ solution. Aside from the presence of a slight impurity, the sample was shown to correspond to that predicted for the title complex. The phenyl protons of the amino-substituent were detected in the range δ_H 7.39-7.30 ppm as a multiplet devoid of fine structure. The C–H groups on

both chiral centres of complex **4.10** were detected as a quartet centred about δ_H 3.96 ppm, and of the remaining signals, only those detected at δ_H 1.75 and 1.74 ppm could be assigned to the CH_3 groups on the amino-substituent. The peaks at δ_H 1.87, 1.84 and 1.73 ppm were determined to equate to nine protons each, therefore allowing them to be assigned as the *exo*-($C(CH_3)_3$) groups on the **Htt** ligand.

Complex **4.10** was detected as a single ion at m/z 982.2535 in the ESI mass spectrum, which was calculated to correspond to a complex ion of formula $C_{34}H_{46}BN_{13}NaO_2S_3W$. The isotope pattern which was collected along with the above value was shown to closely match that calculated for the molecular ion $[M+Na]^+$, and thereby confirmed the presence of complex **4.10**. Elemental microanalysis afforded results which were a good match for those calculated for complex **4.10**. However, in line with the minor impurity observed in the ^1H NMR spectrum, the values obtained for the nitrogen and sulfur content deviated from those calculated by approximately 0.6% and 0.3%, respectively, and could not be accounted for with the inclusion of extraneous solvent.

Crystals suitable for single-crystal X-ray diffraction were not successfully formed of the title complex, even after several attempts.

4.4.10 Synthesis of [TmW(CO)$_2${≡C(*N*,*N*′-diphenylbenzidine)}]

It was hoped that through the use of a bifunctional secondary amine, it may be possible to form complexes bearing two aminocarbyne fragments. To probe this, *N*,*N*′-diphenylbenzidine was utilised in the oxide abstraction reaction protocol with tungsten hexacarbonyl. Two equivalents of all reagents (relative to the amine) were used in an effort to try form the difunctionalised product, but this was ultimately not isolated. The crude reaction mixture was purified *via* silica-gel column chromatography, eluting in a graded manner initially with a 9:1 (v/v) mixture of CH_2Cl_2 and petroleum spirit (60-80°C), before changing to 100% CH_2Cl_2. This resulted in a major orange band traversing down the column which was isolated and concentrated to dryness to afford an orange powder. Spectral analysis of this material revealed it to be the mono-substituted product, [**Tm**W(CO)$_2${≡C(*N*,*N*′-diphenylbenzidine)}] (**4.11**) (**Scheme 4.23**), and no trace of the initially targeted difunctionalised product was detected.

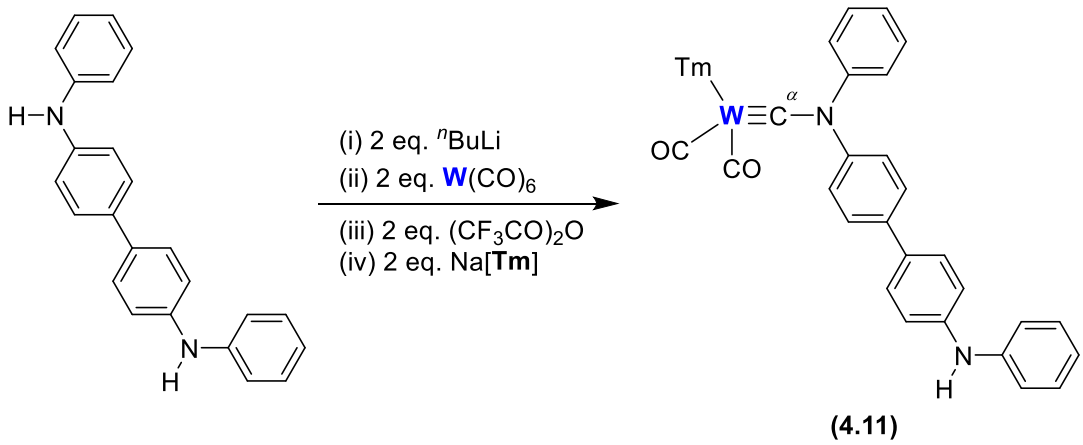

Scheme 4.23. Preparation of complex **4.11**.

Complex **4.11** was found to be soluble in halogenated solvents and was thereby initially analysed *via* infrared spectroscopy as a CH_2Cl_2 solution. Two carbonyl stretching frequencies of approximately equal intensity were detected at ν_{CO} 1953 and 1854 cm^{-1}. Although a concentrated solution was used, the B-H stretching vibration could not be detected.

The ^1H NMR spectrum of complex **4.11** was recorded at room temperature as a $CDCl_3$ solution. A range of aromatic proton signals were detected in the range δ_H 7.51-7.12 ppm which corresponded to the phenyl protons on the amino-backbone. Unfortunately, these signals could not be deconvoluted and assigned to specific rings within the structure. The N-H proton was detected at δ_H 6.85 ppm as a broad singlet, and of the remaining signals, all could be assigned to the framework of the **Tm** ligand. The *exo*-CH_3 groups on the **Tm** ligand were detected as three singlets within the range δ_H 3.75-3.37 ppm, and the protons located in the cyclic alkene moiety were allocated to the multiplets detected at approximately δ_H 6.95 and 6.80 ppm.

A small batch of complex **4.11** was used to determine the gross composition and bulk purity of the sample, whereby it was first analysed *via* ESI mass spectrometry. Two fragments were detected, assigned as $[M+Na]^+$ and $[M-2(CO)]^+$ molecular ions, which closely matched the isotope patterns for complexes of the formulae $C_{39}H_{35}BN_8NaO_2S_3W$ and $C_{37}H_{35}BN_8S_3W$ at m/z 961.1545 and 882.1754, respectively. Furthermore, elemental microanalysis afforded results which coincided well with those calculated for complex **4.11**.

The $^{13}C\{^{1}H\}$ NMR spectrum of complex **4.11** was recorded as a $CDCl_3$ solution at room temperature. Coinciding with the majority of the $^{13}C\{^{1}H\}$ NMR spectra recorded herein, the most downfield signal was assigned as the carbyne carbon ($W\equiv C^{\alpha}$) and was detected at δ_C 238.6 ppm. Both carbon atoms in the carbonyl functional groups were detected as individually resolved signals at δ_C 224.2 and 219.8 ppm. Even although a concentrated sample was used, the spectrum was devoid of coupling data for these groups. The three {C=S} thione fragments were detected at δ_C 161.3, 159.7, and 159.6 ppm, and the remaining cyclic alkene carbon atoms on the **Tm** heterocyclic backbone were found at approximately δ_C 122.7 and 119.6 ppm. All remaining signals across the approximate range δ_C 143.0-121.1 ppm were designated as assorted aromatic signals which could not be assigned to specific carbon atoms.

4.4.11 Synthesis of [(Htt)W(CO)$_2${≡C(*N*,*N*′-diphenylbenzidine)}] and [(Htt)W-(CO)$_2${μ-CN(Ph)-Ph-Ph-N(Ph)C≡}W(CO)$_2$(Htt)]

Once again the bifunctional secondary amine *N*,*N*′-diphenylbenzidine was used in order to target a tungsten complex featuring two tungsten aminocarbyne fragments. In an analogous method to that used to form complex **4.11**, the reaction was carried out with the inclusion of the **Htt** pro-ligand. Interestingly, it was found that two complexes were formed during this procedure, which was in direct contrast to the results described for the analogous **Tm**-ligated complex.

Both these materials were isolated following the addition of Na[**Htt**] into the reaction mixture, where it was subsequently warmed to room temperature overnight with constant stirring. The crude mixture was concentrated to dryness and the residues subjected to chromatographic purification *via* silica-gel column chromatography, eluting with a 7:3 (v/v) mixture of CH_2Cl_2 and petroleum spirit (60-80°C). With the aid of spot thin layer chromatography, it was possible to collate column fractions containing each complex which were then concentrated to dryness. Spectral analysis of the resulting orange powders revealed the materials to be the mono-substituted complex [(**Htt**)W(CO)$_2${≡C(*N*,*N*′-diphenylbenzidine)}] (**4.12**) and the di-substituted complex [(**Htt**)W-(CO)$_2${μ-CN(Ph)-Ph-Ph-N(Ph)C≡}W(CO)$_2$(**Htt**)] (**4.13**) (**Scheme 4.24**).

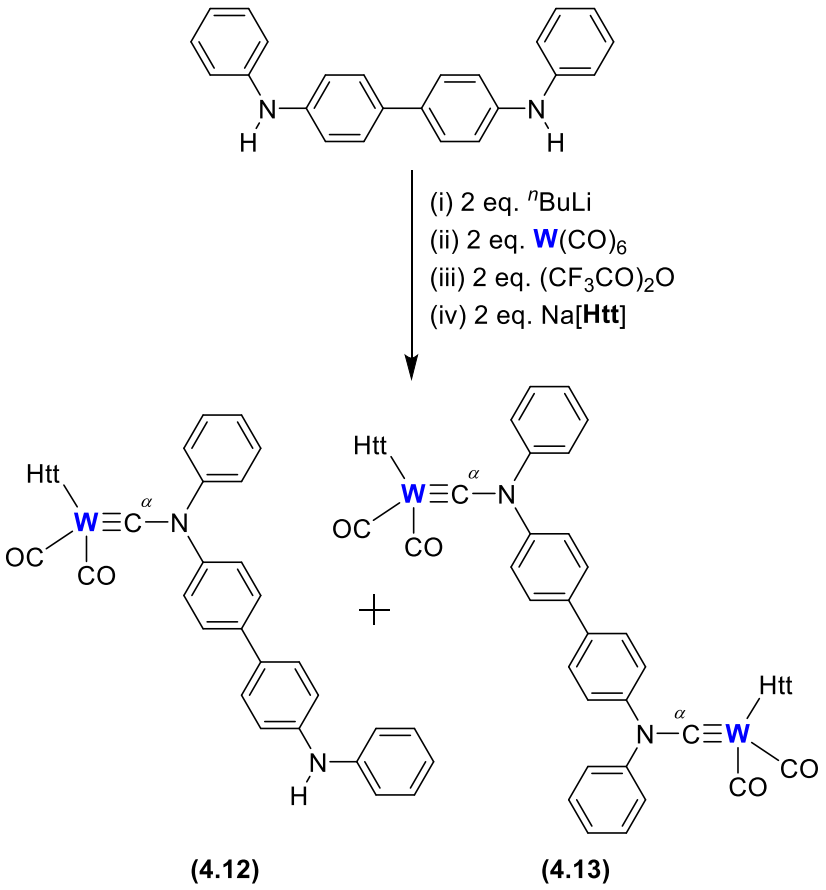

Scheme 4.24. Preparation of complex **4.12** and complex **4.13**.

Both complex **4.12** and complex **4.13** were isolated as orange powders and were found to be readily soluble in halogenated solvents. They were initially probed *via* infrared spectroscopy as CH_2Cl_2 solutions, which revealed two carbonyl bands at ν_{CO} 1966 and 1871 cm^{-1} for complex **4.12**, and two carbonyl bands at ν_{CO} 1967 and 1871 cm^{-1} for complex **4.13**. For both complexes, a B–H stretch was also clearly detected at ν_{BH} 2528 cm^{-1}, whereby the presence of the {B–H} fragment was further corroborated through analysis *via* $^{11}B\{^1H\}$ NMR spectroscopy which revealed a single boron signal.

The ^1H NMR spectra for both complexes were recorded at room temperature as $CDCl_3$ solutions. Some of the most prominent features in these spectra included three individually resolved singlets in the range δ_H 1.90-1.69 ppm which were indicative of the three *exo*-$(C(CH_3)_3)$ groups bound to the **Htt** ligands. These peaks aided with the assignment of complex **4.12** as the mono-functionalised complex, bearing only one aminocarbyne fragment, as the relative integrations of the *exo*-$(C(CH_3)_3)$ groups and the aromatic protons in the range δ_H 7.54-6.97 ppm were calculated to be representative of this type of substitution.

Furthermore, the N–H proton bound to the unreacted secondary amine centre was detected at δ_H 7.14 ppm, which was not present in the ^{1}H NMR spectrum for complex **4.13**. Likewise, it was possible to assign complex **4.13** as the doubly-functionalised complex by direct comparison of the *exo*-($C(CH_3)_3$) groups and the aromatic protons, which revealed a clear doubling in the integrations of the former.

Confidence in these assignments was further bolstered through the recording of ESI mass spectrometry. Complex **4.12** was detected as $[M+Na]^+$ and $[M+H]^+$ molecular ions at m/z 1093.2667 and 1071.2882, respectively. The elemental composition of these ion fragments and their accompanying isotope patterns were calculated to closely match complexes bearing the formulae $C_{42}H_{47}BN_{14}NaO_2S_3W$ and $C_{42}H_{48}BN_{14}O_2S_3W$, respectively. Elemental microanalysis was also recorded for both complex **4.12** and complex **4.13**. For the former, results were found to be in reasonable agreement with those calculated for a complex of formula $C_{34}H_{46}BN_{13}O_2S_3W$, where minor deviations in the nitrogen and sulfur contents were noted. For complex **4.13**, a good match was obtained for a complex of formula $C_{60}H_{74}B_2N_{26}O_4S_6W_2$ mono-solvated with one equivalent of cyclohexane.

Unequivocal structural determination could not be carried out for either complex, as crystals suitable for single crystal X-ray diffraction were not successfully formed, even after several attempts.

4.5 Analysis of Cyclic Voltammetry Data

Although the electrochemical data for various complexes has already been presented in previous sections, a more detailed analysis of the results obtained has been provided below. It should be noted that the results presented are preliminary, and should be subject to further review and study.

Each spectrum clearly indicates one major coupled set of redox events (*i.e.* one oxidation event and one reduction event) which can be easily attributed to a one-electron redox process at the metal centre. It is presumed that this major redox event may be somewhat attenuated depending on the donor ability of the amino-substituent bound to the carbyne carbon. For example, by direct comparison of the $E_{½}$ values for the major redox couple associated with complex **4.2** and complex **4.8** (both bearing tungsten-bound **Htt**-

ligand systems), it can be noted that the $E_{½}$ value recorded for complex **4.8** is approximately double that recorded for complex **4.2** (0.371 V and 0.777 V, respectively). In other words, in order to carry out the oxidation process which is occurring in complex **4.8**, a greater potential is required. This is tentatively attributed to the enhanced electron-releasing capability of the NPh_2 substituent on complex **4.8** which makes it more difficult for the oxidation process to take place, compared to the more frugal electron-releasing ability of NEt_2 substituent on complex **4.2**.

A minor electrochemical redox couple was also noted in each voltammogram, normally centred about higher relative potentials to the major redox couple (**Table 4.3**). It is currently unclear as to what this couple might correspond to, or whether it indicates the presence of an impurity across all samples, or perhaps the presence of a product forming as a result of the redox process. Hence, in lieu of further data, the minor redox events will also be subject to analysis *via* the following method. Analysis of these events may be carried out through the calculation of the Cotton-Kraihanzel constant (k_{CK}),[35] which allows for the carbonyl ligand absorbances which were detected in the liquid IR to be combined into a single number (**Equation 4.1**).

$$k_{CK} = 2.0161\ (\nu_1{}^2 + \nu_2{}^2)$$

Equation 4.1. Cotton-Kraihanzel constant (k_{CK}).

Complex No.	Metal Centre	Ligand	Liquid IR (cm^{-1})	k_{CK} ($N\ m^{-1}$)	Cyclic Voltammetry (V)					
					Major Redox Events			Minor Redox Events		
			ν_{CO}		E_{ox}	E_{Red}	$E_{½}$	E_{ox}	E_{Red}	$E_{½}$
4.1	Mo	**Tm**	1944, 1845	14.482	0.206	0.156	0.181	0.728	–	–
4.2	W	**Htt**	1946, 1847	14.513	0.416	0.326	0.371	0.698	0.650	0.674
4.3	Mo	**Htt**	1959, 1864	14.742	0.602	0.294	0.448	0.826	0.778	0.802
4.4	W	**Htt**	1944, 1845	14.482	0.526	0.286	0.406	0.804	0.692	0.748
4.5	Mo	**Htt**	1958, 1862	14.719	0.522	0.434	0.478	0.844	0.802	0.823
4.8	W	**Htt**	1966, 1871	14.850	0.784	0.770	0.777	0.878	0.324	0.601

Cyclic Voltammetry data measured in CH_2Cl_2. | Liquid IR spectra measured in CH_2Cl_2. | Measured at 25°C.

Table 4.3. Summary of redox events in various aminocarbyne complexes.

In previous examples of tungsten and molybdenum aminocarbyne complexes, it has been possible to display the correlation between k_{CK} and the $E_{½}$ values for all redox events.[32]

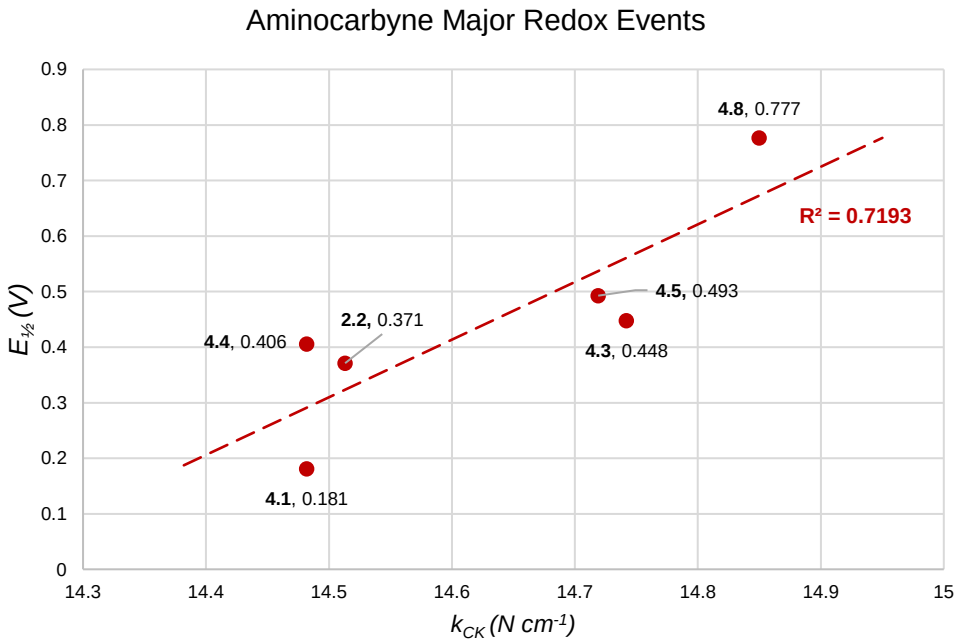

Scheme 4.25. Comparison of electrochemical data for major redox processes with infrared absorbances.

In this work, a significant correlation between these two variables cannot be inferred. Due to the poor ordering of the data, as well as the relatively small range through which the k_{CK} values were calculated to occur, any conclusions drawn from this data may prove to be unreliable. A trend (albeit tenuous) may be fitted for the data associated with the major redox processes (**Scheme 4.25**) which reveals complex **4.1** as having the lowest $E_{½}$ value out of all complexes which were subjected to electrochemical analysis. However, it is noteworthy that the k_{CK} values calculated for complexes **4.1** and **4.4** are closely associated. Although only one aminocarbyne complex bearing the **Tm** ligand was analysed *via* cyclic voltammetry (complex **4.1**), it indicates the those complexes bound with the **Htt** ligand require significantly higher potentials in order to undergo redox processes.

A similar analysis of the minor redox events was carried out and afforded an even more disorganised set of data (**Scheme 4.26**).

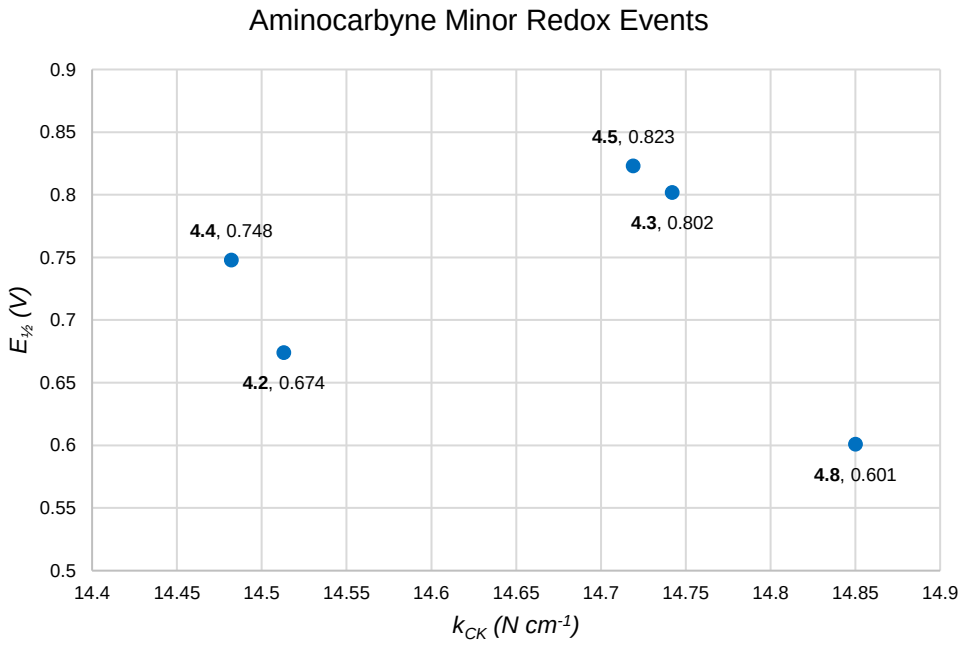

Scheme 4.26. Comparison of electrochemical data for minor redox processes with infrared absorbances.

This is in part caused by the oddly placed minor redox processes which were detected for complex **4.8**. Unlike in all other complexes, the minor oxidation and reduction events were not both found at higher potentials, relative to the major redox couple. Instead, the minor reduction event was found to be at a lower potential, relative to the major redox couple. It is noteworthy that if the datapoint associated with complex **4.8** were to be negated, a somewhat agreeable trend might be installed. However, as this discrepancy cannot be accounted for or explained (*e.g.* through experimental error) it has been included in order to maintain full transparency.

4.6 Summary

Several new aminocarbyne complexes assembled about tungsten and molybdenum centres have been prepared through the course of this work. Predominantly, these complexes feature the rarely encountered **Htt** ligand, but the complexes include one example bearing the closely associated **Tm** ligand. For the complexes formed with simple amino fragments (*e.g.* {NEt_2}, {N^iPr_2}) a comprehensive combinatorial synthetic protocol was attempted, whereby aminocarbyne complexes of the form [(L_{fac})M($CO)_2${$\equiv CNR_2$}] (L_{fac} = **Tm**, **Htt**; M = Mo, W; R = alkyl, aryl) were attempted to be formed for all combinations of metals and

ligands. However, for many, traces of the desired target material were undetectable following chromatographic purification of the crude reaction mixtures.

In addition to commonly encountered secondary amines, chiral secondary amines were successfully utilised in the oxide abstraction reaction protocol. It is believed that through this method, the complexes [**Tm**W(CO)$_2${≡C((*R*)-dimethylbenzylamine)}] and [(**Htt**)W(CO)$_2${≡C((*R*,*R*)-bis(1-phenylethyl)amine)}] serve to be the first two examples of tungsten aminocarbyne complexes ligated with both chiral amino fragments, and soft Scorpionates.

4.7 Chapter 4 - References

1. Fischer, E.O., Kreis, G., Kreissl, F. R., Kalbfus, W., Winkler, E., *J. Organomet. Chem.*, **1974**, *65*, C53.
2. Fischer, E. O, Kreis, G., Kreiter, C. G., Muller, J., Huttner, G., Lorenz, H., *Angew. Chem. Int. Ed. Engl.*, **1973**, *12*, 564.
3. Fischer, E. O, Kreis, G., Kreiter, C. G., Muller, J., Huttner, G., Lorenz, H., *Angew. Chem.*, **1973**, *85*, 618.
4. Morrall, J. P., Dalton, G. T., Humphrey, M. G., *Advances in Organometallic Chemistry*, **2007**, *55*, 61.
5. Chatt, J., Pombeiro, A. J. L., Richards, R. L., Royston, G. H., D., Muir, K. W., Walker, R., *J. Chem. Soc., Chem. Commun.*, **1975**, *17*, 708.
6. Pruchnik, F. P., Duraj, S. A., *Organometallic Chemistry of the Transition Elements*, **1990**, 617.
7. Reglinski, J., Garner, M., Cassidy, I. D., Slavin, P. A., Spicer, M. D., Armstrong, D. R., *J. Chem. Soc., Dalton Trans.*, **1999**, *13*, 2119.
8. Hill, A. F., Schwich, T., Xiong, Y., *Dalton Trans.*, **2019**, *13*, 2119.
9. Goh, L. Y., Weng, Z., Hor, A. T. S., Leong, W. K., *Organometallics*, **2002**, *21*, 4408.
10. Filippou, A. C., Grunleitner, W., *J. Organomet. Chem.*, **1990**, *398*, 99.
11. Lungwitz, B., Filippou, A. C., *J. Organomet. Chem.*, **1995**, *498*, 91.
12. Kim, H. P., Angelici, R. J., *Organometallics*, **1986**, *5*, 2489.
13. Frogley, B. J., Hill, A. F., *Chem. Commun.*, **2018**, *54*, 2126.
14. Cordiner, R. L., Hill, A. F., Wagler, J., *Organometallics*, **2008**, *27*, 4532.
15. Ugi, I., *Isonitrile Chemistry*, Academic Press (Volume 20), **1971**.
16. Malatesta, L., *Progress in Inorganic Chemistry*, **1959**, *1*, 283.
17. Pomberio, A. J. L., Guedes da Silva, M. F. C., Michelin, R. A., *Coord. Chem. Rev.*, **2001**, *218*, 43.
18. Massarotti, A., Brunelli, F., Aprile, S., Giustiniano, M., Tron, G. C., *Chem. Rev.*, **2021**, *121*, 10742.
19. Michelin, R. A., Pomberio, A. J. L., Guedes da Silva, M. F. C., *Coord. Chem. Rev.*, **2001**, *218*, 75.
20. Pombeiro, A. J. L., Carvalho, M. F. N. N., Hitchcock, P. B., Richards, R. L., *J. Chem. Soc., Dalton Trans.*, **1981**, *7*, 1629.
21. Pombeiro, A. J. L., Pickett, C. J., Richards, R. L., *J. Organomet. Chem.*, **1982**, *224*, 285.
22. Chatt, J., Elson, C. M., Pombeiro, A. J. L., Richards, R. L., Royston, G. H. D., *J. Chem. Soc., Dalton Trans.,* **1978**, *2*, 165.
23. Filippou, A. C., Grunleitner, W., *Z. Naturforsch*, **1989**, *44b*, 1572.
24. Filippou, A. C., Grunleitner, W., Fischer, E. O., Imhof, W., Huttner, G., *J. Organomet. Chem.*, **1991**, *413*, 165.
25. Gamble, A. S., White, P. S., Templeton, J. L., *Organometallics*, **1991**, *10*, 693.
26. Fischer, E. O., Winkler, E., Kreiter, C. G., Huttner, G., Krieg, B., *Angew. Chem. Int. Ed. Engl.*, **1971**, *10*, 922.

27. Fischer, H., Motsch, A., Märkl, R., Ackermann, K., *Organometallics*, **1985**, *4*, 726.

28. Fischer, E. O., Wittmann, D., Himmelreich, D., Schubert, U., Ackermann, K., *Chem. Ber.*, **1982**, *115*, 3141.

29. Fischer, E. O., Kleine, W., Kreis, G., Kreissl, F. R., *Chem. Ber.*, **1978**, *111*, 3542.

30. Biancalana, L., Marchetti, F., *Coord. Chem. Rev.*, **2021**, *449*, 214203.

31. Filippou, A. C., Wanninger, K., Mehnert, C., *J. Organomet. Chem.*, **1993**, *461*, 99.

32. Mark, M. R., Hill, A. F., White, A. J. P., Williams, D. J., *Organometallics*, **2003**, *22*, 3831.

33. Foreman, M. R. S. J., Hill, A. F., Smith, M. K., Tshabang, N., *Organometallics*, **2005**, *24*, 5224.

34. Foreman, M. R. S. J., Hill, A. F., Smith, M. K., Tshabang, N., *Organometallics*, **2006**, *25*, 1528.

35. Cotton, F. A., Kraihanzel, C. S., *J. Am. Chem. Soc.,* **1962**, *84*, 4432.

CHAPTER 5.

EXPERIMENTAL

5.1 General Procedures

Unless otherwise stated, all manipulations were carried out under an anaerobic and anhydrous argon atmosphere using standard Schlenk line and glove-box techniques with dried and degassed solvents. Where reference has been made to the exposure of reaction mixtures to 'ambient air' during synthetic procedures (and in the preceding sections of this work), this infers that a reaction flask and its contents were allowed to warm/cool gradually through exposure to the temperature of the atmosphere within the laboratory (approximately 17-21°C). All common reagents were used as obtained from commercial suppliers without further purification. Known compounds were prepared as previously described: [AuCl(PPh$_3$)],[1] [AuCl(SMe$_2$)],[2] [Pd$_2$(dba)$_3$·(CHCl$_3$)],[3] [Pd(PPh$_3$)$_4$],[4] [Pt(nbe)$_3$],[5] [Tp*(CO)$_2$Mo≡C(SnBu$_3$)],[6] [Tp*(CO)$_2$W≡C(SnBu$_3$)],[7] 1-ethynylpyrene,[8] 9-bromo-10-phenylanthracene,[9] 9-ethynylanthracene,[10] 9-ethynylphenanthrene,[11] and *trans*-[RhCl(CO)(PPh$_3$)].[12] The pro-ligand salts Na[Hbt] and Na[Htt] were not prepared during the course of this work. Instead, previously synthesised batches of both salts were used, which were prepared *via* their literature methods. In each case, full spectral characterisation of Na[Hbt] and Na[Htt] have been detailed in the following sections.

NMR spectra were obtained using a Bruker Advance 400, a Bruker Advance 600, or a Bruker Advance 700 spectrometers. Chemical shifts (δ) are reported in ppm, with coupling constants given in Hz, and referenced to the residual solvent peak (^{1}H, ^{13}C), or external reference: 85% H_3PO_4 (^{31}P), 15% BF_3·OEt_2 in $CDCl_3$ (^{11}B). The multiplicities of NMR resonances are denoted by the abbreviations s (singlet), d (doublet), t (triplet), q (quartet), m (multiplet), br (broad) and combinations thereof for more highly coupled systems. Heteronuclear satellites observed in ^{13}C NMR are assigned after the major NMR resonance with '+ multiplicity'. In some cases, distinct peaks were observed in the ^{1}H and ^{13}C{^{1}H} NMR spectra, but to the level of accuracy that is reportable (i.e. 2 decimal places for ^{1}H NMR, 1 decimal place for ^{13}C NMR) they are reported as having the same chemical shift. The abbreviation 'mt' refers to the methimazolyl rings on the hydrotris(methimazolyl) borate (Tm) and dihydrobis(methimazolyl) borate (Bm) ligands. Likewise, the abbreviation 'pz' refers to the pyrazolyl rings on the hydrotris(3,5-dimethylpyrazol-1-yl) borate (Tp*) ligand.

Infrared (IR) spectra were obtained using a Perkin-Elmer Spectrum One FT-IR spectrometer for liquid samples, and a Perkin-Elmer Spectrum Two ATR FT-IR spectrometer for solid samples. The strengths of IR absorptions are denoted by the abbreviations vs (very strong), s (strong), m (medium) and w (weak). Elemental microanalytical data were provided by the London Metropolitan University and Macquarie

University. UV-vis data was collected as solutions in 1 cm quartz cells using a Perkin-Elmer Lambda 950 spectrophotometer.

Electrochemical measurements were recorded using an e-corder 401 potentiostat system from eDaq Pty Ltd. Electrochemical solutions contained 0.1 mol L^{-1} $[Bu_4N][PF_6]$ and *ca.* 10^{-3} mol L^{-1} analyte in CH_2Cl_2 and were purged and maintained under a nitrogen atmosphere. Analytes were internally referenced to the ferrocene/ferrocenium redox couple, which was located at 0.460 V (ΔE = 0.9 – 1.0 V). Scan rates were typically 100 mV s^{-1}. The cell utilised platinum working- and auxiliary-electrodes and a silver wire reference electrode.

High-resolution electrospray ionization mass spectrometry (ESI-MS) were performed by the ANU Research School of Chemistry mass spectrometry service with acetonitrile or methanol as the matrix.

X-ray crystallography data were collected with an Agilent Xcalibur CCD diffractometer using Mo-Kα radiation (λ = 0.71073 Å), Agilent SuperNova CCD diffractometer using Cu-Kα radiation (λ = 1.54184 Å), or at the Australian Synchrotron using the MX1 beamline using silicon double crystal monochromated synchrotron radiation (λ = 0.710762 Å) using CrysAlis PRO software.[ǂǂǂǂ] The structures were solved by direct or Patterson methods and refined by full-matrix least squares on F^2 using SHELXL programs[13] and the Olex2 software.[14] Crystal structures were generated using the CCDC visualization program in Mercury.[15] All X-ray crystallographic datasets were solved by the title author, with marginal input from other group members and SCXRD technicians in some cases.

ǂǂǂǂ CrysAlis PRO, Agilent Technologies Ltd, Yarnton, Oxfordshire, England, 2014.

5.2 Compounds

5.2.1 Ligand Systems

$Na[H_2B(mt)_2]$ (Na[Bm])

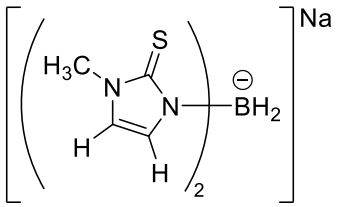

A solution of 2-mercapto-1-methylimidazole (10.5 g, 92.0 mmol) and sodium borohydride (1.44 g, 38.0 mmol) in THF (240 mL) was heated under reflux for 7 hours until all of the sodium borohydride had dissolved. The mixture was allowed to cool to room temperature and evaporated to dryness to afford a white powder. To the crude product mixture, toluene (240 mL) was added and the white suspension heated until boiling. The contents were then poured into a sintered-glass funnel and the solid washed with hot toluene (2 × 50 mL). The solid was air dried on the sintered disk to afford **Na[Bm]** as a white powder. Yield 8.94 g (74%).

IR (ATR): ν_{BH} 2456 w cm^{-1}. NMR ^{1}H (DMSO-d6, 25.05°C, 700.03 MHz): δ 6.98 (d, $^{3}J_{HH}$ 1.9 Hz, 2 H, mtCH), 6.70 (d, $^{3}J_{HH}$ 1.9 Hz, 2 H, mtCH), 3.37 (s, 6 H, $mtCH_3$). $^{11}B\{^{1}H\}$ (DMSO-d6, 24.85°C, 128.38 MHz): δ -9.45. $^{13}C\{^{1}H\}$ (DMSO-d6, 25.95°C, 176.05 MHz): δ 163.2 (2C) (mtCS), 123.8 (2C), 115.5 (2C) (mtCH), 33.8 (2C) ($mtCH_3$). MS (ESI, high resolution): m/z (%) = $[M\text{-}Na]^+$ 239.0601; $[M+Na]^+$ 285.0396. Anal. Calcd. for $C_8H_{12}{}^{11}B_1N_4S_2$: $[M\text{-}Na]^+$ 239.0598; Anal. Calcd. for $C_8H_{12}{}^{11}B_1N_4{}^{23}Na_2S_2$: $[M+Na]^+$ 285.0393. Elemental Anal. Found: C, 36.59; H, 4.70; N, 21.36; S, 24.66%. Calcd. for $C_8H_{12}BN_4NaS_2$: C, 36.66; H, 4.61; N, 21.37%.

$Na[H_2B(tt^{tBu})_2]$ (Na[Hbt])

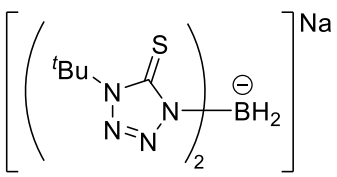

IR (ATR): ν_{BH} 2456, 2444 w cm^{-1}. NMR ^{1}H (DMSO-d6, 24.85°C, 400.13 MHz): δ 1.75 (s, 18 H, $C(CH_3)_3$). $^{11}B\{^{1}H\}$ (DMSO-d6, 24.85°C, 128.38 MHz): δ -10.33. $^{13}C\{^{1}H\}$ (DMSO-d6, 24.85°C, 100.62 MHz): δ 165.2 (2C) (C=S), 60.7 (2C) ($C(CH_3)_3$), 27.1 (6C) ($C(CH_3)_3$). MS (ESI, high resolution): m/z (%) = $[M+Na]^+$ 373.1146. Anal. Calcd. for $C_{10}H_{20}{}^{11}B_1N_8{}^{23}Na_2S_2$: $[M+Na]^+$ 373.1141. Elemental Anal. Found: C, 32.07; H, 5.88; N, 32.07; S, 18.38%. Calcd. for $C_{10}H_{20}BN_8NaS_2$: C, 34.29; H, 5.76; N, 31.99; S, 18.31%.

Na[HB(mt)$_3$] (Na[Tm])

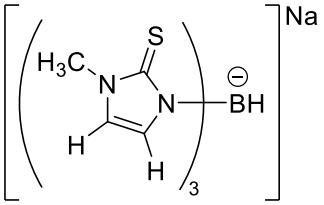

A solution of 2-mercapto-1-methylimidazole (2.93 g, 25.7 mmol) and sodium borohydride (0.330 g, 8.72 mmol) in toluene (40 mL) was heated under reflux for 72 hours until all of the sodium borohydride had dissolved. The mixture was allowed to cool to room temperature and evaporated to dryness to afford a white powder. The contents were then poured into a sintered-glass funnel and the solid washed with hot toluene (2 × 20 mL) and hexane (2 × 20 mL). The solid was air dried on the sintered disk to afford **Na[Tm]** as a white powder. Yield 2.88 g (90%).

IR (ATR): ν_{BH} 2479 w cm^{-1}. NMR ^{1}H (DMSO-d6, 25.05°C, 600.02 MHz): δ 6.78 (d, $^3J_{HH}$ 2.2 Hz, 3 H, mtCH), 6.41 (d, $^3J_{HH}$ 2.2 Hz, 3 H, mtCH), 3.38 (s, 9 H, mtCH$_3$). ^{11}B{^{1}H} (DMSO-d6, 26.85°C, 128.38 MHz): δ -3.17. ^{13}C{^{1}H} (DMSO-d6, 24.85°C, 150.90 MHz): δ 163.4 (3C) (mtCS), 120.8 (3C), 116.5 (3C) (mtCH), 33.6 (3C) (mtCH$_3$). MS (ESI, high resolution): m/z (%) = [M+Na]$^+$ 397.0484. Anal. Calcd. for $C_{12}H_{16}{}^{11}B_1N_6{}^{23}Na_2S_3$: [M+Na]$^+$ 397.0481. Elemental Anal. Found: C, 38.29; H, 4.78; N, 22.25%. Calcd. for $C_{12}H_{16}BN_6NaS_3$: C, 38.51; H, 4.31; N, 22.45%.

Na[HB(tt^{tBu})$_3$] (Na[Htt])

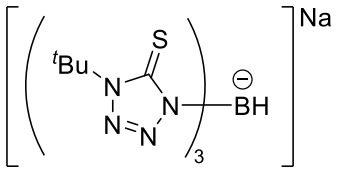

NMR ^{1}H (DMSO-d6, 24.85°C, 400.13 MHz): δ 4.84 (br s, BH$_2$), 1.76 (s, 27 H, C(CH$_3$)$_3$). ^{11}B{^{1}H} (DMSO-d6, 24.85°C, 128.38 MHz): δ -4.66. ^{13}C{^{1}H} (DMSO-d6, 24.85°C, 100.62 MHz): δ 165.7 (3C) (C=S), 61.2 (3C) (*C*(CH$_3$)$_3$), 27.0 (9C) (C(*C*H$_3$)$_3$). MS (ESI, high resolution): m/z (%) = [M+H]$^+$ 507.1794. Anal. Calcd. for $C_{15}H_{29}{}^{11}B_1N_{12}{}^{23}Na_1S_3$: [M+H]$^+$ 507.1791. Elemental Anal. Found: C, 35.61; H, 5.59; N, 32.99; S, 19.22%. Calcd. for $C_{15}H_{28}BN_{12}NaS_3$: C, 35.57; H, 5.57; N, 33.19; S, 18.99%.

5.2.2 Chapter 2 – Propargylidyne & Tricarbido Complexes

TmW(CO)$_2$(≡CC≡CSiMe$_3$) (2.1)

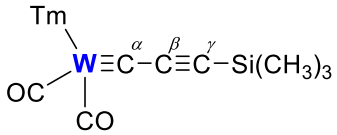

To a 250 mL Schlenk tube, ethynyltrimethylsilane (2.1 mL, 15.159 mmol) was added and dispersed in THF (60 mL). The mixture was cooled to -78°C and ^{n}BuLi (1.6 M,

10.5 mL, 16.800 mmol) was added dropwise and the colourless solution stirred for 10 minutes. The reaction vessel was warmed in ambient air for 10 minutes, then re-cooled to -78°C for another 10 minutes. $[W(CO)_6]$ (5.279 g, 15.001 mmol) was added and after stirring for 15 minutes, the yellow mixture was warmed to room temperature and stirred for 1 h. The resulting red/brown mixture was cooled to -78°C and trifluoroacetic anhydride (2.1 mL, 15.108 mmol) added dropwise. The brown/black mixture was stirred for 15 minutes and then the reaction vessel was warmed in ambient air for 45 minutes. During this time carbon monoxide gas was evolved from the reaction mixture as it warmed. Once re-cooled to -78°C, Na[Tm] (5.627 g, 15.034 mmol) was added to the rapidly stirred mixture which was allowed to slowly warm to room temperature overnight. Stirring of the red/brown reaction mixture was halted after 16 h and concentrated to afford a red/brown residue. All residues were re-dissolved in minimal CH_2Cl_2 and petroleum spirit (40-60°C) was rapidly added to afford a red/brown precipitate which was isolated by vacuum filtration and washed with petroleum spirit (40-60°C), then *n*-pentane. The crude product mixture was purified *via* silica-gel flash column chromatography (Eluent: 2% (v/v) THF/CH_2Cl_2). Collection and subsequent concentration of the major red band afforded **2.1** as a purple powder. Yield 9.201 g (88%).

IR (CH_2Cl_2): ν_{BH} 2436 w; ν_{CO} 1981 vs, 1893 vs cm^{-1}. NMR ^1H ($CDCl_3$, 25.05°C, 700.16 MHz): δ 6.88 (m, 2 H, mtCH), 6.82-6.81 (m, 2 H, mtCH), 6.79 (d, $^3J_{HH}$ 2.1 Hz, 1 H, mtCH), 6.77 (d, $^3J_{HH}$ 2.0 Hz, 1 H, mtCH), 3.77 (s, 3 H, $mtCH_3$), 3.71 (s, 3 H, $mtCH_3$), 3.58 (s, 3 H, $mtCH_3$), 0.14 (s, 9 H, $Si(CH_3)_3$). $^{11}B\{^1H\}$ ($CDCl_3$, 26.85°C, 128.38 MHz): δ -1.75. $^{13}C\{^1H\}$ ($CDCl_3$, 25.75°C, 176.08 MHz): δ 249.9 ($W{\equiv}C^{\alpha}$), 224.8, 219.7 (WCO), 170.2 (WC^{β}), 160.9, 159.0, 158.4 (mtCS), 123.1, 122.9, 120.7, 120.3, 120.1, 120.0 (mtCH), 82.5 (WC^{γ}), 35.3, 34.9, 34.8 ($mtCH_3$), 0.0 ($Si(CH_3)_3$). MS (ESI, high resolution): m/z (%) = $[M+H]^+$ 701.0662. Anal. Calcd. for $C_{20}H_{26}{}^{11}B_1N_6O_2S_3Si_1{}^{184}W_1$: $[M+H]^+$ 701.0651. Elemental Anal. Found: C, 34.32; H, 3.67; N, 11.95; S, 13.88%. Calcd. for $C_{20}H_{25}BN_6O_2S_3SiW$: C, 34.30; H, 3.60; N, 12.00; S, 13.73%.

A crystal suitable for structure determination was grown by vapour diffusion of petroleum spirit (40-60°C) into a CH_2Cl_2 solution at 4°C (**Figure 5.1**). The crystal was found to contain two equivalents of CH_2Cl_2 of solvation, which were modelled across two sites in the asymmetric unit. Crystal Data for $C_{22}H_{29}BCl_4N_6O_2S_3SiW$ (M =870.24 g/mol): monoclinic, space group Cc (no. 9), a = 13.35130(10) Å, b = 14.39740(10) Å, c = 18.2335(2) Å, β = 107.4480(10)°, V = 3343.65(5) Å^3, Z = 4, T = 150.00(10) K, μ(CuKα) =

11.703 mm^{-1}, *Dcalc* = 1.729 g/cm^3, 26074 reflections measured (9.27° ≤ 2Θ ≤ 133.192°), 5312 unique (R_{int} = 0.0273, R_{sigma} = 0.0205) which were used in all calculations. The final R_1 was 0.0365 (I > 2σ(I)) and wR_2 was 0.0959 (all data) for 367 refined parameters with 6 restraints.

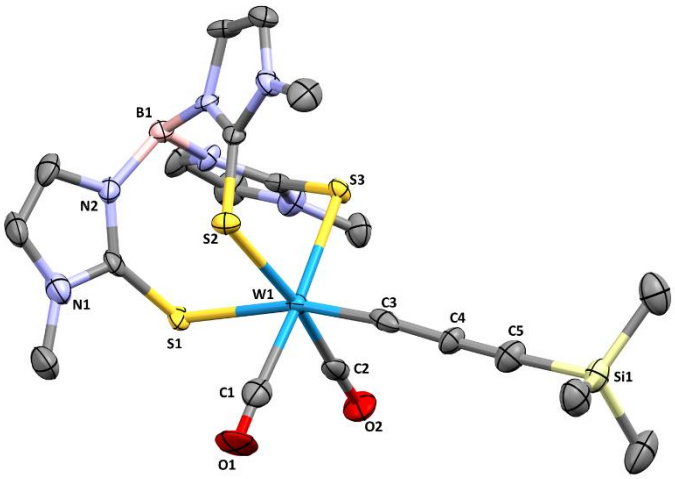

Figure 5.1. Molecular structure of **2.1** (50% displacement ellipsoids) with selected atom labels. Solvent molecules and hydrogen atoms omitted for clarity. Selected bond lengths (Å) and angles (°): W1–C1 2.034(12), W1–C2 1.999(16), W1–S1 2.636(2), W1–S2 2.511(3), W1–S3 2.566(2), W1–C3 1.838(12), C3–C4 1.380(16), C4–C5 1.217(15), C5–Si1 1.848(11); W1–C3–C4 172.4(8), C3–C4–C5 177.5(11).

TmMo(CO)$_2$(≡CC≡CSiMe$_3$) (2.2)

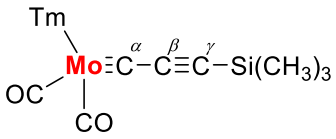

To a 100 mL Schlenk tube, ethynyltrimethylsilylacetylene (0.7 mL, 5.053 mmol) was added and dispersed in THF (30 mL). The mixture was cooled to -78°C and ^{n}BuLi (1.776 M,#### 3.2 mL, 5.683 mmol) was added dropwise and the colourless solution stirred for 10 minutes. The reaction vessel was warmed in ambient air for 10 minutes, then re-cooled to -78°C for another 10 minutes. [Mo(CO)$_6$] (1.321 g, 5.004 mmol) was added and after stirring for 15 minutes, the yellow mixture was warmed to room temperature and stirred for 1 h. The resulting brown mixture was cooled to -78°C and trifluoroacetic anhydride (0.7 mL, 5.036 mmol) added dropwise. The brown/black mixture was stirred for 15 minutes and then the reaction vessel was warmed in ambient air for 30 minutes. During this time carbon monoxide gas was evolved from the reaction mixture as it warmed. Once re-cooled to -78°C Na[Tm] (1.874 g, 5.007 mmol) was added to the rapidly stirred mixture which was allowed to slowly warm to room temperature overnight. Stirring of the red/brown reaction mixture was halted

An old bottle of ^{n}BuLi (2.5 M) was utilised in this preparation. Prior to use, a sample was titrated and calculated to contain 1.776 M ^{n}BuLi in hexanes.

after 16 h and concentrated to afford a red/brown residue. All residues were re-dissolved in CH_2Cl_2 and filtered through a short pad of diatomaceous earth. The resulting filtrate was concentrated to dryness, dissolved in minimal CH_2Cl_2 and purified *via* silica-gel flash column chromatography (Eluent: 2% (v/v) THF/CH_2Cl_2). Collection and subsequent concentration of the major initial red/brown band afforded **2.2** as a red powder. Yield 448 mg (15%).

IR (CH_2Cl_2): ν_{CO} 1995 m, 1915 m cm^{-1}. NMR ^1H ($CDCl_3$, 25.05°C, 699.90 MHz): δ 6.87 (d, $^3J_{HH}$ 2.1 Hz, 1 H, mtCH), 6.85 (d, $^3J_{HH}$ 2.1 Hz, 1 H, mtCH), 6.81 (d, $^3J_{HH}$ 2.1 Hz, 1 H, mtCH), 6.80 (d, $^3J_{HH}$ 2.1 Hz, 1 H, mtCH), 6.76 (d, $^3J_{HH}$ 2.1 Hz, 1 H, mtCH), 6.74 (d, $^3J_{HH}$ 2.1 Hz, 1 H, mtCH), 3.76 (s, 3 H, $mtCH_3$), 3.70 (s, 3 H, $mtCH_3$), 3.58 (s, 3 H, $mtCH_3$), 0.14 (s, 9 H, $Si(CH_3)_3$). $^{11}B\{^1H\}$ (CD_2Cl_2, 26.85°C, 128.38 MHz): δ -1.72. $^{13}C\{^1H\}$ ($CDCl_3$, 25.05°C, 176.02 MHz): δ 257.5 ($Mo{\equiv}C^{\alpha}$), 227.7, 222.7 (MoCO), 161.6, 159.8, 159.1 (mtCS), 123.1, 122.8 (2C), 120.0, 119.9, 119.8 (mtCH), 113.8 (MoC^{β}), 77.9 (MoC^{γ}), 35.2, 34.9, 34.8 ($mtCH_3$). MS (ESI, high resolution): m/z (%) = $[M+H]^+$ 615.0183. Anal. Calcd. for $C_{20}H_{26}{}^{11}B_1Mo_1N_6O_2S_3Si_1$: $[M+H]^+$ 615.0191. After numerous attempts an agreeable elemental microanalysis could not be obtained.

TmW(CO)$_2$(≡CC≡CSi^{i}Pr$_3$) (2.3)

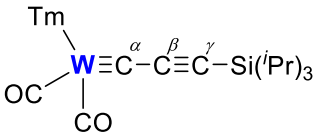

To a 100 mL Schlenk tube, ethynyltriisopropylsilane (1.2 mL, 5.349 mmol) was added and dispersed in THF (30 mL). The mixture was cooled to -78°C and ^{n}BuLi (1.6 M, 3.5 mL, 5.600 mmol) was added dropwise and the colourless solution stirred for 10 minutes. The reaction vessel was warmed in ambient air for 10 minutes, then re-cooled to -78°C for another 10 minutes. $[W(CO)_6]$ (1.759 g, 4.999 mmol) was added and after stirring for 15 minutes, the yellow mixture was warmed to room temperature and stirred for 1 h. The resulting red/brown mixture was cooled to -78°C and trifluoroacetic anhydride (0.7 mL, 5.040 mmol) added dropwise. The brown/black mixture was stirred for 15 minutes and then the reaction vessel was warmed in ambient air for 30 minutes. During this time carbon monoxide gas was evolved from the reaction mixture as it warmed. Once re-cooled to -78°C Na[Tm] (1.882 g, 5.028 mmol) was added to the rapidly stirred mixture which was allowed to slowly warm to room temperature overnight. Stirring of the brown reaction mixture was halted after 16 h and concentrated to afford a red/brown residue. All residues were re-dissolved in CH_2Cl_2 and filtered through a short pad of diatomaceous earth. The resulting filtrate was concentrated to dryness, dissolved in minimal CH_2Cl_2 and purified *via* silica-gel

flash column chromatography (Eluent: CH_2Cl_2). Collection and subsequent concentration of the major red band afforded **2.3** as a pink/red powder. Yield 1.829 g (47%).

IR (CH_2Cl_2): ν_{BH} 2436 w; ν_{CO} 1980 vs, 1892 vs cm^{-1}. NMR ^1H ($CDCl_3$, 25.05°C, 699.90 MHz): δ 6.88 (m, 1 H, mtCH), 6.87 (m, 1 H, mtCH), 6.82-6.81 (m, 2 H, mtCH), 6.80 (m, 1 H, mtCH), 6.76 (m, 1 H, mtCH), 3.77 (s, 3 H, $mtCH_3$), 3.69 (s, 3 H, $mtCH_3$), 3.57 (s, 3 H. $mtCH_3$), 1.03 (s, 21 H, $Si(^iPr)_3$). $^{11}B\{^1H\}$ (CD_2Cl_2, 24.85°C, 128.38 MHz): δ -1.63. $^{13}C\{^1H\}$ ($CDCl_3$, 25.05°C, 176.02 MHz): δ 251.0 ($W{\equiv}C^{\alpha}$, $^1J_{WC}$ 202.7 Hz), 224.9 (WCO, $^1J_{WC}$ 168.9 Hz), 219.6 (WCO, $^1J_{WC}$ 161.3 Hz), 161.2, 159.0, 158.5 (mtCS), 123.0, 122.9 (2C), 120.2, 120.1, 120.0 (mtCH), 80.9 (WC^{β}), 53.6 (WC^{γ}), 35.0, 34.9, 34.8 ($mtCH_3$), 18.8, 11.5 ($Si(^iPr)_3$). MS (ESI, high resolution): m/z (%) = $[M+H]^+$ 785.1566. Anal. Calcd. for $C_{26}H_{38}{}^{11}B_1N_6O_2S_3Si_1{}^{184}W_1$: $[M+H]^+$ 785.1585. Elemental Anal. Found: C, 39.82; H, 4.88; N, 10.80; S, 12.30%. Calcd. for $C_{26}H_{37}BN_6O_2S_3SiW$: C, 39.80; H, 4.75; N, 10.71; S, 12.26%.

TmW(CO)$_2$(≡CC≡C^{t}Bu) (2.4)

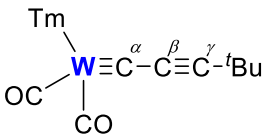

To a 100 mL Schlenk tube, 3,3-dimethyl-1-butyne (1.2 mL, 9.744 mmol) was added and dispersed in THF (30 mL). The mixture was cooled to -78°C and ^{n}BuLi (1.6 M, 3.5 mL, 5.600 mmol) was added dropwise and the colourless solution stirred for 10 minutes. The reaction vessel was warmed in ambient air for 10 minutes, then re-cooled to -78°C for another 10 minutes. $[W(CO)_6]$ (1.761 g, 5.004 mmol) was added and after stirring for 15 minutes, the yellow mixture was warmed to room temperature and stirred for 1 h. The resulting red/brown mixture was cooled to -78°C and trifluoroacetic anhydride (0.7 mL, 5.036 mmol) added dropwise. The brown/black mixture was stirred for 15 minutes and then the reaction vessel was warmed in ambient air for 45 minutes. During this time carbon monoxide gas was evolved from the reaction mixture as it warmed. Once re-cooled to -78°C Na[Tm] (1.879 g, 5.020 mmol) was added to the rapidly stirred mixture which was allowed to slowly warm to room temperature overnight. Stirring of the red/brown reaction mixture was halted after 16 h and concentrated to afford a red/brown residue. All residues were re-dissolved in minimal CH_2Cl_2 and petroleum spirit (40-60°C) was rapidly added to afford a red/brown precipitate which was isolated by vacuum filtration and washed with petroleum spirit (40-60°C), then pentane. The crude product mixture was purified *via* silica-gel flash column chromatography (Eluent: 2% (v/v) THF/CH_2Cl_2). Collection and subsequent concentration of the major red band afforded **2.4** as an orange/peach powder. Yield 616 mg (18%).

IR (CH_2Cl_2): ν_{BH} 2434 w; ν_{CO} 1975 vs, 1886 vs cm^{-1}. NMR ^1H ($CDCl_3$, 24.65°C, 700.03 MHz): δ 6.87 (s, 2 H, mtCH), 6.81 (m, 2 H, mtCH), 6.79 (d, $^3J_{HH}$ 2.0 Hz, 1 H, mtCH), 6.77 (d, $^3J_{HH}$ 2.0 Hz, 1 H, mtCH), 3.77 (s, 3 H, $mtCH_3$), 3.71 (s, 3 H, $mtCH_3$), 3.58 (s, 3 H, $mtCH_3$), 1.20 (s, 9 H, $C(CH_3)_3$). $^{11}B\{^1H\}$ ($CDCl_3$, 26.85°C, 128.38 MHz): δ -1.60. $^{13}C\{^1H\}$ ($CDCl_3$, 25.85°C, 176.04 MHz): δ 251.7 ($W{\equiv}C^{\alpha}$), 224.7, 219.8 (WCO), 161.1, 159.2, 158.8 (mtCS), 123.0, 122.9, 122.8, 120.2, 120.0 (2C) (mtCH), 97.9 (WC^{β}), 85.8 (WC^{γ}), 35.2, 35.0, 34.8 ($mtCH_3$), 30.6 ($C(CH_3)_3$). MS (ESI, high resolution): m/z (%) = $[M+H]^+$ 685.0870. Anal. Calcd. for $C_{21}H_{26}{}^{11}B_1N_6O_2S_3{}^{184}W_1$: $[M+H]^+$ 685.0879. Elemental Anal. Found: C, 37.05; H, 3.59; N, 12.22%. Calcd. for $C_{21}H_{25}BN_6O_2S_3W$: C, 36.86; H, 3.68; N, 12.28%.

A crystal suitable for structure determination was grown by vapour diffusion of petroleum spirit (40-60°C) into a CH_2Cl_2 solution at 4°C (**Figure 5.2**). Crystal Data for $C_{21}H_{25}BN_6O_2S_3W$ (M =684.31 g/mol): monoclinic, space group $P2_1/c$ (no. 14), a = 9.38240(10) Å, b = 31.9700(5) Å, c = 11.1690(2) Å, β = 95.091(2)°, V = 3336.98(9) $Å^3$, Z = 5, T = 150.01(10) K, μ(CuKα) = 10.459 mm^{-1}, $Dcalc$ = 1.703 g/cm^3, 24167 reflections measured (8.416° ≤ 2Θ ≤ 147.48°), 6720 unique (R_{int} = 0.0302, R_{sigma} = 0.0299) which were used in all calculations. The final R_1 was 0.0661 (I > 2σ(I)) and wR_2 was 0.1869 (all data) for 313 refined parameters with 0 restraints.

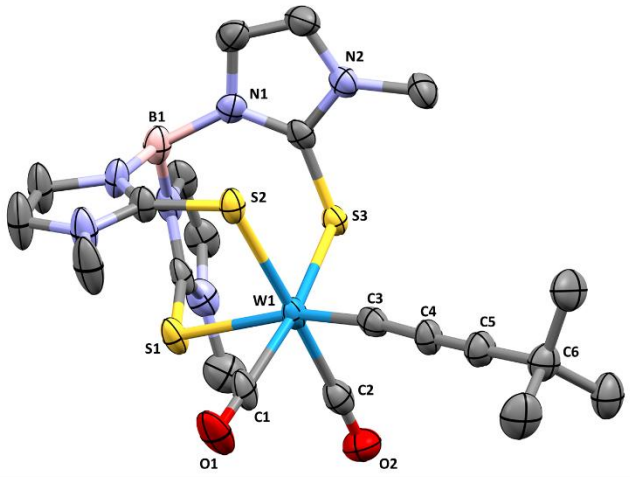

Figure 5.2. Molecular structure of **2.4** (50% displacement ellipsoids) with selected atom labels. Hydrogen atoms omitted for clarity. Selected bond lengths (Å) and angles (°): W1–C1 1994(9), W1–C2 2.020(11), W1–S1 2.633(2), W1–S2 2.575(2), W1–S3 2.5373(19), W1–C3 1.843(9), C3–C4 1.359(12), C4–C5 1.230(13), C5–C6 1.472(12); W1–C3–C4 172.7(7), C3–C4–C5 177.9(10).

TmW(CO)$_2$(≡CC≡CPh) (2.5)

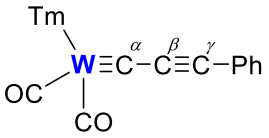

To a 100 mL Schlenk tube, ethynylbenzene (0.6 mL, 5.464 mmol) was added and dispersed in THF (30 mL). The mixture was cooled to -78°C and ^{n}BuLi (1.776 M, 3.2 mL, 5.683 mmol) was added dropwise and the yellow solution stirred for 10 minutes. The reaction vessel was warmed in ambient air for 10 minutes, then re-cooled to -78°C for another 10 minutes. [W(CO)$_6$] (1.760 g, 5.001 mmol) was added and after stirring for 15 minutes, the dark green mixture was warmed to room temperature and stirred for 1 h. The resulting brown mixture was cooled to -78°C and trifluoroacetic anhydride (0.7 mL, 5.036 mmol) added dropwise. The brown/black mixture was stirred for 15 minutes and then the reaction vessel was warmed in ambient air for 30 minutes. During this time carbon monoxide gas was evolved from the reaction mixture as it warmed. Once re-cooled to -78°C Na[Tm] (1.875 g, 5.009 mmol) was added to the rapidly stirred mixture which was allowed to slowly warm to room temperature overnight. Stirring of the red/brown reaction mixture was halted after 16 h and concentrated to afford a red/brown residue. All residues were re-dissolved in CH_2Cl_2 and filtered through a short pad of diatomaceous earth. The resulting filtrate was concentrated to dryness, dissolved in minimal CH_2Cl_2 and purified *via* silica-gel flash column chromatography (Eluent: 2% (v/v) THF/CH_2Cl_2). Collection and subsequent concentration of the major initial red/brown band afforded **2.5** as a red/brown powder. Yield 231 mg (7%).

IR (CH_2Cl_2): ν_{BH} 2412 w; ν_{CO} 1979 vs, 1890 vs cm^{-1}. NMR ^{1}H (CD_2Cl_2, 24.55°C, 700.03 MHz): δ 7.45 (br d, $^3J_{HH}$ 7.6 Hz, 2 H, C_6H_5), 7.34 (br t, $^3J_{HH}$ 7.5 Hz, 1 H, C_6H_5), 7.27 (br t, $^3J_{HH}$ 7.7 Hz, 2 H, C_6H_5), 6.94 (d, $^3J_{HH}$ 2.1 Hz, 1 H, mtCH), 6.92 (d, $^3J_{HH}$ 2.1 Hz, 1 H, mtCH), 6.87 (m, 2 H, mtCH), 6.84 (d, $^3J_{HH}$ 2.1 Hz, 1 H, mtCH), 6.81 (d, $^3J_{HH}$ 2.1 Hz, 1H, mtCH), 3.75 (s, 3 H, mtCH$_3$), 3.69 (s, 3 H, mtCH$_3$), 3.56 (s, 3 H, mtCH$_3$). ^{11}B{^{1}H} ($CDCl_3$, 24.85°C, 128.38 MHz): δ -1.78. ^{13}C{^{1}H} (CD_2Cl_2, 25.45°C, 176.05 MHz): δ 246.8 (W≡C$^\alpha$), 225.4, 220.6 (WCO), 160.6, 158.8, 158.3 (mtCS), 132.4, 128.8, 128.5 (C_6H_5), 123.5, 123.4, 123.3 (mtCH), 123.0 (C_6H_5), 120.6, 120.5, 120.4 (mtCH), 107.3 (WC$^\beta$), 74.8 (WC$^\gamma$), 68.2 (C_6H_5), 35.2, 35.0, 34.9 (mtCH$_3$), 26.0 (C_6H_5). MS (ESI, high resolution): *m*/*z* (%) = [M-(CO)]$^+$ 677.0620; [M-2(CO)]$^+$ 649.0668. Anal. Calcd. for $C_{22}H_{21}{}^{11}B_1N_6O_1S_3{}^{184}W_1$: [M-(CO)]$^+$ 677.0614; Anal. Calcd. for $C_{21}H_{21}{}^{11}B_1N_6S_3{}^{184}W_1$: [M-2(CO)]$^+$ 649.0665. Elemental Anal. Found: C, 40.78; H, 3.63; N, 10.40; S, 12.13%. Calcd. for $C_{23}H_{21}BN_6O_2S_3W\cdot C_4H_8O$: C, 41.77; H, 3.76; N, 10.82; S, 12.39%.

A crystal suitable for structure determination was grown by vapour diffusion of petroleum spirit (40-60°C) into a CH_2Cl_2 solution at 4°C (**Figure 5.3**). Crystal Data for

$C_{23}H_{21}BN_6O_2S_3W$ (M =704.30 g/mol): monoclinic, space group $P2_1/c$ (no. 14), a = 9.6170(2) Å, b = 17.7851(3) Å, c = 17.4575(3) Å, β = 105.196(2)°, V = 2881.51(10) Å^3, Z = 4, T = 150.01(10) K, μ(CuKα) = 9.714 mm^{-1}, $Dcalc$ = 1.623 g/cm^3, 5876 reflections measured (7.228° ≤ 2Θ ≤ 133.188°), 4308 unique (R_{int} = 0.0185, R_{sigma} = 0.0343) which were used in all calculations. The final R_1 was 0.0297 (I > 2σ(I)) and wR_2 was 0.0763 (all data) for 328 refined parameters with 0 restraints.

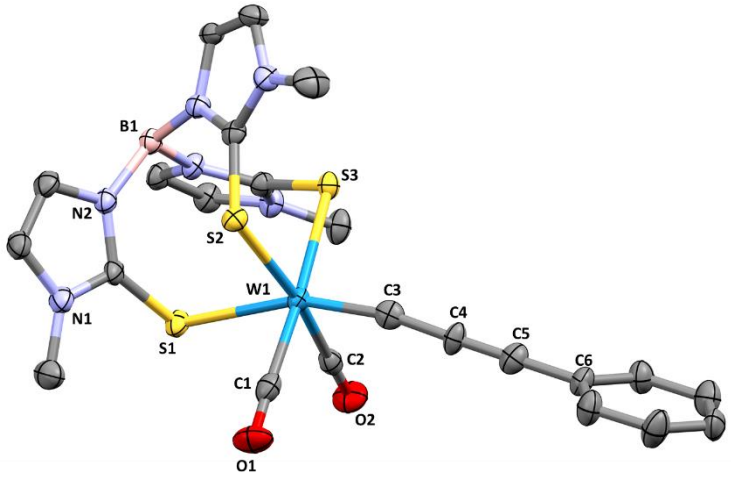

Figure 5.3. Molecular structure of **2.5** (50% displacement ellipsoids) with selected atom labels. Hydrogen atoms omitted for clarity. Selected bond lengths (Å) and angles (°): W1–C1 1.999(6), W1–C2 1.992(5), W1–S1 2.6337(11), W1–S2 2.5353(11), W1–S3 2.5788(11), W1–C3 1.856(5), C3–C4 1.356(7), C4–C5 1.222(7), C5–C6 1.437(7); W1–C3–C4 168.6(4), C3–C4–C5 178.3(6).

[TmW(CO)$_2$I(≡CC≡CSiMe$_3$)][I$_3$] (2.6)

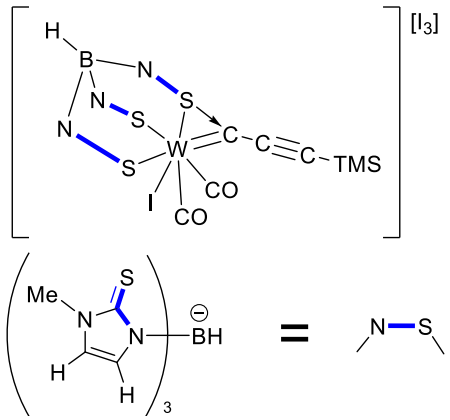

To a 100 mL round-bottom flask, [TmW(CO)$_2$(≡CC≡CSiMe$_3$)] (**2.1**: 200 mg, 0.286 mmol) was dissolved in CH_2Cl_2 (30 mL) under aerobic conditions. Solid iodine (164 mg, 0.646 mmol) was added to the red mixture and stirred at room temperature for 5 minutes. During this time, the mixture underwent two changes in colour: (i) from red to green, (ii) from green to brown. The brown reaction mixture was concentrated to dryness to afford a brown residue. To remove any remaining unreacted iodine *n*-hexane (15 mL) was added and the flask sonicated for approximately 10 seconds, ensuring that the flask was turned whilst in the ultrasonic bath to allow all residues to come into contact with the solvent. After allowing the subsequent mixture to settle for approximately 30 seconds, the pink supernatant fluid was decanted *via* a Pasteur pipette and this process repeated twice

more. Once dried under high vacuum, this afforded **2.6** as a brown powder. Yield 208 mg (57%).

IR (CH_2Cl_2): ν_{BH} 2472 w; ν_{CO} 2050 vs, 1990 vs cm^{-1}. NMR ^1H ($CDCl_3$, 25.05°C, 699.90 MHz): δ 7.51 (d, $^3J_{HH}$ 2.1 Hz, 1 H, mtCH), 7.33 (br s, 1 H, mtCH), 7.27 (br s, 1 H, mtCH), 7.13 (d, $^3J_{HH}$ 2.1 Hz, 1 H, mtCH), 7.10 (d, $^3J_{HH}$ 2.1 Hz, 1 H, mtCH), 7.04 (d, $^3J_{HH}$ 2.1 Hz, 1 H, mtCH), 4.16 (s, 3 H, $mtCH_3$), 3.85 (s, 3 H, $mtCH_3$), 3.81 (s, 3 H, $mtCH_3$), 0.29 (s, 9 H, $Si(CH_3)_3$). $^{11}B\{^1H\}$ ($CDCl_3$, 24.85°C, 128.38 MHz): δ -1.15. $^{13}C\{^1H\}$ ($CDCl_3$, 25.05°C, 176.02 MHz): δ 203.3, 198.9 (WCO), 186.5 ($W{\equiv}C^{\alpha}$), 158.1, 157.0, 140.5 (mtCS), 127.9, 126.9 (mtCH), 126.6 (WC^{β}), 126.4, 124.6, 122.5, 122.1 (mtCH), 110.9 (WC^{γ}), 39.8, 36.2, 35.8 ($mtCH_3$), 2.1, -0.7 ($Si(CH_3)_3$). MS (ESI, high resolution): m/z (%) = $[M]^+$ 826.9617. Anal. Calcd. for $C_{20}H_{25}{}^{11}B_1{}^{127}I_1N_6O_2S_3Si_1{}^{184}W_1$: $[M]^+$ 826.9617. Elemental Anal. Found: C, 17.60; H, 2.10; N, 6.45; S, 7.42%. Calcd. for $C_{20}H_{25}BI_4N_6O_2S_3SiW{\cdot}CH_2Cl_2$: C, 19.51; H, 2.10; N, 6.50; S, 7.44%.

A crystal suitable for structure determination was grown by vapour diffusion of petroleum spirit (40-60°C) into a CH_2Cl_2 solution at 4°C (**Figure 5.4**).

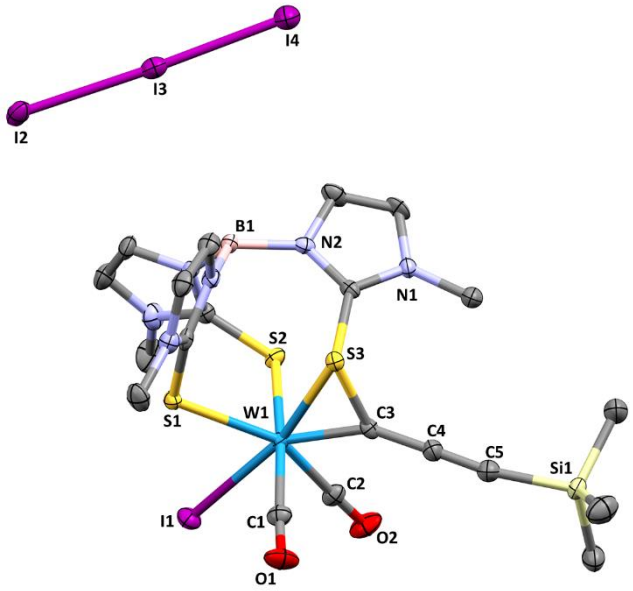

Figure 5.4. Molecular structure of **2.6** (50% displacement ellipsoids) with selected atom labels. Solvent molecules and hydrogen atoms omitted for clarity. Selected bond lengths (Å) and angles (°): W1–I1 2.8028(4), W1–C1 2.040(5), W1–C2 1.999(5), W1–S1 2.5568(12), W1–S2 2.5002(11), W1–S3 2.4922(11), W1–C3 1.951(4), C3–C4 1.381(6), C4–C5 1.219(7), C5–Si1 1.852(5); W1–S3–C3 51.10(14), W1–C3–C4 149.7(4), C3–C4–C5 176.8(6).

The crystal was found to contain one equivalent of CH_2Cl_2 of solvation, which was modelled across one site in the asymmetric unit. Crystal Data for $C_{21}H_{27}BCl_2I_4N_6O_2S_3SiW$

(M =1292.91 g/mol): monoclinic, space group $P2_1/c$ (no. 14), a = 20.1958(10) Å, b = 11.0262(3) Å, c = 19.5454(9) Å, β = 118.116(6)°, V = 3838.8(3) Å^3, Z = 4, T = 150.00(10) K, μ(MoKα) = 6.588 mm^{-1}, $Dcalc$ = 2.237 g/cm^3, 36288 reflections measured (7.098° ≤ 2Θ ≤ 60.182°), 9319 unique (R_{int} = 0.0384, R_{sigma} = 0.0388) which were used in all calculations. The final R_1 was 0.0307 (I > 2σ(I)) and wR_2 was 0.0689 (all data) for 376 refined parameters with 0 restraints.

TmW(CO)$_2${μ-≡CC≡C}(Au(PPh$_3$)) (2.7)

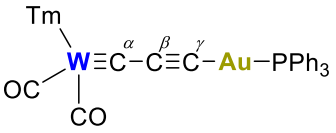

To a 50 mL round-bottom flask, [TmW(CO)$_2$(≡CC≡CSiMe$_3$)] (**2.1**: 101 mg, 0.144 mmol) and [AuCl(PPh$_3$)] (73 mg, 0.148 mmol) were added and dissolved in CH_2Cl_2 (20 mL) under aerobic conditions. Slowly, and with constant stirring, tetrabutylammonium fluoride (1.0 M in THF, 0.3 mL, 0.300 mmol) was added and the mixture stirred at room temperature for 15 minutes. The reaction mixture was combined with ethanol (20 mL) in a 50 mL round bottom flask and slowly evaporated to afford a precipitate. The precipitate was isolated *via* vacuum filtration and washed with ethanol, then *n*-pentane which afforded **2.7** as an orange powder. Yield 88 mg (56%).

IR (CH_2Cl_2): ν_{BH} 2434 w; ν_{CO} 1965 m, 1877 m cm^{-1}. NMR ^{1}H ($CDCl_3$, 24.85°C, 400.13 MHz): δ 7.53-7.43 (m, 15 H, P(C_6H_5)$_3$), 6.85 (br s, 2 H, mtCH), 6.78 (br s, 3 H, mtCH), 6.75 (m, 1 H, mtCH), 3.74 (s, 3 H, mtCH$_3$), 3.72 (s, 3 H, mtCH$_3$), 3.56 (s, 3 H, mtCH$_3$). ^{11}B{^{1}H} ($CDCl_3$, 24.85°C, 128.38 MHz): δ -1.47. ^{31}P ($CDCl_3$, 24.85°C, 161.97 MHz): δ 42.3. A ^{13}C{^{1}H} NMR of this complex could not be obtained due to its tendency to precipitate out of deuterated solvents over several hours. MS (ESI, high resolution): m/z (%) = [M+H]$^+$ 1087.0752. Anal. Calcd. for $C_{35}H_{32}{}^{197}Au_1{}^{11}B_1N_6O_2P_1S_3{}^{184}W_1$: [M+H]$^+$ 1087.0754. Elemental Anal. Found: C, 35.07; H, 2.88; N, 7.38; S, 8.38%. Calcd. for $C_{35}H_{31}AuBN_6O_2PS_3W\cdot CH_2Cl_2$: C, 36.91; H, 2.84; N, 7.17; S, 8.21%.

TmW(CO)$_2${μ-≡CC≡C}(Rh(CO)(PPh$_3$)$_2$) (2.8)

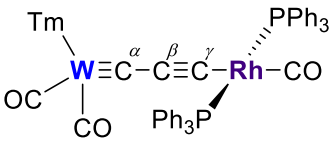

To a 100 mL Schlenk tube, [TmW(CO)$_2$(≡CC≡CSiMe$_3$)] (**2.1**: 0.100 g, 0.143 mmol) and *trans*-[RhCl(CO)(PPh$_3$)$_2$] (0.098 g, 0.142 mmol) were added and dispersed in CH_2Cl_2 (40 mL). To this cherry-red mixture, tetrabutylammonium fluoride (1.0 M in THF, 0.3 mL, 0.300 mmol) was added slowly dropwise and the subsequent brown solution was stirred at room temperature for 30 minutes. The reaction mixture was

combined with ethanol (15 mL) in a 100 mL round bottom flask and slowly evaporated to afford a brown precipitate. The precipitate was isolated *via* vacuum filtration and washed with ethanol, then *n*-pentane which afforded **2.8** as a brown powder. Yield 72 mg (40%).

IR (CH_2Cl_2): ν_{CO} 1973 m, 1940 m, 1863 m cm^{-1}. NMR ^1H (CD_2Cl_2, 26.85°C, 400.13 MHz): δ 7.70 (br m, 15 H, PPh_3), 7.41 (br m, 15 H, PPh_3), 6.80 (d, $^3J_{HH}$ 2.0 Hz, 1 H, mtCH), 6.79-6.78 (m, 2 H, mtCH), 6.76 (d, $^3J_{HH}$ 2.0 Hz, 1 H, mtCH), 6.73 (br m, 2 H, mtCH), 3.66 (s, 3 H, $mtCH_3$), 3.48 (s, 3 H, $mtCH_3$), 3.03 (s, 3 H, $mtCH_3$). ^1H (CD_2Cl_2, 24.95°C, 699.90 MHz: δ 7.69 (br s, 15 H, PPh_3), 7.41 (m, 15 H, PPh_3), 6.81 (d, $^3J_{HH}$ 2.1 Hz, 1 H, mtCH), 6.79 (d, $^3J_{HH}$ 2.1 Hz, 1 H, mtCH), 6.78 (d, $^3J_{HH}$ 2.1 Hz, 1 H, mtCH), 6.76 (d, $^3J_{HH}$ 2.1 Hz, 1 H, mtCH), 6.73 (d, $^3J_{HH}$ 2.1 Hz, 2 H, mtCH), 3.67 (s, 3 H, $mtCH_3$), 3.48 (s, 3 H, $mtCH_3$), 3.04 (s, 3 H, $mtCH_3$). $^{31}P\{^1H\}$ (CD_2Cl_2, 26.85°C, 161.97 MHz): δ 30.5, 29.9 (d, $^1J_{PRh}$ 84.5 Hz, PPh_3). $^{13}C\{^1H\}$ (CD_2Cl_2, 25.05°C, 176.02 MHz): δ 253.7 ($W{\equiv}C^{\alpha}$), 226.6, 222.3 (WCO), 161.7, 160.2, 159.6 (mtCS), 150.4, 143.3, 143.2 ($P(C_6H_5)_3$), 134.8 (WC^{γ}), 132.4, 132.3 (2C), 132.2, 130.2, 128.9, 128.8 ($P(C_6H_5)_3$), 128.5 (WC^{β}), 122.8 (2C), 120.0, 119.9, 119.8 (mtCH), 34.9, 34.8 (2C) ($mtCH_3$). MS (ESI, high resolution): m/z (%) = $[M]^+$ 1282.0947. Anal. Calcd. for $C_{54}H_{46}{}^{11}B_1N_6O_3P_2{}^{103}Rh_1S_3{}^{184}W_1$: $[M]^+$ 1282.0926. After numerous attempts an agreeable elemental microanalysis could not be obtained.

A crystal suitable for structure determination was grown by vapour diffusion of *n*-hexane into a CH_2Cl_2 solution at 4°C (**Figure 5.5**). Crystal Data for $C_{54}H_{46}BN_6O_3P_2RhS_3W$ (M =1283.17 g/mol): triclinic, space group P-1 (no. 2), a = 11.7310(6) Å, b = 15.1450(10) Å, c = 18.6729(10) Å, α = 77.083(5)°, β = 72.796(5)°, γ = 75.188(5)°, V = 3024.2(3) $Å^3$, Z = 2, T = 150.00(10) K, μ(CuKα) = 7.493 mm^{-1}, $Dcalc$ = 1.409 g/cm^3, 5831 reflections measured (7.266° ≤ 2Θ ≤ 140.92°), 4444 unique (R_{int} = 0.0307, R_{sigma} = 0.0484) which were used in all calculations. The final R_1 was 0.0418 (I > 2σ(I)) and wR_2 was 0.1064 (all data) for 464 refined parameters with 0 restraints.

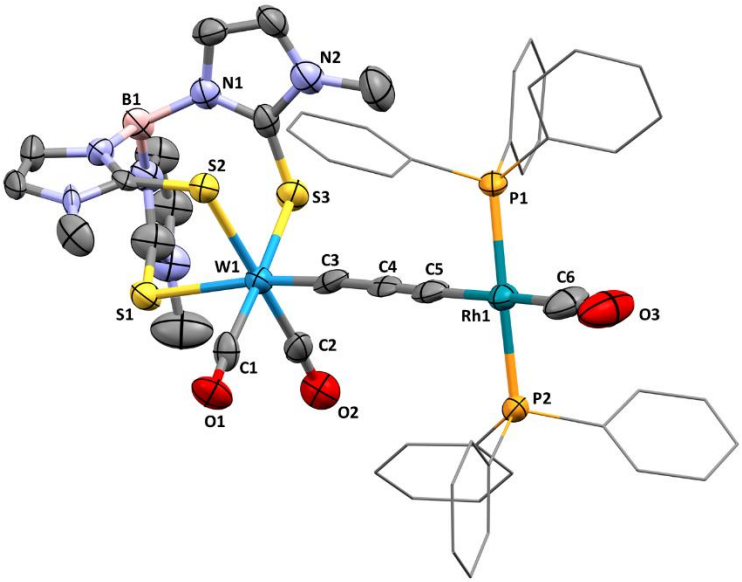

Figure 5.5. Molecular structure of **2.8** (50% displacement ellipsoids) with selected atom labels. Solvent molecules and hydrogen atoms omitted, and phenyl rings have been simplified for clarity. Selected bond lengths (Å) and angles (°): W1–C1 1.995(10), W1–C2 1.914(14), W1–S1 2.663(3), W1–S2 2.577(3), W1–S3 2.542(2), W1–C3 1.800(13), C3–C4 1.406(16), C4–C5 1.251(15), C5–Rh1 1.982(14), Rh1–C6 1.806(16), Rh1–P1 2.303(2), Rh1–P2 2.304(3); W1–C3–C4 174.9(8), C3–C4–C5 178.0(12), C4–C5–Rh1 178.4(8), C5–Rh1–P1 84.7(3), C5–Rh1–P2 91.5(3), C5–Rh1–C6 176.9(6).

5.2.3 Chapter 3 – Polycyclic Aromatic Hydrocarbon-containing Carbynes

BmW(CO)$_2${≡C-(Mesityl)} (3.1)

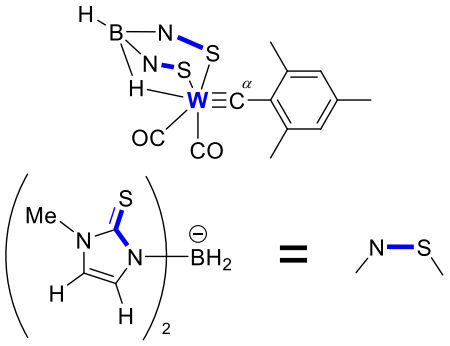

To a 100 mL Schlenk tube, [Br(pic)$_2$(CO)$_2$W≡C(Mes)] (99 mg, 0.144 mmol) and Na[Bm] (39 mg, 0.149 mmol) were added, dispersed in CH_2Cl_2 (20 mL), and the bright orange mixture stirred at room temperature for 3 h. The reaction mixture was concentrated to dryness and the orange residues were subjected to silica-gel column chromatography (Eluent: CH_2Cl_2), where isolation and concentration of the major orange band which moved off the baseline afforded **3.1** as an orange residue. Yield 51 mg (58%).

IR (CH_2Cl_2): ν_{BH} 2437 w; ν_{CO} 1986 vs, 1904 vs cm^{-1}. NMR ^{1}H ($CDCl_3$, 24.85°C, 400.15 MHz): δ 6.80 (s, 2 H, MesCH), 6.76 (s, 2 H, mtCH), 6.70 (s, 2 H, mtCH), 3.56 (s, 6 H,

mtCH$_3$), 2.49 (s, 6 H, MesCH$_3$), 2.17 (s, 3 H, MesCH$_3$), -2.49 (br, 1 H, BHW). ^{1}H (CD_2Cl_2, 25.05°C, 700.03 MHz): δ 6.86 (s, 2 H, MesCH), 6.82 (s, 2 H, mtCH), 6.72 (s, 2 H, mtCH), 3.55-3.54 (m, 6 H, mtCH$_3$), 2.44 (s, 6 H, MesCH$_3$), 2.17 (s, 3 H, MesCH$_3$), -2.50 (br, 1 H, BHW). ^{11}B{^{1}H} ($CDCl_3$, 24.85°C, 128.38 MHz): δ 42.55. A ^{13}C{^{1}H} NMR of this complex could not be obtained due to its tendency to precipitate out of deuterated solvents over several hours. MS (ESI, high resolution): *m*/*z* (%) = $[M+H]^+$ 611.0941. Calcd. for $C_{20}H_{24}{}^{11}B_1N_4O_2S_2{}^{184}W_1$: $[M+H]^+$ 611.0943. Elemental Anal. Found: C, 39.31; H, 3.79; N, 9.39; S, 10.61%. Calcd. for $C_{20}H_{23}BN_4O_2S_2W$: C, 39.97; H, 3.80; N, 9.18; S, 10.51%.

TmW(CO)$_2${≡C-(Mesityl)} (3.2)

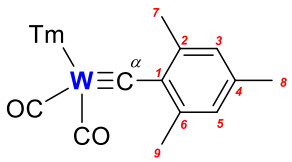

To a 100 mL Schlenk tube, [Br(pic)$_2$(CO)$_2$W≡C(Mes)] (102 mg, 0.149 mmol) and Na[Tm] (56 mg, 0.150 mmol) were added, dispersed in CH_2Cl_2 (20 mL), and the bright orange mixture stirred at room temperature for 3 h. The reaction mixture was concentrated to dryness and the orange residues were subjected to silica-gel column chromatography (Eluent: CH_2Cl_2), where isolation and concentration of the major orange band which moved off the baseline afforded **3.2** as an orange residue. Yield 76 mg (70%).

IR (CH_2Cl_2): ν_{BH} 2431 w; ν_{CO} 1966 vs, 1874 vs cm^{-1}. NMR ^{1}H ($CDCl_3$, 25.05°C, 700.03 MHz): δ 6.89 (d, $^3J_{HH}$ 2.0 Hz, 1 H, mtCH), 6.84 (d, $^3J_{HH}$ 2.0 Hz, 1 H, mtCH), 6.83 (d, $^3J_{HH}$ 2.0 Hz, 1 H, mtCH), 6.80 (d, $^3J_{HH}$ 2.1 Hz, 2 H, mtCH), 6.77 (d, $^3J_{HH}$ 2.0 Hz, 1 H, mtCH), 6.69 (s, 2 H, MesCH), 3.77 (s, 3 H, mtCH$_3$), 3.63 (s, 3 H, mtCH$_3$), 3.62 (s, 3 H, mtCH$_3$), 2.56 (s, 6 H, MesCH$_3$), 2.16 (MesCH$_3$). ^{11}B{^{1}H} ($CDCl_3$, 24.85°C, 128.38 MHz): δ 48.32. ^{13}C{^{1}H} ($CDCl_3$, 25.05°C, 176.05 MHz): δ 284.1 (W≡C$^\alpha$, $^1J_{WC}$ 196.5 Hz), 225.4 (WCO, $^1J_{WC}$ 173.7 Hz), 220.9 (WCO, $^1J_{WC}$ 168.9 Hz), 160.9, 159.5, 159.4 (mtCS), 145.2 (C^1[C_9H_{11}], $^2J_{WC}$ 39.4 Hz), 140.5 (C^3[C_9H_{11}]), 136.7 (C^5[C_9H_{11}]), 127.7 (3C) (C^{2,4,6}[C_9H_{11}]) , 123.1, 122.8, 122.5, 119.9 (2C), 119.8 (mtCH), 34.9, 34.8 (2C) (mtCH$_3$), 21.6 (C^8[C_9H_{11}]), 20.8 (2C) (C^{7,9}[C_9H_{11}]). MS (ESI, high resolution): *m*/*z* (%) = $[M]^+$ 722.0971; $[M-CO]^+$ 694.1017; $[M-2(CO)]^+$ 666.1066. Calcd. for $C_{24}H_{27}{}^{11}B_1N_6O_2S_3{}^{184}W_1$: $[M]^+$ 722.0960; Calcd. for $C_{23}H_{27}{}^{11}B_1N_6O_1S_3{}^{184}W_1$: $[M-CO]^+$ 694.1011; Calcd. for $C_{22}H_{27}{}^{11}B_1N_6S_3{}^{184}W_1$: $[M-2(CO)]^+$ 666.1062. Elemental Anal. Found: C, 39.89; H, 3.54; N, 11.65; S, 13.06%. Calcd. for $C_{24}H_{27}BN_6O_2S_3W$: C, 39.91; H, 3.77; N, 11.63; S, 13.32%.

(Hbt)W(CO)$_2${≡C-(Mesityl)} (3.3)

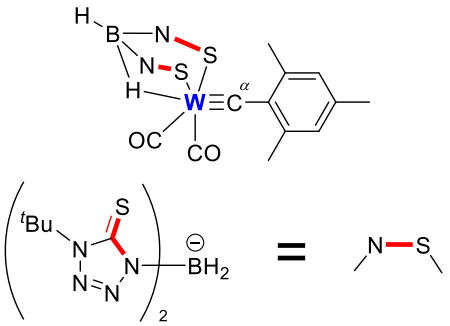

In a flame dried 100 mL Schlenk tube [Br(pic)$_2$(CO)$_2$W≡C-Mes] (203 mg, 0.296 mmol) and Na[Hbt] (104 mg, 0.297 mmol) were dispersed in CH_2Cl_2 (40 mL) and stirred at room temperature for 12 h. the bright orange reaction mixture was concentrated to dryness and purified *via* silica-gel column chromatography (Eluent: CH_2Cl_2). The single brown band which moved off the baseline was collected and concentrated to dryness to provide **3.3** as a brown residue. Yield 65 mg (31%).

IR (CH_2Cl_2): ν_{CO} 1996 vs, 1917 vs cm^{-1}. NMR ^{1}H ($CDCl_3$, 24.85°C, 400.13 MHz): δ 6.75 (s, 2 H, MesCH), 2.51 (s, 6 H, MesCH$_3$), 2.20 (s, 3 H, MesCH$_3$), 1.81 (s, 18 H, C(CH$_3$)$_3$), -2.24 (br, 1 H, BHW). ^{11}B{^{1}H} ($CDCl_3$, 24.85°C, 128.38 MHz): δ -10.25. A ^{13}C{^{1}H} NMR of this complex could not be obtained due to its tendency to precipitate out of deuterated solvents over several hours. MS (ESI, high resolution): *m/z* (%) = [M+H]$^+$ 699.1682. Calcd. for $C_{22}H_{32}{}^{11}B_1N_8O_2{}^{23}Na_1S_2{}^{184}W_1$: [M+H]$^+$ 699.1692. Elemental Anal. Found: C, 37.90; H, 4.44; N, 15.94; S, 8.85%. Calcd. for $C_{22}H_{31}BN_8O_2S_2W$: C, 37.84; H, 4.47; N, 16.05; S, 9.18%.

(Htt)W(CO)$_2${≡C-(Mesityl)} (3.4)

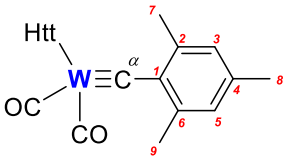

To a 100 mL Schlenk tube, [Br(pic)$_2$(CO)$_2$W≡C-Mes] (202 mg, 0.295 mmol) and Na[Htt] (149 mg, 0.294 mmol) were dispersed in CH_2Cl_2 (40 mL) and stirred at RT for 12 h. the bright orange reaction mixture was concentrated to dryness and purified *via* column chromatography, using neutral alumina as the stationary phase (Eluent: CH_2Cl_2). The major bright orange band which moved off the baseline was collected and concentrated to dryness to provide **3.4** as a vivid orange powder. Yield 86 mg (34%).

IR (CH_2Cl_2): ν_{BH} 2529; ν_{CO} 1980 vs, 1893 vs cm^{-1}. NMR ^{1}H ($CDCl_3$, 24.95°C, 700.03 MHz): δ 6.70 (s, 2 H, MesCH), 2.61 (s, 6 H, MesCH$_3$), 2.19 (s, 3 H, MesCH$_3$), 1.94 (s, 9 H, C(CH$_3$)$_3$), 1.86 (s, 9 H, C(CH$_3$)$_3$), 1.79 (s, 9 H, C(CH$_3$)$_3$). ^{11}B{^{1}H} ($CDCl_3$, 24.85°C, 128.38 MHz): δ -2.75. ^{13}C{^{1}H} ($CDCl_3$, 24.95°C, 176.05 MHz) δ 287.5 (W≡C$^\alpha$, $^1J_{WC}$ 193.6 Hz), 220.2 (WCO, $^1J_{WC}$ 175.4 Hz), 216.8 (WCO, $^1J_{WC}$ 172.2 Hz), 166.8, 164.4, 164.2 (C=S), 144.0 (C^1[C$_9$H$_{11}$], $^2J_{WC}$ 38.0 Hz), 141.2 (C^2[C$_9$H$_{11}$]), 138.6 (C^6[C$_9$H$_{11}$]), 127.9 (C^4[C$_9$H$_{11}$]), 65.1, 64.9 (C^{3,5}[C$_9$H$_{11}$]), 28.7, 28.6, 28.3 (C(*C*H$_3$)$_3$), 21.7 (C^8[C$_9$H$_{11}$]), 20.4 (2C) (C^{7,9}[C$_9$H$_{11}$]). MS (ESI,

high resolution): m/z (%) = $[M+Na]^+$ 877.1972. Calcd. for $C_{27}H_{39}{}^{11}B_1N_{12}{}^{23}Na_1O_2S_3{}^{184}W_1$ $[M+Na]^+$: 877.1981. Elemental Anal. Found: C, 37.94; H, 4.57; N, 19.41; S, 10.97%. Calcd. for $C_{27}H_{39}BN_{12}O_2S_3W$: C, 37.95; H, 4.60; N, 19.67; S, 11.26%.

TmW(CO)$_2${≡C-(Thienyl)} (3.5)

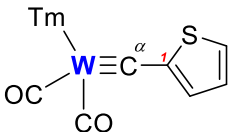

To a 100 mL round-bottom flask, thiophene (0.24 mL, 2.998 mmol) was added and dispersed in THF (10 mL). The mixture was cooled to -78°C and ^{n}BuLi (1.6 M, 2.0 mL, 3.200 mmol) was added dropwise, then the mixture stirred for 10 minutes. The reaction vessel was warmed to 0°C for 4 h to promote the formation of 2-thienyllithium, then re-cooled to -78°C. Separately, to a 100 mL Schlenk tube, $[W(CO)_6]$ (1.002 g, 2.847 mmol) was added and dispersed in THF (40 mL). The colourless mixture was cooled to -78°C and the freshly prepared 2-thienyllithium solution was added dropwise and the mixture stirred for 15 minutes, then warmed in ambient air for 30 minutes. The resulting dark red mixture was re-cooled to -78°C and trifluoroacetic anhydride (0.40 mL, 2.878 mmol) added dropwise. The purple mixture was stirred for 15 minutes and warmed in ambient air for 30 minutes. During this time carbon monoxide was evolved as the reaction mixture warmed. Once re-cooled to -78°C, Na[Tm] (1.090 g, 2.912 mmol) was added to the rapidly stirred mixture and slowly warmed to room temperature overnight. Stirring of the brown reaction mixture was halted after 16 h and concentrated to afford a brown residue. The crude product mixture was purified *via* silica-gel flash column chromatography (Eluent: 8:2 (v/v) CH_2Cl_2/Petroleum spirit 40-60°C). Collection and subsequent concentration of the major red band afforded **3.5** as a bright red powder. Yield 436 mg (22%).

IR (CH_2Cl_2): ν_{CO} 1970 vs, 1880 vs cm^{-1}. NMR ^1H ($CDCl_3$, 24.85°C, 700.03 MHz): δ 7.09 (dd, $^3J_{HH}$ 5.0, 1.0 Hz, 1 H, C_4H_3S), 6.97 (dd, $^3J_{HH}$ 3.6, 1.0 Hz, 1 H, C_4H_3S), 6.87 (q, $^3J_{HH}$ 2.1 Hz, 2 H, mtCH), 6.82-6.81 (m, 4 H, mtCH), 6.79 (d, $^3J_{HH}$ 2.1 Hz, 1 H, C_4H_3S), 3.75 (s, 3 H, $mtCH_3$), 3.71 (s, 3 H, $mtCH_3$), 3.61 (s, 3 H, $mtCH_3$). $^{11}B\{^1H\}$ ($CDCl_3$, 24.85°C, 128.38 MHz): δ 48.34. $^{13}C\{^1H\}$ ($CDCl_3$, 25.05°C, 176.05 MHz): δ 264.2 ($W{\equiv}C^\alpha$, $^1J_{WC}$ 197.4 Hz), 223.7 (WCO, $^1J_{WC}$ 170.5 Hz), 218.8 (WCO, $^1J_{WC}$ 163.7 Hz), 161.2, 159.3, 158.8 (mtCS), 155.3 ($C^1[C_4H_3S]$, $^2J_{WC}$ 49.9 Hz), 128.1, 126.3, 125.5 (C_4H_3S), 122.9 (2C), 122.8, 120.1, 120.0 (2C) (mtCH), 35.0, 34.9, 34.8 ($mtCH_3$). MS (ESI, high resolution): m/z (%) = $[M-2(CO)]^+$ 630.0175; $[M+H]^+$ 687.0142; $[M+Na]^+$ 708.9962. Anal. Calcd. for $C_{17}H_{19}{}^{11}B_1N_6S_4{}^{184}W_1$: $[M-2(CO)]^+$ 630.0156. Anal. Calcd. for $C_{19}H_{20}{}^{11}B_1N_6O_2S_4{}^{184}W_1$: $[M+H]^+$ 687.0133. Anal. Calcd. for $C_{19}H_{19}{}^{11}B_1N_6{}^{23}Na_1O_2S_4{}^{184}W_1$: $[M+Na]^+$ 708.9952. Elemental Anal. Found: C, 33.06; H,

2.89; N, 11.69; S, 18.68%. Calcd. for $C_{19}H_{19}BN_6O_2S_4W$: C, 33.25; H, 2.79; N, 12.25; S, 18.69%.

TmW(CO)$_2${≡C-(1-Naphthyl)} (3.6)

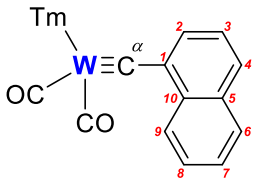

To a 100 mL Schlenk tube, 1-bromonaphthalene (503 mg, 2.429 mmol) was added and dispersed in THF (40 mL). The mixture was cooled to -78°C and ^{n}BuLi (1.6 M, 1.8 mL, 2.880 mmol) was added dropwise and the light yellow/green solution stirred for 10 minutes. The reaction vessel was warmed in ambient air for 10 minutes, then re-cooled to -78°C for another 10 minutes to afford an orange mixture. [W(CO)$_6$] (852 mg, 2.421 mmol) was added and after stirring for 15 minutes, the mixture was warmed to room temperature and stirred for 1 h. The resulting brown mixture was cooled to -78°C and trifluoroacetic anhydride (0.35 mL, 2.518 mmol) added dropwise. The dark red mixture was stirred for 15 minutes and then the reaction vessel was warmed in ambient air for 45 minutes. During this time carbon monoxide gas was evolved from the reaction mixture as it warmed. Once re-cooled to -78°C Na[Tm] (906 mg, 2.421 mmol) was added to the rapidly stirred mixture which was allowed to slowly warm to room temperature overnight. Stirring of the red reaction mixture was halted after 16 h and concentrated to afford a red/brown residue. The crude product mixture was purified *via* silica-gel flash column chromatography (Eluent: CH_2Cl_2). Collection and subsequent concentration of the major red band afforded **3.6** as a cherry red powder. Yield 1.04 g (59%).

IR (CH_2Cl_2): ν_{BH} 2435 w; ν_{CO} 1970 vs, 1879 vs cm^{-1}. NMR ^{1}H ($CDCl_3$, 24.85°C, 700.03 MHz): δ 8.87 (d, $^3J_{HH}$ 8.3 Hz, 1 H, $C_{10}H_7$), 7.76 (d, $^3J_{HH}$ 8.1 Hz, 1 H, $C_{10}H_7$), 7.71 (d, $^3J_{HH}$ 8.1 Hz, 1 H, $C_{10}H_7$), 7.51-7.50 (m, 1 H, $C_{10}H_7$), 7.48-7.46 (m, 1 H, $C_{10}H_7$), 7.41-7.40 (m, 1 H, $C_{10}H_7$), 7.33-7.30 (m, 1 H, $C_{10}H_7$), 6.91 (d, $^3J_{HH}$ 2.0 Hz, 1 H, mtCH), 6.87 (d, $^3J_{HH}$ 2.0 Hz, 1 H, mtCH), 6.84 (d, $^3J_{HH}$ 2.1 Hz, 1 H, mtCH), 6.83 (d, $^3J_{HH}$ 2.1 Hz, 1 H, mtCH), 6.83 (d, $^3J_{HH}$ 2.1 Hz, 1 H, mtCH), 6.82 (d, $^3J_{HH}$ 2.1 Hz, 1 H, mtCH), 3.80 (s, 3 H, mtCH$_3$), 3.65 (s, 3 H, mtCH$_3$), 3.64 (s, 3 H, mtCH$_3$). ^{11}B{^{1}H} ($CDCl_3$, 24.85°C, 128.38 MHz): δ 48.44. ^{13}C{^{1}H} ($CDCl_3$, 24.85°C, 176.05 MHz) δ 279.5 (W≡C$^\alpha$, $^1J_{WC}$ 192.6 Hz), 223.8 (WCO, $^1J_{WC}$ 171.4 Hz), 219.2 (WCO, $^1J_{WC}$ 165.2 Hz), 161.0, 159.2 (2C) (mtCS), 146.9 (C^1[$C_{10}H_7$], $^2J_{WC}$ 41.7 Hz), 133.3 (C^{10}[$C_{10}H_7$]), 132.8 (C^5[$C_{10}H_7$]), 128.7 (C^9[$C_{10}H_7$]), 127.9 (C^6[$C_{10}H_7$]), 126.9 (2C) (C^{2,3}[$C_{10}H_7$]), 126.1 (C^8[$C_{10}H_7$]), 126.0 (C^7[$C_{10}H_7$]), 125.4 (C^4[$C_{10}H_7$]), 123.1, 122.9, 122.7, 120.1, 120.0 (2C) (mtCH), 35.0, 34.9, 34.8 (mtCH$_3$). MS (ESI, high resolution): *m*/*z* (%) = $[M+H]^+$ 731.0724; $[M+Na]^+$ 753.0554. Anal. Calcd. for $C_{25}H_{24}{}^{11}B_1N_6O_2S_3{}^{184}W_1$: $[M+H]^+$ 731.0725; Anal. Calcd.

for $C_{25}H_{23}{}^{11}B_1N_6{}^{23}Na_1O_2S_3{}^{184}W_1$: $[M+Na]^+$ 753.0545. Elemental Anal. Found: C, 41.11; H, 3.25; N, 10.82; S, 12.11%. Calcd. for $C_{25}H_{23}BN_6O_2S_3W$: C, 41.11; H, 3.17; N, 11.51; S, 13.17%.

TmMo(CO)$_2${≡C-(1-Naphthyl)} (3.7)

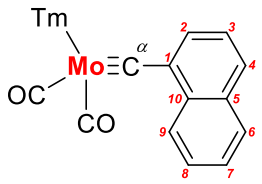

To a 100 mL Schlenk tube, 1-bromonaphthalene (0.34 mL, 2.429 mmol) was added and dispersed in THF (40 mL). The mixture was cooled to -78°C and ^{n}BuLi (1.6 M, 1.8 mL, 2.880 mmol) was added dropwise and the light yellow/green mixture stirred for 10 minutes. The reaction vessel was warmed in ambient air for 10 minutes then re-cooled to -78°C for a further 10 minutes to afford an orange mixture. $[Mo(CO)_6]$ (640 mg, 2.424 mmol) was added and after stirring for 15 minutes, the mixture was warmed to room temperature for 1 h. The resulting mixture was re-cooled to -78°C and trifluoroacetic anhydride (0.35 mL, 2.518 mmol) added dropwise. The green mixture was stirred for 15 minutes and warmed in ambient air for 30 minutes. During this time carbon monoxide was evolved as the reaction mixture warmed. Once re-cooled to -78°C, Na[Tm] (907 mg, 2.423 mmol) was added to the rapidly stirred mixture and slowly warmed to room temperature overnight. Stirring of the red reaction mixture was halted after 16 h and concentrated to afford a red/brown residue. The crude product mixture was purified *via* silica-gel flash column chromatography (Eluent: CH_2Cl_2). Collection and subsequent concentration of the major red band afforded **3.7** as a cherry red powder. Yield 925 mg (80%).

IR (CH_2Cl_2): ν_{BH} 2434 m; ν_{CO} 1984 vs, 1900 vs cm^{-1}. NMR ^1H ($CDCl_3$, 25.05°C, 700.03 MHz): δ 8.96 (d, $^3J_{HH}$ 7.6 Hz, 1 H, $C_{10}H_7$), 7.76 (d, $^3J_{HH}$ 7.5 Hz, 1 H, $C_{10}H_7$), 7.69 (d, $^3J_{HH}$ 7.5 Hz, 1 H, $C_{10}H_7$), 7.60 (d, $^3J_{HH}$ 6.5 Hz, 1 H, $C_{10}H_7$), 7.50 (t, $^3J_{HH}$ 7.5 Hz, 1 H, $C_{10}H_7$), 7.43 (t, $^3J_{HH}$ 7.4 Hz, 1 H, $C_{10}H_7$), 7.32 (t, $^3J_{HH}$ 7.6 Hz, 1 H, $C_{10}H_7$), 6.89 (m, 1 H, mtCH), 6.86 (m, 1 H, mtCH), 6.84-6.79 (m, 4 H, mtCH), 3.79 (s, 3 H, $mtCH_3$), 3.64 (s, 3 H, $mtCH_3$), 3.63 (s, 3 H, $mtCH_3$). $^{11}B\{^1H\}$ ($CDCl_3$, 24.85°C, 128.38 MHz): δ 48.47. $^{13}C\{^1H\}$ ($CDCl_3$, 25.05°C, 176.05 MHz) δ 290.3 ($Mo{\equiv}C^{\alpha}$), 226.5, 222.1 (MoCO), 161.6, 159.7, 159.6 (mtCS), 143.0 ($C^1[C_{10}H_7]$), 132.9 ($C^{10}[C_{10}H_7]$), 132.6 ($C^5[C_{10}H_7]$), 128.8 ($C^9[C_{10}H_7]$), 127.7 ($C^6[C_{10}H_7]$), 127.6 ($C^2[C_{10}H_7]$), 126.6 ($C^3[C_{10}H_7]$), 126.3 ($C^8[C_{10}H_7]$), 125.9 ($C^7[C_{10}H_7]$), 125.1 ($C^4[C_{10}H_7]$), 122.8, 122.6, 122.3, 119.7 (3C) (mtCH), 34.7 (2C), 34.6 ($mtCH_3$). MS (ESI, high resolution): *m/z* (%) = $[M+Na]^+$ 667.0096. Anal. Calcd. for $C_{25}H_{23}{}^{11}B_1{}^{98}Mo_1N_6{}^{23}Na_1O_2S_3$: $[M+Na]^+$ 667.0089.

Elemental Anal. Found: C, 48.65; H, 3.83; N, 11.89; S, 13.28%. Calcd. for $C_{25}H_{23}BMoN_6O_2S_3 \cdot C_4H_8O$: C, 48.74; H, 4.37; N, 11.76; S, 13.46%.

TmW(CO)$_2${≡C-(9-Phenanthryl)} (3.8)

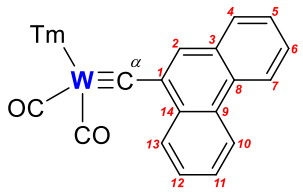

To a 100 mL Schlenk tube, 9-bromophenanthrene (503 mg, 1.956 mmol) was added and dispersed in THF (40 mL). The mixture was cooled to -78°C and ^{n}BuLi (1.6 M, 1.4 mL, 2.240 mmol) was added dropwise and the bright yellow mixture stirred for 10 minutes. The reaction vessel was warmed in ambient air for 10 minutes then re-cooled to -78°C for a further 10 minutes to afford a yellow/green mixture. [W(CO)$_6$] (687 mg, 1.952 mmol) was added and after stirring for 15 minutes, the mixture was warmed to room temperature for 1 h. The resulting mixture was re-cooled to -78°C and trifluoroacetic anhydride (0.30 mL, 2.157 mmol) added dropwise. The red/brown mixture was stirred for 15 minutes and warmed in ambient air for 30 minutes. During this time carbon monoxide was evolved as the reaction mixture warmed. Once re-cooled to -78°C, Na[Tm] (729 mg, 1.948 mmol) was added to the rapidly stirred mixture and slowly warmed to room temperature overnight. Stirring of the red/brown reaction mixture was halted after 16 h and concentrated to afford a red/brown residue. The crude product mixture was purified *via* silica-gel flash column chromatography (Eluent: CH_2Cl_2). Collection and subsequent concentration of the red band afforded **3.8** as a red residue. Yield 755 mg (50%).

IR (CH_2Cl_2): ν_{BH} 2435 w; ν_{CO} 1970 vs, 1880 vs cm^{-1}. NMR ^{1}H ($CDCl_3$, 24.85°C, 700.03 MHz): δ 9.04-9.02 (m, 1 H, $C_{14}H_9$), 8.61-8.59 (m, 1 H, $C_{14}H_9$), 8.53 (d, $^3J_{HH}$ 8.2 Hz, 1 H, $C_{14}H_9$), 7.83 (d, $^3J_{HH}$ 7.3 Hz, 1 H, $C_{14}H_9$), 7.78 (s, 1 H, $C_{14}H_9$), 7.60-7.58 (m, 3 H, $C_{14}H_9$), 7.52-7.49 (m, 1 H, $C_{14}H_9$), 6.92-6.91 (m, 1 H, mtCH), 6.87 (d, $^3J_{HH}$ 2.0 Hz, 1 H, mtCH), 6.86 (d, $^3J_{HH}$ 2.1 Hz, 1 H, mtCH), 6.85 (d, $^3J_{HH}$ 2.1 Hz, 1 H, mtCH), 6.84 (d, $^3J_{HH}$ 2.1 Hz, 1 H, mtCH), 6.83 (d, $^3J_{HH}$ 2.1 Hz, 1 H, mtCH), 3.83 (s, 3 H, mtCH$_3$), 3.66 (s, 3 H, mtCH$_3$), 3.65 (s, 3 H, mtCH$_3$). ^{11}B{^{1}H} ($CDCl_3$, 24.85°C, 128.38 MHz): δ 48.26. ^{13}C{^{1}H} ($CDCl_3$, 24.85°C, 176.06 MHz) δ 279.5 (W≡C$^\alpha$), 233.8, 219.2 (WCO), 161.0, 159.2, 159.1 (mtCS), 145.3 (C^1[$C_{14}H_9$]), 131.9 (C^3[$C_{14}H_9$]), 131.5 (C^8[$C_{14}H_9$]), 130.1 (C^9[$C_{14}H_9$]), 129.7 (C^4[$C_{14}H_9$]), 129.5 (C^{13}[$C_{14}H_9$]), 128.7 (C^{14}[$C_{14}H_9$]), 127.8 (C^2[$C_{14}H_9$]), 126.9 (C^5[$C_{14}H_9$]), 126.7 (C^{12}[$C_{14}H_9$]), 126.6 (C^6[$C_{14}H_9$]), 126.5 (C^{11}[$C_{14}H_9$]), 123.1 (C^7[$C_{14}H_9$]), 123.0 (C^{10}[$C_{14}H_9$]), 122.8, 122.7, 122.5, 120.1, 120.0 (2C) (mtCH), 35.0 (2C), 34.9 (mtCH$_3$). MS (ESI, high resolution): m/z (%) = [M]$^+$ 780.0820. Anal. Calcd. for $C_{29}H_{25}{}^{11}B_1N_6O_2S_3{}^{184}W_1$: [M]$^+$ 780.0802. Elemental Anal. Found: C, 44.56; H, 3.22; N, 10.41; S, 12.25%. Calcd. for $C_{29}H_{25}BN_6O_2S_3W$: C, 44.63; H, 3.23; N, 10.77; S, 12.33%.

$TmMo(CO)_2\{\equiv C\text{-}(9\text{-Phenanthryl})\}$ (3.9)

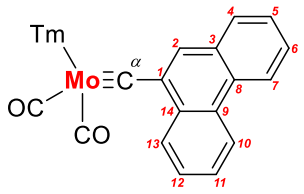

To a 100 mL Schlenk tube, 9-bromophenanthrene (502 mg, 1.952 mmol) was added and dispersed in THF (40 mL). The mixture was cooled to -78°C and ^{n}BuLi (1.6 M, 1.4 mL, 2.240 mmol) was added dropwise and the bright yellow mixture stirred for 10 minutes. The reaction vessel was warmed in ambient air for 10 minutes then re-cooled to -78°C for a further 10 minutes to afford a yellow/green mixture. $[Mo(CO)_6]$ (515 mg, 1.951 mmol) was added and after stirring for 15 minutes the mixture was warmed to room temperature for 1 h. The resulting mixture was re-cooled to -78°C and trifluoroacetic anhydride (0.30 mL, 2.157 mmol) added dropwise. The brown mixture was stirred for 15 minutes and warmed in ambient air for 30 minutes. During this time carbon monoxide was evolved as the reaction mixture warmed. Once re-cooled to -78°C, Na[Tm] (729 mg, 1.948 mmol) was added to the rapidly stirred mixture and slowly warmed to room temperature overnight. Stirring of the red/brown reaction mixture was halted after 16 h and concentrated to afford a red/brown residue. The crude product mixture was purified *via* silica-gel flash column chromatography (Eluent: 4:1 (v/v) CH_2Cl_2/Petroleum spirit (40-60 °C)). Initially a brown band was observed, but after continued elution of the column this separated into two distinct bands. Collection and subsequent concentration of the second red band to elute from the column afforded **3.9** as a red residue. Yield 226 mg (17%).

IR (CH_2Cl_2): ν_{BH} 2434 w; ν_{CO} 1984 vs, 1900 vs cm^{-1}. NMR ^1H ($CDCl_3$, 24.85°C, 700.03 MHz): δ 9.12 (m, 1 H, $C_{14}H_9$), 8.60 (m, 1 H, $C_{14}H_9$), 8.54 (d, $^3J_{HH}$ 7.7 Hz, 1 H, $C_{14}H_9$), 7.88 (s, 1 H, $C_{14}H_9$), 7.84 (d, $^3J_{HH}$ 7.0 Hz, 1 H, $C_{14}H_9$), 7.61-7.58 (m, 3 H, $C_{14}H_9$), 7.54-7.53 (m, 1 H, $C_{14}H_9$), 6.89 (s, 1 H, mtCH), 6.85 (m, 3 H, mtCH), 6.80 (d, $^3J_{HH}$ 7.2 Hz, 2 H, mtCH), 3.81 (s, 3 H, $mtCH_3$), 3.66 (s, 3 H, $mtCH_3$), 3.63 (s, 3 H, $mtCH_3$). $^{11}B\{^1H\}$ ($CDCl_3$, 24.85°C, 128.38 MHz): δ 48.49. $^{13}C\{^1H\}$ ($CDCl_3$, 24.85°C, 176.05 MHz) δ 290.2 ($Mo\equiv C^{\alpha}$), 226.6, 222.1 (MoCO), 161.5, 159.7, 159.5 (mtCS), 141.4 ($C^1[C_{14}H_9]$), 131.2 ($C^3[C_{14}H_9]$), 131.0 ($C^8[C_{14}H_9]$), 130.0 ($C^9[C_{14}H_9]$), 129.7 (2C) ($C^{4,13}[C_{14}H_9]$), 128.7 ($C^{14}[C_{14}H_9]$), 127.4 ($C^2[C_{14}H_9]$), 127.0 ($C^5[C_{14}H_9]$), 126.6 ($C^{12}[C_{14}H_9]$), 126.6 ($C^6[C_{14}H_9]$), 126.5 ($C^{11}[C_{14}H_9]$), 122.8 ($C^7[C_{14}H_9]$), 122.6 ($C^{10}[C_{14}H_9]$), 122.3 (3C), 119.7 (2C), 119.6 (mtCH), 34.7 (2C), 34.6 ($mtCH_3$). MS (ESI, high resolution): m/z (%) = $[M+Na]^+$ 717.0247. Anal. Calcd. for $C_{29}H_{25}{}^{11}B_1{}^{98}Mo_1N_6{}^{23}Na_1O_2S_3$: $[M+Na]^+$ 717.0246. Elemental Anal. Found: C, 52.56; H, 4.12; N, 10.81; S, 12.56%. Calcd. for $C_{29}H_{25}BMoN_6O_2S_3 \cdot C_4H_8O$: C, 51.84; H, 4.35; N, 10.99; S, 12.58%.

TmW(CO)$_2${≡C-(9-Anthracenyl)} (3.10)

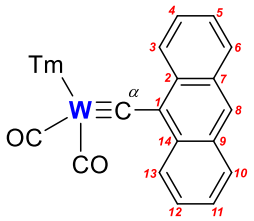

To a 100 mL Schlenk tube, 9-bromoanthracene (503 mg, 1.956 mmol) was added and dispersed in THF (40 mL). The mixture was cooled to -78°C and ^{n}BuLi (1.6 M, 1.4 mL, 2.240 mmol) was added dropwise and the bright orange mixture stirred for 10 minutes. The reaction vessel was warmed in ambient air for 10 minutes then re-cooled to -78°C for a further 10 minutes. [W(CO)$_6$] (686 mg, 1.949 mmol) was added and after stirring for 15 minutes, the mixture was warmed to room temperature for 1 h. The resulting orange mixture was re-cooled to -78°C and trifluoroacetic anhydride (0.30 mL, 2.158 mmol) added dropwise. The dark brown mixture was stirred for 15 minutes and warmed in ambient air for 30 minutes. During this time carbon monoxide was evolved as the reaction mixture warmed. Once re-cooled to -78°C, Na[Tm] (730 mg, 1.950 mmol) was added to the rapidly stirred mixture and slowly warmed to room temperature overnight. Stirring of the brown reaction mixture was halted after 16 h and concentrated to afford an orange/brown residue. The crude product mixture was purified *via* silica-gel flash column chromatography (Eluent: CH_2Cl_2). Collection and subsequent concentration of the major brown band afforded **3.10** as a brown powder. Yield 324 mg (21%).

IR (CH_2Cl_2): ν_{CO} 1970 s, 1880 s cm^{-1}. NMR ^{1}H ($CDCl_3$, 24.85°C, 700.03 MHz): δ 9.25 (d, $^3J_{HH}$ 8.7 Hz, 2 H, $C_{14}H_9$), 8.36 (s, 1 H, $C_{14}H_9$), 7.92 (d, $^3J_{HH}$ 8.4 Hz, 2 H, $C_{14}H_9$), 7.53-7.50 (m, 2 H, $C_{14}H_9$), 7.39-7.37 (m, 2 H, $C_{14}H_9$), 6.93 (d, $^3J_{HH}$ 2.1 Hz, 1 H, mtCH), 6.88 (d, $^3J_{HH}$ 2.1 Hz, 1 H, mtCH), 6.85 (q, $^3J_{HH}$ 2.2 Hz, 3 H, mtCH), 6.84 (d, $^3J_{HH}$ 2.1 Hz, 1 H, mtCH), 3.87 (s, 3 H, mtCH$_3$), 3.68 (s, 3 H, mtCH$_3$), 3.55 (s, 3 H, mtCH$_3$). ^{11}B{^{1}H} ($CDCl_3$, 24.85°C, 128.38 MHz): δ 48.38. ^{13}C{^{1}H} ($CDCl_3$, 24.85°C, 176.06 MHz): δ 279.4 (W≡C$^\alpha$), 225.1, 220.8 (WCO), 160.8, 159.4, 159.3 (mtCS), 141.9 (C^1[$C_{14}H_9$]), 132.6 (2C) (C^{7,9}[$C_{14}H_9$]), 131.5 (2C) (C^{2,14}[$C_{14}H_9$]), 128.4 (2C) (C^{4,12}[$C_{14}H_9$]), 127.8 (2C) (C^{3,13}[$C_{14}H_9$]), 126.4 (C^8[$C_{14}H_9$]), 126.1 (2C) (C^{6,10}[$C_{14}H_9$]), 125.6 (2C) (C^{5,11}[$C_{14}H_9$]), 123.2, 123.0, 122.8, 120.1, 120.0 (2C) (mtCH), 35.0, 34.9 (2C) (mtCH$_3$). MS (ESI, high resolution): *m/z* (%) = [M+Na]$^+$ 803.0688. Anal. Calcd. for $C_{29}H_{25}{}^{11}B_1N_6{}^{23}Na_1O_2S_3{}^{184}W_1$: [M+Na]$^+$ 803.0701. Elemental Anal. Found: C, 44.68; H, 3.22; N, 10.43; S, 12.43%. Calcd. for $C_{29}H_{25}BN_6O_2S_3W$: C, 44.63; H, 3.23; N, 10.77; S, 12.33%.

TmMo(CO)$_2${≡C-(9-Anthracenyl)} (3.11)

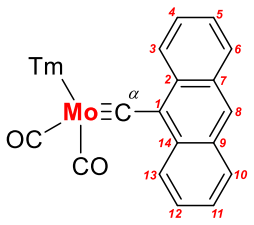

To a 100 mL Schlenk tube, 9-bromoanthracene (500 mg, 1.945 mmol) was added and dispersed in THF (40 mL). The mixture was cooled to -78°C and ^{n}BuLi (1.6 M, 1.4 mL, 2.240 mmol) was added dropwise and the bright orange mixture stirred for 10 minutes. The reaction vessel was warmed in ambient air for 10 minutes then re-cooled to -78°C for a further 10 minutes. [Mo(CO)$_6$] (515 mg, 1.951 mmol) was added and after stirring for 15 minutes, the mixture was warmed to room temperature for 1 h. The resulting orange mixture was re-cooled to -78°C and trifluoroacetic anhydride (0.30 mL, 2.158 mmol) added dropwise. The dark brown mixture was stirred for 15 minutes and warmed in ambient air for 30 minutes. During this time carbon monoxide was evolved as the reaction mixture warmed. Once re-cooled to -78°C, Na[Tm] (730 mg, 1.950 mmol) was added to the rapidly stirred mixture and slowly warmed to room temperature overnight. Stirring of the brown reaction mixture was halted after 16 h and concentrated to afford an orange/brown residue. The crude product mixture was purified *via* silica-gel flash column chromatography (Eluent: CH_2Cl_2). Collection and subsequent concentration of the major brown band afforded **3.11** as a black/brown powder. Yield 520 mg (39%).

IR (CH_2Cl_2): ν_{BH} 2400 w; ν_{CO} 1984 vs, 1901 vs cm^{-1}. NMR ^{1}H ($CDCl_3$, 24.85°C, 700.03 MHz): δ 9.35 (d, $^3J_{HH}$ 8.7 Hz, 2 H, $C_{14}H_9$), 8.28 (s, 1 H, $C_{14}H_9$), 7.91 (d, $^3J_{HH}$ 8.4 Hz, 2 H, $C_{14}H_9$), 7.53 (t, $^3J_{HH}$ 7.7 Hz, 2 H, $C_{14}H_9$), 7.40 (t, $^3J_{HH}$ 7.2 Hz, 2 H, $C_{14}H_9$), 6.90 (d, $^3J_{HH}$ 1.8 Hz, 1 H, mtCH), 6.87 (d, $^3J_{HH}$ 1.9 Hz, 1 H, mtCH), 6.85 (d, $^3J_{HH}$ 2.0 Hz, 1 H, mtCH), 6.83 (t, $^3J_{HH}$ 2.3 Hz, 2 H, mtCH), 6.81 (d, $^3J_{HH}$ 2.0 Hz, 1 H, mtCH), 3.86 (s, 3 H mtCH$_3$), 3.67 (s, 3 H mtCH$_3$), 3.54 (s, 3 H mtCH$_3$). ^{11}B{^{1}H} ($CDCl_3$, 24.85°C, 128.38 MHz): δ 48.56. ^{13}C{^{1}H} ($CDCl_3$, 24.85°C, 176.06 MHz): δ 291.8 (Mo≡C$^{\alpha}$), 228.2, 224.0 (MoCO), 161.7, 160.1, 160.0 (mtCS), 138.6 (C^1[$C_{14}H_9$]), 133.0 (C^{7,9}[$C_{14}H_9$]), 131.4 (C^{2,14}[$C_{14}H_9$]), 128.6(C^{4,12}[$C_{14}H_9$]), 127.6 (C^{3,13}[$C_{14}H_9$]), 127.4 (C^8[$C_{14}H_9$]), 126.7 (C^{6,10}[$C_{14}H_9$]), 125.6 (C^{5,11}[$C_{14}H_9$]), 123.1, 122.9, 122.6, 119.8 (2C), 119.7 (mtCH), 35.0, 34.9, 34.8 (mtCH$_3$). MS (ESI, high resolution): *m/z* (%) = [M+Na]$^+$ 717.0256. Anal. Calcd. for $C_{29}H_{25}{}^{11}B_1{}^{98}Mo_1N_6{}^{23}Na_1O_2S_3$: [M+Na]$^+$ 717.0246. Elemental Anal. Found: C, 50.29; H, 3.59; N, 11.95; S, 14.19%. Calcd. for $C_{29}H_{25}BMoN_6O_2S_3$: C, 50.30; H, 3.64; N, 12.14; S, 13.89%.

TmW(CO)$_2${≡C-(1-Pyrenyl)} (3.12)

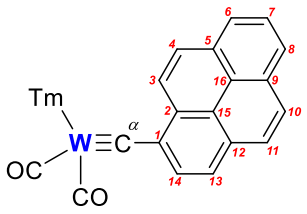

To a 100 mL Schlenk tube, 1-bromopyrene (501 mg, 1.782 mmol) was added and dispersed in THF (40 mL). The mixture was cooled to -78°C and ^{n}BuLi (1.6 M, 1.4 mL, 2.240 mmol) was added dropwise and the light orange mixture stirred for 10 minutes. The reaction vessel was warmed in ambient air for 10 minutes then re-cooled to -78°C for a further 10 minutes to afford a red mixture. [W(CO)$_6$] (628 mg, 1.785 mmol) was added and after stirring for 15 minutes, the mixture was warmed to room temperature for 1 h. The resulting mixture was re-cooled to -78°C and trifluoroacetic anhydride (0.25 mL, 1.799 mmol) added dropwise. The brown/black mixture was stirred for 15 minutes and warmed in ambient air for 30 minutes. During this time carbon monoxide was evolved as the reaction mixture warmed. Once re-cooled to -78°C, Na[Tm] (668 mg, 1.785 mmol) was added to the rapidly stirred mixture and slowly warmed to room temperature overnight. Stirring of the brown reaction mixture was halted after 16 h and concentrated to afford an orange/brown residue. The crude product mixture was purified *via* silica-gel flash column chromatography (Eluent: 2:1 (v/v) CH_2Cl_2/Petrol (40-60°C)). Collection and subsequent concentration of the orange/brown band afforded **3.12** as a brown powder. Yield 330 mg (23%).

IR (CH_2Cl_2): ν_{CO} 1969 vs, 1880 vs cm^{-1}. NMR ^{1}H ($CDCl_3$, 24.95°C, 700.03 MHz): δ 9.11 (d, $^3J_{HH}$ 9.0 Hz, 1 H, $C_{16}H_9$), 8.14-8.12 (m, 2 H, $C_{16}H_9$), 8.07 (d, $^3J_{HH}$ 9.0 Hz, 1 H, $C_{16}H_9$), 8.01 (d, $^3J_{HH}$ 8.8 Hz, 1 H, $C_{16}H_9$), 7.97-7.92 (m, 4 H, $C_{16}H_9$), 6.92 (d, $^3J_{HH}$ 2.1 Hz, 1 H, mtCH), 6.88 (d, $^3J_{HH}$ 2.1 Hz, 1 H, mtCH), 6.86-6.84 (m, 2 H, mtCH), 6.83 (m, 2 H, mtCH), 3.83 (s, 3 H, $mtCH_3$), 3.68 (s, 3 H, $mtCH_3$), 3.67 (s, 3 H, $mtCH_3$). ^{11}B{^{1}H} ($CDCl_3$, 24.85°C, 128.38 MHz): δ 48.34. ^{13}C{^{1}H} ($CDCl_3$, 24.95°C, 176.05 MHz): δ 280.0 (W≡C$^\alpha$), 224.1, 219.6 (WCO), 161.1, 159.3, 159.2 (mtCS), 144.7 (C^1[$C_{16}H_9$]), 131.8 (C^{12}[$C_{16}H_9$]), 131.6 (C^9[$C_{16}H_9$]), 130.9 (C^{14}[$C_{16}H_9$]), 130.0 (C^{13}[$C_{16}H_9$]), 128.5 (C^8[$C_{16}H_9$]), 127.8 (C^{10}[$C_{16}H_9$]), 127.5 (C^{11}[$C_{16}H_9$]), 127.3 (C^4[$C_{16}H_9$]), 126.4 (C^6[$C_{16}H_9$]), 126.1 (C^7[$C_{16}H_9$]), 124.9 (C^5[$C_{16}H_9$]), 124.8 (C^3[$C_{16}H_9$]), 124.6 (2C) (C^{15,16}[$C_{16}H_9$]), 124.5 (C^2[$C_{16}H_9$]), 123.1, 123.0, 122.8, 120.1, 120.0 (2C) (mtCH), 35.0, 34.9, 34.3 ($mtCH_3$). MS (ESI, high resolution): m/z (%) = $[M+H]^+$ 805.0887; $[M-CO]^+$ 776.0882. Anal. Calcd. for $C_{31}H_{26}{}^{11}B_1N_6O_2S_3{}^{184}W_1$: $[M+H]^+$ 805.0882; $C_{30}H_{25}{}^{11}B_1N_6O_1S_3{}^{184}W_1$: $[M-CO]^+$ 776.0854. After numerous attempts an agreeable elemental microanalysis could not be obtained.

$TmMo(CO)_2\{\equiv C\text{-}(1\text{-}Pyrenyl)\}$ (3.13)

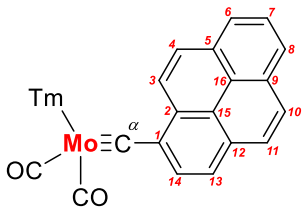

To a 100 mL Schlenk tube, 1-bromopyrene (501 mg, 1.782 mmol) was added and dispersed in THF (40 mL). The mixture was cooled to -78°C and ^{n}BuLi (1.6 M, 1.4 mL, 2.240 mmol) was added dropwise and the light orange mixture stirred for 10 minutes. The reaction vessel was warmed in ambient air for 10 minutes then re-cooled to -78°C for a further 10 minutes to afford a red mixture. $[Mo(CO)_6]$ (471 mg, 1.784 mmol) was added and after stirring for 15 minutes, the mixture was warmed to room temperature for 1 h. The resulting mixture was re-cooled to -78°C and trifluoroacetic anhydride (0.25 mL, 1.799 mmol) added dropwise. The brown mixture was stirred for 15 minutes and warmed in ambient air for 30 minutes. During this time carbon monoxide was evolved as the reaction mixture warmed. Once re-cooled to -78°C, Na[Tm] (668 mg, 1.785 mmol) was added to the rapidly stirred mixture and slowly warmed to room temperature overnight. Stirring of the brown reaction mixture was halted after 16 h and concentrated to afford an orange/brown residue. The crude product mixture was purified *via* silica-gel flash column chromatography (Eluent: 2:1 (v/v) CH_2Cl_2/Petrol (40-60°C)). Collection and subsequent concentration of the orange/brown band afforded **3.13** as a brown powder. Yield 279 mg (22%).

IR (CH_2Cl_2): ν_{BH} 2399 w; ν_{CO} 1983 vs, 1900 vs cm^{-1}. NMR ^{1}H ($CDCl_3$, 24.95°C, 699.90 MHz): δ 9.21 (d, $^{3}J_{HH}$ 8.2 Hz, 1 H, $C_{16}H_9$), 8.15-8.13 (m, 2 H, $C_{16}H_9$), 8.11 (d, $^{3}J_{HH}$ 9.2 Hz, 1 H, $C_{16}H_9$), 8.09 (d, $^{3}J_{HH}$ 7.8 Hz, 1 H, $C_{16}H_9$), 8.05 (d, $^{3}J_{HH}$ 8.4 Hz, 1 H, $C_{16}H_9$), 7.96 (m, 3 H, $C_{16}H_9$), 6.91 (br s, 1 H, mtCH), 6.88 (br s, 1 H, mtCH), 6.85 (m, 2 H, mtCH), 6.82 (m, 2 H, mtCH), 3.82 (s, 3 H, $mtCH_3$), 3.67 (s, 6 H, $mtCH_3$). $^{11}B\{^{1}H\}$ ($CDCl_3$, 24.85°C, 128.38 MHz): δ 48.51. A $^{13}C\{^{1}H\}$ NMR of this complex could not be obtained due to its tendency to precipitate out of deuterated solvents over several hours. MS (ESI, high resolution): *m/z* (%) = $[M\text{-}2(CO)]^+$ 662.0463; $[M+Na]^+$ 741.0260. Anal. Calcd. for $C_{29}H_{25}{}^{11}B_1{}^{98}Mo_1N_6S_3$: $[M\text{-}2(CO)]^+$ 662.0450; Anal. Calcd. for $C_{31}H_{25}{}^{11}B_1{}^{98}Mo_1N_6{}^{23}Na_1O_2S_3$: $[M+Na]^+$ 741.0246. Elemental Anal. Found: C, 51.97; H, 3.53; N, 10.70; S, 11.92%. Calcd. for $C_{31}H_{25}BMoN_6O_2S_3$: C, 51.96; H, 3.52; N, 11.73; S, 13.42%.

TmW(CO)$_2${≡C-(3-Perylenyl)} (3.14)

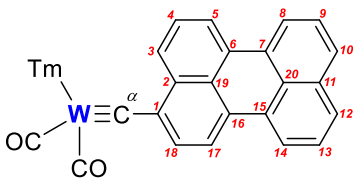

To a 100 mL Schlenk tube, 3-bromoperylene (501 mg, 1.513 mmol) was added and dispersed in THF (40 mL). The mixture was cooled to -78°C and ^{n}BuLi (1.6 M, 1.1 mL, 1.760 mmol) was added dropwise and the orange mixture stirred for 10 minutes. The reaction vessel was warmed in ambient air for 10 minutes then re-cooled to -78°C for a further 10 minutes to afford a brown/red mixture. [W(CO)$_6$] (533 mg, 1.515 mmol) was added and after stirring for 15 minutes, the mixture was warmed to room temperature for 1 h. The resulting mixture was re-cooled to -78°C and trifluoroacetic anhydride (0.22 mL, 1.583 mmol) added dropwise. The dark red mixture was stirred for 15 minutes and warmed in ambient air for 30 minutes. During this time carbon monoxide was evolved as the reaction mixture warmed. Once re-cooled to -78°C, Na[Tm] (567 mg, 1.515 mmol) was added to the rapidly stirred mixture and slowly warmed to room temperature overnight. Stirring of the red reaction mixture was halted after 16 h and concentrated to afford a dark red residue. The crude product mixture was purified *via* silica-gel flash column chromatography (Eluent: CH_2Cl_2). After the initial yellow and orange bands (highly fluorescent) were eluted off the column, a major dark band was observed. After further elution of the column this dark band split into three segments; the central segment being the apparent major component. The segments were successfully separated with the help of a bright light being shone through the column to help illuminate the small regions between each band. The peripheral red and deep purple bands were discarded, while the central brown/red band was retained. Further purification of this product was required for the purpose of recording spectroscopic data. The crude product was further purified *via* silica-gel flash column chromatography (Eluent: CH_2Cl_2). Collection and subsequent concentration of the brown/red band afforded **3.14** as a semi-crystalline dark green residue. Yield 262 mg (20%).

IR (CH_2Cl_2): ν_{CO} 1969 s, 1879 s cm^{-1}. NMR ^{1}H ($CDCl_3$, 24.85°C, 700.03 MHz): δ 8.75 (d, $^3J_{HH}$ 8.1 Hz, 1 H, $C_{20}H_{11}$), 8.14 (d, $^3J_{HH}$ 7.5 Hz, 1 H, $C_{20}H_{11}$), 8.11 (t, $^3J_{HH}$ 7.5 Hz, 2 H, $C_{20}H_{11}$), 7.99 (d, $^3J_{HH}$ 8.0 Hz, 1 H, $C_{20}H_{11}$), 7.65 (t, $^3J_{HH}$ 8.5 Hz, 2 H, $C_{20}H_{11}$), 7.50-7.46 (m, 2 H, $C_{20}H_{11}$), 7.44-7.41 (m, 2 H, $C_{20}H_{11}$), 6.90 (d, $^3J_{HH}$ 2.0 Hz, 1 H, mtCH), 6.88 (d, $^3J_{HH}$ 2.0 Hz, 1 H, mtCH), 6.84 (d, $^3J_{HH}$ 2.0 Hz, 1 H, mtCH), 6.83 (d, $^3J_{HH}$ 2.1 Hz, 1 H, mtCH), 6.82 (d, $^3J_{HH}$ 2.1 Hz, 1 H, mtCH), 6.81 (d, $^3J_{HH}$ 2.1 Hz, 1 H, mtCH), 3.81 (s, 3 H, mtCH$_3$), 3.67 (s, 3 H, mtCH$_3$), 3.65 (s, 3 H, mtCH$_3$). ^{11}B{^{1}H} ($CDCl_3$, 24.85°C, 128.38 MHz): δ 48.38. ^{13}C{^{1}H} ($CDCl_3$, 24.85°C, 176.05 MHz): δ 279.2 (W≡C$^\alpha$, $^1J_{WC}$ 193.9 Hz), 223.9 (WCO, $^1J_{WC}$ 170.9 Hz),

219.4 (WCO, 164.6 Hz), 161.0, 159.2, 159.1 (mtCS), 146.7 ($C^{1}[C_{20}H_{11}]$, $^{2}J_{WC}$ 42.5 Hz), 134.9 ($C^{20}[C_{20}H_{11}]$), 134.1 ($C^{11}[C_{20}H_{11}]$), 131.7 ($C^{7}[C_{20}H_{11}]$), 131.0 ($C^{16}[C_{20}H_{11}]$), 129.7 ($C^{17}[C_{20}H_{11}]$), 129.5 ($C^{2}[C_{20}H_{11}]$), 128.6 (2C) ($C^{6,15}[C_{20}H_{11}]$), 127.6 (2C) ($C^{9,13}[C_{20}H_{11}]$), 127.1 ($C^{19}[C_{20}H_{11}]$), 126.9 ($C^{4}[C_{20}H_{11}]$), 126.7 ($C^{3}[C_{20}H_{11}]$), 126.6 ($C^{10,12}[C_{20}H_{11}]$), 123.1, 123.0, 122.8, 120.6, 120.5, 120.1 (mtCH), 120.1 (2C) ($C^{8,14}[C_{20}H_{11}]$), 120.0 ($C^{5}[C_{20}H_{11}]$), 35.0, 34.9, 34.8 ($mtCH_3$). MS (ESI, high resolution): m/z (%) = $[M+H]^+$ 855.1039. Anal. Calcd. for $C_{35}H_{28}{}^{11}B_1N_6O_2S_3{}^{184}W_1$: $[M+H]^+$ 855.1038. Elemental Anal. Found: C, 49.27; H, 3.29; N, 9.12; S, 10.30%. Calcd. for $C_{35}H_{27}BN_6O_2S_3W$: C, 49.20; H, 3.18; N, 9.84; S, 11.26%.

$TmMo(CO)_2${≡C-(3-Perylenyl)} (3.15)

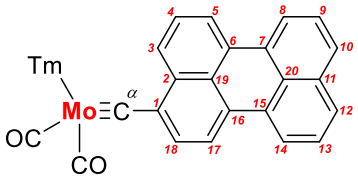

To a 100 mL Schlenk tube, 3-bromoperylene (501 mg, 1.513 mmol) was added and dispersed in THF (40 mL). The mixture was cooled to -78°C and ^{n}BuLi (1.6 M, 1.1 mL, 1.760 mmol) was added dropwise and the orange mixture stirred for 10 minutes. The reaction vessel was warmed in ambient air for 10 minutes then re-cooled to -78°C for a further 10 minutes to afford a brown/red mixture. $[Mo(CO)_6]$ (399 mg, 1.511 mmol) was added and after stirring for 15 minutes, the mixture was warmed to room temperature for 1 h. The resulting mixture was re-cooled to -78°C and trifluoroacetic anhydride (0.22 mL, 1.583 mmol) added dropwise. The dark red mixture was stirred for 15 minutes and warmed in ambient air for 30 minutes. During this time carbon monoxide was evolved as the reaction mixture warmed. Once re-cooled to -78°C, Na[Tm] (567 mg, 1.515 mmol) was added to the rapidly stirred mixture and slowly warmed to room temperature overnight. Stirring of the red reaction mixture was halted after 16 h and concentrated to afford a dark red residue. The crude product mixture was purified *via* silica-gel flash column chromatography (Eluent: CH_2Cl_2). After the initial yellow and orange bands (highly fluorescent) were eluted off the column, a major dark band was observed. After further elution of the column this dark band split into three segments; the central segment being the apparent major component. The segments were successfully separated with the help of a bright light being shone through the column to help illuminate the small regions between each band. The peripheral red and red/purple bands were discarded, while the central brown/red band was retained. Further purification of this product was required for the purpose of recording spectroscopic data. The crude product was further purified *via* silica-gel flash column chromatography (Eluent: CH_2Cl_2). Collection and subsequent concentration of the brown/red band afforded **3.15** as a semi-crystalline dark green residue. Yield 306 mg (26%).

IR (CH_2Cl_2): ν_{BH} 2400 w; ν_{CO} 1983 s, 1899 s cm^{-1}. NMR ^1H ($CDCl_3$, 24.85°C, 700.03 MHz): δ 8.84 (d, $^3J_{HH}$ 7.8 Hz, 1 H, $C_{20}H_{11}$), 8.13 (t, $^3J_{HH}$ 7.1 Hz, 3 H, $C_{20}H_{11}$), 8.09 (d, $^3J_{HH}$ 7.1 Hz, 1 H, $C_{20}H_{11}$), 7.97 (d, $^3J_{HH}$ 7.6 Hz, 1 H, $C_{20}H_{11}$), 7.65 (m, 2 H, $C_{20}H_{11}$), 7.57 (d, $^3J_{HH}$ 7.7 Hz, 1 H, $C_{20}H_{11}$), 7.49 (t, $^3J_{HH}$ 7.6 Hz, 1 H, $C_{20}H_{11}$), 7.43 (q, $^3J_{HH}$ 6.8 Hz, 1 H, $C_{20}H_{11}$), 6.89 (s, 1 H, mtCH), 6.87 (s, 1 H, mtCH), 6.84 (d, $^3J_{HH}$ 6.6 Hz, 2 H, mtCH), 6.80 (d, $^3J_{HH}$ 7.6 Hz, 2 H, mtCH), 3.80 (s, 3 H, $mtCH_3$), 3.66 (s, 6 H, $mtCH_3$). $^{11}B\{^1H\}$ ($CDCl_3$, 24.85°C, 128.38 MHz): δ 48.54. $^{13}C\{^1H\}$ ($CDCl_3$, 24.85°C, 176.05 MHz): δ 290.1 (Mo≡C^{α}), 226.9, 222.4 (WCO), 161.7, 159.8, 159.7 (mtCS), 142.8 ($C^1[C_{20}H_{11}]$), 134.7 ($C^{20}[C_{20}H_{11}]$), 134.1 ($C^{11}[C_{20}H_{11}]$), 131.3 ($C^7[C_{20}H_{11}]$), 131.1 ($C^{16}[C_{20}H_{11}]$), 131.0 ($C^{15}[C_{20}H_{11}]$), 130.6 ($C^6[C_{20}H_{11}]$), 129.8 ($C^{17}[C_{20}H_{11}]$), 128.4 ($C^2[C_{20}H_{11}]$), 128.3 ($C^{19}[C_{20}H_{11}]$), 127.9 ($C^{13}[C_{20}H_{11}]$), 127.7 ($C^9[C_{20}H_{11}]$), 126.9 ($C^4[C_{20}H_{11}]$), 126.8 ($C^3[C_{20}H_{11}]$), 126.7 ($C^{12}[C_{20}H_{11}]$), 126.6 ($C^{10}[C_{20}H_{11}]$), 123.0, 122.8, 122.5 120.8, 120.5, 120.2 (mtCH), 119.8 (3C) ($C^{5,8,14}[C_{20}H_{11}]$), 34.9, 34.8, 34.7 ($mtCH_3$). MS (ESI, high resolution): m/z (%) = $[M+H]^+$ 769.0579. Anal. Calcd. for $C_{35}H_{28}{}^{11}B_1{}^{98}Mo_1N_6O_2S_3$: $[M+H]^+$ 769.0583. Elemental Anal. Found: C, 54.78; H, 3.53; N, 10.26; S, 11.57%. Calcd. for $C_{35}H_{27}BMoN_6O_2S_3$: C, 54.84; H, 3.55; N, 10.96; S, 12.55%.

$TmW(CO)_2\{\equiv CC\equiv C$-(3-Phenanthryl)$\}$ (3.16)

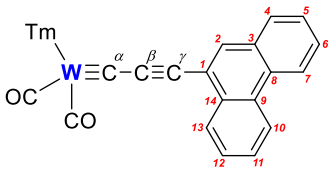

To a 100 mL Schlenk tube, 9-ethynylphenanthrene (1.160 g, 5.735 mmol) was added and dispersed in THF (30 mL). The mixture was cooled to -78°C and ^{n}BuLi (1.6 M, 4.0 mL, 6.400 mmol) was added dropwise and the solution stirred for 10 minutes. The reaction vessel was warmed in ambient air for 10 minutes, then re-cooled to -78°C for another 10 minutes. $[W(CO)_6]$ (2.056 g, 5.843 mmol) was added and after stirring for 15 minutes, the marshy-green mixture was warmed to room temperature and stirred for 1 h. The resulting brown mixture was cooled to -78°C and trifluoroacetic anhydride (0.8 mL, 5.755 mmol) added dropwise. The purple mixture was stirred for 15 minutes and then the reaction vessel was warmed in ambient air for 45 minutes. During this time carbon monoxide gas was evolved from the reaction mixture as it warmed. Once re-cooled to -78°C Na[Tm] (2.154 g, 5.755 mmol) was added to the rapidly stirred mixture which was allowed to slowly warm to room temperature overnight. Stirring of the brown reaction mixture was halted after 16 h and concentrated to afford a brown residue. The crude product mixture was purified *via* silica-gel flash column chromatography (Eluent: CH_2Cl_2). Collection and subsequent concentration of the major brown/red band afforded **3.16** as a brown/black powder. Yield 1.885 g (41%).

IR (CH_2Cl_2): ν_{BH} 2435 w; ν_{CO} 1979 vs, 1891 vs cm^{-1}. NMR ^1H ($CDCl_3$, 25.05°C, 700.03 MHz): δ 8.64-8.62 (m, 1 H, $C_{14}H_9$), 8.59 (d, $^3J_{HH}$ 8.3 Hz, 1 H, $C_{14}H_9$), 8.41-8.40 (m, 1 H, $C_{14}H_9$), 8.03 (s, 1 H, $C_{14}H_9$), 7.80 (d, $^3J_{HH}$ 7.7 Hz, 1 H, $C_{14}H_9$), 7.65-7.63 (m, 3 H, $C_{14}H_9$), 7.55 (t, $^3J_{HH}$ 7.7 Hz, 1 H, $C_{14}H_9$), 6.91 (d, $^3J_{HH}$ 2.0 Hz, 1 H, mtCH), 6.90 (d, $^3J_{HH}$ 2.0 Hz, 1 H, mtCH), 6.84-6.83 (m, 2 H, mtCH), 6.82 (d, $^3J_{HH}$ 2.1 Hz, 1 H, mtCH), 6.79 (d, $^3J_{HH}$ 2.0 Hz, 1 H, mtCH), 3.82 (s, 3 H, $mtCH_3$), 3.78 (s, 3 H, $mtCH_3$), 3.62 (s, 3 H, $mtCH_3$). $^{11}B\{^1H\}$ ($CDCl_3$, 24.85°C, 128.38 MHz): δ -1.65. $^{13}C\{^1H\}$ ($CDCl_3$, 24.95°C, 176.02 MHz): δ 247.1 ($W{\equiv}C^{\alpha}$, $^1J_{WC}$ 203.8 Hz), 225.1 (WCO, $^1J_{WC}$ 167.8 Hz), 220.0 (WCO, $^1J_{WC}$ 160.2 Hz), 160.9, 159.0, 158.4 (mtCS), 132.9 ($C^3[C_{14}H_9]$), 131.7 ($C^8[C_{14}H_9]$), 131.3 ($C^9[C_{14}H_9]$), 130.2 ($C^4[C_{14}H_9]$), 130.1 ($C^{13}[C_{14}H_9]$), 128.5 ($C^{14}[C_{14}H_9]$), 127.6 ($C^2[C_{14}H_9]$), 127.4 ($C^5[C_{14}H_9]$), 127.2 ($C^6[C_{14}H_9]$), 127.1 (2C) ($C^{11,12}[C_{14}H_9]$), 123.1 ($C^7[C_{14}H_9]$), 123.0 (mtCH), 123.0 ($C^{10}[C_{14}H_9]$), 122.8, 122.7, 120.3, 120.2, 120.1 (mtCH), 119.7 ($C^1[C_{14}H_9]$), 112.1 (WC^{β}, $^2J_{WC}$ 59.9 Hz), 73.2 (WC^{γ}, $^3J_{WC}$ 7.6 Hz), 35.2, 35.0, 34.8 ($mtCH_3$). MS (ESI, high resolution): m/z (%) = 805.0891 $[M+H]^+$. Anal. Calcd. for $C_{31}H_{26}{}^{11}B_1N_6O_2S_3{}^{184}W_1$: $[M+H]^+$ 805.0881. Elemental Anal. Found: C, 46.30; H, 3.12; N, 9.85; S, 11.70%. Calcd. for $C_{31}H_{25}BN_6O_2S_3W$: C, 46.29; H, 3.13; N, 10.45; S, 11.96%.

A crystal suitable for structure determination was grown by vapour diffusion of toluene into a CH_2Cl_2 solution at 4°C (**Figure 5.6**).

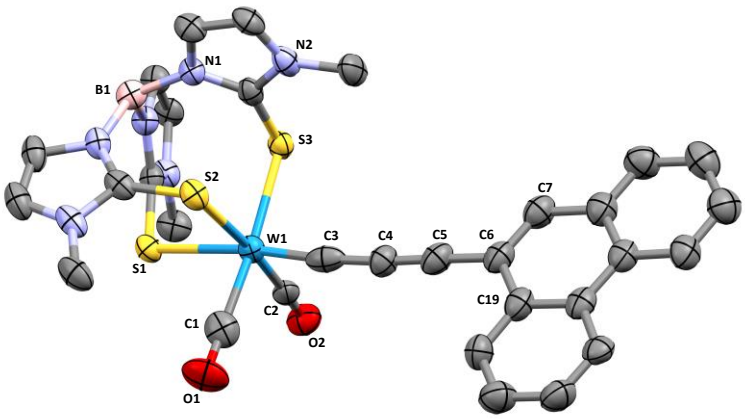

Figure 5.6. Molecular structure of **3.16** (50% displacement ellipsoids) with selected atom labels. Solvent molecules and hydrogen atoms omitted for clarity. Selected bond lengths (Å) and angles (°): W1–C1 1.992(7), W1–C2 1.984(6), W1–S1 2.6677(12), W1–S2 2.5726(13), W1–S3 2.5374(12), W1–C3 1.835(7), C3–C4 1.360(9), C4–C5 1.226(8), C5–C6 1.422(8); W1–C3–C4 172.8(5), C3–C4–C5 174.6(6), C4–C5–C6 178.9(7). The alternative enantiomer is generated by crystallographic symmetry (n-glide).

Crystal Data for $C_{45}H_{41}BN_6O_2S_3W$ (M =988.68 g/mol): tetragonal, space group $P4_2/n$ (no. 86), a = 25.5387(3) Å, c = 12.7864(3) Å, V = 8339.6(3) $Å^3$, Z = 8, T = 150.01(10) K, μ(CuKα) = 6.904 mm^{-1}, $Dcalc$ = 1.575 g/cm^3, 29195 reflections measured

(7.732° ≤ 2Θ ≤ 147.386°), 8362 unique (R_{int} = 0.0276, R_{sigma} = 0.0265) which were used in all calculations. The final R_1 was 0.0442 (I > 2σ(I)) and wR_2 was 0.1217 (all data) for 400 refined parameters with 0 restraints.

TmW(CO)$_2${≡CC≡C-(9-Anthracenyl)} (3.17)

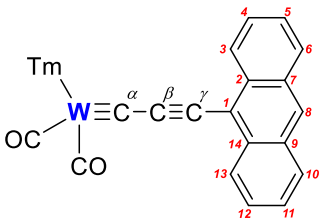

To a 100 mL Schlenk tube, 9-ethynylanthracene (324 mg, 1.602 mmol) was added and dispersed in THF (30 mL). The system was cooled to -78°C and ^{n}BuLi (1.6 M, 1.10 mL, 1.762 mmol) was added dropwise and the mixture stirred for 10 minutes. The reaction vessel was warmed in ambient air for 10 minutes then re-cooled to -78°C for a further 10 minutes. [W(CO)$_6$] (565 mg, 1.606 mmol) was added and after stirring for 15 minutes, the mixture was warmed to room temperature for 1 h. The resulting mixture was re-cooled to -78°C and trifluoroacetic anhydride (0.23 mL, 1.655 mmol) added dropwise, then stirred for 15 minutes and warmed in ambient air for 30 minutes. During this time carbon monoxide was evolved as the reaction mixture warmed. Once re-cooled to -78°C, Na[Tm] (603 mg, 1.611 mmol) was added to the rapidly stirred mixture and slowly warmed to room temperature overnight. Stirring of the brown reaction mixture was halted after 16 h and concentrated to afford a brown residue which was subsequently extracted with CH_2Cl_2 and filtered through a short plug of diatomaceous earth (Eluent: CH_2Cl_2). The filtrate was concentrated to dryness and purified *via* silica-gel flash column chromatography (Eluent: 1:1 (v/v) CH_2Cl_2/Petroleum spirit (40-60°C)). Four distinct bands were isolated from the column (in order of elution): (i) bright red (fluorescent blue); (ii) orange/red (fluorescent blue); (iii) yellow (fluorescent light blue/green); (iv) dark brown (not fluorescent). Collection and subsequent concentration of the dark brown band afforded **3.17** as a brown powder. Yield 176 mg (14%).

IR (CH_2Cl_2): ν_{CO} 1978 w, 1891 w cm^{-1}. NMR ^{1}H ($CDCl_3$, 25.05°C, 700.03 MHz): δ 8.50 (d, $^3J_{HH}$ 8.6 Hz, 2 H, $C_{14}H_9$), 8.39 (s, 1 H, $C_{14}H_9$), 7.96 (d, $^3J_{HH}$ 8.4 Hz, 2 H, $C_{14}H_9$), 7.54-7.52 (m, 2 H, $C_{14}H_9$), 7.46-7.44 (m, 2 H, $C_{14}H_9$), 6.92 (d, $^3J_{HH}$ 1.9 Hz, 1 H, mtCH), 6.90 (d, $^3J_{HH}$ 1.9 Hz, 1 H, mtCH), 6.84 (d, $^3J_{HH}$ 2.0 Hz, 1 H, mtCH), 6.84 (d, $^3J_{HH}$ 1.9 Hz, 1 H, mtCH), 6.82 (d, $^3J_{HH}$ 2.0 Hz, 1 H, mtCH), 6.79 (d, $^3J_{HH}$ 1.9 Hz, 1 H, mtCH), 3.82 (s, 3 H, mtCH$_3$), 3.79 (s, 3 H, mtCH$_3$), 3.63 (s, 3 H, mtCH$_3$). ^{13}C{^{1}H} ($CDCl_3$, 25.65°C, 176.05 MHz) δ 246.5 (W≡C$^\alpha$, $^1J_{WC}$ 203.8 Hz), 225.2 (WCO, $^1J_{WC}$ 168.9 Hz), 220.0 (WCO, $^1J_{WC}$ 160.5 Hz), 161.0, 159.0, 158.5 (mtCS), 133.5 (2C) (C^{2,14}[$C_{14}H_9$]), 131.5 (2C) (C^{7,9}[$C_{14}H_9$]), 128.7 (2C) (C^{4,12}[$C_{14}H_9$]), 127.5 (C^{3,13}[$C_{14}H_9$]), 127.1 (C^8[$C_{14}H_9$]), 126.6 (C^{6,10}[$C_{14}H_9$]), 126.0 (C^{5,11}[$C_{14}H_9$]),

123.1, 123.0 (2C), 120.3, 120.2, 120.1 (mtCH), 118.9 (WC^{β}), 117.5 ($C^{1}[C_{14}H_{9}]$), 72.1 (WC^{γ}), 35.2, 35.0, 34.9 ($mtCH_3$). MS (ESI, high resolution): m/z (%) = $[M+Na]^+$ 827.0704. Anal. Calcd. for $C_{31}H_{25}{}^{11}B_1N_6{}^{23}Na_1O_2S_3{}^{184}W_1$: $[M+Na]^+$ 827.0701. After numerous attempts an agreeable elemental microanalysis could not be obtained.

TmW(CO)$_2${≡CC≡C-(1-Pyrenyl)} (3.18)

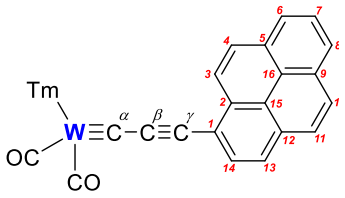

To a 100 mL Schlenk tube, 1-ethynylpyrene (151 mg, 0.667 mmol) was added and dispersed in THF (25 mL). The mixture was cooled to -78°C and ^{n}BuLi (1.6 M, 0.47 mL, 0.752 mmol) was added dropwise and the green mixture stirred for 10 minutes. The reaction vessel was warmed in ambient air for 10 minutes then re-cooled to -78°C for a further 10 minutes. $[W(CO)_6]$ (235 mg, 0.668 mmol) was added and after stirring for 15 minutes, the mixture was warmed to room temperature for 1 h. The resulting brown mixture was re-cooled to -78°C and trifluoroacetic anhydride (0.10 mL, 0.719 mmol) added dropwise, then stirred for 15 minutes and warmed in ambient air for 30 minutes. During this time carbon monoxide was evolved as the reaction mixture warmed. Once re-cooled to -78°C, Na[Tm] (249 mg, 0.665 mmol) was added to the rapidly stirred mixture and slowly warmed to room temperature overnight. Stirring of the brown reaction mixture was halted after 16 h and concentrated to afford a red/brown residue which was subsequently extracted with CH_2Cl_2 and filtered through a short plug of diatomaceous earth (Eluent: CH_2Cl_2). The crude product mixture was purified *via* silica-gel flash column chromatography (Eluent: Gradient from 1:1 (v/v) CH_2Cl_2/Petroleum spirits (40-60°C) to 100 % CH_2Cl_2). Following the elution of the initial strong brown band and the second yellow (fluorescent blue) band, the polarity of the eluent mixture was gradually increased. This allowed the third orange band to be isolated followed by the fourth dark brown band. Collection and subsequent concentration of the dark brown band afforded **3.18** as a brown powder. Yield 57 mg (10%).

NMR ^{1}H ($CDCl_3$, 25.05°C, 700.03 MHz): δ 8.54 (d, $^{3}J_{HH}$ 9.0 Hz, 1 H, $C_{16}H_9$), 8.20 (d, $^{3}J_{HH}$ 7.5 Hz, 1 H, $C_{16}H_9$), 8.17 (d, $^{3}J_{HH}$ 7.5 Hz, 1 H, $C_{16}H_9$), 8.13 (d, $^{3}J_{HH}$ 9.0 Hz, 1 H, $C_{16}H_9$), 8.10 (d, $^{3}J_{HH}$ 8.0 Hz, 1 H, $C_{16}H_9$), 8.08 (d, $^{3}J_{HH}$ 8.0 Hz, 1 H, $C_{16}H_9$), 8.01-7.98 (m, 3 H, $C_{16}H_9$), 6.93-6.92 (m, 2 H, mtCH), 6.85 (m, 2 H, mtCH), 6.84-6.83 (m, 1 H, mtCH), 6.81 (m, 1 H, mtCH), 3.84 (s, 3 H, $mtCH_3$), 3.81 (s, 3 H, $mtCH_3$), 3.63 (s, 3 H, $mtCH_3$). $^{13}C\{^{1}H\}$ ($CDCl_3$, 25.75°C, 176.05 MHz): δ 247.0 ($W{\equiv}C^{\alpha}$), 225.1, 220.0 (WCO), 161.1, 159.1, 158.6 (mtCS), 132.9 ($C^{5}[C_{16}H_9]$), 131.5 (2C) ($C^{6,14}[C_{14}H_9]$), 131.0 ($C^{2}[C_{14}H_9]$), 130.5 ($C^{4}[C_{14}H_9]$), 128.2

(C[10][C14H9]), 128.1 (C[11][C14H9]), 127.6 (C[7][C14H9]), 126.4 (2C) (C[8,13][C14H9]), 125.6 (C[9][C14H9]), 125.4 (C[12][C14H9]), 124.8 (C[16][C14H9]), 124.7 (C[15][C14H9]), 124.4 (C[3][C14H9]), 123.1, 123.0 (2C), 120.3, 120.2, 120.1 (mtCH), 117.8 (WC$^{\beta}$), 113.4 (C[1][C14H9]), 74.0 (WC$^{\gamma}$), 35.3, 35.0, 34.9 (mtCH$_3$). MS (ESI, high resolution): m/z (%) = [M+Na]$^+$ 851.0687. Anal. Calcd. for $C_{33}H_{25}{}^{11}B_1N_6{}^{23}Na_1O_2S_3{}^{184}W_1$: [M+Na]$^+$ 851.0701. After numerous attempts an agreeable elemental microanalysis could not be obtained.

Tp*W(CO)$_2${≡C(1-(1,2,4,5-dehydro[2.2]paracyclophane))} (3.19)

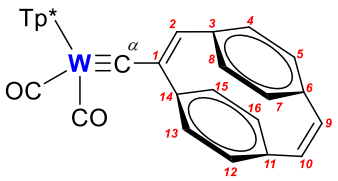

To a two-neck round bottom flask, [Tp*(CO)$_2$W≡C(SnBu$_3$)] (442 mg, 0.527 mmol), 1-bromo-1,2,4,5-dehydro[2.2]paracyclophane[§§§§§] (151 mg, 0.533 mmol), [Pd(PPh$_3$)$_4$] (61 mg, 0.053 mmol) and [AuCl(SMe$_2$)] (16 mg, 0.054 mmol) were combined, dispersed in toluene (40 mL), and the dark red mixture was stirred overnight at 90-100°C. Once cooled to room temperature, the mixture was concentrated to dryness and purified *via* silica-gel column chromatography (Eluent: Toluene), where collection and concentration of the major red band afforded **3.19** as a pink powder. Yield 306 mg (77%).

IR (CH_2Cl_2): ν_{BH} 2554 w; ν_{CO} 1973 vs, 1882 vs cm^{-1}. NMR ^{1}H ($CDCl_3$, 24.95°C, 700.03 MHz): δ 7.49 (s, 1 H, CH$_{alkene}$), 7.19 (s, 2 H, CH$_{alkene}$), 6.60 (s, 1 H, C$_6$H$_4$), 6.59 (s, 1 H, C$_6$H$_4$), 6.53-6.51 (m, 3 H, C$_6$H$_4$), 6.50-6.48 (m, 3 H, C$_6$H$_4$), 5.90 (s, 2 H, pzCH), 5.78 (s, 1 H, pzCH), 2.65 (s, 6 H, pzCH$_3$), 2.44 (s, 3 H, pzCH$_3$), 2.38 (s, 6 H, pzCH$_3$), 2.35 (s, 3 H, pzCH$_3$). ^{11}B{^{1}H} ($CDCl_3$, 24.85°C, 128.38 MHz): δ 40.95. ^{13}C{^{1}H} ($CDCl_3$, 25.05°C, 176.05 MHz): δ 271.9 (W≡C$^{\alpha}$, $^1J_{WC}$ 187.5 Hz), 224.1 (WCO, $^1J_{WC}$ 165.4 Hz), 160.2 (C[1][C16H11], $^2J_{WC}$ 44.3 Hz), 152.5, 152.1 (2C), 145.2, 144.5 (2C) (pz*C*CH$_3$), 138.1 (2C) (C$_6$H$_4$), 137.9 (C[9][C16H11]), 137.6 (C[10][C16H11]), 137.3 (2C) (C$_6$H$_4$), 137.2 (C[2][C16H11]), 137.1 (2C), 131.2 (2C), 130.7, 130.3, 129.2, 128.4 (C$_6$H$_4$), 106.8, 106.6 (2C) (pzCH), 16.9 (2C), 15.4, 12.8 (3C) (pzCH$_3$). MS (ESI, high resolution): m/z (%) = [M+H]$^+$ 753.2357. Calcd for $C_{34}H_{33}{}^{11}B_1N_6O_2{}^{184}W_1$: [M+H]$^+$ 753.2346. Elemental Anal. Found: C, 55.44; H, 4.56; N, 10.79%. Calcd. for $C_{34}H_{33}BN_6O_2W{\cdot}0.25(C_7H_8)$: C, 55.38; H, 4.55; N, 10.84%.

§§§§§ This compound, derived from [2.2]paracyclophane, is also referred to as (2*E*,5*Z*)-2-bromo-1,4(1,4)-dibenzenacyclohexaphane-2,5-diene.

[Tp*(CO)$_2$W≡C]$_2$-{1,9/10-(1,2,4,5-dehydro[2.2]paracyclophane)} (3.20)

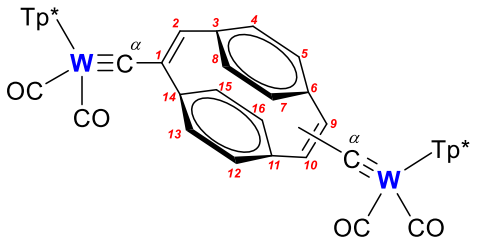

To a three-neck round bottom flask, [Tp*(CO)$_2$W≡C(SnBu$_3$)] (927 mg, 1.105 mmol), 1,9/10-dibromo-1,2,4,5-dehydro[2.2]-paracyclophane[******] (201 mg, 0.555 mmol), [Pd(PPh$_3$)$_4$] (129 mg, 0.112 mmol) and [AuCl(SMe$_2$)] (35 mg, 0.119 mmol) were combined, dispersed in toluene (80 mL), and the dark red mixture was stirred overnight at 90-100°C. Once cooled to room temperature, the mixture was concentrated to dryness and purified *via* silica-gel column chromatography (Eluent: Toluene), where collection and concentration of the major red band afforded **3.20** as a red powder. Yield 276 mg (38%).

IR (CH_2Cl_2): ν_{BH} 2554 m; ν_{CO} 1974 vs, 1883 vs cm^{-1}. NMR ^{1}H ($CDCl_3$, 24.95°C, 700.03 MHz): δ 7.48 (s, 2 H, C_6H_4), 6.58 (s, 3 H, C_6H_4), 6.50 (s, 3 H, C_6H_4), 5.90 (s, 4 H, pzCH), 5.78 (s, 2 H, pzCH), 2.64 (s, 12 H, pzCH_3), 2.51 (s, 2 H, CH_{alkene}), 2.44 (s, 6 H, pzCH_3), 2.37 (s, 12 H, pzCH_3), 2.34 (s, 6 H, pzCH_3). ^{11}B{^{1}H} ($CDCl_3$, 24.85°C, 128.38 MHz): δ 40.69. ^{13}C{^{1}H} ($CDCl_3$, 25.05°C, 176.05 MHz): δ 271.9 (W≡C$^\alpha$), 224.1 (WCO, $^1J_{WC}$ 165.5 Hz), 160.2 (WC*C*), 152.5, 152.1 (2C), 145.1, 144.5 (2C) (pz*C*CH$_3$), 138.2, 138.0, 137.8, 137.2, 131.5, 130.9, 130.6, 130.1, 129.3, 129.2, 128.4, 128.1 (C_6H_4), 127.5, 125.4 (CH_{alkene}), 106.7, 106.6 (2C) (pzCH), 21.6 (CH_{alkene}), 16.9 (2C), 16.7, 15.4, 12.8 (2C) (pzCH_3). MS (ESI, high resolution): *m*/*z* (%) = [M+Na]$^+$ 1323.3522; [M+H]$^+$ 1301.3702. Calcd. for $C_{52}H_{54}{}^{11}B_2N_{12}{}^{23}Na_1O_4{}^{184}W_2$: [M+Na]$^+$ 1323.3493; Calcd. for $C_{52}H_{55}{}^{11}B_2N_{12}O_4{}^{184}W_2$: [M+H]$^+$ 1301.3674. Elemental Anal. Found: C, 49.65; H, 4.17; N, 12.33%. Calcd. for $C_{52}H_{54}B_2N_{12}O_4W_2 \cdot 0.5(C_7H_8)$: C, 49.51; H, 4.34; N, 12.48%.

TmW(CO)$_2${≡C(9-[10-phenyl-anthracenyl])} (3.21)

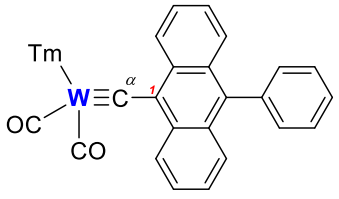

To a 100 mL Schlenk tube, 9-bromo-10-phenylanthracene (339 mg, 1.017 mmol) was added and dispersed in THF (40 mL), cooled to -78°C and ^{n}BuLi (1.6 M, 0.70 mL, 1.120 mmol) was added dropwise. The reaction mixture was maintained at -78°C for 10 minutes before being warmed in

[******] This compound, derived from [2.2]paracyclophane, is believed to contain a mixture of dibrominated products (based on ^{13}C{^{1}H} NMR). The isomers present in this mixture are also referred to as (2*E*,5*E*)-2,5-dibromo-1,4(1,4)-dibenzenacyclohexaphane-2,5-diene and (2*E*,5*E*)-2,6-dibromo-1,4(1,4)-dibenzenacyclohexaphane-2,5-diene. It is implied through the use of the name 1,9/10-dibromo-1,2,4,5-dehydro[2.2]-paracyclophane (above) that the mixture consists of approximately equal amounts of both isomers.

ambient air for 10 minutes, then re-cooled to -78°C. [$W(CO)_6$] (720 mg, 2.046 mmol) was added and stirred for 15 minutes before the mixture was warmed in ambient air for 30 minutes, then re-cooled to -78°C. Trifluoroacetic anhydride (0.15 mL, 1.079 mmol) was added dropwise into the orange mixture, stirred for 10 minutes, then warmed in ambient air for 30 minutes to promote the liberation of carbon monoxide gas. Finally, whilst cooled to -78°C, Na[Tm] (382 mg, 1.021 mmol) was added in a single batch and the brown reaction mixture slowly warmed to room temperature overnight. Stirring was halted after 16 h and the resulting brown reaction mixture was concentrated to dryness to afford a brown residue. The crude product mixture was purified *via* silica-gel column chromatography (Eluent: CH_2Cl_2), where isolation and concentration of the major brown band which moved off the baseline afforded **3.21** as a dark brown powder. Yield 484 mg (56%).

IR (CH_2Cl_2): ν_{BH} 2435 w; ν_{CO} 1969 vs, 1880 vs cm^{-1}. NMR ^1H ($CDCl_3$, 25.05°C, 700.03 MHz): δ 9.39 (d, $^3J_{HH}$ 8.7 Hz, 2 H, $C_{14}H_8$), 7.58 (d, $^3J_{HH}$ 8.8 Hz, 2 H, $C_{14}H_8$), 7.55-7.51 (m, 5 H, C_6H_5), 7.37 (m, 1 H, $C_{14}H_8$), 7.36 (m, 1 H, $C_{14}H_8$), 7.27-7.25 (m, 2 H, $C_{14}H_8$), 6.93 (d, $^3J_{HH}$ 1.9 Hz, 1 H, mtCH), 6.88 (d, $^3J_{HH}$ 2.1 Hz, 1 H, mtCH), 6.86 (q, $^3J_{HH}$ 2.1 Hz, 3 H, mtCH), 6.84 (d, $^3J_{HH}$ 2.1 Hz, 1 H, mtCH), 3.89 (s, 3 H, $mtCH_3$), 3.69 (s, 3 H, $mtCH_3$), 3.58 (s, 3 H, $mtCH_3$). $^{11}B\{^1H\}$ ($CDCl_3$, 24.85°C, 128.38 MHz): δ 48.48. $^{13}C\{^1H\}$ ($CDCl_3$, 25.05°C, 176.05 MHz): δ 279.5 (W≡C^{α}, $^1J_{WC}$ 196.2 Hz), 225.1 (WCO, $^1J_{WC}$ 172.2 Hz), 220.9 (WCO, $^1J_{WC}$ 165.7 Hz), 160.8, 159.3 (2C) (mtCS), 141.9 ($C^1[C_{20}H_{13}]$, $^2J_{WC}$ 40.3 Hz), 139.6, 136.8, 132.2, 131.0, 130.2, 128.4, 127.9, 127.4, 127.0, 125.8, 125.5 (aromatic), 123.2, 123.0, 122.8, 120.1, 120.0 (2C) (mtCH), 35.0, 34.9 (2C) ($mtCH_3$). MS (ESI, high resolution): m/z (%) = $[M]^+$ 856.1116; $[M-(CO)]^+$ 828.1165. Calcd. for $C_{35}H_{29}{}^{11}B_1N_6O_2S_3{}^{184}W_1$: $[M]^+$ 856.1116; Calcd. for $C_{34}H_{29}{}^{11}B_1N_6O_1S_3{}^{184}W_1$: $[M-(CO)]^+$ 828.1167. Elemental Anal. Found: C, 49.02; H, 3.45; N, 9.68; S, 11.13%. Calcd. for $C_{35}H_{29}BN_6O_2S_3W$: C, 49.08; H, 3.41; N, 9.81; S, 11.23%.

$TmW(CO)_2${≡C(9-[10-bromo-anthracenyl])} (3.22)

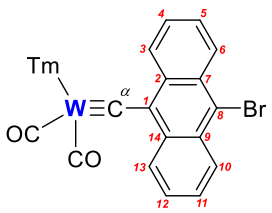

To a 250 mL Schlenk tube, 9,10-dibromoanthracene (3.00 g, 8.934 mmol) was added and dispersed in a 1:1 mixture of THF and Et_2O (120 mL), cooled to -78°C and ^{n}BuLi (1.6 M, 6.0 mL, 9.600 mmol) was added dropwise. The reaction mixture was maintained at -78°C for 10 minutes before being warmed in ambient air for 5 minutes, then re-cooled to -78°C. [$W(CO)_6$] (3.15 g, 8.963 mmol) was added and stirred for 15 minutes before the mixture was warmed in ambient air for 1 h, then re-cooled to -78°C. Trifluoroacetic anhydride (1.30 mL, 9.353 mmol) was added dropwise at

into the brown/red mixture, stirred for 15 minutes, then warmed in ambient air for 30 minutes to promote the liberation of carbon monoxide gas. Finally, whilst cooled to -78°C, Na[Tm] (3.36 g, 8.980 mmol) was added in a single batch and the brown/red reaction mixture slowly warmed to room temperature overnight. Stirring was halted after 16 h and the resulting orange/brown reaction mixture was concentrated to dryness to afford a brown solid. The crude product mixture was purified *via* silica-gel column chromatography (Eluent: CH_2Cl_2), where isolation and concentration of the major brown band which moved off the baseline afforded **3.22** as a brown powder which had a green shimmer. Yield 6.86 g (89%).

IR (CH_2Cl_2): ν_{BH} 2411 w; ν_{CO} 1972 vs, 1884 vs cm^{-1}. NMR ^1H ($CDCl_3$, 25.05°C, 700.03 MHz): δ 9.34 (d, $^3J_{HH}$ 8.6 Hz, 2 H, $C_{14}H_8$), 8.49 (d, $^3J_{HH}$ 8.7 Hz, 2 H, $C_{14}H_8$), 7.57-7.55 (m, 2 H, $C_{14}H_8$), 7.52-7.50 (m, 2 H, $C_{14}H_8$), 6.91 (d, $^3J_{HH}$ 1.9 Hz, 1 H, mtCH), 6.87 (d, $^3J_{HH}$ 2.0 Hz, 1 H, mtCH), 6.85 (d, $^3J_{HH}$ 2.0 Hz, 1 H, mtCH), 6.84 (t, $^3J_{HH}$ 2.1 Hz, 2 H, mtCH), 6.83 (d, $^3J_{HH}$ 2.0 Hz, 1 H, mtCH), 3.87 (s, 3 H, $mtCH_3$), 3.67 (s, 3 H, $mtCH_3$), 3.52 (s, 3 H, $mtCH_3$). $^{11}B\{^1H\}$ ($CDCl_3$, 24.85°C, 128.38 MHz): δ 48.28. $^{13}C\{^1H\}$ ($CDCl_3$, 24.95°C, 176.05 MHz): δ 277.4 (W≡C^{α}, $^1J_{WC}$ 196.2 Hz), 225.0 (WCO, $^1J_{WC}$ 171.1 Hz), 220.7 (WCO, $^1J_{WC}$ 164.6 Hz), 160.6, 159.1, 159.0 (mtCS), 142.4 ($C^1[C_{14}H_8]$, $^2J_{WC}$ 40.3 Hz), 133.0 ($C^{2,14}[C_{14}H_8]$), 130.5 ($C^{7,9}[C_{14}H_8]$), 128.4 ($C^{4,12}[C_{14}H_8]$), 127.8 ($C^{3,13}[C_{14}H_8]$), 127.2 ($C^{6,10}[C_{14}H_8]$), 126.2 ($C^{5,11}[C_{14}H_8]$), 123.2, 123.0, 122.8 (mtCH), 121.5 ($C^8[C_{14}H_8]$), 120.1 (2C), 120.0 (mtCH), 34.9 (2C), 34.8 ($mtCH_3$). MS (ESI, high resolution): m/z (%) = $[M(^{79}Br)]^+$ 858.9975; $[M(^{81}Br)]^+$ 860.9996; $[M(^{79}Br)\text{-}2(CO)\text{-}2H]^+$ 800.9937; $[M(^{81}Br)\text{-}2(CO)\text{-}2H]^+$ 802.9954. Calcd. for $C_{29}H_{25}{}^{11}B_1{}^{79}Br_1N_6O_2S_3{}^{184}W_1$: $[M(^{79}Br)]^+$ 858.9987; Calcd. for $C_{29}H_{25}{}^{11}B_1{}^{81}Br_1N_6O_2S_3{}^{184}W_1$: $[M(^{81}Br)]^+$ 860.9966; Calcd. for $C_{27}H_{23}{}^{11}B_1{}^{79}Br_1N_6S_3{}^{184}W_1$: $[M(^{79}Br)\text{-}2(CO)\text{-}2H]^+$ 800.9932; Calcd. for $C_{27}H_{23}{}^{11}B_1{}^{81}Br_1N_6S_3{}^{184}W_1$: $[M(^{81}Br)\text{-}2(CO)\text{-}2H]^+$ 802.9912. Elemental Anal. Found: C, 40.41; H, 2.94; N, 9.74; S, 11.43%. Calcd. for $C_{29}H_{25}BBrN_6O_2S_3W$: C, 40.49; H, 2.93; N, 9.77; S, 11.18%.

A crystal suitable for structure determination was grown by vapour diffusion of petroleum spirits (40-60°C) into a CH_2Cl_2 solution at 4°C (**Figure 5.7**). Crystal Data for $C_{29}H_{23}BBrN_6O_2S_3W$ (M =858.28 g/mol): monoclinic, space group $P2_1/c$ (no. 14), a = 9.4825(3) Å, b = 15.3301(4) Å, c = 22.6473(7) Å, β = 93.208(3)°, V = 3287.03(17) Å^3, Z = 4, T = 150.00(10) K, μ(CuKα) = 10.018 mm^{-1}, $Dcalc$ = 1.734 g/cm^3, 17260 reflections measured (7.82° ≤ 2Θ ≤ 133.182°), 5795 unique (R_{int} = 0.0390, R_{sigma} = 0.0399) which were used in all calculations. The final R_1 was 0.0566 (I > 2σ(I)) and wR_2 was 0.1584 (all data) for 391 refined parameters with 0 restraints.

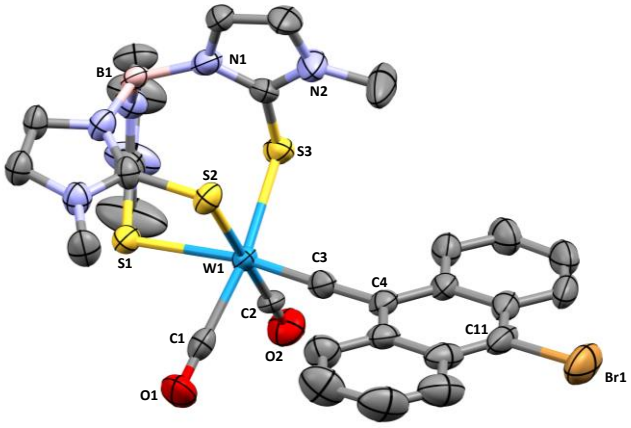

Figure 5.7. Molecular structure of **3.22** (50% displacement ellipsoids) with selected atom labels. Solvent molecules and hydrogen atoms omitted for clarity. Selected bond lengths (Å) and angles (°): W1–C1 2.033(9), W1–C2 2.025(9), W1–S1 2.655(2), W1–S2 2.567(2), W1–S3 2.525(2), W1–C3 1.837(9), C3–C4 1.441(12), C11–Br1 1.922(9); W1–C3–C4 178.6(7).

$TmW(CO)_2$={SC(9-[10-bromo-anthracenyl])} (3.23)

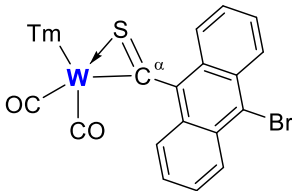

To a 100 mL three-neck round bottom flask, [$Tm(CO)_2W{\equiv}C$(9-[10-bromo-anthracenyl])] (**3.22**: 253 mg, 0.294 mmol) and excess S_8 (51 mg, 1.590 mmol) were combined and dispersed in THF (40 mL). The brown reaction mixture was heated at reflux overnight. Stirring was halted after 16 h and the reaction mixture was cooled to room temperature before being concentrated to dryness. The crude reaction mixture was purified *via* silica-gel column chromatography (Eluent: CH_2Cl_2), where isolation and concentration of the dark green band afforded **3.23** as a green/brown residue. Yield 42 mg (16%).

IR (CH_2Cl_2): ν_{CO} 1971 m, 1870 m cm^{-1}. NMR ^1H ($CDCl_3$, 24.85°C, 400.15 MHz): δ 8.50 (d, $^3J_{HH}$ 8.7 Hz, 2 H, $C_{14}H_8$), 8.09 (d, $^3J_{HH}$ 7.6 Hz, 2 H, $C_{14}H_8$), 7.54-7.50 (m, 2 H, $C_{14}H_8$), 7.47-7.44 (m, 2 H, $C_{14}H_8$), 7.05 (br s, 1 H, mtCH), 6.96-6.95 (m, 3 H, mtCH), 6.88 (d, $^3J_{HH}$ 1.7 Hz, 1 H, mtCH), 6.83 (d, $^3J_{HH}$ 1.8 Hz, 1 H, mtCH), 3.93 (br s, 3 H, $mtCH_3$), 3.82 (s, 3 H, $mtCH_3$), 3.68 (s, 3 H, $mtCH_3$). $^{11}B\{^1H\}$ ($CDCl_3$, 24.85°C, 128.38 MHz): δ 48.55. A $^{13}C\{^1H\}$ NMR of this complex could not be obtained due to its tendency to precipitate out of deuterated solvents over several hours. MS (ESI, high resolution): m/z (%) = $[M(^{79}Br)\text{-}2(CO)]^+$ 833.9712; $[M(^{81}Br)\text{-}2(CO)]^+$ 835.9733. Calcd. for $C_{27}H_{24}{}^{11}B_1{}^{79}Br_1N_6S_4{}^{184}W_1$: $[M(^{79}Br)\text{-}2(CO)]^+$ 833.9731; Calcd. for $C_{27}H_{24}{}^{11}B_1{}^{81}Br_1N_6S_4{}^{184}W_1$: $[M(^{81}Br)\text{-}2(CO)]^+$ 835.9711. Elemental Anal. Found: C, 39.06; H, 3.04; N, 9.04; S, 14.37%. Calcd. for $C_{29}H_{24}BBrN_6O_2S_4W$: C, 39.08; H, 2.71; N, 9.43; S, 14.39%.

TmW(CO)$_2${≡C(9-[10-bromo-triptycenyl])} (3.24)

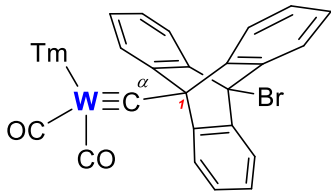

To a 100 mL Schlenk tube, [Tm(CO)$_2$W≡C(9-[10-bromo-anthracenyl])] (**3.22**: 500 mg, 0.582 mmol) was added, dispersed in THF (30 mL), and cooled to -78°C. To the brown mixture, 2-(trimethylsilyl)phenyl trifluoromethane sulfonate (0.70 mL, 2.884 mmol) was added *via* syringe, followed by TBAT‡‡‡‡‡‡ (1571 mg, 2.910 mmol) and stirring was continued for 15 minutes, before being allowed to slowly warm to room temperature overnight. Stirring was halted after 16 h and the brown reaction mixture was concentrated and purified *via* silica-gel column chromatography (Eluent: CH_2Cl_2), where isolation and concentration of the brown band which moved off the baseline afforded **3.24** as a brown powder. Yield 172 mg (32%).

IR (CH_2Cl_2): ν_{CO} 1972 w, 1884 w cm^{-1}. NMR ^{1}H ($CDCl_3$, 25.05°C, 700.03 MHz): δ 9.34 (d, $^3J_{HH}$ 8.6 Hz, 2 H, $C_{20}H_{12}$), 8.49 (d, $^3J_{HH}$ 8.7 Hz, 2 H, $C_{20}H_{12}$), 7.64 (dd, $^3J_{HH}$ 8.0, 1.3 Hz, 2 H, $C_{20}H_{12}$), 7.57-7.55 (m, 2 H, $C_{20}H_{12}$), 7.52-7.50 (m, 2 H, $C_{20}H_{12}$), 7.39 (t, $^3J_{HH}$ 7.3 Hz, 2 H, $C_{20}H_{12}$), 6.92 (d, $^3J_{HH}$ 2.0 Hz, 1 H, mtCH), 6.88 (d, $^3J_{HH}$ 2.1 Hz, 1 H, mtCH), 6.86 (d, $^3J_{HH}$ 2.1 Hz, 1 H, mtCH), 6.85 (d, $^3J_{HH}$ 2.0 Hz, 1 H, mtCH), 6.84 (t, $^3J_{HH}$ 2.4 Hz, 2 H, mtCH), 3.88 (s, 3 H, mtCH$_3$), 3.67 (s, 3 H, mtCH$_3$), 3.52 (s, 3 H, mtCH$_3$). ^{11}B{^{1}H} ($CDCl_3$, 24.85°C, 128.38 MHz): δ 48.45. ^{13}C{^{1}H} ($CDCl_3$, 25.05°C, 176.05 MHz): δ 277.5 (W≡C$^\alpha$, $^1J_{WC}$ 197.4 Hz), 225.0 (WCO, $^1J_{WC}$ 171.3 Hz), 220.7 (WCO, $^1J_{WC}$ 165.6 Hz), 160.7, 159.1 (2C) (mtCS), 142.4 (WC^1[$C_{20}H_{12}$Br], $^2J_{WC}$ 40.7 Hz), 135.4, 135.3 (2C), 135.1 (2C), 133.0, 130.5, 130.3, 128.4 (2C), 128.1 (2C), 127.8 (2C), 127.2 (2C), 126.2 (2C) ($C_{20}H_{12}$Br), 123.2, 123.0, 122.8 (mtCH), 121.6 ($C_{20}H_{12}$), 120.1 (2C), 120.0 (mtCH), 34.9 (3C) (mtCH$_3$). MS (ESI, high resolution): *m*/*z* (%) = [M(^{79}Br)-2(CO)+H]$^+$ 879.0370; [M(^{81}Br)-2(CO)+H]$^+$ 881.0386. Calcd. for $C_{33}H_{29}{}^{11}B_1{}^{79}Br_1N_6S_3{}^{184}W_1$: [M(^{79}Br)-2(CO)+H]$^+$ 879.0402; Calcd. for $C_{33}H_{29}{}^{11}B_1{}^{81}Br_1N_6S_3{}^{184}W_1$: [M(^{81}Br)-2(CO)+H]$^+$ 881.0381. Elemental Anal. Found: C, 44.92; H, 3.06; N, 8.47; S, 9.87%. Calcd. for $C_{35}H_{28}BBrN_6O_2S_3W$: C, 44.94; H, 3.02; N, 8.98; S, 10.28%.

‡‡‡‡‡ TBAT – Tetrabutylammonium difluorotriphenylsilicate. CAS Registry No.: 163931-61-1.

[TmW(CO)$_2${≡C(9-[10-bromo-anthracenyl])}]$_2$Pt (3.25)

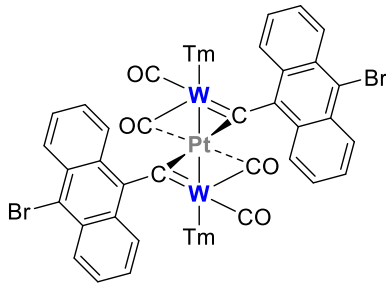

To a 100 mL round-bottom flask, [Tm(CO)$_2$W≡C(9-[10-bromo-anthracenyl])] (**3.22**: 100 mg, 0.116 mmol) and [Pt(nbe)$_3$] (nbe = norbornene) (28 mg, 0.059 mmol) were combined, dispersed in CH_2Cl_2 (20 mL), and stirred at room temperature for 1 h. The brown reaction mixture was concentrated to dryness to afford a brown residue and purified *via* silica-gel column chromatography (Eluent: 5% (v/v) THF/CH_2Cl_2). Isolation and subsequent concentration of the dark brown band which moved off the baseline afforded **3.25** as a brown powder. Yield 40 mg (36%).

IR (CH_2Cl_2): ν_{CO} 1949 s, 1927 s, 1792 br cm^{-1}. ^{1}H and ^{13}C{^{1}H} NMR data of this complex could not be obtained due to its tendency to rapidly precipitate out of deuterated solvents. ^{11}B{^{1}H} ($CDCl_3$, 24.85°C, 128.38 MHz): δ 48.48. MS (ESI, high resolution): *m/z* (%) = [M(^{79}Br$_2$)]$^+$ 1910.9453; [M(^{79}Br, ^{81}Br)]$^+$ 1912.9470; [M(^{81}Br$_2$)]$^+$ 1914.9482. Calcd. for $C_{58}H_{48}{}^{11}B_2{}^{79}Br_2N_{12}O_4{}^{195}Pt_1S_6{}^{184}W_2$: [M(^{79}Br$_2$)]$^+$ 1910.9465; Calcd. for $C_{58}H_{48}{}^{11}B_2{}^{79}Br_1{}^{81}Br_1N_{12}O_4{}^{195}Pt_1S_6{}^{184}W_2$: [M(^{79}Br, ^{81}Br)]$^+$ 1912.9445; Calcd. for $C_{58}H_{48}{}^{11}B_2{}^{81}Br_2N_{12}O_4{}^{195}Pt_1S_6{}^{184}W_2$: [M(^{81}Br$_2$)]$^+$ 1914.9424. Elemental Anal. Found: C, 38.62; H, 2.90; N, 8.54; S, 9.56%. Calcd. for $C_{58}H_{48}B_2Br_2N_{12}O_4PtS_6W_2 \cdot 2(C_4H_8O)$: C, 38.52; H, 3.13; N, 8.17; S, 9.35%.

A crystal suitable for structure determination was grown by vapour diffusion of ethanol into a $CHCl_3$ solution at 4°C (**Figure 5.8**). A region of highly disordered solvent could not be adequately modelled and were removed using a solvent mask; the data which follows is presented excluding solvent. Crystal data for $C_{58}H_{48}B_2Br_2N_{12}O_4PtS_6W_2$ (M = 1913.67 g/mol): triclinic, space group P-1 (no. 2), a = 16.120(3), b = 16.920(3), c = 18.522(4) Å, α = 85.80(3)°, β = 70.72(3)°, γ = 68.87(3)°, V = 4441.9(19) Å^3, Z = 2, T = 100.0(2) K, μ(Synchrotron) = 5.235 mm^{-1}, D_{calc} = 1.431 g cm^{-3}, 81298 reflections measured (2.332° ≤ 2Θ ≤ 64.49°), 23122 unique (R_{int} = 0.0800, R_{sigma} = 0.0725) which were used in all calculations. The final R_1 was 0.0616 (I > 2σ(I)) and wR_2 was 0.1846 (all data) for 792 refined parameters with 6 restraints.

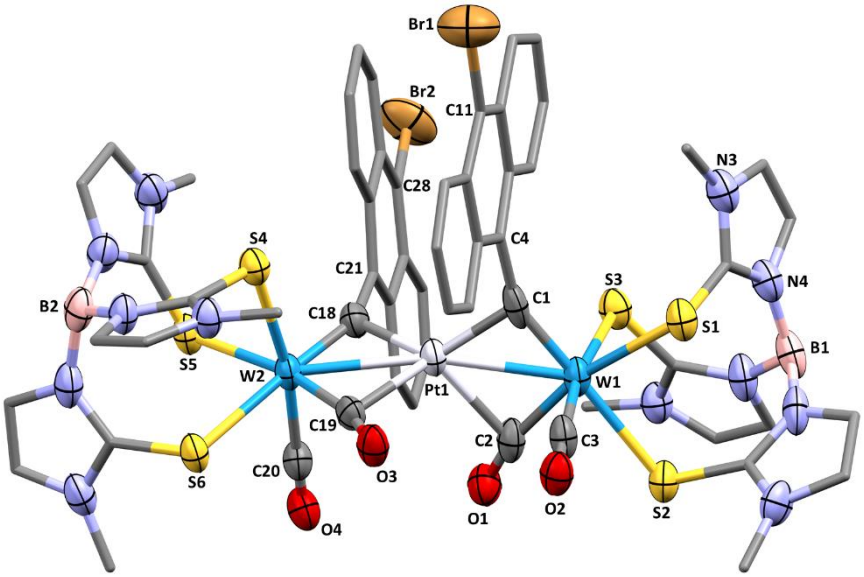

Figure 5.8. Molecular structure of **3.25** (30% displacement ellipsoids) with selected atom labels. Solvent molecules and hydrogen atoms omitted for clarity. Selected distances (Å) and angles (°): W1–Pt1 2.7208(7), W2–Pt1 2.7254(7), Pt1–C1 2.020(8), Pt1–C2 2.272(10), Pt1–C18 2.024(8), Pt1–C19 2.283(7), W1–C1 1.872(11), W1–C2 1.997(11), W2–C18 1.905(8), W2–C19 2.010(9), C1–C4 1.499(13), C18–C21 1.458(11), C11–Br1 1.901(12), C28–Br2 1.938(8), W1–Pt1–W2 166.550(18), C1–Pt1–C2 89.5(4), W1–C1–Pt1 88.6(4), W1–C1–C4 153.6(6), W1–C2–O1 166.7(8), W2–C18–Pt1 87.8(3), W2–C18–C21 152.9(6), W2–C19–O2 164.8(6).

[TmW(CO)$_2${≡C(9-[10-bromo-anthracenyl])}]$_2$Pd (3.26)

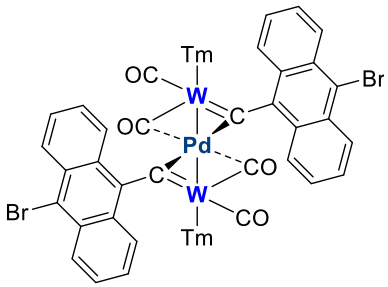

To a 100 mL round-bottom flask, [Tm(CO)$_2$W≡C(9-[10-bromo-anthracenyl])] (**3.22**: 201 mg, 0.234 mmol) and [Pd$_2$(dba)$_3$·CHCl$_3$] (dba = dibenzylideneacetone) (61 mg, 0.059 mmol) were combined, dispersed in CH$_2$Cl$_2$ (30 mL), and stirred at room temperature for 1.5 h. The brown reaction mixture was concentrated to dryness to afford a brown residue and purified *via* silica-gel column chromatography (Eluent: Gradient 100% CH$_2$Cl$_2$ to 4% (v/v) THF/CH$_2$Cl$_2$). Isolation and subsequent concentration of the dark red/brown band which moved off the baseline afforded **3.26** as a brown/red powder. Yield 106 mg (50%).

IR (CH$_2$Cl$_2$): ν_{CO} 1945 s, 1923 s, 1808 br cm^{-1}. ^{1}H (CDCl$_3$, -40.05°C, 700.03 MHz): δ 9.27 (d, $^3J_{HH}$ 8.6 Hz, 4 H, C$_{14}$H$_8$), 8.47 (d, $^3J_{HH}$ 8.6 Hz, 4 H, C$_{14}$H$_8$), 7.57 (t, $^3J_{HH}$ 8.3 Hz, 4 H, C$_{14}$H$_8$), 7.52 (t, $^3J_{HH}$ 7.0 Hz, 4 H, C$_{14}$H$_8$), 6.95 (d, $^3J_{HH}$ 1.8 Hz, 2 H, mtCH), 6.92-6.90 (m, 6 H, mtCH), 6.87 (d, $^3J_{HH}$ 1.9 Hz, 2 H, mtCH), 6.85 (d, $^3J_{HH}$ 1.9 Hz, 2 H, mtCH), 3.86 (s, 6 H, mtCH$_3$), 3.67 (s, 6 H, mtCH$_3$), 3.55 (s, 6 H, mtCH$_3$). The intrinsic insolubility of this complex

in $CDCl_3$ precluded the identification of all expected $^{13}C\{^1H\}$ NMR signals. The following incomplete data are included here and with some tentative peak assignments. $^{13}C\{^1H\}$ ($CDCl_3$, -40.05°C, 176.05 MHz): δ 224.9, 220.2 (WCO), 159.6, 158.2, 158.1 (mtCS), 141.9, 135.4, 134.4, 133.3, 132.8, 130.8, 130.1, 128.7, 128.0, 127.8, 127.3, 127.2, 127.1, 126.9, 126.3, 125.7, 124.3, 123.1, 122.8, 122.7, 121.8, 120.2, 120.0 ($C_{14}H_8$ & mtCH), 35.1, 35.0, 34.3, 30.2, 29.9, 25.7 ($mtCH_3$). MS (ESI, high resolution): *m/z* (%) = $[M(^{79}Br_2)]^+$ 1821.8843; $[M(^{79}Br, ^{81}Br)]^+$ 1823.8853; $[M(^{81}Br_2)]^+$ 1825.8866. Calcd. for $C_{58}H_{48}{}^{11}B_2{}^{79}Br_2N_{12}O_4{}^{106}Pd_1S_6{}^{184}W_2$: $[M(^{79}Br_2)]^+$ 1821.8852; Calcd. for $C_{58}H_{48}{}^{11}B_2{}^{79}Br_1{}^{81}Br_1N_{12}O_4{}^{106}Pd_1S_6{}^{184}W_2$: $[M(^{79}Br, ^{81}Br)]^+$ 1823.8832; Calcd. for $C_{58}H_{48}{}^{11}B_2{}^{81}Br_2N_{12}O_4{}^{106}Pd_1S_6{}^{184}W_2$: $[M(^{81}Br_2)]^+$ 1825.8811. Elemental Anal. Found: C, 38.18; H, 2.67; N, 9.24; S, 10.29%. Calcd. for $C_{58}H_{48}B_2Br_2N_{12}O_4PdS_6W_2$: C, 38.17; H, 2.65; N, 89.21; S, 10.54%.

A crystal suitable for structure determination was grown by vapour diffusion of ethanol into a $CHCl_3$ solution at 4°C (**Figure 5.9**).

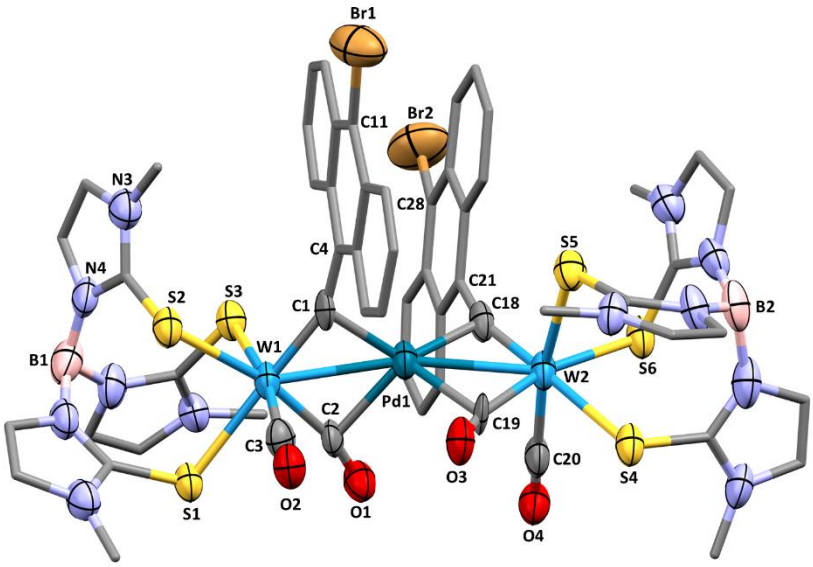

Figure 5.9. Molecular structure of **3.26** (30% displacement ellipsoids) with selected atom labels. Solvent molecules and hydrogen atoms omitted for clarity. Due to the low quality of this synchrotron data, the extensive use of restraints and the solvent mask that was required, this dataset is only included as evidence of connectivity.

A region of highly disordered solvent could not be adequately modelled and were removed using a solvent mask; the data which follows is presented excluding solvent. Crystal data for $C_{58}H_{48}B_2Br_2N_{12}O_4PtS_6W_2$ (M = 1913.67 g/mol): triclinic, space group P-1 (no. 2), a = 16.120(3), b = 16.920(3), c = 18.522(4) Å, α = 85.80(3)°, β = 70.72(3)°, γ = 68.87(3)°, V = 4441.9(19) Å^3, Z = 2, T = 100.0(2) K, μ(Synchrotron) = 5.235 mm^{-1}, *Dcalc* =1.431 g cm^{-3},

81298 reflections measured (2.332° ≤ 2Θ ≤64.49°), 23122 unique (R_{int} = 0.0800, R_{sigma} = 0.0725) which were used in all calculations. The final R_1 was 0.0616 (I > 2σ(I)) and wR_2 was 0.1846 (all data) for 792 refined parameters with 6 restraints.

TmW(CO)$_2${μ-C-(9,10-anthracenyl)-C≡}W(CO)$_2$Tp* (3.27)

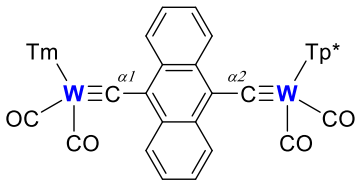

To a 100 mL three-neck round bottom flask, [Tm(CO)$_2$W≡C(9-[10-bromo-anthracenyl])] (**3.22**: 200 mg, 0.233 mmol), [Tp*(CO)$_2$W≡C(SnBu$_3$)] (200 mg, 0.238 mmol), [AuCl(SMe$_2$)] (8 mg, 0.027 mmol) and [Pd(PPh$_3$)$_4$] (27 mg, 0.023 mmol) were combined, dispersed in toluene (40 mL) and the brown mixture stirred at 90°C for 3 h. Once cooled to room temperature, the purple reaction mixture was concentrated to dryness and purified *via* silica-gel column chromatography (Eluent: CH_2Cl_2), where isolation and concentration of the major vivid purple band which moved off the baseline afforded **3.27** as a dark purple solid. Yield 198 mg (64%)

IR (CH_2Cl_2): ν_{CO} 1974 s, 1966 s, 1884 s cm^{-1}. NMR ^{1}H ($CDCl_3$, 24.95°C, 700.03 MHz): δ 9.28 (d, $^3J_{HH}$ 8.5 Hz, 2 H, $C_{14}H_8$), 7.57-7.55 (m, 1 H, $C_{14}H_8$), 7.52-7.50 (m, 1 H, $C_{14}H_8$), 7.45 (br, 2 H, $C_{14}H_8$), 6.92 (d, $^3J_{HH}$ 2.0 Hz, 1 H, mtCH), 6.87 (d, $^3J_{HH}$ 2.0 Hz, 1 H, mtCH), 6.85-6.84 (m, 3 H, mtCH), 6.83 (d, $^3J_{HH}$ 2.1 Hz, 1 H, mtCH), 5.84 (s, 2 H, pzCH), 5.81 (s, 1 H, pzCH), 3.86 (s, 3 H, mtCH$_3$), 3.67 (s, 3 H, mtCH$_3$), 3.55 (s, 3 H, mtCH$_3$), 2.53 (s, 3 H, pzCH$_3$), 2.46 (s, 6 H, pzCH$_3$), 2.39 (s, 3 H, pzCH$_3$), 2.22 (s, 6 H, pzCH$_3$). ^{1}H ($CDCl_3$, -40.05°C, 700.03 MHz): δ 9.30-9.27 (m, 1 H, $C_{14}H_8$), 9.18 (d, $^3J_{HH}$ 7.8 Hz, 1 H, $C_{14}H_8$), 9.13 (d, $^3J_{HH}$ 8.1 Hz, 1 H, $C_{14}H_8$), 7.68-7.66 (m, 1 H, $C_{14}H_8$), 7.58-7.51 (m, 2 H, $C_{14}H_8$), 7.39-7.37 (m, 1 H, $C_{14}H_8$), 7.12-7.10 (m, 1 H, $C_{14}H_8$), 6.94 (d, $^3J_{HH}$ 1.9 Hz, 1 H, mtCH), 6.90 (br s, 2 H, mtCH), 6.88 (d, $^3J_{HH}$ 2.0 Hz, 1 H, mtCH), 6.85 (d, $^3J_{HH}$ 2.1 Hz, 1 H, mtCH), 6.84 (d, $^3J_{HH}$ 2.0 Hz, 1 H, mtCH), 5.84 (s, 2 H, pzCH), 5.82 (s, 1 H, pzCH), 3.85 (s, 3 H, mtCH$_3$), 3.66 (s, 3 H, mtCH$_3$), 3.55 (s, 3 H, mtCH$_3$), 2.52 (s, 3 H, pzCH$_3$), 2.45 (s, 6 H, pzCH$_3$), 2.38 (s, 3 H, pzCH$_3$), 2.18 (s, 6 H, pz CH$_3$). ^{11}B{^{1}H} ($CDCl_3$, 24.85°C, 128.38 MHz): δ 48.41. ^{13}C{^{1}H} ($CDCl_3$, -39.95°C, 176.05 MHz): δ 282.0, 279.3 (W≡C), 227.6, 227.5, 225.4, 220.8 (WCO), 159.7, 158.2 (2C) (mtCS), 152.2, 152.1 (2C), 145.2, 144.4 (2C) (pz*C*CH$_3$), 141.7, 139.6, 134.0, 132.8, 132.1, 131.8, 131.2, 130.1, 128.0, 127.8, 127.2, 126.8 (2C), 126.3 ($C_{14}H_8$), 123.1, 122.8, 122.7, 120.1 (2C), 120.0 (mtCH), 106.6, 106.2 (2C) (pzCH), 35.1, 35.0 (2C) (mtCH$_3$), 16.1 (2C), 15.6, 13.2 (2C), 12.9 (pzCH$_3$). MS (ESI, high resolution): *m*/*z* (%) = [M]$^+$ 1329.2211; [M-CO]$^+$ 1301.2244. Calcd. for $C_{47}H_{47}{}^{11}B_1N_{12}O_4S_3{}^{184}W_2$: [M]$^+$ 1329.2210; Calcd. for

$C_{46}H_{47}{}^{11}B_1N_{12}O_3S_3{}^{184}W_2$: $[M\text{-}CO]^+$ 1301.2261. Elemental Anal. Found: C, 42.43; H, 3.54; N, 12.13; S, 7.42%. Calcd. for $C_{47}H_{47}B_2N_{12}O_4S_3W_2$: C, 42.46; H, 3.56; N, 12.64; S, 7.24%.

A crystal suitable for structure determination was grown by vapour diffusion of *n*-pentane into a CH_2Cl_2 solution at 4°C (**Figure 5.10**).

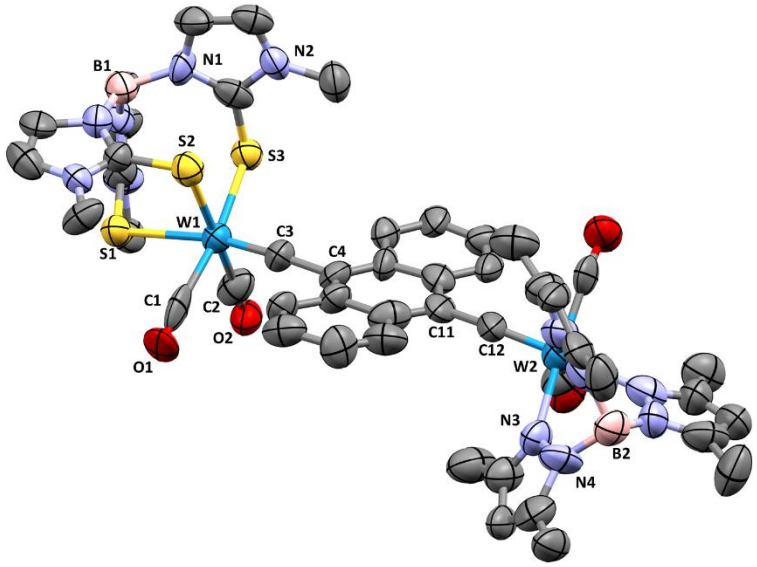

Figure 5.10. Molecular structure of **3.27** (50% displacement ellipsoids) with selected atom labels. Solvent molecules and hydrogen atoms omitted for clarity. The low quality of the acquired synchrotron data means that this structural model is included only as evidence of connectivity.

The low quality of the acquired synchrotron data means that this structural model is included only as evidence of connectivity. Crystal Data for $C_{47}H_{46}B_2N_{12}O_4S_3W_2$ (M =1328.46 g/mol): triclinic, space group P-1 (no. 2), a = 10.394(8) Å, b = 14.743(8) Å, c = 16.870(9) Å, a = 84.501(14)°, β = 89.910(17)°, γ = 80.987(12)°, V = 2541(3) Å^3, Z = 2, T = 293(2) K, μ(MoKα) = 4.702 mm^{-1}, *Dcalc* = 1.736 g/cm^3, 29629 reflections measured (2.426° ≤ 2Θ ≤ 57.056°), 8699 unique (R_{int} = 0.0989, R_{sigma} = 0.0949) which were used in all calculations. The final R_1 was 0.0987 (I > 2σ(I)) and wR_2 was 0.3237 (all data) for 641 refined parameters with 66 restraints.

$TmW(CO)_2\{\mu\text{-}C\text{-}(9,10\text{-anthracenyl})\text{-}C{\equiv}\}Mo(CO)_2Tp^*$ (3.28)

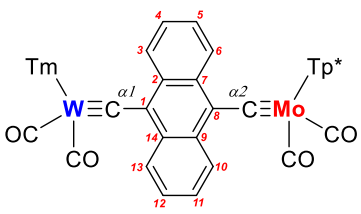

To a 100 mL three-neck round-bottom flask, [$Tm(CO)_2W{\equiv}C$(9-[10-bromo-anthracenyl])] (**3.22**: 202 mg, 0.235 mmol), [$Tp^*(CO)_2Mo{\equiv}C(Sn^nBu_3)$] (180 mg, 0.240 mmol), [$Pd(PPh_3)_4$] (28 mg, 0.024 mmol) and [$AuCl(SMe_2)$] (8 mg, 0.027 mmol) were combined,

dispersed in toluene (40 mL), and the brown reaction mixture heated to 90°C overnight. Stirring was halted after 16 h and the purple reaction mixture cooled to room temperature and concentrated to afford a purple residue. The crude reaction mixture was purified *via* silica-gel column chromatography (Eluent: CH_2Cl_2), where isolation and concentration of the major purple band afforded **3.28** as a dark purple micro-crystalline powder. Yield 133 g (46%).

IR (CH_2Cl_2): ν_{CO} 1987 vs, 1970 vs, 1903 vs, 1884 vs cm^{-1}. NMR ^1H ($CDCl_3$, 25.05°C, 700.03 MHz): δ 9.25 (s, 2 H, $C_{14}H_8$), 8.84 (br 2 H, $C_{14}H_8$), 7.48-7.37 (br, 4 H, $C_{14}H_8$), 6.93-6.85 (br, 6 H, mtCH), 5.79 (m, 3 H, pzCH), 3.87, (s, 3 H, $mtCH_3$), 3.67 (s, 3 H, $mtCH_3$), 3.55 (s, 3 H, $mtCH_3$), 2.48 (s, 3 H, $pzCH_3$), 2.45 (s, 6 H, $pzCH_3$), 2.39 (s, 3 H, $pzCH_3$), 2.20 (s, 6 H, $pzCH_3$). NMR ^1H ($CDCl_3$, -50.05°C, 700.03 MHz): δ 9.27 (d, $^3J_{HH}$ 7.6 Hz, 1 H, $C_{14}H_8$), 9.20 (d, $^3J_{HH}$ 6.9 Hz, 1 H, $C_{14}H_8$), 9.14 (d, $^3J_{HH}$ 7.4 Hz, 1 H, $C_{14}H_8$), 8.48 (d, $^3J_{HH}$ 7.0 Hz, 1 H, $C_{14}H_8$), 7.66 (br, 1 H, $C_{14}H_8$), 7.58 (br, 1 H, $C_{14}H_8$), 7.42 (br, 1 H, $C_{14}H_8$), 7.15 (br, 1 H, $C_{14}H_8$), 6.95 (s, 1 H, mtCH), 6.92-6.90 (br m, 3 H, mtCH), 6.85 (d, $^3J_{HH}$ 7.2 Hz, 2 H, mtCH), 5.80 (s, 3 H, pzCH), 3.85 (s, 3 H, $mtCH_3$), 3.66 (s, 3 H, $mtCH_3$), 3.56 (s, 3 H, $mtCH_3$), 2.47 (s, 3 H, $pzCH_3$), 2.44 (s, 3 H, $pzCH_3$), 2.38 (s, 3 H, $pzCH_3$), 2.16 (s, 3 H, $pzCH_3$). $^{13}C\{^1H\}$ ($CDCl_3$, -50.05°C, 176.05 MHz): δ 249.1 ($Mo{\equiv}C^{\alpha 2}$), 278.2 ($W{\equiv}C^{\alpha 1}$), 229.3, 229.2, 225.2, 220.5 (CO), 159.4, 157.9 (2C) (mtCS), 151.2 ($pzCCH_3$), 145.1 ($C^1[C_{14}H_8]$), 144.4 ($pzCCH_3$), 142.3 ($C^8[C_{14}H_8]$), 136.2 ($C^2[C_{14}H_8]$), 134.5 ($C^{14}[C_{14}H_8]$), 131.8 ($C^9[C_{14}H_8]$), 131.5 ($C^7[C_{14}H_8]$), 131.3 ($C^4[C_{14}H_8]$), 128.3 ($C^{12}[C_{14}H_8]$), 127.9 ($C^{11}[C_{14}H_8]$), 127.4 ($C^5[C_{14}H_8]$), 127.1 ($C^3[C_{14}H_8]$), 126.6 ($C^{13}[C_{14}H_8]$), 126.3 ($C^6[C_{14}H_8]$), 126.2 ($C^{10}[C_{14}H_8]$), 123.1, 122.8, 122.7, 120.2 (2C), 120.0 (mtCH), 106.3, 105.8 (2C) (pzCH), 35.1 (2C), 35.0 ($mtCH_3$), 15.4 (2C), 15.0, 13.3 (2C), 13.0 ($pzCH_3$). MS (ESI, high resolution): m/z (%) = $[M]^+$ 1242.1711. Calcd. for $C_{47}H_{46}{}^{11}B_2{}^{98}Mo_1N_{12}O_4{}^{184}W_1$: $[M]^+$ 1242.1677. Elemental Anal. Found: C, 45.52; H, 3.61; N, 12.73; S, 7.61%. Calcd. for $C_{47}H_{46}B_2MoN_{12}O_4S_3W$: C, 45.50; H, 3.74; N, 13.55; S, 7.75%.

A crystal suitable for structure determination was grown by vapour diffusion of ethanol into a $CHCl_3$ solution at 4°C (**Figure 5.11**). Crystal data for $C_{47}H_{46}B_2MoN_{12}O_4S_3W$ (M = 1240.55 g/mol): triclinic, space group P-1 (no. 2), a = 10.324(2), b = 14.829(3), c = 17.015(3) Å, α = 84.43(3)°, β = 90.00(3)°, γ = 80.97(3)°, V = 2560.1(9) Å^3, Z = 2, T = 100.0(2) K, μ(Synchrotron) = 2.667 mm^{-1}, D_{calc} = 1.609 Mg m^{-3}, 31968 reflections measured (2.406° ≤ 2Θ ≤ 52.738°), 9542 unique (R_{int} = 0.1066, R_{sigma} = 0.0998) which were used in all calculations. The final R_1 was 0.0747 (I > 2σ(I)) and wR_2 was 0.2384 (all data) for 648 refined parameters without restraints.

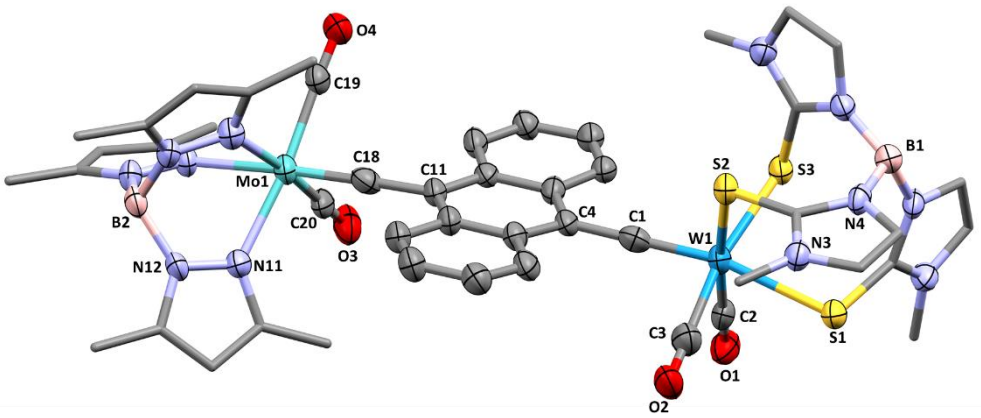

Figure 5.11. Molecular structure of **3.28** (30% displacement ellipsoids) with selected atom labels. Solvent molecules and hydrogen atoms omitted for clarity. Selected bond lengths (Å) and angles (°): W1–S3 2.540(3), W1–S2 2.546(3), W1–S1 2.652(3), W1–C1 1.817(12), Mo1–N7 2.319(9), Mo1–N9 2.224(9), Mo1–N11 2.233(8), Mo1–C18 1.796(11), C1–C4 1.456(15), C11–C18 1.478(14), C25–S3–W1 108.0(4), C29–S2–W1 104.4(4), C21–S1–W1 105.5(4), C4–C1–W1 178.6(9), C11–C18–Mo1 171.9(9).

5.2.4 Chapter 4 – Aminocarbyne Complexes

TmMo(CO)$_2${≡CN(Et$_2$)} (4.1)

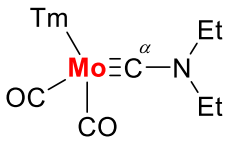

To a 100 mL Schlenk tube, diethylamine (0.21 mL, 2.030 mmol) was dispersed in THF (40 mL), cooled to -78°C and ^{n}BuLi (2.5 M, 0.88 mL, 2.200 mmol) was added dropwise. The reaction mixture was maintained at -78°C for 5 minutes before being warmed in ambient air for 15 minutes, then re-cooled to -78°C and stirred for a further 10 minutes. [Mo(CO)$_6$] (529 mg, 2.004 mmol) was added and stirred for 15 minutes before the light yellow mixture was warmed in ambient air for 10 minutes, causing it to turn orange, then re-cooled to -78°C for 20 minutes. Trifluoroacetic anhydride (0.28 mL, 2.014 mmol) was added slowly dropwise into the reaction mixture, stirred for 10 minutes, then warmed in ambient air to promote the liberation of carbon monoxide gas. Stirring was continued until bubbles of carbon monoxide gas were no longer observed in the solution. Finally, whilst cooled to -78°C, Na[Tm] (751 mg, 2.007 mmol) was added in single batch and the brown dispersion slowly warmed to room temperature overnight. The resulting brown mixture was concentrated to dryness and purified *via* silica-gel column chromatography (Eluent: 2% (v/v) THF/CH_2Cl_2). The major orange band which moved off the baseline was collected and concentrated to dryness to provide **4.1** as a beige powder. Yield 107 mg (9%).

IR (CH_2Cl_2): ν_{CO} 1944 vs, 1845 vs cm^{-1}. NMR ^1H ($CDCl_3$, 24.95°C, 700.03 MHz): δ 6.78 (br s, 6 H, 6 × mtC*H*), 3.63 (br s, 9 H, 3 × mtC*H*$_3$), 3.23 (m, 4 H, 2 × C*H*$_2$CH$_3$), 1.29 (t, $^3J_{HH}$ 7.2 Hz, 6 H, 2 × CH$_2$C*H*$_3$). ^1H ($CDCl_3$, -40.05°C, 700.03 MHz): δ 6.82 (d, $^3J_{HH}$ 1.9 Hz, 2 H, 2 × mtC*H*), 6.80 (d, $^3J_{HH}$ 1.9 Hz, 2 H, 2 × mtC*H*), 6.77 (d, $^3J_{HH}$ 2.0 Hz, 1 H, mtC*H*), 6.75 (d, $^3J_{HH}$ 2.0 Hz, 1 H, mtC*H*), 3.69 (s, 3 H, mtC*H*$_3$), 3.62 (2 × s overlapping, 6 H, 2 × mtC*H*$_3$), 3.27-3.22 (m, 2 H, C*H*$_2$CH$_3$), 3.21-3.16 (m, 2 H, C*H*$_2$CH$_3$), 1.27 (t, $^3J_{HH}$ 7.2 Hz, 6 H, 2 × CH$_2$C*H*$_3$). $^{11}B\{^1H\}$ ($CDCl_3$, 24.85°C, 128.38 MHz): δ -1.54. $^{13}C\{^1H\}$ ($CDCl_3$, -40.05°C, 176.05 MHz) δ 256.2 (Mo≡C$^{\alpha}$), 229.9, 225.1 (MoCO), 161.4, 160.0, 159.8 (mtCS), 122.4, 122.3, 122.1, 119.6, 119.5, 119.3 (mtCH), 45.6 (2C) (*C*H$_2$CH$_3$), 35.0, 34.9, 34.6 (mtCH$_3$), 14.7 (2C) (CH$_2$*C*H$_3$). MS (ESI, high resolution): *m*/*z* (%) = $[M–2(CO)]^+$ 533.0550. Calcd. for $C_{17}H_{26}{}^{11}B_1{}^{98}Mo_1N_7S_3$: $[M–2(CO)]^+$ 533.0559. Elemental Anal. Found: C, 38.84; H, 4.78; N, 16.55; S, 16.50%. Calcd. for $C_{19}H_{26}BMoN_7O_2S_3$: C, 38.85; H, 4.46; N, 16.69; S, 16.38%.

(Htt)W(CO)$_2${≡CN(Et$_2$)} (4.2)

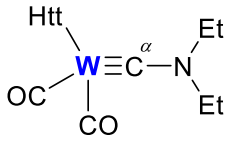

To a 100 mL Schlenk tube, diethylamine (0.21 mL, 2.030 mmol) was dispersed in THF (40 mL), cooled to -78°C and ^{n}BuLi (1.6 M, 1.4 mL, 2.240 mmol) added dropwise over 2 minutes. The colourless mixture was stirred at -78°C for 5 minutes before being warmed in ambient air for 15 minutes. After re-cooling to -78°C for 10 minutes, [W(CO)$_6$] (706 mg, 2.006 mmol) was added and the light-yellow dispersion stirred for 15 minutes, warmed in ambient air for 10 minutes, and finally re-cooled to -78°C for 20 minutes. Trifluoroacetic anhydride (0.28 mL, 2.014 mmol) was added slowly dropwise at -78°C and the resulting yellow reaction mixture stirred for 10 minutes, before being warmed in ambient air to promote the liberation of carbon monoxide gas. Stirring was continued until bubbles of carbon monoxide gas were no longer observed in the solution. Finally, whilst cooled to -78°C, Na[Htt] (1.013 g, 2.002 mmol) was added in single batch and the light yellow dispersion slowly warmed to room temperature overnight. Stirring of the resulting clear orange/brown solution was halted after 16 h and concentrated to dryness. The crude reaction mixture was purified *via* silica-gel column chromatography (Eluent: CH_2Cl_2). Collection and subsequent concentration of the major orange band afforded **4.2** as an orange powder. Yield 407 mg (25%).

IR (CH_2Cl_2): ν_{BH} 2530 w; ν_{CO} 1946 vs, 1847 vs cm^{-1}. NMR ^1H ($CDCl_3$, 25.05°C, 700.03 MHz): δ 3.30-3.25 (m, 2 H, NC*H*$_2$CH$_3$), 3.22-3.17 (m, 2 H, NC*H*$_2$CH$_3$), 1.87 (br s, 27 H, 3 × ^{t}Bu), 1.28 (t, $^3J_{HH}$ 7.2 Hz, 6 H, 2 × NCH$_2$C*H*$_3$). $^{11}B\{^1H\}$ ($CDCl_3$, 24.85°C, 128.38 MHz):

δ -2.80. $^{13}C\{^{1}H\}$ ($CDCl_3$, 25.05°C, 176.05 MHz) δ 250.3 (W≡C^{α}, $^{1}J_{WC}$ 216.5 Hz), 222.3 (WCO, $^{1}J_{WC}$ 173.3 Hz), 217.8 (WCO, $^{1}J_{WC}$ 173.2 Hz), 166.7, 165.9, 165.0 (C=S), 64.6 (2 × $C(CH_3)_3$), 62.3 ($C(CH_3)_3$), 44.7 (2 × NCH_2CH_3), 28.5, 27.8 (3 × $C(CH_3)_3$), 14.6 (2 × NCH_2CH_3). MS (ESI, high resolution): *m/z* (%) = $[M+Na]^+$ 830.1924. Calcd. for $C_{22}H_{38}{}^{11}B_1N_{13}{}^{23}Na_1O_2S_3{}^{184}W_1$: $[M+Na]^+$ 830.1934. Elemental Anal. Found: C, 32.78; H, 4.87; N, 22.48; S, 11.95%. Calcd. for $C_{22}H_{38}BN_{13}O_2S_3W$: C, 32.72; H, 4.74; N, 22.55; S, 11.91%.

(Htt)Mo(CO)$_2${≡CN(Et$_2$)} (4.3)

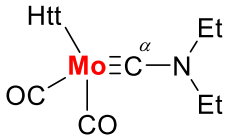

To a 100 mL Schlenk tube, diethylamine (0.10 mL, 0.967 mmol) was dispersed in THF (40 mL), cooled to -78°C and ^{n}BuLi (2.5 M, 0.45 mL, 1.125 mmol) was added dropwise. The reaction mixture was maintained at -78°C for 5 minutes before being warmed in ambient air for 15 minutes, then re-cooled to -78°C and stirred for a further 10 minutes. $[Mo(CO)_6]$ (258 mg, 0.977 mmol) was added and stirred for 15 minutes before the light yellow mixture was warmed in ambient air for 10 minutes, causing it to turn orange, then re-cooled to -78°C for 20 minutes. Trifluoroacetic anhydride (0.14 mL, 1.007 mmol) was added slowly dropwise into the reaction mixture, stirred for 10 minutes, then warmed in ambient air to promote the liberation of carbon monoxide gas. Stirring was continued until bubbles of carbon monoxide gas were no longer observed in the solution. Finally, whilst cooled to -78°C, Na[Htt] (491 mg, 0.970 mmol) was added in single batch and the orange/brown dispersion slowly warmed to room temperature overnight. The resulting brown mixture was concentrated to dryness and purified *via* silica-gel column chromatography (Eluent: CH_2Cl_2). The major orange band which moved off the baseline was collected and concentrated to dryness to provide **4.3** as an orange powder. Yield 240 mg (34%).

IR (CH_2Cl_2): ν_{BH} 2519 w; ν_{CO} 1959 vs, 1864 vs cm^{-1}. NMR ^{1}H ($CDCl_3$, 24.95°C, 700.03 MHz): δ 3.29-3.24 (m, 2 H, CH_3CH_2), 3.22-3.17 (m, 2 H, CH_3CH_2), 1.87 (br s, 27 H, 3 × ^{t}Bu), 1.29 (t, $^{3}J_{HH}$ 7.3 Hz, 6 H, 2 × CH_3CH_2). $^{11}B\{^{1}H\}$ ($CDCl_3$, 24.85°C, 128.38 MHz): δ -2.66. $^{13}C\{^{1}H\}$ ($CDCl_3$, 24.95°C, 176.05 MHz): δ 256.7 (Mo≡C^{α}), 226.5, 222.9 (MoCO), 165.8 (3 × C=S), 64.3 (3 × $C(CH_3)_3$), 45.6 (2 × CH_2CH_3), 28.5 (3 × $C(CH_3)_3$), 14.6 (2 × CH_2CH_3). MS (ESI, high resolution): *m/z* (%) = $[M+Na]^+$ 744.1484. Calcd. for $C_{22}H_{38}{}^{11}B_1{}^{98}Mo_1N_{13}{}^{23}Na_1O_2S_3$: $[M+Na]^+$ 744.1478. Elemental Anal. Found: C, 37.53; H, 5.48; N, 25.17; S, 13.73%. Calcd. for $C_{22}H_{38}BMoN_{13}O_2S_3$: C, 36.72; H, 5.32; N, 25.30; S, 13.37%.

(Htt)W(CO)$_2${≡CN(^{i}Pr$_2$)} (4.4)

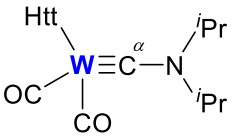

To a 100 mL Schlenk tube, [W(CO)$_6$] (706 mg, 2.006 mmol) was dispersed in THF (40 mL), cooled to -78°C and LDA (2.0 M, 1.1 mL, 2.200 mmol) added dropwise over 2 minutes. The yellow/orange mixture was stirred at -78°C for 15 minutes, then warmed in ambient air for 10 minutes. It was noted that carbon monoxide gas was liberated upon warming, so the reaction mixture was quickly re-cooled to -78°C for 20 minutes to arrest this process. Trifluoroacetic anhydride (0.28 mL, 2.014 mmol) was added slowly dropwise at -78°C and the resulting brown reaction mixture stirred for 10 minutes, before being warmed in ambient air to promote the liberation of carbon monoxide gas. Stirring was continued until bubbles of carbon monoxide gas were no longer observed in the solution. Finally, whilst cooled to -78°C, Na[Htt] (1.016 g, 2.006 mmol) was added in a single batch and the orange/brown reaction mixture slowly warmed to room temperature overnight. Stirring of the resulting red solution was halted after 16 h and concentrated to dryness. The crude reaction mixture was purified *via* silica-gel column chromatography (Eluent: CH_2Cl_2). Collection and subsequent concentration of the major orange band afforded **4.4** as an orange powder. Yield 981 mg (59%).

IR (CH_2Cl_2): ν_{BH} 2526 w; ν_{CO} 1944 vs, 1845 vs cm^{-1}. NMR ^{1}H ($CDCl_3$, 24.95°C, 700.03 MHz): δ 3.31 (sept, $^3J_{HH}$ 6.7 Hz, 2 H, 2 × $(CH_3)_2CH$), 1.87 (br s, 27 H, 3 × ^{t}Bu), 1.38 (d, $^3J_{HH}$ 6.7 Hz, 6 H, $(CH_3)_2CH$), 1.23 (d, $^3J_{HH}$ 6.6 Hz, 6 H, $(CH_3)_2CH$). ^{11}B{^{1}H} ($CDCl_3$, 24.85°C, 128.38 MHz): δ -2.74. ^{13}C{^{1}H} ($CDCl_3$, 24.95°C, 176.05 MHz) δ 249.7 (W≡C$^\alpha$, $^1J_{WC}$ 217.8 Hz), 224.2 (WCO, $^1J_{WC}$ 172.2 Hz), 217.8 (WCO, $^1J_{WC}$ 176.5 Hz), 165.0 (3 × C=S), 64.6 (3 × $C(CH_3)_3$), 52.1 ($(CH_3)_2CH$), 28.7 (3 × $C(CH_3)_3$), 23.4, 22.9 ($(CH_3)_2CH$). MS (ESI, high resolution): m/z (%) = [M+Na]$^+$ 858.2243. Calcd. for $C_{24}H_{42}{}^{11}B_1N_{13}{}^{23}Na_1O_2S_3{}^{184}W_1$: [M+Na]$^+$ 858.2247. Elemental Anal. Found: C, 34.57; H, 5.19; N, 21.61; S, 11.22%. Calcd. for $C_{24}H_{42}BN_{13}O_2S_3W$: C, 34.50; H, 5.07; N, 21.79; S, 11.51%.

(Htt)Mo(CO)$_2${≡CN(^{i}Pr$_2$)} (4.5)

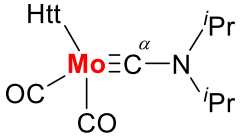

To a 100 mL Schlenk tube, [Mo(CO)$_6$] (528 mg, 2.000 mmol) was dispersed in THF (40 mL), cooled to -78°C and LDA (2.0 M, 1.1 mL, 2.200 mmol) added dropwise over 2 minutes. The orange mixture was stirred at -78°C for 15 minutes, then warmed in ambient air for 10 minutes and finally re-cooled to -78°C for 20 minutes. Trifluoroacetic anhydride (0.28 mL, 2.014 mmol) was added slowly dropwise at -78°C and the resulting

brown/black reaction mixture stirred for 10 minutes, before being warmed in ambient air to promote the liberation of carbon monoxide gas. Stirring was continued until bubbles of carbon monoxide gas were no longer observed in the solution. Finally, whilst cooled to -78°C, Na[Htt] (1.013 g, 2.000 mmol) was added in single batch and the brown reaction mixture slowly warmed to room temperature overnight. Stirring of the orange/brown mixture was halted after 16 h and concentrated to dryness. The crude reaction mixture was purified *via* silica-gel column chromatography (Eluent: CH_2Cl_2). Collection and subsequent concentration of the major orange band afforded **4.5** as an orange powder. Yield 972 mg (65%).

IR (CH_2Cl_2): ν_{BH} 2516 w; ν_{CO} 1958 vs, 1862 vs cm^{-1}. NMR ^1H ($CDCl_3$, 25.05°C, 700.03 MHz): δ 3.32 (sept, $^3J_{HH}$ 6.7 Hz, 2 H, 2 × $(CH_3)_2CH$), 1.88 (br s, 27 H, 3 × ^{t}Bu), 1.40 (d, $^3J_{HH}$ 6.7 Hz, 6 H, $(CH_3)_2CH$), 1.27 (d, $^3J_{HH}$ 6.7 Hz, 6 H, $(CH_3)_2CH$). $^{11}B\{^1H\}$ ($CDCl_3$, 24.85°C, 128.38 MHz): δ -2.63. $^{13}C\{^1H\}$ ($CDCl_3$, 24.95°C, 176.05 MHz) δ 257.4 (Mo≡C^α), 228.3, 223.4 (MoCO), 165.8 (3 × C=S), 64.2 (3 × $C(CH_3)_3$), 53.4 ($(CH_3)_2CH$), 28.6 (3 × $C(CH_3)_3$), 23.4, 23.0 ($(CH_3)_2CH$). MS (ESI, high resolution): m/z (%) = $[M+Na]^+$ 772.1791. Calcd. for $C_{24}H_{42}{}^{11}B_1{}^{98}Mo_1{}^{23}Na_1N_{13}O_2S_3$: $[M+Na]^+$ 772.1791. Elemental Anal. Found: C, 38.55; H, 5.78; N, 24.12; S, 12.81%. Calcd. for $C_{24}H_{42}BMoN_{13}O_2S_3$: C, 38.56; H, 5.66; N, 24.35; S, 12.87%.

TmW(CO)$_2${≡CN(Ph$_2$)} (4.6)

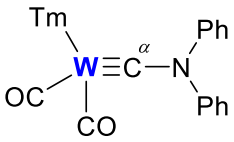

To a 100 mL Schlenk tube, diphenylamine (339 mg, 2.003 mmol) was dispersed in THF (40 mL), cooled to -78°C and ^{n}BuLi (2.5 M, 0.88 mL, 2.200 mmol) was added dropwise. The reaction mixture was maintained at -78°C for 5 minutes before being warmed in ambient air for 30 minutes, then re-cooled to -78°C and stirred for a further 10 minutes. $[W(CO)_6]$ (705 mg, 2.003 mmol) was added and stirred for 15 minutes before the yellow mixture was warmed in ambient air for 30 minutes, then re-cooled to -78°C for 20 minutes. Trifluoroacetic anhydride (0.28 mL, 2.014 mmol) was added slowly dropwise into the reaction mixture, stirred for 10 minutes, then warmed in ambient air to promote the liberation of carbon monoxide gas. Stirring was continued until bubbles of carbon monoxide gas were no longer observed in the solution. Finally, whilst cooled to -78°C, Na[Tm] (749 mg, 2.001 mmol) was added in a single batch and the orange mixture slowly warmed to room temperature overnight. Stirring was halted after 16 h and the resulting orange/red reaction mixture was concentrated to dryness and purified *via* silica-gel column chromatography

(Eluent: CH_2Cl_2). The major orange band which moved off the baseline was collected and concentrated to dryness to afford **4.6** as an orange powder. Yield 654 mg (42%)

IR (CH_2Cl_2): ν_{CO} 1952 vs, 1853 vs cm^{-1}. NMR ^1H ($CDCl_3$, 24.95°C, 700.03 MHz): δ 7.43-7.41 (m, 4 H, C_6H_5), 7.31-7.29 (m, 4 H, C_6H_5), 7.11-7.09 (m, 2 H, C_6H_5), 6.84 (m, 1 H, mtCH), 6.81-6.79 (m, 4 H, mtCH), 6.78 (m, 1 H, mtCH), 3.74 (s, 3 H, $mtCH_3$), 3.62 (s, 3 H, $mtCH_3$), 3.36 (s, 3 H, $mtCH_3$). $^{11}B\{^1H\}$ ($CDCl_3$, 24.85°C, 128.38 MHz): δ -1.59. $^{13}C\{^1H\}$ ($CDCl_3$, 25.05°C, 176.05 MHz): δ 238.8 (W≡C^{α}, $^1J_{WC}$ 230.7 Hz), 224.0 (WCO, $^1J_{WC}$ 171.9 Hz), 219.7 (WCO, $^1J_{WC}$ 167.5 Hz), 161.3, 159.7, 159.6 (mtCS), 140.9, 129.1, 124.7 (C_6H_5), 122.8, 122.7, 122.6 (mtCH), 122.2 (C_6H_5), 119.8 (2C), 119.6 (mtCH), 34.8 (2C), 34.4 ($mtCH_3$). MS (ESI, high resolution): m/z (%) = $[M]^+$ 771.0917; $[M\text{-}CO]^+$ 743.0970; $[M\text{-}2(CO)]^+$ 715.1015. Calcd. for $C_{27}H_{26}{}^{11}B_1N_7O_2S_3{}^{184}W_1$: $[M]^+$ 771.0912. Calcd. for $C_{26}H_{26}{}^{11}B_1N_7O_1S_3{}^{184}W_1$: $[M\text{-}CO]^+$ 743.0963. Calcd. for $C_{25}H_{26}{}^{11}B_1N_7S_3{}^{184}W_1$: $[M\text{-}2(CO)]^+$ 715.1014. Elemental Anal. Found: C, 42.06; H, 3.56; N, 11.83; S, 11.80%. Calcd. for $C_{27}H_{26}BN_7O_2S_3W{\cdot}CH_3Cl$: C, 40.92; H, 3.56; N, 11.93; S, 11.70%.

$TmMo(CO)_2\{\equiv CN(Ph_2)\}$ (4.7)

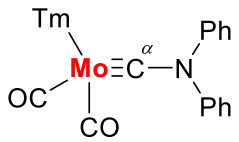

To a 100 mL Schlenk tube, diphenylamine (343 mg, 2.027 mmol) was dispersed in THF (40 mL), cooled to -78°C and ^{n}BuLi (2.5 M, 0.88 mL, 2.200 mmol) was added dropwise. The reaction mixture was maintained at -78°C for 5 minutes before being warmed in ambient air for 30 minutes, then re-cooled to -78°C and stirred for a further 10 minutes. $[Mo(CO)_6]$ (530 mg, 2.008 mmol) was added and stirred for 15 minutes before the yellow mixture was warmed in ambient air for 30 minutes, then re-cooled to -78°C for 20 minutes. Trifluoroacetic anhydride (0.28 mL, 2.014 mmol) was added slowly dropwise into the reaction mixture, stirred for 10 minutes, then warmed in ambient air to promote the liberation of carbon monoxide gas. Stirring was continued until bubbles of carbon monoxide gas were no longer observed in the solution. Finally, whilst cooled to -78°C, Na[Tm] (750 mg, 2.004 mmol) was added in a single batch and the brown mixture slowly warmed to room temperature overnight. Stirring was halted after 16 h and the resulting brown reaction mixture was concentrated to dryness and purified *via* silica-gel column chromatography (Eluent: CH_2Cl_2). The major orange band which moved off the baseline was collected and concentrated to dryness to afford **4.7** as an orange powder. Yield 114 mg (8%)

IR (CH_2Cl_2): ν_{CO} 1966 vs, 1871 vs cm^{-1}. NMR ^1H ($CDCl_3$, 24.95°C, 699.90 MHz): δ 7.41 (br s, 2 H, C_6H_5), 7.40 (m, 2 H, C_6H_5), 7.33 (br s, 1 H, C_6H_5), 7.32 (br s, 2 H, C_6H_5), 7.30 (br s, 1 H, C_6H_5), 7.13 (t, $^3J_{HH}$ 7.4 Hz, 2 H, C_6H_5), 6.82 (s, 1 H, mtCH), 6.80 (d, $^3J_{HH}$ 5.0 Hz, 1 H, mtCH), 6.78-6.77 (m, 3 H, mtCH), 3.72 (s, 3 H, $mtCH_3$), 3.61 (s, 3 H, $mtCH_3$), 3.39 (s, 3 H, $mtCH_3$). $^{11}B\{^1H\}$ ($CDCl_3$, 24.85°C, 128.38 MHz): δ -1.44. $^{13}C\{^1H\}$ ($CDCl_3$, 25.05°C, 176.02 MHz): δ 243.0 (Mo≡C^{α}), 227.6, 223.5 (MoCO), 162.2, 160.6, 160.4 (mtCS), 141.2, 129.8, 129.7, 129.5, 129.3, 129.2, 125.2 (C_6H_5), 122.8, 122.7, 122.5 (mtCH), 122.4 (C_6H_5), 119.6, 119.4, 117.9 (mtCH), 34.8, 34.7, 34.4 ($mtCH_3$). MS (ESI, high resolution): m/z (%) = $[M+Na]^+$ 708.0354; $[M-2(CO)]^+$ 629.0564. Calcd. for $C_{27}H_{26}{}^{11}B_1{}^{98}Mo_1N_7{}^{23}Na_1O_2S_3$: $[M+Na]^+$ 708.0355. Calcd. for $C_{25}H_{26}{}^{11}B_1{}^{98}Mo_1N_7S_3$: $[M-2(CO)]^+$ 629.0559. Elemental Anal. Found: C, 49.37; H, 4.29; N, 13.24; S, 13.02%. Calcd for $C_{27}H_{26}BMoN_7O_2S_3 \cdot C_4H_8O$: C, 49.28; H, 4.54; N, 12.98; S, 12.73%.

(Htt)W(CO)$_2${≡CN(Ph$_2$)} (4.8)

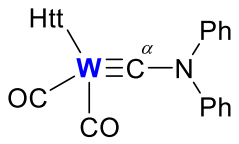

To a 100 mL Schlenk tube, diphenylamine (341 mg, 2.015 mmol) was dispersed in THF (40 mL), cooled to -78°C and ^{n}BuLi (2.5 M, 0.88 mL, 2.200 mmol) was added dropwise. The reaction mixture was maintained at -78°C for 5 minutes before being warmed in ambient air for 30 minutes, then re-cooled to -78°C and stirred for a further 10 minutes. $[W(CO)_6]$ (706 mg, 2.006 mmol) was added and stirred for 15 minutes before the yellow mixture was warmed in ambient air for 30 minutes, then re-cooled to -78°C for 20 minutes. Trifluoroacetic anhydride (0.28 mL, 2.014 mmol) was added slowly dropwise into the reaction mixture, stirred for 10 minutes, then warmed in ambient air to promote the liberation of carbon monoxide gas. Stirring was continued until bubbles of carbon monoxide gas were no longer observed in the solution. Finally, whilst cooled to -78°C, Na[Htt] (1.015 g, 2.004 mmol) was added in a single batch and the orange mixture slowly warmed to room temperature overnight. Stirring was halted after 16 h and the resulting orange/red reaction mixture was concentrated to dryness and purified *via* silica-gel column chromatography (Eluent: CH_2Cl_2). The major orange band which moved off the baseline was collected and concentrated to dryness to afford **4.8** as an orange powder. Yield 1.489 g (82%)

IR (CH_2Cl_2): ν_{BH} 2528 w; ν_{CO} 1966 vs, 1871 vs cm^{-1}. NMR ^1H ($CDCl_3$, 24.95°C, 700.03 MHz): δ 7.39-7.37 (m, 4 H, C_6H_5), 7.35-7.32 (m, 4 H, C_6H_5), 7.19-7.16 (m, 2 H, C_6H_5), 1.89 (s, 9 H, $C(CH_3)_3$), 1.85 (s, 9 H, $C(CH_3)_3$), 1.67 (s, 9 H, $C(CH_3)_3$). $^{11}B\{^1H\}$ ($CDCl_3$, 24.85°C, 128.38 MHz): δ -2.69. $^{13}C\{^1H\}$ ($CDCl_3$, 24.95°C, 176.05 MHz): δ 240.2 (W≡C^{α}, $^1J_{WC}$ 229.6

Hz), 220.3 (WCO, $^{1}J_{WC}$ 172.9 Hz), 216.3 (WCO, $^{1}J_{WC}$ 168.9 Hz), 191.3 (C_6H_5), 166.4, 164.8, 164.4 (C=S), 139.7, 129.5, 129.3, 125.7, 122.3 (C_6H_5), 64.9 (3C) ($C(CH_3)_3$), 28.6 (2C), 28.1 ($C(CH_3)_3$). MS (ESI, high resolution): *m/z* (%) = $[M]^+$ 903.2040; $[M\text{-}CO]^+$ 875.2086. Calcd. for $C_{30}H_{38}{}^{11}B_1N_{13}O_2S_3{}^{184}W_1$: $[M]^+$ 903.2036; Calcd. for $C_{29}H_{38}{}^{11}B_1N_{13}O_1S_3{}^{184}W_1$: $[M\text{-}CO]^+$ 875.2087. Elemental Anal. Found: C, 39.80; H, 4.23; N, 19.35; S, 10.56%. Calcd. for $C_{30}H_{38}BN_{13}O_2S_3W$: C, 39.88; H, 4.24; N, 20.15; S, 10.65%.

TmW(CO)$_2${≡C((*R*)-dimethylbenzylamine)} (4.9)

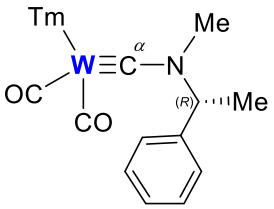

To a 100 mL Schlenk tube, (*R*)-(+)-*N*-α-dimethylbenzylamine (0.25 mL, 1.709 mmol) was dispersed in THF (40 mL), cooled to -78°C and ^{n}BuLi (2.5 M, 0.80 mL, 2.000 mmol) was added dropwise. The reaction mixture was maintained at -78°C for 10 minutes before being warmed in ambient air for 15 minutes, then re-cooled to -78°C. [W(CO)$_6$] (605 mg, 1.719 mmol) was added and stirred for 15 minutes before the mixture was warmed in ambient air for 1 h, then re-cooled to -78°C for 10 minutes. Trifluoroacetic anhydride (0.24 mL, 1.727 mmol) was added dropwise into the orange mixture, stirred for 10 minutes, then warmed in ambient air to promote the liberation of carbon monoxide gas. Stirring was continued for 45 minutes until bubbles of carbon monoxide were no longer observed in solution. Finally, whilst cooled to -78°C, Na[Tm] (644 mg, 1.701 mmol) was added in a single batch and the brown mixture slowly warmed to room temperature overnight. Stirring was halted after 16 h and the resulting orange reaction mixture was concentrated to dryness to afford an orange residue. The crude product mixture was purified *via* silica-gel column chromatography (Eluent: CH_2Cl_2), where isolation and concentration of the bright orange/red band which moved off the baseline afforded **4.9** as an orange powder. Yield 575 mg (46%).

IR (CH_2Cl_2): ν_{CO} 1932 s, 1830 s cm^{-1}. Many signals in the ^{1}H and ^{13}C{^{1}H} NMR spectra appear doubled, due to the presence of two distinct atropisomers which form through the conformational locking of the Tm cage when bound to the metal centre. NMR ^{1}H ($CDCl_3$, 24.95°C, 699.90 MHz): δ 7.47-7.44 (m, 4 H, C_6H_5), 7.34-7.32 (m, 5 H, C_6H_5), 7.25-7.24 (m, 1 H, C_6H_5), 6.80 (br s, 12 H, mtCH), 4.27-4.24 (m, 2 H, NCH), 3.82-3.73 (m, 7 H, mtCH$_3$), 3.64-3.31 (m, 11 H, mtCH$_3$), 2.86 (s, 3 H, NCH$_3$), 2.86 (s, 3 H, NCH$_3$), 1.71-1.70 (m, 6 H, NCCH$_3$). ^{1}H ($CDCl_3$, -40.05°C, 699.90 MHz): δ 7.49 (d, $^{3}J_{HH}$ 6.9 Hz, 2 H, C_6H_5), 7.46 (d, $^{3}J_{HH}$ 7.0 Hz, 2 H, C_6H_5), 7.34 (t, $^{3}J_{HH}$ 7.7 Hz, 5 H, C_6H_5), 7.27 (m, 1 H, C_6H_5), 6.86 (d, $^{3}J_{HH}$ 2.1 Hz, 1 H, mtCH), 6.86-6.84 (m, 3 H, mtCH), 6.83-6.81 (m, 6 H, mtCH), 6.78 (d,

$^{3}J_{HH}$ 2.1 Hz, 1 H, mtCH), 6.78 (d, $^{3}J_{HH}$ 2.1 Hz, 1 H, mtCH), 4.23-4.19 (m, 2 H, NCH), 3.75 (s, 3 H, mtCH$_3$), 3.73 (s, 3 H, mtCH$_3$), 3.64 (s, 3 H, mtCH$_3$), 3.63 (s, 3 H, mtCH$_3$), 3.57 (s, 3 H, mtCH$_3$), 3.49 (s, 3 H, mtCH$_3$), 2.85 (s, 3 H, NCH$_3$), 2.84 (s, 3 H, NCH$_3$), 1.69-1.67 (m, 6 H, NCCH$_3$). $^{13}C\{^{1}H\}$ ($CDCl_3$, -39.95°C, 176.02 MHz): δ 248.7 (W≡C$^{\alpha}$), 227.1, 226.2, 220.9, 220.1 (WCO), 160.3, 160.2, 159.5 (2C), 159.0, 158.9 (mtCS), 142.4, 142.3, 128.6 (2C), 127.5 (2C), 127.0, 126.9 (C_6H_5), 122.8, 122.7, 122.5 (2C), 122.3 (2C), 119.8 (2C), 119.7, 119.5 (mtCH), 61.2, 61.0 (N*C*CH$_3$), 36.3, 36.1 (NCH$_3$), 35.0 (2C), 34.9 (2C), 34.7 (2C) (mtCH$_3$), 22.0, 21.7 (NC*C*H$_3$). MS (ESI, high resolution): m/z (%) = $[M+Na]^+$ 760.0974; $[M]^+$ 737.1077. Calcd. for $C_{24}H_{28}{}^{11}B_1N_7{}^{23}Na_1O_2S_3{}^{184}W_1$: $[M+Na]^+$ 760.0967; Calcd. for $C_{24}H_{28}{}^{11}B_1N_7O_2S_3{}^{184}W_1$: $[M]^+$ 737.1069. Elemental Anal. Found: C, 39.00; H, 4.22; N, 12.73; S, 12.63%. Calcd. for $C_{24}H_{28}BN_7O_2S_3W\cdot(C_3H_6O)_{0.5}$: C, 39.54; H, 3.95; N, 13.04; S, 12.79%.

(Htt)W(CO)$_2${≡C((*R*,*R*)-bis[1-phenylethyl]amine)} (4.10)

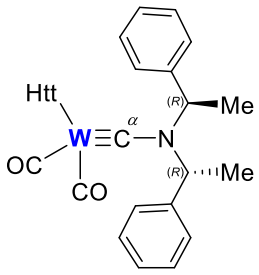

To a 100 mL Schlenk tube, (+)-bis[(*R*)-1-phenylethyl]amine (0.46 mL, 2.011 mmol) was dispersed in THF (40 mL), cooled to -78°C and ^{n}BuLi (2.5 M, 0.88 mL, 2.200 mmol) was added dropwise. The peach reaction mixture was maintained at -78°C for 5 minutes before being warmed in ambient air for 30 minutes, then re-cooled to -78°C and stirred for a further 10 minutes. $[W(CO)_6]$ (706 mg, 2.006 mmol) was added and stirred for 15 minutes before the pale-yellow mixture was warmed in ambient air for 30 minutes, then re-cooled to -78°C for 20 minutes. Trifluoroacetic anhydride (0.28 mL, 2.014 mmol) was added dropwise into the yellow/orange reaction mixture, stirred for 10 minutes, then warmed in ambient air to promote the liberation of carbon monoxide gas. Stirring was continued until bubbles if carbon monoxide gas were no longer observed in solution. Finally, whilst cooled to -78°C, Na[Htt] (1.015 g, 2.004 mmol) was added in a single batch and the light orange mixture slowly warmed to room temperature overnight. Stirring was halted after 16 h and the resulting red reaction mixture was concentrated to dryness and purified *via* silica-gel column chromatography (Eluent: CH_2Cl_2). The initial major orange band which moved off the baseline was collected and concentrated to dryness to afford **4.10** as an orange powder. Yield 709 mg (37%)

IR (CH_2Cl_2): ν_{BH} 2528 w; ν_{CO} 1947 s, 1850 s cm^{-1}. NMR ^{1}H ($CDCl_3$, -40.15°C, 699.90 MHz): δ 7.39-7.30 (m, 10 H, 2 × C_6H_5), 3.96 (q, $^{3}J_{HH}$ 7.0 Hz, 2 H, 2 × NCH), 1.87 (s, 9 H, C(CH$_3$)$_3$), 1.84 (s, 9 H, C(CH$_3$)$_3$), 1.75 (d, $^{3}J_{HH}$ 7.0 Hz, 6 H, 2 × NC(C*H*$_3$)), 1.73 (s, 9 H, C(CH$_3$)$_3$). $^{11}B\{^{1}H\}$ ($CDCl_3$, 24.85°C, 128.38 MHz): δ -2.58. $^{13}C\{^{1}H\}$ ($CDCl_3$, -39.95°C,

176.02 MHz): δ 246.3 (W≡C$^{\alpha}$), 223.1, 220.4 (WCO), 165.6, 164.8, 164.5 (C=S), 142.6, 129.2, 128.9 (2C), 127.9, 127.0, 126.2 (C_6H_5), 64.7, 64.6, 64.4 ($C(CH_3)_3$), 59.4 (2C) (NCH), 28.3, 28.2, 28.1 ($C(CH_3)_3$), 22.8, 22.1 ($NC(CH_3)$). MS (ESI, high resolution): m/z (%) = $[M+Na]^+$ 982.2535. Calcd. for $C_{34}H_{46}{}^{11}B_1N_{13}{}^{23}Na_1O_2S_3{}^{184}W_1$: $[M+Na]^+$ 982.2560. Elemental Anal. Found: C, 42.66; H, 4.91; N, 18.34; S, 9.69%. Calcd. for $C_{34}H_{46}BN_{13}O_2S_3W$: C, 42.55; H, 4.83; N, 18.97; S, 10.02%.

TmW(CO)$_2${≡C(*N,N'*-diphenylbenzidine)} (4.11)

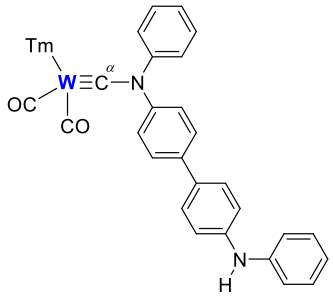

To a 100 mL Schlenk tube, *N,N'*-diphenylbenzidine (336 mg, 0.999 mmol) was dispersed in THF (30 mL), cooled to -78°C and ^{n}BuLi (2.5 M, 0.9 mL, 2.250 mmol) was added dropwise. The greyish pink reaction mixture was maintained at -78°C for 5 minutes before being warmed in ambient air for 30 minutes, then re-cooled to -78°C and stirred for a further 10 minutes. $[W(CO)_6]$ (777 mg, 2.208 mmol) was added and stirred for 15 minutes before the mixture was warmed in ambient air for 30 minutes, then re-cooled to -78°C for 20 minutes. Trifluoroacetic anhydride (0.30 mL, 2.158 mmol) was added dropwise into the yellow reaction mixture, stirred for 10 minutes, then warmed in ambient air to promote the liberation of carbon monoxide gas. Stirring was continued until bubbles of carbon monoxide gas were no longer observed in solution. Finally, whilst cooled to -78°C, Na[Tm] (822 mg, 2.196 mmol) was added in a single batch and the brown/red mixture slowly warmed to room temperature overnight. Stirring was halted after 16 h and the resulting brown reaction mixture was concentrated to dryness to afford a brown residue. The crude product mixture was purified *via* silica-gel column chromatography (Eluent: Gradient 9:1 (v/v) CH_2Cl_2/Petroleum spirit (60-80°C) to 100% CH_2Cl_2), where isolation and concentration of the major orange band afforded **4.11** as an orange powder. Yield 391 mg (42%).

IR (CH_2Cl_2): ν_{CO} 1953 s, 1854 s cm^{-1}. NMR ^{1}H ($CDCl_3$, 24.85°C, 699.90 MHz): δ 7.51-7.45 (m, 9 H, aromatic), 7.34-7.31 (m, 2 H, C_6H_5), 7.30-7.27 (m, 2 H, C_6H_5), 7.14-7.11 (m, 5 H, aromatic), 6.95 (t, $^3J_{HH}$ 7.3 Hz, 1 H, mtCH), 6.85 (br s, 1 H, NH), 6.82-6.80 (m, 4 H, mtCH), 6.78 (br s, 1 H, mtCH), 3.75 (s, 3 H, $mtCH_3$), 3.63 (s, 3 H, $mtCH_3$), 3.37 (s, 3 H, $mtCH_3$). ^{11}B{^{1}H} ($CDCl_3$, 24.85°C, 128.38 MHz): δ -1.64. ^{13}C{^{1}H} ($CDCl_3$, 24.85°C, 176.02 MHz): δ 238.6 (W≡C$^{\alpha}$), 224.2, 219.8 (WCO), 161.3, 159.7, 159.6 (mtCS), 143.0, 142.4, 140.8, 139.7, 137.0, 133.4, 129.5, 129.1, 127.8, 127.5, 127.0, 124.9, 123.3 (aromatic), 122.8, 122.7, 122.6 (mtCH), 122.5, 122.1, 121.4, 121.3, 121.1 (aromatic), 119.9, 119.8, 119.6 (mtCH), 119.4,

118.2, 118.1, 118.0, 117.9 (aromatic), 34.9, 34.8, 34.4 (mtCH_3). MS (ESI, high resolution): m/z (%) = $[M+Na]^+$ 961.1545; $[M-2(CO)]^+$ 882.1754. Calcd. for $C_{39}H_{35}{}^{11}B_1N_8{}^{23}Na_1O_2S_3{}^{184}W_1$: $[M+Na]^+$ 961.1545; Calcd. for $C_{37}H_{35}{}^{11}B_1N_8S_3{}^{184}W_1$: $[M-2(CO)]^+$ 882.1749. Elemental Anal. Found: C, 49.60; H, 4.03; N, 11.33; S, 9.98%. Calcd. for $C_{39}H_{35}BN_8O_2S_3W$: C, 49.91; H, 3.76; N, 11.94; S, 10.25%.

(Htt)W(CO)$_2${≡C(*N,N'*-diphenylbenzidine)} (4.12)

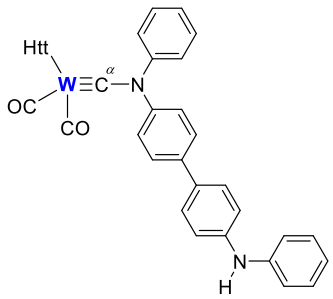

To a 100 mL Schlenk tube, *N,N'*-diphenylbenzidine (337 mg, 1.002 mmol) was dispersed in THF (30 mL), cooled to -78°C and ^{n}BuLi (2.5 M, 0.9 mL, 2.250 mmol) was added dropwise. The greyish pink reaction mixture was maintained at -78°C for 5 minutes before being warmed in ambient air for 30 minutes, then re-cooled to -78°C and stirred for a further 10 minutes. $[W(CO)_6]$ (777 mg, 2.208 mmol) was added and stirred for 15 minutes before the mixture was warmed in ambient air for 30 minutes, then re-cooled to -78°C for 20 minutes. Trifluoroacetic anhydride (0.31 mL, 2.230 mmol) was added dropwise into the yellow/orange reaction mixture, stirred for 10 minutes, then warmed in ambient air to promote the liberation of carbon monoxide gas. Stirring was continued until bubbles of carbon monoxide gas were no longer observed in solution. Finally, whilst cooled to -78°C, Na[Htt] (825 mg, 2.204 mmol) was added in a single batch and the brown mixture slowly warmed to room temperature overnight. Stirring was halted after 16 h and the resulting red reaction mixture was concentrated to dryness to afford a green residue. The crude product mixture was partially purified *via* silica-gel column chromatography (Eluent: CH_2Cl_2), where isolation and concentration of the major orange band which moved off the baseline afforded an orange powder. This was further purified *via* silica-gel column chromatography (Eluent: 7:3 (v/v) CH_2Cl_2/Petroleum spirit (60-80°C)) which allowed for the separation of two orange bands from the crude mixture. Collection and subsequent concentration of the second orange band which developed from the baseline afforded an orange powder, which still contained a mixture of products. Definitive resolution of this product mixture was carried out *via* silica-gel column chromatography (Eluent: 7:3 (v/v) CH_2Cl_2/Petroleum spirit (60-80°C)) and the collection of 5 mL fractions as the orange band eluted through the column. Comparative TLC on aluminium-backed silica plates (Eluent: 7:3 (v/v) CH_2Cl_2/Petroleum spirit (60-80°C)) was used to aid with the combination of column fractions, which showed the presence of two major products. Combination of the initial column fractions and

subsequent concentration under reduced pressure afforded **4.12** as a bright orange powder. Yield 166 mg (15%).

IR (CH_2Cl_2): ν_{BH} 2528 w; ν_{CO} 1966 vs, 1871 vs cm^{-1}. NMR ^1H ($CDCl_3$, 25.05°C, 699.90 MHz): δ 7.53 (d, $^3J_{HH}$ 8.7 Hz, 2 H, C_6H_4), 7.50 (d, $^3J_{HH}$ 8.7 Hz, 2 H, C_6H_4), 7.43-7.41 (m, 4 H, C_6H_5), 7.36 (t, $^3J_{HH}$ 8.0 Hz, 2 H, C_6H_5), 7.31-7.28 (m, 2 H, C_6H_5), 7.20 (t, $^3J_{HH}$ 7.4 Hz, 1 H, C_6H_5), 7.16-7.14 (m, 4 H, C_6H_5), 6.98 (t, $^3J_{HH}$ 7.3 Hz, 1 H, C_6H_5), 1.91 (s, 9 H, $C(CH_3)_3$), 1.86 (s, 9 H, $C(CH_3)_3$), 1.69 (s, 9 H, $C(CH_3)_3$). $^{11}B\{^1H\}$ ($CDCl_3$, 24.85°C, 128.38 MHz): δ -2.40. $^{13}C\{^1H\}$ ($CDCl_3$, 25.05°C, 176.02 MHz): δ 240.1 (W≡C^{α}, $^1J_{WC}$ 229.4 Hz), 220.4 (WCO, $^1J_{WC}$ 173.3 Hz), 216.4 (WCO, $^1J_{WC}$ 168.9 Hz), 166.4, 164.8, 164.5 (C=S), 142.5, 139.6, 138.3 (2C), 138.1 (2C), 129.6, 129.4, 127.9, 127.6 (2C), 127.3, 125.9, 122.5, 122.3, 118.7, 118.6, 118.2, 118.1 (aromatic), 64.9 (3C) ($C(CH_3)_3$), 28.6 (2C), 28.2 ($C(CH_3)_3$). MS (ESI, high resolution): m/z (%) = $[M+Na]^+$ 1093.2667; $[M+H]^+$ 1071.2882. Calcd. for $C_{42}H_{47}{}^{11}B_1N_{14}{}^{23}Na_1O_2S_3{}^{184}W_1$: $[M+Na]^+$ 1093.2669; Calcd. for $C_{42}H_{48}{}^{11}B_1N_{14}O_2S_3{}^{184}W_1$: $[M+H]^+$ 1071.2849. Elemental Anal. Found: C, 42.66; H, 4.91; N, 18.34; S, 9.69%. Calcd. for $C_{34}H_{46}BN_{13}O_2S_3W$: C, 42.55; H, 4.83; N, 18.97; S, 10.02%.

$(Htt)W(CO)_2\{\mu$-C-N(Ph)-Ph-Ph-N(Ph)-C≡$\}W(CO)_2(Htt)$ (4.13)

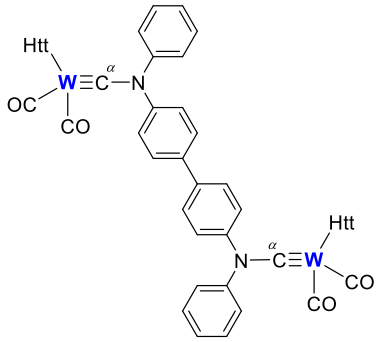

To a 100 mL Schlenk tube, *N,N'*-diphenylbenzidine (337 mg, 1.002 mmol) was dispersed in THF (30 mL), cooled to -78°C and ^{n}BuLi (2.5 M, 0.9 mL, 2.250 mmol) was added dropwise. The greyish pink reaction mixture was maintained at -78°C for 5 minutes before being warmed in ambient air for 30 minutes, then re-cooled to -78°C and stirred for a further 10 minutes. $[W(CO)_6]$ (777 mg, 2.208 mmol) was added and stirred for 15 minutes before the mixture was warmed in ambient air for 30 minutes, then re-cooled to -78°C for 20 minutes. Trifluoroacetic anhydride (0.31 mL, 2.230 mmol) was added dropwise into the yellow/orange reaction mixture, stirred for 10 minutes, then warmed in ambient air to promote the liberation of carbon monoxide gas. Stirring was continued until bubbles of carbon monoxide gas were no longer observed in solution. Finally, whilst cooled to -78°C, Na[Htt] (825 mg, 2.204 mmol) was added in a single batch and the brown mixture slowly warmed to room temperature overnight. Stirring was halted after 16 h and the resulting red reaction mixture was concentrated to dryness to afford a green residue. The crude product mixture was partially purified *via* silica-gel column chromatography (Eluent: CH_2Cl_2), where isolation and concentration of the major orange

band which moved off the baseline afforded an orange powder. This was further purified *via* silica-gel column chromatography (Eluent: 7:3 (v/v) CH_2Cl_2/Petroleum spirit (60-80°C)) which allowed for the separation of two orange bands from the crude mixture. Collection and subsequent concentration of the second orange band which developed from the baseline afforded an orange powder, which still contained a mixture of products. Definitive resolution of this product mixture was carried out *via* silica-gel column chromatography (Eluent: 7:3 (v/v) CH_2Cl_2/Petroleum spirit (60-80°C)) and the collection of 5 mL fractions as the orange band eluted through the column. Comparative TLC on aluminium-backed silica plates (Eluent: 7:3 (v/v) CH_2Cl_2/Petroleum spirit (60-80°C)) was used to aid with the combination of column fractions, which showed the presence of two major products. Combination of the latter column fractions and subsequent concentration under reduced pressure afforded **4.13** as an orange powder. Yield 64 mg (4%).

IR (CH_2Cl_2): ν_{BH} 2528 w; ν_{CO} 1967 vs, 1871 vs cm^{-1}. NMR ^1H ($CDCl_3$, 24.85°C, 699.90 MHz): δ 7.54-7.52 (m, 4 H, C_6H_4), 7.45-7.41 (m, 8 H, C_6H_5), 7.38-7.36 (m, 4 H, C_6H_5), 7.21 (t, $^3J_{HH}$ 7.3 Hz, 1 H, C_6H_5), 1.90 (s, 18 H, 2 × $C(CH_3)_3$), 1.86 (s, 18 H, 2 × $C(CH_3)_3$), 1.70 (s, 18 H, 2 × $C(CH_3)_3$). $^{11}B\{^1H\}$ ($CDCl_3$, 24.85°C, 128.38 MHz): δ -2.48. $^{13}C\{^1H\}$ ($CDCl_3$, 24.85°C, 176.02 MHz): δ 239.7 (W≡C^α, $^1J_{WC}$ 230.0 Hz), 220.4 (WCO, $^1J_{WC}$ 173.3 Hz), 216.3 (WCO, $^1J_{WC}$ 168.9 Hz), 166.3, 164.7, 164.4 (C=S), 139.6, 139.4, 139.1, 138.3, 138.1, 137.3, 129.6, 129.5, 129.4, 127.9, 127.6, 127.3, 126.1, 122.8, 122.5, 122.3, 122.0, 118.7, 118.2 (aromatic), 64.9, 64.8 ($C(CH_3)_3$), 28.6 (2C), 28.2 ($C(CH_3)_3$). MS (ESI, high resolution): *m/z* (%) = $[M+Na]^+$ 1827.3768; $[M+H]^+$ 1805.3925. Calcd. for $C_{60}H_{74}{}^{11}B_2N_{26}{}^{23}Na_1O_4S_6{}^{184}W_1$: $[M+Na]^+$ 1827.3813; Calcd. for $C_{60}H_{74}{}^{11}B_2N_{26}O_4S_6{}^{184}W_1$: $[M+H]^+$ 1805.3994. Elemental Anal. Found: C, 42.72; H, 4.53; N, 19.22; S, 10.09%. Calcd for $C_{60}H_{74}B_2N_{26}O_4S_6W_2{\cdot}(C_6H_{12})$: C, 41.96; H, 4.59; N, 19.28; S, 10.18%.

5.3 Chapter 5 - References and Notes

1. Bruce, M. I., Nicholson, B. K., Shawkataly, O. B., Shapley, J. R., Henly, T., *Inorg. Synth.*, **1989**, *26*, 324.

2. Hooper, T. N., Butts, C. P., Green, M., Haddow, M. F., McGrady, J. E., Russell, C. A., *Chem. -Eur. J.*, **2009**, *15*, 12196.

3. (a) Takahashi, Y., Ito, T., Sakai, S., Ishii, Y., *J. Chem. Soc. D*, 1970, 1065.; (b) Ishii, Y., *Ann. N. Y. acad. Sci.*, **1974**, *239*, 114.

4. Coulson, D. R., *Inorg, Synth.*, **1990**, *28*, 107.

5. $[Pt(nbe)_3]$ (tris(bicyclo[2.2.1]heptane)platinum(0); nbe = norbornene) was prepared from dichloro(1,5-cyclooctadiene)platinum(II) by variation of the literature method (Crascall, L. E., Spencer, J. L., Doyle, R. A., Angelici, R. J., *Inorg. Synth.*, **1990**, *28*, 126.) using triethylsilane rather than (1,3,5,7-cyclooctatetraene)dilithium as the reductant, as reported by Spencer and co-workers (Vaughan, T. F., Koedyk, D. J., Spencer, J. L., *Organometallics*, **2011**, *30*, 5170.)

6. Frogley, B. J., Hill, A. F., Shang, R., Sharma, M., Willis, A. C., *Chem. -Eur. J.*, **2020**, *26*, 8819.

7. Reinholdt, A., Bendix, J., Hill, A. F., Manzano, R. A., Manzano, *Dalton Trans.*, **2018**, *47*, 14893.

8. Keller, S., Yi, C., Li, C., Liu, S.-X., Blum, C., Frie, G., Sereda, O., Neels, A., Wandlowski, T., Decurtins, S., *Org. Biomol. Chem.*, **2011**, *9*, 6410.

9. Hu, J.-Y., Pu, Y.-J., Yamashita, Y., Satoh, F., Kawata, S., Katagiri, H., Sasabe, H., Kido, J., *J. Mater. Chem. C*, **2013**, *1*, 3871.

10. Zdobinsky, T., Maiti, P. S., Klajn, R., *J. Am., Chem. Soc.*, **2014**, *136*, 2711.

11. Procedure adapted from: Wu, Z., Li, A., Fan, B., Xue, F., Adachi, C., Ouyang, J., *Solar Energy Materials & Solar Cells*, **2011**, 95, 2516.

12. D. Evans, J. A. Osborn, G. Wilkinson, R. Paine, R. W. Parry, *Inorg. Synth.*, **1990**, *28*, 79.

13. G. Sheldrick, *Acta Crystallogr. C*, **2015**, *71*, 3.

14. O. V. Dolomanov, L. J. Bourhis, R. J. Gildea, J. A. K. Howard, H. Puschmann, *J. Appl. Crystallogr.*, **2009**, *42*, 339.

15. C. F. Macrae, I. J. Bruno, J. A. Chisholm, P. R. Edgington, P. McCabe, E. Pidcock, L. Rodriguez-Monge, R. Taylor, J. van de Streek, P. A. Wood, *J. Appl. Crystallogr.*, **2008**, *41*, 466.

CHAPTER 6.

CONCLUDING REMARKS

6.1 Concluding Remarks

Over the course of the work carried out herein, it has been noted on several occasions that the 'soft' sulfur-containing Scorpionate ligands **Bm**, **Hbt**, **Tm**, and **Htt** are yet to be utilised to their fullest potential. In comparison to the various chemistries of their 'hard' nitrogen-containing predecessors (e.g. **Tp** and **Tp***), their respective fields within organometallic chemistry are only just beginning to become developed. With reference to the organometallic and coordination chemistry of **Tp** and **Tp***, significant success has been noted during efforts to incorporate these facially capping ligand systems into group 6 carbyne, propargylidyne, and aminocarbyne complexes. Prior to this report, few attempts had been made to carry out analogous studies using soft Scorpionate ligand systems.

Throughout early literature reports on the topic of **Tm** chemistry, repeated attempts were made to draw comparison to the similarities of Cp, **Tp*** and **Tm** ligand systems. Superficially, this can be rationalised due their shared preference for the facially capping coordination mode on appropriate metal centres with octahedral coordination environments, as well as their anionic charge, and six-electron donor capabilities. However, upon deconvolution of the coordination chemistry which **Tm** displays, it is now recognised that a significant and commensurate difference exists between all three ligand systems.

Inherently, the environments formed through the κ^3-coordination of the **Tm** ligand to metal centres are very different to those similarly formed by **Tp**/**Tp*** ligands. Due to the warping of the **Tm** cage about the metal centre, not only are two isomeric structures likely to form, but the additional flexibility of the cage allows incoming reactants to more easily access the **Tm**-ligated metal centre. Furthermore, the relatively soft donor ability of the thione groups on **Tm** allows for the enhanced potential for non-innocent coordination behaviours. This has been noted during the course of this study, whereby the oxidative addition of a single iodine atom to a **Tm**-ligated tungsten silylpropargylidyne complex invoked slippage of one methimazolyl arm from the metals centre and into a semi-bridging position between the metal centre and the (originally) carbyne carbon.

Regrettably, the additional lability exhibited by the **Tm** ligand has in some cases limited progress. This was especially evident during efforts which were made to form various mixed bi-metallic tricarbido complexes *via* an *in situ* desilylation and metalation approach of a preformed silylpropargylidyne complex. Although two tricarbido complexes bearing Au and Rh fragments were successfully prepared, several other complexes bearing a range of

metal fragments were synthetically targeted, but never isolated. This was somewhat unexpected, given that many of the analogous complexes bearing the **Tp*** ligand have been previously reported using similar reaction routes. However, these shortcomings did not halt progress during the preparation of a library of propargylidyne complexes assembled about tungsten and molybdenum centres, and featuring either silyl-, alkyl-, or aryl-termini.

More success was noted during the formation of tungsten and molybdenum carbyne complexes featuring polycyclic aromatic hydrocarbons (PAH). In recognition of the potential for electronic conjugation within such complexes, a range of PAH compounds were chosen due to their pre-existing optical and electronic-properties, with the aim to harnessing these attributes. Beginning from appropriately mono-brominated PAH starting materials, these compounds were utilised in the ubiquitous oxide abstraction protocol to form metallocarbyne complexes. This approach allows for a significant degree of tailoring and control, and tends to afford relatively high yields when compared to alternative reaction pathways. Unfortunately, no notable optoelectronic properties were observed in the resulting Scorpionate-ligated complexes, more than likely as a result of the heavy metals facilitating intramolecular quenching mechanisms. Efforts were made to try and invoke optical and electronic properties through extension of the conjugated systems within various **Tm** complexes. However, these once again proved to be ineffective in this regard. Conversely, these efforts allowed for the preparation of two examples of precious metal 'butterfly' complexes, which were specifically targeted following the serendipitous formation of the Pd-variant during an attempted Sonogashira cross-coupling reaction.

Aminocarbyne complexes are well documented to have unique electronic structures, on account of the significant contribution the 2-azavinylidene resonance form has within these species. Empirically, this can be detected through the relatively sluggish reactivity these materials display when compared to more typical carbyne complexes, resulting from the increased delocalisation of the electronic structure within such complexes. Using the rarely encountered **Htt** ligand system, a library of simple aminocarbyne complexes were formed about tungsten and molybdenum centres. Where appropriate, electrochemical testing of these speices was undertaken, and revealed both major and minor redox couples, the latter of which could not be accounted for. Furthermore, through the use of chiral secondary amines, it was possible to form mixtures of cage-locked aminocarbyne complexes which were interrogated *via* various spectroscopic means.

It is hoped that through the work which has been briefly summarised above, research will continue into the application of soft Scorpionate ligands in the fields of organometallic and coordination chemistry. Compared to the nitrogen-based Scorpionate ligands which have been widely used over the past several decades, the reactivity of the new homologue of soft sulfur-containing Scorpionates proves to be significantly disparate. In some instances, the differences between these two types of ligand systems has been all too apparent during the course of this work. However, this justifies the need for continued work in this field, and for a better understanding of the chemistry these materials display to be developed.